

Aus dem Institut für Schlaganfall- und Demenzforschung (ISD)
Klinikum der Ludwig-Maximilians-Universität München
Direktor: Prof. Dr. Martin Dichgans



Investigating the Nuclease Activity of MIF and MIF-2 and Their Effects on DNA Damage

Dissertation

zum Erwerb des Doktorgrades der Naturwissenschaften (Dr. rer. nat.)
an der Medizinischen Fakultät der
Ludwig-Maximilians-Universität München

vorgelegt von

Buket Bulut Impraim

aus Augsburg

2023

Mit Genehmigung der Medizinischen Fakultät
der Universität München

Betreuer(in): Prof. Dr. rer. nat. Jürgen Bernhagen

Zweitgutachter: Prof. Dr. rer. nat. Wolfgang Enard

Dekan: Prof. Dr. med. Thomas Gudermann

Tag der mündlichen Prüfung: 19.Juni 2024

Table of contents

Table of contents	I
Summary	IV
Zusammenfassung	VI
List of figures	VIII
Abbreviations	XI
1. Introduction	1
1.1. An overview of brain anatomy and physiology	1
1.1.2 Functions of brain cells	2
1.2. The impact of age on cognitive health	3
1.3. Neurodegenerative diseases: mechanisms and implications.	5
1.3.1. Inflammasomes and their impact on neurodegenerative diseases	6
1.3.2. Cellular diversity in neurodegenerative	8
1.4. The biology of aging: mechanisms and implications	9
1.4.1. Genomic instability and DNA damage.....	9
1.4.2. Altered intercellular communication and immune function	10
1.4.3. The Role of oxidative stress and cell death.....	11
1.5. Protein aggregation.....	12
1.6. Neuroinflammation and neurodegeneration	14
1.7. Genomic damage and neurodegeneration.....	14
1.8. The impact of cytokines on biological processes.....	17
1.9. The role of cytokines and chemokines in the brain	18
1.10. Macrophage migration inhibitory factor (MIF)	19
1.11. Structure and function of MIF	19
1.12. D-Dopachrome tautomerase (D-DT/MIF-2).....	21
1.13. MIF: a crucial regulator of inflammation	22
1.14. MIF and its involvement in neurodegenerative disorders	23
1.15. The multiple functions of MIF as a moonlighting protein.....	23
1.15.1. The nuclease function of MIF	27
1.15.2. Nucleases: key players in cell death processes	29
2. Aim of this study	31

3. Material	32
3.1. Chemicals and reagents	32
3.2. MIF family protein samples	33
3.3. Buffer and solution.....	33
3.4. Buffer and solution (SDS-PAGE, western blot immunodetection)	34
3.5. Media and solutions for culture of primary mouse neurons	34
3.6. Solutions for Coomassie brilliant blue staining	35
3.7. Bacteria and plasmids	36
3.8. Buffers and solutions for protein expression and purification.....	36
3.9. Primary antibodies	36
3.10. Cell lines and primary cultures	37
3.11. Mouse lines	37
3.12. Consumables	37
3.13. Kits.....	38
3.14. Devices	38
3.15. Software	39
4. Method	40
4.1. Cell culture	40
4.1.1. Human embryonic kidney (HEK).....	40
4.1.2. Neuronal culture isolation	40
4.1.3. Astrocyte culture isolation	41
4.2. Toxic treatments.....	42
4.3. Digestion of DNA by restriction endonucleases	43
4.4. Nuclease agarose assay	43
4.5. Real-time nuclease assay	44
4.6. Agarose gel electrophoresis and DNA detection	44
4.7. Comet assay (single-cell gel electrophoresis)	45
4.8. Cloning	46
4.9. Trizol RNA isolation (brain tissue).....	47
4.10. Transgenic mice	48
4.10.1. Transgenic rat.....	49
4.11. CRISPR/Cas	50
4.12. Confocal microscopy analysis.....	52
4.13. Statistics	52
5. Results	53

5.1.	Initial results	53
5.2.	Nuclease properties of MIF and MIF-2.....	57
5.3.	MIF-2 is a novel nuclease	67
5.3.1.	MIF-2 exhibits nuclease activity similar to MIF.....	68
5.3.2.	MIF and MIF-2 nuclear enrichment after excitotoxicity.....	73
5.4.	Indication of DSB and cell survival change in <i>Mif KO</i> and <i>Mif-2 KO</i> ..	77
5.5.	MIF related to DNA damage.....	79
5.5.1.	MIF's topological driven function.....	79
5.6.	<i>Mif KO</i> rat	85
5.6.1.	Designing CRISPR/Cas9 guide RNA.....	88
6.	Discussion	97
6.1.	Aging associated neurodegenerative diseases	97
6.2.	MIF-2 is a potential nuclease.....	98
6.3.	MIF is related to DNA damage.....	104
6.4.	Validation of MIF/MIF-2 enzymatic activity.....	108
6.5.	MIF and MIF-2 are key players in various diseases	109
6.6.	Validation of <i>Mif</i> -deficient rat	115
6.7.	<i>Mif</i> -deficient rat as a novel research model.....	117
	References.....	119
	Acknowledgement	147
	Affidavit.....	149
	List of publications	150

Summary

The multifunctional inflammatory protein macrophage migration inhibitory factor (MIF) and its paralog D-dopachrome tautomerase (D-DT)/MIF-2 have important functions in various neurodegenerative diseases. This work aimed to study the relationship between the topological location of MIF and MIF-2 in different neuronal cell compartments and their functions. The focus of this study was to describe the complex modes of action of MIF and MIF-2 in the brain, as well as the discovery and function of the nuclease activity of MIF-2. In 2016, MIF was identified as a new member of the PD-D/E(X)K class of nucleases. Similar catalytic properties were discovered in this dissertation for MIF-2, where the PD-D/E(X)K nuclease domains are only partially conserved when compared with MIF. Glutamic acid at position 22 of human and mouse MIF is relevant for nuclease function. Similarly in this work, glutamic acid was identified at position 88 as being critical for the nuclease activity of human MIF-2.

Moreover, the subcellular localization of MIF was found to be similar to that of MIF-2, with both homologs present in the cytoplasm, nucleus, and extracellular space, indicating a potential "moonlighting" function for MIF-2. Moonlighting proteins serve multiple functions despite originating from a single gene. Changes at catalytic sites or interactions with other proteins can cause different functions. The MIF family has different functions, both intracellularly and extracellularly. This work's second focus was the interaction between MIF and the protein apoptosis-inducing factor (AIF), since MIF is the essential nuclease in AIF-induced programmed cell death (parthanatos). AIF is assumed to escort MIF from the cytosol to the nucleus. My work detected MIF in both wild-type cells and *Mif-2*-deficient primary astrocyte cultures. Conversely, *Mif-2* was localized to the nucleus in both wild-type cells and *Mif*-deficient cells. In addition, it is assumed that the translocation of MIF and MIF-2 takes place independently of one another. It has been identified that the nuclease function of MIF is an Mg²⁺- and Ca²⁺-dependent 3' exonuclease activity. In my study, MIF-2 nuclease function was inhibited using various methods, including ethylenediaminetetraacetate (EDTA), which forms chelate complexes with positively charged metal ions. The results highlight the pleiotropic effects of MIF and MIF-2, but my study focused on their roles in cellular stress and apoptosis. PARP1 inhibition has been identified as an attractive target for acute neurological diseases. Using DNA double-strand break markers and comet assays, a reduction of DNA damage was observed in *Mif*- and *Mif-2*-deficient cells compared to wild-type cells. Work in my thesis found that primary mixed neuronal cultures obtained from *Mif* KO animals and primary astrocytes isolated from *Mif-2* KO animals showed fewer γ H2AX

and 53BP1 markers compared to the wild-type. This highlights the potential role of MIF and MIF-2 in DNA damage and neurodegenerative diseases.

Laboratory mice and rats have long been indispensable tools in research, with mice being the by far predominant model for most diseases. This dissertation explored the unique advantages of a rat model, particularly in the context of studying the macrophage migration inhibitory factor (MIF) family. Rats, with their larger size and weight, offer significant benefits for various research applications, including investigations into MIF-related conditions like stroke and Alzheimer's disease.

In this study, reverse genetic tools, including genome editing methods, were employed to establish a *Mif* KO rat model for investigating the critical role of MIF proteins in important biological processes. The rat model's establishment remains crucial for replicating essential insights from mouse models.

In conclusion, this dissertation explored the roles of MIF and MIF-2 in neurodegenerative diseases, revealing their nuclease activity, subcellular localization, and involvement in programmed cell death together with AIF. Overall, this research enhanced our understanding of MIF and MIF-2 in neurodegenerative diseases and their potential in treating acute neurological conditions.

Zusammenfassung

Das im Jahr 1966 erstmals beschriebene Protein "macrophage migration inhibitory factor" (MIF) und sein Paralog D-dopachrome tautomerase (DDT) / MIF-2 nehmen wichtige Funktionen in verschiedenen neurodegenerativen Erkrankungen ein. Im Rahmen dieser Arbeit sollte der Zusammenhang der topologischen Lage von MIF und MIF-2 innerhalb der Zellkompartimente und deren Funktion dargestellt werden. Im Fokus dieser Arbeit stand die Beschreibung der vielfältigen Wirkungsweisen im Gehirn von MIF und MIF-2 sowie die Entdeckung und Nuklease Funktion von MIF-2. Im Jahr 2016 wurde MIF als neues Mitglied der PD-D/E(X)K-Klasse von Nukleasen identifiziert. In dieser Dissertation wurden auch ähnliche katalytische Eigenschaften für MIF-2 entdeckt, wobei die PD-D/E(X)K-Nuklease-Domänen im Vergleich zu MIF nur teilweise konserviert waren. Die Aminosäure Glutaminsäure an Position 22 von humanem und Maus MIF wurde im Jahr 2016 als relevante Aminosäure für die Nuklease Funktion beschrieben. In dieser Arbeit wurde die Glutaminsäure an Position 88 im humanen MIF-2 als kritische Aminosäure für die Nuklease Funktion identifiziert. Die topologischen Lokalisationen, die für MIF bekannt sind, wurden auch für MIF-2 detektiert. Beide Homologe wurden extrazellulär, im Zytoplasma sowie im Nukleus lokalisiert. Dementsprechend wurde eine topologisch regulierte "Moonlight"-Funktion auch für MIF-2 beobachtet. Der Begriff "Moonlighting-Proteine" beschreibt Proteine, die von einem einzigen Gen abstammen, aber mehrere Funktionen erfüllen. Die MIF-Familie ist ein Sonderfall, da sie sowohl intrazellulär als auch extrazellulär unterschiedliche Funktionen aufweist. In dieser Arbeit stand insbesondere die Interaktion von MIF und dem Protein Apoptosis Inducing Factor (AIF) im Mittelpunkt. Dies wurde damit begründet, dass MIF als essenzielle Nuklease beim AIF-induzierten programmierten Zelltod (Apoptose) bekannt ist. Dieser experimentelle Befund wurde durch einen Chromatin-Immunoprecipitation (ChIP)-Assay und eine nachfolgende "Deep Sequencing"-Analyse erlangt. In Zellen, in denen die MIF-Gene durch RNA-Interferenz künstlich stillgelegt wurden, konnte AIF im Nukleus detektiert werden. Es wurde jedoch keine Translokation von MIF in den Zellkern beobachtet. In dieser Studie konnte MIF sowohl in Wildtyp-Zellen als auch in MIF-2-defizienten primären Astrozytenkulturen nachgewiesen werden. Umgekehrt wurde MIF-2 sowohl in Wildtyp-Zellen als auch in MIF-defizienten KO-Zellen im Nukleus lokalisiert. Darüber hinaus wurde angenommen, dass die Translokation von MIF bzw. MIF-2 unabhängig voneinander stattfindet. Nuklease Funktion von MIF wurde als Mg^{2+} , und Ca^{2+} -abhängige 3' Exonuklease identifiziert. In dieser Studie wurden diese Daten reproduziert, und es wurde eine Inhibition der Nuklease Funktion von MIF-2 durch

Ethylendiamintetraacetat (EDTA) erreicht, das Chelatkomplexe mit positiv geladenen Metallionen bildet. Angesichts dieser Ergebnisse zeigt diese Arbeit die Vielzahl von pleiotropen Wirkungen von MIF und MIF-2 auf. Der Schwerpunkt dieser Studie lag jedoch vor allem auf der Rolle von MIF und MIF-2 bei zellulärem Stress und der Apoptose. In vielen Apoptose-Studien wird die Hemmung von PARP 1 als attraktives Ziel für akute neurologische Erkrankungen genannt. In dieser Arbeit wurde gezeigt, dass in MIF- und MIF-2-defizienten Zellen im Vergleich zu Wildtyp-Zellen eine Reduktion von DNA-Schäden durch DNA-Doppelstrangbruchmarker und Comet-Essays festgestellt wurde. Zum Beispiel wurden in primären neuronalen Mischkulturen, die von *Mif*-KO-Tieren gewonnen wurden, und in primären Astrozyten, die aus *Mif-2* KO-Tieren isoliert wurden, im Vergleich zum Wildtyp weniger γ H2AX- und 53BP1-Marker detektiert. DNA-Schäden werden schon seit längerem im Rahmen neurodegenerativer Erkrankungen untersucht. In dieser Arbeit lag der Fokus auf der PARP 1-Aktivierung und der daraus resultierenden Freisetzung von AIF aus den Mitochondrien bei der Signalisierung des Zelltods. Angesichts dieser Ergebnisse stellt die Nukleaseaktivität von MIF sowie von MIF-2 ein attraktives Ziel für die Behandlung akuter neurologischer Erkrankungen dar. Betrachtet man die Ergebnisse, wird deutlich, dass MIF und MIF-2 Proteine mit unterschiedlichen komplexen Funktionen sind. Die Rolle von MIF und MIF-2 wird einerseits durch die Topologie innerhalb der Zelle definiert und andererseits durch externe Bedingungen, unter denen sich die Zelle befindet, wie beispielsweise oxidativer Stress oder Replikationsstress. Neben der Nukleaseaktivität von MIF und MIF-2 sowie der Reduktion von DNA-Schäden in *Mif*-KO - und *MIF-2*-KO-Zellen wurde in dieser Studie auch ein potenzielles neues Forschungsmodell etabliert, nämlich die *Mif*-KO-transgene Ratte. In der vorliegenden Arbeit wurde mithilfe von reversen genetischen Werkzeugen (Genome-Editing-Methoden) ein Rattenmodell mit *Mif*-KO zur Untersuchung der Schlüsselrolle der MIF-Proteine in kritischen biologischen Prozessen etabliert. Die Etablierung des Rattenmodells bleibt entscheidend, um wesentliche Erkenntnisse aus Mausmodellen zu replizieren.

List of figures

Figure 1-1: Schematic representation of mouse and human brain; modified by using Biorender.	2
Figure 1-2: Schematic representation of healthy brain and Alzheimer’s brain; generated and modified by using Biorender.....	5
Figure 1-3: Schematic representation of summarized multitasking/moonlighting functions of MIF family member proteins.....	26
Figure 4-1: Schematic representation of primary astrocyte culture.....	42
Figure 5-1: Presentation of the purity of the in-house produced recombinant MIF, MIF-2, and their mutants.	54
Figure 5-2: Representation of the sequence analysis of a variety of animals as well as human MIF and their schematic phylogenetic tree with the focus of the nuclease domains.	55
Figure 5-3: Heatmap of MIF family proteins and their receptors, nucleases DNA2 and FEN1as well as PARP1 in human tissues.	56
Figure 5-4 : Heatmap of MIF family proteins and their receptors, nucleases DNA2 and FEN1as well as PARP1 during prenatal human brain development.....	58
Figure 5-5: Heatmap of MIF-receptor family proteins, nucleases (DNA2, Dnase1 and FEN1), proteins involved in DNA sensing process (Cyclic GMP-AMP synthase (CGas)) and mechanistic Target of Rapamycin (MTOR).....	60
Figure 5-6 : Heatmap of MIF family proteins and their receptors, nucleases (DNA2, Dnase1 and FEN1), DNA sensing process proteins (Cyclic GMP-AMP synthase (CGas)) and mechanistic Target of Rapamycin (MTOR).....	61
Figure 5-7: Heatmap of MIF family proteins and their receptors, S100A9 also known as migration inhibitory factor-related protein 14 (MRP14), and Bromodomain Adjacent to Zinc Finger Domain 1A, including (BAZ1A).	63
Figure 5-8: Identifying the possible Nuclease domains by the crystal structure of human MIF and MIF-2.....	64
Figure 5-9: Identifying the possible Zinc finger domains.....	65
Figure 5-10: Sequence analysis of a variety of animals as well as human MIF-2 and their schematic phylogenetic tree.....	66
Figure 5-11: MIF-2 nuclease function is conserved within the crystal structure.....	69
Figure 5-12: Quantification of the relative fluorescence Intensity indicate different sequence affinities of MIF and MIF-2 by using the real time nuclease assay.....	70

Figure 5-13: In vitro agarose gel electrophoreses nuclease assay of MIF and MIF-2 with various concentration, buffer conditions, with known inhibitors as well as with different MIF mutants.	72
Figure 5-14: MIF and MIF-2 enrichment in the nucleus in excitotoxicity in astrocyte culture and neuronal primary culture. AIF translocation is not affected by MIF or MIF-2 deficiency.	74
Figure 5-15: AIF, MIF and MIF-2 enrichment in the nucleus after MNNG excitotoxicity in HEK-cells.	76
Figure 5-16: Decrease of DSB in Mif KO and Mif-2 KO indicated by the neutral comet assay analysis of the tail moment, and by DSB marker γ H2AX, 53BP1, as well as increase of cell survival after MNNG excitotoxicity.	77
Figure 5-17: Imapris representative of cellular MIF topology in primary neuronal mixed culture.	80
Figure 5-18: Representative of DNA damage related with MIF and MIF deficient cells by the neutral comet assay as well as the Co-staining of MIF , MIF-2 with DSB-marker γ H2AX and 53BP1.	81
Figure 5-19: Representative of DNA (Dapi) and (extracellular) DNA damage, colocalized MIF and MIF-2.....	82
Figure 5-20: Decrease of DSB in Mif KO indicated by the neutral comet assay from brain tissue and immunocytochemistry primary neuronal culture.	83
Figure 5-21: Decrease of DSB in Mif KO transgenic mice indicated by the neutral comet assay of brain tissue from WT, Mif KO, transgenic 5XFAD and 5XFAD/Mif ko mice.	84
Figure 5-22: Targeted MIF gene in rat genome with the help of uniprot tools (https://www.uniprot.org).	86
Figure 5-23: Schematic representation of MIF gene Editing by CRISPR/Cas9 method, modified by using Biorender.....	88
Figure 5-24: Design of Targeted gene side, with the help of the PAM sequence and sgRNA.....	90
Figure 5-25: Representation of CRISPR guide efficiency (Agilent Technologies 5190-7716).....	91
Figure 5-26: Selection of targeted gene side (PCR F2-R7) of F0 and F1 genotyping results.	92
Figure 5-27: Sanger Sequencing results of the founder animals for the transgenic Mif KO rat.	93
Figure 5-28: Illustration of experimental design for rat tissue collection.	94
Figure 5-29: Illustration of experimental design for WT and Mif KO rat tissue collection.	95

Figure 5-30: Western Blot Validation of the CRISPR/Cas9 transgenic WT and Mif KO rat, by AIF and MIF detection, by using brain tissue.96

Figure 6-1: Schematic representation of summarized MIF and MIF function. 113

Abbreviations

°C	Degree Celsius	µg	Microgram
µM	Micromolar		
µm	Micrometer		
µl	Microliter		
3-NP	3-nitropropionic acid		
4-IPP	4-iodo-6-phenylpyrimidine		
Aβ	Amyloid-β		
ACK	Atypical chemokine		
AIF	Apoptosis-inducing factor		
ALS	Amyotrophic lateral sclerosis		
AMPK	AMP-activated protein kinase	APC	Antigen-presenting cell
ApoE	Apolipoprotein e		
APE1	AP endonuclease 1		
APP	Amyloid-Precursor-Protein		
ATP	Adenosine triphosphate		
BBB	Blood-brain barrier		
BD	Bipolar disorder		
Bcl2	B-cell lymphoma 2		
BER	Base excision repair		
BSA	Bovine serum albumin		
cDNA	Complementary DNA		
c-NHEJ	Canonical DNA non-homologous end-joining		
CNS	Central nervous system		
CR	Calorie restriction		
CRISPR	Clustered Regularly Interspaced Short Palindromic Repeats		
DAMPs	Damage-associated molecular patterns		
ddH ₂ O	Double-distilled water		
D-DT	D-Dopachrome tautomerase (MIF-2)		
DDR	DNA damage response mechanism		
DEG	Differential gene expression		
DNA	Deoxyribonucleic acid		
DRG	Dorsal root ganglia		
DSB	Double Strand Break		
EDTA	Ethylene diamine tetraacetic acid		
EdU	5-Ethynyl-2'-deoxyuridine		

e.g.	For example
ERK	Extracellular signal-regulated kinase
FACS	Fluorescence-activated cell sorting
FasL	Fas-Fas ligand
FCS	Fetal calf serum
FSH	Follicle-stimulating hormone
FTD	Frontotemporal dementia
GaAsP	Galliumarsenidphosphid
h	Hour
HCG	Human chorionic gonadotropin
HD	Huntington's disease
HMGB1	High mobility group box protein 1
HO	Hydroxyl radical
H ₂ O ₂	Hydrogen peroxide
HR	Homologous recombination
HRP	Horseradish peroxidase
ICC	Immunocytochemistry staining
IFN- γ	Interferon- γ
IHC	Immunohistochemistry
IL	Interleukin
ISO-1	(S,R)-3-(4-hydroxyphenyl)-4,5-dihydro-5-isoxazole acetic acid methyl ester
IVF	In vitro fertilization
JAB1	JUN activation domain-binding protein 1
JNK	c-Jun <i>N</i> -terminal kinase
lncRNAs	long non-coding RNAs
LPS	Lipopolysaccharide
MACS	Magnetic cell separation
MAPK	Mitogen-activated protein kinase
M-CSF	Macrophage colony-stimulating factor
mDC	Monocyte-derived dendritic cell
MFI	Mean fluorescence intensity
mg	Milligram
mGluR5	Metabotropic type 5 receptor
MHC	Major histocompatibility complex
MIF	Macrophage migration inhibitory factor
min	Minute

ml	Milliliter
mM	Millimolar
mm	Millimeter
MMPs	The matrix metalloproteinases
MNNG	N-methyl-N'-nitro-N-nitrosoguanidine
MRI	Magnetic resonance imaging
MS	Multiple sclerosis
Mt	Mitochondrial
n	Quantity
NDs	Neurodegenerative diseases
Nf- κ B	Nuclear factor 'kappa-light-chain-enhancer' of activated B cells
NFTs	Neurofibrillary tangles
ng	Nanogram
Nlrp3	Pyrin-domain containing 3
nm	Nanometer
NMDA	N-methyl-D-aspartic
ns	Non-significant
N-terminal	Amino-terminal
O (O ₂)	Oxygen
OPA1	Optic atrophy protein-1
OS	Oxidative stress
PAM	Protospacer adjacent motif
PAR	poly-ADP-ribose (trees)
PARP	Poly(ADP-ribose)-Polymerase 1
PBS	Phosphate-buffered saline
PD	Parkinson disease
PET	Positron emission tomography
PFA	Paraformaldehyde
pH	<i>Potentia hydrogenii</i>
PI3K	Phosphoinositide 3-kinase
PNS	Peripheral nervous system
PQC	Protein quality control
PSEN1/2	presenilin 1/2
PTM	Post-translational modifications
RA	Rheumatoid arthritis
RAGE	Receptor of advanced glycation endproducts
RCD	Regulated cell death

RGEN	RNA-Guided Nuclease
RNA	Ribonucleic acid
RNAseq	RNA-sequencing
ROS	Reactive oxygen species
RT	Room temperature
RT-qPCR	Reverse transcription and quantitative real-time PCR
SAR	Structure-activity relationship
SASP	Senescence-associated secretory phenotype
scRNAseq	Single cell RNA-sequencing
SD	Standard deviation
SEB	Staphylococcus aureus enterotoxin B
sec	Second
SEM	Standard error of mean
SNPs	Single nucleotide polymorphisms
SRSRs	Short Regularly Spaced Repeats
SSBs	Single Strand Breaks
SSN	Sequence-specific nucleases
TALENs	Transcription activator-like Effector Nucleases
TCR	T cell receptor gene (TCR)
TH2	T-helper
tMCAo	Temporary occlusion of the middle cerebral artery
TNF- α	Tumor necrosis factor- α
TPOR	Thiol protein oxidoreductase
tracrRNA	The transactivating CRISPR-RNA
TREM2	Triggering receptor, expressed on myeloid cells 2
U	Unit
UBC	Ubiquitin-conjugating enzyme
VCAM-1	Vascular cell adhesion protein-1
WT	Wild type

1. Introduction

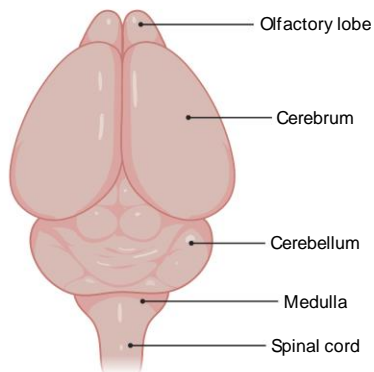
1.1. An overview of brain anatomy and physiology

The brain serves as the central organ of the human body and acts as the control center for the central nervous system (CNS), consisting of a vast number of nerve and glial cells and weighing approximately 1.4 kg. It can be broadly divided into three parts, namely the cerebrum (the largest part), the brain stem, and the cerebellum, as depicted in Figure 1-1¹. The cerebrum connects to the brain stem, which, in turn, links to the spinal cord.

Within the neural structure, the brain stem emerges as a foundational element, comprising the midbrain, medulla oblongata, and pons. Further beneath the expanse of the cerebral cortex, a network of essential structures including the thalamus, hypothalamus, pituitary gland, amygdala, hippocampus, and pineal gland finds its abode. The brain regulates various bodily activities, including the integration and coordination of sensory information and other cognitive functions. The structure known as the corpus callosum serves as the bridge between the brain's left and right hemispheres. Meanwhile, the brain's four primary lobes—the frontal lobe, temporal lobe, parietal lobe, and occipital lobe—assume distinct roles in performing various cognitive functions.

For instance, the frontal lobe controls cognitive functions, memory, and language, while the temporal lobe is responsible for hearing. The parietal lobe controls sensory information such as temperature, taste, and touch. While the mouse model is advantageous for preclinical studies due to its physiological similarity to humans and ease of animal model maintenance and breeding, differences between the two organisms should not be underestimated. Recent studies have revealed significant differences between human and mouse organisms in non-neuronal cells, suggesting that these have undergone significant evolutionary changes, and different expression patterns were shown for the cells of mice and humans. However, viewed as an overall organization, the two models remain comparable. Therefore, the mouse model remains an essential resource for preclinical studies.

Mouse Brain Anatomy



Human Brain Anatomy

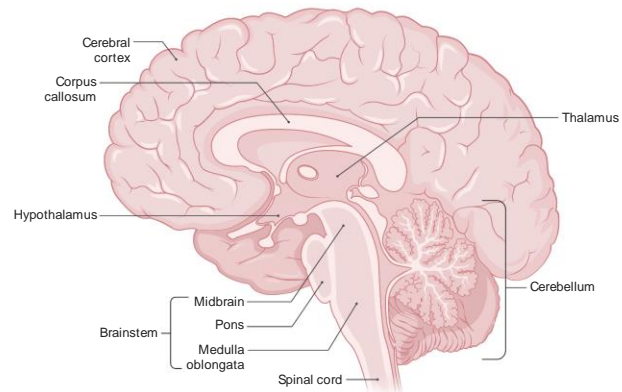


Figure 1-1: Schematic representation of mouse and human brain; modified by using Biorender.

The figure illustrates a side-by-side comparison of the mouse and human brain. On the left side of the panel, a schematic depiction of the mouse brain is presented, highlighting its major areas, including the cerebellum, cerebrum, and olfactory lobe. Similarly, on the right side, the human brain is shown on a side view, emphasizing key brain regions such as the cortex, corpus callosum, and cerebellum.

Please note that the sizes of the brain illustrations have been adjusted for illustrative purposes and do not accurately represent the relative sizes of the mouse and human brains. This schematic serves as a visual aid and should not be used for direct size comparison.

1.1.2 Functions of brain cells

Current estimates suggest that an average, healthy adult brain typically comprises around 86 billion neurons. The interplay between neurons and glial cells is now known to be essential for proper brain function. Neurons receive and transmit electrical or biochemical signals to muscles, other organs in the body, or other neurons. A neuron is composed of the soma, dendrites, and axon. Brain cells such as astrocytes or microglia, along with specific interconnected brain areas, allow us to perceive our environment, control body movements, and engage in understanding, learning, and memory processes². Glial cells build a supportive environment around neurons, with the word "glia" deriving from the Latin word "glue." These cells play a vital role in signal transmission and are necessary for neural functions. Oligodendrocytes, microglia, and astrocytes are different types of glial cells. Oligodendrocytes are known as "axon isolators" and contribute to the accelerated long-distance transmission of electrical signals^{3,4}. Microglia are the resident immune cells of the CNS and communicate with

many other brain cells, including star-shaped astrocytes, which support the blood-brain barrier (BBB)^{5,6}. The BBB plays an important role in the supply of nutrients to the brain. It controls the ion, oxygen and molecular flow between the blood and the brain. Moreover, it acts as a barrier and protects the brain from toxins as well as pathogens. In this way, it also regulates hormone levels and water in the brain environment. However, the selective permeability of the BBB is a major challenge for the delivery of therapeutic drugs. Because drugs or therapeutic antibodies often cannot overcome the BBB or cross it only to a small, unpredictable extent^{7,8}. The brain is an important central point of control. Therefore a functional disorder caused by brain diseases can affect aspects of the entire body. Keeping the brain intact, therefore depends highly on internal and external factors. Damage to different brain areas can be caused by physical and emotional trauma (brain injuries and psychiatric illness), disruption of the blood supply (stroke), or chemical insults that trigger neurotoxicity. That is why brain diseases are divided into two main categories: one is neurodegenerative diseases, and the other is neuropsychiatric diseases. Both forms are complex and therapeutic approaches are still being researched or improved to suppress or treat the symptoms of these diseases. In addition, the next forms must not be left unmentioned, because they also contribute to the pathology of the brain, such as the craniocerebral trauma, brain injury, brain metastases, or stroke.

1.2. The impact of age on cognitive health

With an aging population comes new challenges, as we live longer and are more prone to developing age-related diseases. Neurodegenerative diseases (NDs) are a group of diseases that afflict many individuals in their old age. It is rare to find a healthy brain in the current population of older people, especially in industrialized economies. Two prominent neurodegenerative disorders that have gained significant recognition are Alzheimer's disease (AD) and Parkinson's disease (PD), both of which have an increased risk of development in advanced age (above 65). Studies analyzing the prevalence of AD in relation to age have shown that about 50% of individuals aged ≥ 95 years suffer from AD in the USA. Figure 1-2 illustrates the differences between a healthy brain and an AD brain, examining plaque formation and disintegrated microtubules. Alongside AD, the prevalence of PD and Amyotrophic lateral sclerosis (ALS) also increases within the population of older people^{9,10}.

As a result, an aging population can become a severe socio-economic burden on patients, families, and communities. Therefore, there is an urgent need for novel therapies to better cope with these disorders, as the treatments already on the market

have little to no effect on NDs. Hence, understanding the fundamental mechanisms of aging is one of the new medical and scientific challenges. Examining the role of the aging mechanism will provide a comprehensive overview and insights into the onset and progression of any neurodegenerative disease¹¹. In addition to age, genetics and environmental factors also play a role in the progression of neurodegenerative diseases. Nevertheless, the aging process has the greatest impact on these disorders. Genomic instability or mitochondrial dysfunction in cells, which can result in neurodegeneration, are the hallmarks of aging. To identify abnormal deposits of aggregated proteins, such as amyloid- β (A β) and α -synuclein, in the brain tissue of older patients, imaging technologies such as MRI or PET have been employed. Nevertheless, the extent to which the accumulation of these protein deposits can be linked to cognitive decline remains uncertain, given our current understanding¹²⁻¹⁴.

Studies of early human development have linked early developmental defects to changes in the brain structure. However, cognitive impairment is only evident in later timepoints. Some findings have been made when studying genetics in the early stages of development. As an example, an imaging study using MRI on infants who carry the apolipoprotein E (APOE) ϵ 4 allele, revealed that the white matter myelin water fraction and grey matter volume across different brain regions were different from those of infants who are not carriers of the gene^{15,16}. Besides, also external factors have a critical impact on our neurological health. It has been found that exposure to trauma, drugs or toxins through pollution during development has dire consequences later in life e.g., regarding neuroplasticity^{17,18}. Thus, exposure to harmful environmental factors during life increases the risk of developing neurodegenerative disorders in advanced age. Since many different factors play a role in the pathophysiology of neurodegenerative diseases, an in-depth study is required to fully understand their impacts. As a multipotent protein, the MIF protein family are key players as proinflammatory factors and play an essential role in programmed cell death or in various cell survival-promoting pathways supported by receptor CD74 or other cell survival-promoting pathways nuclease activity that does not promote PARP1-dependent cell death but also potentially DNA repair¹⁹.

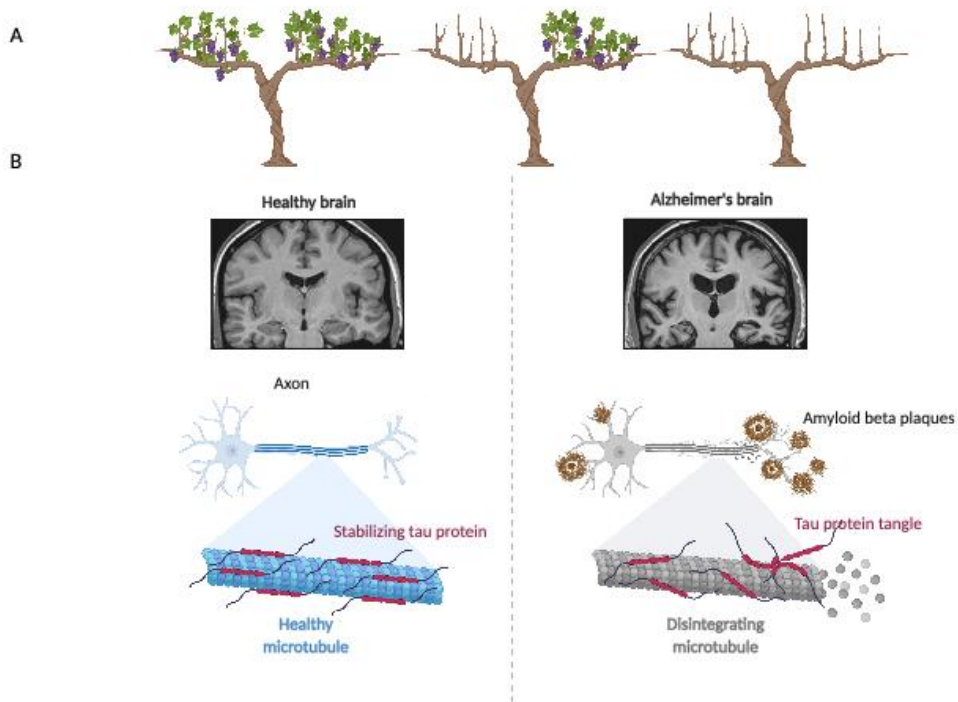


Figure 1-2: Schematic representation of healthy brain and Alzheimer's brain; generated and modified by using Biorender.

The Positron-Emissions-Tomographie (PET) images were obtained from Biorender. The figure presents a visual comparison between a healthy brain and an Alzheimer's brain. The schematic illustration, created using Biorender, incorporates caricatured elements to depict disease progression, represented by the loss of leaves on a tree. On the left side of the figure, the healthy brain is depicted, showing intact axons represented in blue. Conversely, on the right side, the Alzheimer's brain is illustrated, highlighting the presence of amyloid beta plaques in brown and dislocated tau protein forming tangles. These pathological features symbolize the characteristic changes associated with Alzheimer's disease. This sketch aims to emphasize the degradation of cell density and the reduction in intercellular connectivity observed in Alzheimer's disease. It is important to note that the visual changes portrayed in this illustration are for illustrative purposes only and may not precisely represent specific pathological conditions or stages of disease progression.

1.3. Neurodegenerative diseases: mechanisms and implications.

We tend to classify neurodegenerative diseases into distinct clinical units based on the affected regions, pathology, and symptoms. However, repetitive patterns have been observed in neurodegeneration, at the genetic, molecular, and cellular levels, with common key actors. These diseases can be categorized based on the affected cell population and how the pathologies develop, yet the mechanisms underlying selective vulnerability remain poorly understood. At their core, neurodegenerative conditions share a common feature – the decline of functionality in distinct brain areas, resulting in similar clinical features across various disorders. For instance, cognitive impairments are

prevalent in conditions like Alzheimer's disease, vascular dementia, and frontotemporal dementia (FTD). Additionally, motor system dysfunctions manifest in tandem with diseases such as amyotrophic lateral sclerosis (ALS) and Huntington's disease (HD)^{20,21}. Aging significantly increases the risk of developing these disorders, and with a growing population reaching higher ages, the prevalence of these disorders is increasing concurrently with the accumulation of environmental factors.

It is crucial to investigate the pathological mechanisms of neurodegenerative diseases in detail due to the increasing prevalence of these disorders in aging populations. This requires a thorough understanding of the pathways involved in the pathophysiology, as well as the consequences of disruptions to these pathways. While neuronal loss has traditionally been the main characteristic of neurodegenerative diseases, this definition fails to capture the complexity of these disorders, given the varied tasks of different cell types in the brain, including neurons and astrocytes.

Accumulation of unfolded or misfolded proteins is a known hallmark of neurodegenerative diseases, with the formation of neurofibrillary tangles and plaques leading to neuronal cytotoxicity. Thus, understanding the mechanisms underlying the building and processing of these protein aggregates is critical for developing effective therapies. However, while specific protein aggregates have been identified in different neurodegenerative diseases (e.g. AD, PD, HD, and ALS), no potent treatment currently exists to tackle them effectively²²⁻²⁴.

1.3.1. Inflammasomes and their impact on neurodegenerative diseases

The NLRP3 inflammasome is activated in microglia in response to defective protein or beta-amyloid aggregates. Other inflammasomes, such as pyrin-domain containing 3 (Nlrp3), also play an essential role in microglia, astrocytes, or neurons^{25,26}. It is believed that the activation and subsequent cleavage of caspase 1 promotes the development of Alzheimer's disease²⁷. When developing therapies against neurodegeneration, attention is also given to environmental factors and potential risk areas for epigenetic changes. For instance, an increased expression of HDAC6, a class II histone deacetylase, has been found in Alzheimer's patients, particularly in the hippocampal region, where it colocalizes with tau proteins associated with tau phosphorylation. Reducing the HDAC6 level has been shown to improve perception^{28,29}. Abnormalities in metabolic processes are frequently observed in neurodegenerative diseases. It is currently believed that

metabolic disorders may contribute to the development of neurodegenerative diseases, although it remains uncertain whether these disorders are a cause or a consequence of neurodegeneration. A better understanding of the affected metabolic processes during disease progression is therefore essential. Proteins play a critical role in glucose metabolism, cell growth, survival, and migration. Aβ is thought to promote tau hyperphosphorylation and is involved in the pathogenesis of Alzheimer's disease. The presence of the apolipoprotein E4 (APOE4) allele is associated with early-onset forms of Parkinson's disease¹⁵. Apolipoproteins act as transporters for lipids, and cholesterol and are produced in the liver and brain. ApoE4 is an essential factor in neuronal plasticity and synaptogenesis, and carriers of the APOE4 allele are thought to have a higher risk of developing Alzheimer's disease. The mammalian target of rapamycin (mTOR) is also related to Alzheimer's disease. It belongs to the insulin and PI3K signaling pathways and is an essential player within the mTORC complex. Cell death is a complex process that can occur due to apoptosis, mitophagy, necroptosis, and autophagy³⁰. Mutations that alter the cell death pathways can contribute to uncontrolled neuronal cell death (necrosis) or promote the apoptosis mechanism, thereby contributing to the progression of neurodegenerative diseases. Other mechanisms that promote neuronal cell death are mitochondrial dysfunction, dysregulation of autophagy, or activation of the necrosome by stress or inflammation. Herein, PARP is a critical player in DNA repair, cell death, chromatin function, and genomic stability^{31,32}. PARP is activated in addition to ATM or p53 after the detection of DNA damage. If caspase 3 is cleaved between Asp214 and Gly215, the N-terminally cleaved fragment's DNA repair enzyme is inhibited^{33,34}. This drives neurons to apoptosis. The characterization of PARP-deficient mouse models has revealed the involvement of PARP in the pathogenesis of stroke and Parkinson's disease, thereby creating new opportunities for targeted treatments. Cellular stress, including DNA damage or oxidative stress, can cause an irreversible growth blockage called "cellular senescence"^{35,36}.

Neurodegenerative diseases can be detected by various senescence markers. Namely, one example of many: In tau pathology, p16 (Ink4a) accumulates in senescent astrocytes and microglia. P16 (Ink4a) is a tumor suppressor; it is an INK4 family member of cyclin-dependent kinase inhibitors. It affects the cell cycle in the G1 phase by stopping its progression^{37,38}. It is a critical player in responding to DNA damage signals caused by telomere dysfunction^{39,40}. In connection with amyloid plaque pathology, the accumulation of p16 and p27 is also observed. This allows senescent cells to be recognized and removed by immune cells^{41,42}. Stem cells in the bone marrow supply the body with important immune cells. These include neutrophils, lymphocytes such as B cells, and T cells. But also, monocytes, macrophages, and dendritic cells. Tumor necrosis factor

(TNF- α) is a cytokine, which plays a crucial role in most inflammatory mechanisms. It activates different types of immune cells. In addition, it can promote cell differentiation and the release of other cytokines. Dysregulation of TNF- α is shown in Alzheimer's disease and Parkinson's disease; patients' brain tissue is implicated in an increased level of TNF- α ^{43,44}.

1.3.2. Cellular diversity in neurodegenerative

The brain is composed of various brain areas, each of which contains different cell types, including neurons, microglia, oligodendrocytes, and astrocytes, which take on different functions. Cell-specific antibodies can be used as protein biomarkers to localize target cells.

Neurons are key components of the peripheral sensory and motor systems, as well as the spinal cord. They are electrically excitable and highly specialized, processing information quickly. Neurons transmit electrical signals and neurotransmitters across synapses and can be expressed in various morphologies in the nervous system, with signals mostly received at the cell body or dendrites and sent along the axon. To gain a broader insight into neurodegenerative diseases, non-cellular autonomous mechanisms that cause neuronal loss are also being studied, and the role of astrocytes is being increasingly recognized.

Reactive astrocytes are characterized by an increase in glial fibrillary acid protein (GFAP), a standard marker. This increase is distinctive in many CNS diseases but is not always proportional to the severity of disease or injury due to differences in astrocyte region and content. A decrease in GFAP has been reported in the spinal cord of the amyotrophic lateral sclerosis (ALS) mouse model, possibly due to caspase 3 cleavage⁴⁵. Changes in morphology, physiology, or transcription regulation can lead to the loss or upregulation of homeostatic functions, resulting in an exchange of functions. However, a connection between AIF-induced cell death and downregulation of GFAP is also possible⁴⁶. Astrocytes play a pivotal role in the degeneration of motor neurons in ALS. Concurrently, previous investigations have indicated that astrocytes undergo transcriptional alterations in response to the influences and the unique microenvironment within the affected central nervous system. This is reflected in their morphology and reactivity. These reactivated astrocytes are in turn divided into two different groups: A1 astrocytes, which are classified as neurotoxic and A2 astrocytes, classified as neuroprotective. However, only a rough classification is shown here because by continuing the scientific analyses, especially in the single-cell or single-nucleus transcriptome analyses, new disease-specific astrocyte clusters are discovered. Protein

quality control (PQC) systems are utilized to monitor protein folding quality, thus limiting the toxicity of misfolded proteins within the cell. Chaperones play a crucial role in the refolding of misfolded proteins or their breakdown to minimize toxicity and the accumulation of misfolded proteins in the cell. This process is well documented in literature⁴⁷⁻⁴⁹.

1.4. The biology of aging: mechanisms and implications

Aging is an irreversible process characterized by physical changes. The main features of aging include genomic instability, epigenetic changes, telomere shortening, and loss of proteostasis. In contrast, mitochondrial dysfunction, cellular senescence, and deregulated nutrient perception are antagonistic elements. Initially, these responses cause damage, but over time, they can become deleterious themselves. The accumulation of damage induced by these hallmarks results in the dysfunction associated with aging. The brain is not only one of the essential organs but also sensitive to the effects of aging due to its composition of primarily postmitotic cells. It is known that postmitotic cells, such as neurons, are especially vulnerable to DNA damage⁵⁰⁻⁵². Therefore, the brain may play an important role in the etiology of age-associated neurodegenerative diseases.

1.4.1. Genomic instability and DNA damage

One of the primary hallmarks of aging is genomic instability and DNA damage. Several types of DNA damage are counted, such as DNA single-strand breaks, double-strand breaks, or insertions and deletions. Besides the DNA damage, it caused endogenous reactive oxygen species (ROS). This can promote neurodegenerative diseases or cancer⁵³. As a response to DNA damage, DNA repair pathways are activated. Among others, base excision repair (BER), nucleotide excision repair (NER), mismatch repair, DNA double-strand break repair (DSBR), and direct reversal are counted⁵⁴. Oxidative base damage and single-strand breaks is primarily repaired by the BER mechanism. Dysfunction of the BER pathway genes promotes the risk of neurodegeneration, next to

aging. The BER is composed of two BER sub pathways: a short-patch and a long-patch. The repair mechanism involves a DNA glycosylase, recognizing the damaged DNA base and removing it by leaving a basic site. One of the main, and especially for this work, important results is the activation of PARP1 by DNA damage. PARP1 then increases PARylation; PAR polymers are promoted to be formed. PARP1 activation undergoes a NAD⁺ depletion. However, also senescence and inflammation are factors, which are promoted by DNA damage^{55,56}.

1.4.2. Altered intercellular communication and immune function

The immune system has a significant role in brain development. Nonetheless, as individuals age, alterations within both the nervous and immune systems can lead to a loss of immune response regulation in the brain, potentially fostering long-term neurodegenerative processes. Changes in intercellular communication and immune function can also contribute to neurodegeneration. In addition, dysfunctional hormone levels, including among other leptin, or insulin, can cause neuronal damage. Therefore, comprehending the involvement of innate and adaptive immune responses in disease pathogenesis is imperative. Recent research has unveiled that neurodegenerative diseases' pathological mechanisms encompass microglia and other supportive glial cells, including astrocytes and oligodendrocytes. In addition, T cells play a pivotal role in preserving the peripheral immune equilibrium and the central nervous system's immune privilege. Maintaining effective cellular crosstalk is essential for proper immune system function and the prevention of neurodegenerative diseases. The changes in immune responses associated with aging and the heightened susceptibility to neurodegenerative diseases offer valuable insights into communication processes. During aging process, inflammation also becomes upregulated. Although low levels of inflammation have a beneficial potential, uncontrolled inflammation can cause age- chronic neurodegenerative diseases, as well as, AD or PD^{57,58}. Studies of expression levels in aging human brains have indicated the importance of inflammation, with their main actors in neurodegenerative diseases. In the statute of Chronic inflammation, microglia are activated and pro-inflammatory mediators such as cytokines are increased as well as oxidative stress. All these factors are associated with age-related neurodegenerative processes. This is consequential for cell-type-specific diseases of the brain. This mechanism is evident in the system level of the brain. This paper specifically highlights the fact that, moonlight proteins with multipotent functions play a significant role. Therefore, understanding the various mechanisms of moonlight proteins does not have

to be researched in tissue, brain area, or cell type. Even their potential topology-driven mechanism within a cell needs to be understood. Since research at the cell organ level is not possible in human experiments, analysis depends on animal models, cell lines, or even primary cells. Over the years, researchers have had new technologies available to modify these research objects genetically. In this paper, genetically modified animal models by CRISPR / Cas are being mainly dealt with. Furthermore, the focus is on primary neuronal mixed culture as well as on primary astrocyte culture. The constantly new technological possibilities and the research results discovered through them give a closer and better look at the clinical-pathological description of, for example, degenerative diseases, cancer diseases, and psychological disorders. The cascade of activated microglia elicits ROS. Dysfunctional mitochondria are known to lead to ROS production, and this again results in an NF- κ B signaling increase. In addition, aging processes promote NLRP3 inflammasomes, which leads to IL-1 β release in the brain. The increase of IL-1 β via NLRP3 inflammasome secretion is activated in Alzheimer's disease by Aggregated A β fibrils, in Parkinson's disease by mutant α -synuclein, as well as the superoxide dismutase 1 (SOD1) mutant protein SOD1G93A in ALS^{20,59,60}. Thus, protein aggregation might be induced by exacerbation of A β deposition in AD or α -synuclein might be induced in PD by Inflammation mechanisms. In this way, promoted inflammation positively supports the accumulation of unfolded or misfolded proteins in neurodegenerative diseases. However, as mentioned before, other factors are known to contribute to the inflammation mechanism and, therefore, to the pathogenesis of neurodegenerative disorders, such as the defective proteasome, cellular senescence, oxidative DNA damage, DNA repair dysfunction, and decreased innate immunity and adaptive immune system responses as well as toxic environmental insults. For decades there has been continued therapeutic research in finding new treatments to combat these inflammatory processes, which our aging society is facing. This field is still not redundant.

Therefore, it is necessary to investigate the neuroinflammatory processes further with a focus on anti-inflammatory drugs. The challenge is still to develop drugs that can cross the blood-brain barrier.

1.4.3. The Role of oxidative stress and cell death

Free radicals are being produced by the normal aerobic cellular metabolism. To prevent the accumulation of these harmful ROS, the body has several mechanisms to build antioxidants. However due to aging processes and environmental influences, the

defense mechanism of antioxidants can be weakened, and therefore lead to cell loss, and neurodegeneration.

Neuronal and other cell type loss or sensory dysfunction are key factors in neurodegenerative diseases. Various environmental and genetic influences, including oxidative stress (OS) are among the many causes of free radical production, and this too contributes to neurodegeneration. The human body needs Oxygen to survive, however an imbalanced metabolism which can result in an increase in reactive oxygen species (ROS), could lead to a variety of disorders such as Alzheimer's disease, and other neural disorders associated with aging. In Neurodegenerative diseases, it is indicated that brain cells as well as cells from the spinal cord lose their functionality (ataxia) or can lead to a sensory dysfunction (dementia).

As mentioned before, the free radicals mediated ROS, and activated proteins, which resulted in DNA dysfunction and inflammation. These can also contribute to tissue damage and subsequent cellular apoptosis. Alongside diet, therapeutic recourses are also becoming interesting as a source of antioxidants. Besides there is evidence that, antioxidant therapy is beneficial for chelating free radicals and ROS, to inhibit neuronal degeneration⁶¹.

In relation to Alzheimer's disease (AD), it is known that Mitochondrial (Mt) dysfunctions and excitotoxicity can lead to apoptosis as a pathological cause of aging.

1.5. Protein aggregation

Biomolecular aggregates can lead to the development of Biopolymers. In cell biology condensates have important implications for cell organization and cell physiology. The build-up of condensate plays an important role, and it is strictly controlled in the intracellular environment. If this regulation is disturbed, it leads to protein misfolding and thus ultimately to unwanted aggregation, which is regarded as one of the causes of age-related diseases. The mechanisms, and regulations for the build-up or dissolution of condensate are very complex and contribute to aging and the diseases that result from it. Dysfunction of the regulatory factors results in: the reduction in homeostasis; the increase in cellular stress and thus also ROS production. It also leads to the decrease in protein quality control which in turn results in disease-specific aggregations. In the cytosol of the cells, there are numerous polymers (including nucleic acids and cytoskeleton). Although the protein density in the cytosol is quite high, under normal physiological conditions, they do not form any insoluble protein aggregates due to undesired interactions between the molecules. Since proteins are supposed to interact

with each other, to form signal cascades, this interaction must be well regulated. The cytosol is not a uniformly homogeneous substance but rather houses organized biomolecular condensates, which are formed with the help of mechanisms of phase separation. Condensate-forming proteins are segments or domains that are intrinsically disordered. This allows dynamic interaction networks to be formed and aggregates to be built up. However, this is exactly the function that promotes the accumulation of incorrect folds and thus unwanted aggregation. In aging organisms, there is an increased preference for misfolded proteins. As a result, the cell loses the ability to maintain homeostasis. Researchers see a close relationship between condensation-forming proteins and age-related diseases, such as neurodegenerative diseases and cancer. Research has made significant progress in understanding the physical, chemical, cellular, and regulatory mechanisms of aggregate formation. Post-translational mechanisms or the protein quality control machinery (PQC) regulate the amount and quality of aggregate formation with the help of chaperones. Nowadays, researchers are wondering how the PQC machinery regulates the integrity of condensates; how the various environmental influences affect the formation of aggregates, and how aging affects the systems. Of course, the molecular mechanisms are closely monitored in order to secure functional protein aggregates and an intact PQC system⁶². These results could help to develop therapeutic approaches. Newly synthesized proteins fold into three-dimensional structures under normal conditions and can also form protein complexes with one another. The mechanism of the folding process is fragile and sometimes undermines cellular and physical stress, which in turn leads to unfolding and misfolding. Hence, maintaining optimal conditions is important. Factors such as thermodynamic conditions influence the quality of protein folding. Oxidative stress can cause misfolding or unfolding. The resulting non-native structures can form fibrils. Amyloid fibrils are formed within Alzheimer's disease and consist of 3–6 filaments¹². Covalent and non-covalent interactions can promote the formation of clusters and thereby also inhibit biological activity. Since the interaction between hydrophobic areas acts in aggregates, it can lead to insoluble. The van der Waals forces or electrostatic interactions are required for self-aggregation and belong to the non-covalent interactions. Covalent aggregates can be formed by disulfide bridges over their free thiol groups. Proteins bound via disulfide bridges form aggregated via β -elimination⁶³. Aggregates are clustered in different groups, irreversible or reversible; the non-covalently or covalently bound and the group of smaller soluble aggregates. Neurodegenerative diseases can be a consequence of protein aggregation.

1.6. Neuroinflammation and neurodegeneration

Genetic studies, in addition to clinical studies, have revealed that immunological mechanisms underlie many neurodegenerative diseases. Alzheimer's disease is an example where neuroinflammatory processes play a crucial role in disease progression. Therefore, understanding the neuroimmune interactions of the CNS is crucial. Healthy donors' microglia show expression levels of CX3CR1 or P2RY12, while patients with MS exhibit a downregulated signature⁶⁴⁻⁶⁶. Single-cell RNA- and single-nucleus RNA sequencing have revealed that antigen presentation signature genes were increased in MS patients, leading to the conclusion that autoreactive T cells play a critical role in MS pathology. Additionally, an upregulation of galectin-1 was observed, which is known to weaken the cytotoxic CD8+ T-cell function. Recent studies have utilized transposase-accessible chromatin and chromatin immunoprecipitation followed by sequencing (ChIP-seq) to combine with single-nucleus sorting utilizing sequencing (ATAC-seq). The objective is to understand single nucleotide polymorphisms (SNPs) associated with resistance or susceptibility to disease by localizing promoters as proximal and distal enhancers. These and other studies have shown that SNPs are associated with psychiatric disorders, and those associated with Alzheimer's disease are primarily found in microglia enhancers. Overall, technologies like scRNA-seq and snRNA-seq provide researchers with new possibilities to depict the brain in a single-cell resolution and provide a multidimensional molecular description of the differentiation between control groups and the disease. These technologies justify an expansion into human studies to investigate the transcriptomic changes during pathogenesis. The results obtained can be validated through proteome analysis, leading to the identification of new diagnostic and prognostic biomarkers. Moreover, new molecular targets for a therapeutic approach could also be identified. To sum up, while modest levels of inflammation can be beneficial, excessive or prolonged inflammation is detrimental and plays a role in the development of age-related chronic neurodegenerative conditions like Alzheimer's disease^{67,68}.

1.7. Genomic damage and neurodegeneration

As mentioned initially, neurodegenerative illnesses represent an ever more significant challenge in an aging society. Due to the complex mechanisms to which it is subjected, it is necessary to develop therapeutic strategies. In order to study the associated

biological mechanisms, it is inevitable to have a detailed understanding of the disease and its various forms. However, since this is closely connected to a detailed understanding of the disease states, studying the associated biological mechanisms is inevitable. Studies show that genomic instability is a significant challenge in neurodegenerative diseases. The role of DNA double-strand breaks (DSBs) is the main focus of studies. DNA double-strand breaks (DSBs) have been implicated in the progression of neuronal loss. The accumulation of DNA double-strand breaks within the neuronal cells poses a problem since neurons are not proliferative cell types and show a high metabolic activity, which means they are more susceptible to exposure. However, research is still being conducted into whether DNA damage is the main contributor to cell death and thus neuronal loss. Neurons with a lack of proliferation and at the same time a high metabolic activity are naturally susceptible to DNA damage. Various groups are listed within the DNA damage, one of them being the DSBs, which are more harmful. These can activate cell death mechanisms. In order to counteract this, the cell has developed various types of repair mechanisms, which will be discussed in more detail at a later point in time. As already mentioned, the progression of neurodegenerative diseases causes an increasing deterioration in brain function. Researchers have found that an imbalance between DNA damage and the associated repair mechanisms promotes neuronal damage. DNA is exposed to several harmful factors, including intracellular metabolism, physiological neuronal activity, transcription, replication, and genotoxic agents from the environment. The accumulation of DNA damage is a common phenotype in AD, PD, and ALS patients⁶⁹. Under normal physiological conditions, up to 10,000 single-stranded DNA breaks and 10 to 50 double-stranded DNA breaks occur nearly every day. If there is an accumulation of unrepaired DSBs in proliferating cells, the cell cycle can be paused until cell death mechanisms are activated. Since DSBs increase the likelihood of mutations and deletions and even lead to chromosomal translocations, it is a risk factor, especially for non-proliferating cells. In contrast to proliferating cells, DSBs can be repaired with the help of sister chromatids through homologous recombination (HR), but this does not apply to postmitotic neurons. We note that Neurons use the non-homologous end connection (NHEJ), which is, however, more prone to errors⁷⁰. Therefore, DSBs represent a major risk for neural function. In addition to homologous recombination, the NHEJ also represents a way of repairing DSBs. DNA is an important but complex molecule, so it is essential to be precise and cautious in correcting errors. Such errors can lead to long-term irreversible damage, which can include defective RNA and protein products. As a result, an accumulation of unrepaired or incorrectly repaired DSBs in neurons leads to a loss of genome integrity. The repair mechanisms, chromatin remodeling or inflammation mechanisms also play an important

role. These ultimately decide between apoptosis or survival. If DSBs are formed, post-translational modification is promoted, and proteins are mobilized at broken DNA ends and the surrounding chromatin. The phosphorylation of the histone H2A.X can be observed as an example of histone modification. This belongs to the subfamily of the histone H2A. The H2Ax for example is phosphorylated instead of serine 139, resulting in γ H2AX. For repair mechanisms like homologous recombination (HR) and the non-homologous end connection (NHEJ), γ H2Ax is a point of control. So, a successful repair, in turn, restrains effector proteins, which also include 53BP1.

A stable function of the DNA Damage Response (DDR) is important during neural development but also in the adult stage⁷¹. The recent γ H2Ax domains can spread over the neighboring chromatin along the chromosome. The γ H2Ax domains have various mechanisms of damage reactions, repression of transcription, and of the promotion of GDR mechanisms, forming a DSB location. Therefore, for genome stability and thus for maintaining cell function, it is essential to balance the GDR mechanisms and the accumulation of DSBs. Further repair mechanisms are activated, including the MRN complex. This assures that the DSBs end up close to each other. Further, ATMs are activated, and H2AX histones are phosphorylated. γ H2AX foci arise⁷². These are also identified in this paper with the help of immunofluorescence-based assays, and thus the possibility of analysis is given. The activated ATM monomer, in turn, phosphorylates p53, which promotes apoptosis or cell cycle arrest. Most DSBs are repaired by c-NHEJ in both phases of the cell cycle⁷³. Other DSBs, in the G2 phase via HR. With the help of mitogens, the S-phase can be initiated in the cell. These mitogenic factors can be growth factors, binding cell surface receptors and thereby inducing intracellular signaling. Among other things, the mitogen-activated protein kinase (MAPK) pathway is activated. After the activation of the subsequent transcription factor (e.g., c-Myc), the cell enters the controlled and S-phase⁷⁴. However, the entry into the S-phase can be inhibited by DNA damage. As mentioned above, these can accumulate through various triggers, including oxygen species (ROS). In addition to SSBs and DSBs, ROS can drive the ATM or p53 signal cascade, which suppresses entry into the S phase of the cell⁷⁵.

Incorrect chromosome replication leads to considerable damage and even chromosomal abnormalities in cancer cells. Endogenous and exogenous events pose a risk to genome integrity and, thus, also to DNA replication. Since DNA replication is a complex and important mechanism, many control checkpoints are switched on. This is because a blocked replication fork and a disruption in the restart of replication can lead to an accumulation of mutations.

1.8. The impact of cytokines on biological processes

Research results, from the last decade showed that cytokines play an important role in the communication between immune cells and signaling to the brain. Cytokine activity can cause neurochemical, neuroimmune, or behavioral changes, among other things. Cytokines can play important roles in the pathophysiology of some psychiatric disorders, including depression, schizophrenia, and Alzheimer's disease. Therefore, it is essential to examine the effect of cytokines in the central nervous system on their specific mechanism leading to patients' "disease behavior", especially with severe infections, cancer, or neuropsychiatric side effects after interferon treatment. This is because the improved understanding of the cytokine mechanisms involved in various brain activities can exclude specific psychobiological mechanisms of neurodegenerative diseases and thus approaches for treatment interventions. Research into cytokines brings two scientific areas together: neuroscience, and immunology. The cytokines are known to act as chemical messengers between the immune cells. Therefore, one of their key roles is mediating inflammatory and immune responses⁷⁶. The brain also acts as a control center for the body. Information about infections and injuries that reach the brain is processed, and metabolic and behavioral pathways are set in motion. These mechanisms, in turn, serve to maintain homeostasis or, in the event of an unbalance, restore the healthy state. The cytokines are thought to be immune system hormones that regulate communication between cells. The comparison to the hormones is also reinforced by the fact that their properties are comparable to those of the classic hormones of the endocrine system. The induction of early cytokines controls the expression of later cytokines. Cytokines are in close interaction with their functional receptor. This enables the physiological reaction to be activated and regulated by the cytokines⁷⁷. Cytokine receptors can occur in soluble form but also as membrane-anchored receptors. However, a complex can also arise between the soluble form of the receptor and the cytokine, which in turn increases the biological activity of the cytokine. This was observed when IL-6 binds to its soluble receptor. Which, being complex, increases the activity of IL-6. The cytokines were mainly named after their biological activity. Cytokines are pleiotropic proteins because they are usually involved in several physical activities. Research projects often work on a protein but investigate different functions of the cytokines. After successful gene sequencing, interleukin numbers are assigned to cytokines, should this be possible, and they are not seen as part of another superfamily. Many cytokines (e.g., TNF, interferon, and IL-1) come in varying forms; for this reason, they are usually given a suffix from the Greek alphabet (α , β , γ). Cytokines are structurally homologous to one another to a limited extent, but they bind to the same

surface receptors and cause similar biological reactions. Cytokines can also be grouped into proinflammatory and anti-inflammatory cytokines. The cytokines to which proinflammatory function is attributed include IL-1, IL-6, and TNF. These increase the immune response, primarily to eliminate pathogens and dissolve a cluster of inflammation more quickly³³. Another example of a pleiotropic protein, which will be discussed in more detail in the following chapter, is the macrophage migration inhibitory factor (MIF). This is also assigned a function comparable to that of the proinflammatory cytokines. Cytokines can lead to proinflammatory effects in various ways. Cells can be activated, and the metabolic rate or the temperature regulation can also be changed. These changes aim to increase inflammatory responses.

1.9. The role of cytokines and chemokines in the brain

The effects of cytokines in the brain can unfold in multiple ways. The cytokine signal transmission in the brain can be mediated by passive transport to circumventricular points where the blood-brain barrier is missing^{78,79}. The cytokines can also bind to the cerebral vascular endothelium, which enables the formation of secondary messenger substances. Cytokines can also stimulate the peripheral afferent nerve endings, where they are released in turn. Finally, with the help of carrier-mediated transport, cytokines can also enter the brain via the blood-brain barrier. All these mechanisms provide a means of overcoming the blood-brain barrier. Cytokines are also synthesized and released in the central nervous system. Furthermore, astrocytes and also microglia can be secreted. The cytokines in the brain regulate various brain activities, including immunological, neurochemical, and neuroendocrine activities. The balance and feedback loops of cytokines are an important part of the homeostatic mechanism. Dysfunction can lead to severe illnesses such as infections, cancer, or autoimmune diseases. Some studies focus on the influence of physical stress as a result of infection on cytokine production, and psychological stress factors on cytokine secretion are also examined. Because cytokines are influenced by stress and, at the same time, are associated with neurotransmitters, studies repeatedly bring cytokines into the focus of psychiatric diseases.

In research groups focusing on psychiatric diseases, specific cytokine abnormalities were observed in schizophrenia patients. In Alzheimer's disease, inflammatory and immune mechanisms are at the center of research. It is assumed that it is precisely the acute phase proteins that are mediated by cytokines. Higher levels of IL-1, IL-6, and TNF were observed in Alzheimer's patients⁸⁰

1.10. Macrophage migration inhibitory factor (MIF)

The naming of MIF basically steers in the wrong direction, which goes back to the late 1950s when MIF was originally identified as a T cell-derived mediator that inhibits random movement of macrophages^{81,82}. In 1966, MIF was simultaneously characterized by Bloom and Bennet and by David as a soluble factor that is produced by activated T lymphocytes^{83,84}. In the years following, MIF was also identified as a key player in general macrophage activation, which includes the spreading of phagocytosis and also enhancing tumoricidal activity^{85,86}.

However, one should not neglect the fact that the source of the MIF in these studies originate from the conditioned media of activated T cells. Additionally, other mediators, such as interleukin (IL)-4 and interferon (IFN)-gamma, influence the inhibitory effect on the migration of macrophages^{87,88}. Progress in MIF studies reached new heights when a cDNA encoding human MIF was isolated from transfected COS-1 cells⁸⁹. Through this advancement, the biological, biochemical and biophysical properties of human MIF were able to be studied. All of this laid the foundation for Prof. Jürgen Bernhagen, who was the first to clone and purify murine MIF released by the anterior pituitary gland after the administration of the endotoxin LPS⁹⁰. Just a year later, studies found that MIF is also produced by activated macrophages. Not only were macrophages an important target, but they were now also a source of MIF proteins *in vivo*^{90,91}. In 1999, an MIF knockout mouse model was established, while studying the biological role of MIF as a pleiotropic cytokine during sepsis⁹². Just a few years later, the now well-known receptors were found, such as the cell surface receptor CD74^{93,94}, and the chemokine receptors CXCR2 and CXCR4. Having a more or less complete picture of the MIF family members, formed the understanding that MIF has an important role not only in inflammatory diseases but also in other disease pathologies^{95,96}.

1.11. Structure and function of MIF

The cytokine Macrophage migration inhibitory factor (MIF) is a small Protein of about 12,5 kDa. RNA expression of MIF has been detected in all human tissue. The protein is mostly expressed in the cytoplasm including immune cells. Additionally, in most cases the RNA expressions are not different from the protein expression levels, except for some tissue. There are few exceptions, these include blood and the muscle tissue.

The expression of MIF has been demonstrated both in embryonic^{97,98} stages and in adults⁹⁹.

Thierry Roger indicated a 10-fold increase of expression levels for migration inhibitory factor (MIF) during neonatal stage compared with adults. It is believed that MIF in the neonatal stage is counter regulating adenosine and prostaglandin E2-mediated immunosuppression. However, it is also known, that already existing infection in the neonatal stage has a further negative effect on the course of the disease^{100,101}. This reveals the unique role of MIF in the regulation of neonatal innate immune response. It is partly protective while reducing susceptibility to infection during the neonatal period and MIF is partly identified to promote uncontrolled inflammation during sepsis which may lead to negative results¹⁰⁰. The MIF expression levels differ not only between adult and neonates or cell types it also changes within the disease course¹⁰². Expression levels of MIF and their known functionally-related genes, D-DT, CD74, CD44, CXCR2 and CXCR4 are not only increases in atherosclerosis^{103,104} related diseases but in particular they play critical roles in the carcinogenesis such as glioblastoma¹⁰⁵⁻¹⁰⁷. In the present studies, MIF and its family relevant proteins are more and more in the focus of Alzheimer's disease¹⁰⁸⁻¹¹⁰. The human MIF gene consists of 115 amino acids, with three short exons of 107, 172 and 66 base pairs and two introns of 188 and 94 base pairs. Monomeric MIF has a molecular weight of 12,5 kDa⁸⁹.

The trimeric arrangement of MIF three identical monomers was reported in 1996¹¹¹. MIF is highly conserved across species^{112,113}. Within mammalian (human, mouse and rat) MIF have a homology around 90%. As a result, one can assume that MIF might have an important biological function. Every single monomer contains two anti-parallel alpha helices, which are packed against a four stranded beta sheet. In addition, each monomer contains two beta strands that interact with the beta sheets of adjacent subunits($\beta\alpha\beta\beta\alpha\beta\beta$). This complex forms the interface between the monomers. All three beta sheets are arranged in a cylinder that provides a solvent-accessible channel that runs through the center of the protein along a molecular triple axis. The important structural elements of the MIF monomer are presented by the N-like loop and the pseudo (E) LR motif. The (E) LR motif is very similar to the chemokine's ELR motif. The only difference is that the amino acid glutamic acid has been replaced by aspartic acid. Compared to classical chemokines, MIF does not have an N-terminal signal sequence that is required for the classical secretory pathway via the endoplasmic reticulum and the Golgi apparatus. Instead, a so-called "non-classical export pathway" secretion occurred in response to various stimuli, such as hypoxia or bacterial lipopolysaccharides (LPS)^{114,115}.

Only recently a new role was discovered for MIF, in addition to the already familiar ones. MIF was found to be the unknown nuclease of the AIF dependent apoptosis pathways during a screen for AIF interacting proteins. MIF has been classified as a member of the

PD-D/E(x)K similar to EcoRI, EcoRV, ExoIII and PvuII^{116,117}. This new finding will be the main focus of this thesis^{118,119}.

1.12. D-Dopachrome tautomerase (D-DT/MIF-2)

Identifying the surface receptor CD74, led to the discovery of D-dopachrome tautomerase (D-DT) or MIF-2. Several reports showed that the deletion of MIF still generated similar phenotypes when compared to the immunoneutralization or genetic deletion of MIF. The measured effect is about 2-fold more pronounced in receptor-deficient cells. Due to these observations, a second receptor-ligand interaction pair was proposed⁹⁵. D-dopachrome tautomerase (D-DT) was the ligand. It appeared for the first time in literature in 1993 as an enzyme detected in the cytoplasm of human melanoma cells, human liver cells and the cells of rat organs, which converts *D*-dopachrome to 5,6-dihydroxyindole¹²⁰. It is also called MIF-2, because it was found to be a homolog of MIF in the mammalian genome. MIF-2 also shares three-dimensional homology with MIF¹²¹. Since then, the enzymatic activity of MIF-2 was detected in the epidermis of the skin, and its level was found to increase after UV irradiation¹²². Additionally, a critical role for MIF-2 and CD74 in kidney disease has been detected¹²³. D-dopachrome tautomerase (D-DT) also called MIF-2, has come to the fore after it was discovered as the second CD74 receptor ligand. From this time forward MIF-2 has been described as the newly cytokine and a member of the macrophage MIF protein superfamily. It is known that MIF-2 binds to the MIF cell surface receptor complex CD74 / CD44 with a very high affinity^{124,125}. As already mentioned at the beginning, in the human genome the gene for MIF-2, is located in close proximity (~80 kb apart) to chromosome 22. It is hypothesized that an early DNA duplication event played a pivotal role in shaping the current gene structure. This hypothesis gains support from the observation that the human and mouse MIF, along with MIF-2, are closely associated with two theta-class glutathione S-transferase genes. In addition, MIF-2 also consists of three exons (exon 1: 108 bp, exon 2: 176 bp and exon 3: 70 bp) merely the non-coding intron has different lengths (intron 1: 363 bp, intron 2: 2144 bp)^{126,127}. In addition, that triggers similar cell signal and effector functions. New findings show that the MIF and MIF-2 work cooperatively. A neutralization or systemic knockout of MIF-2 in vivo significantly reduces inflammatory reactions. It was recently shown that the biological role of MIF-2 has a very narrow functional spectrum with MIF. This can perhaps also be explained by the fact that in the human genome, MIF-2 loci is in close proximity to MIF. This, in turn, indicates that MIF and MIF-2 gene clusters arise from an ancestral duplication event¹²⁷. The second ligand, MIF-2, has a molecular weight of approximately 13 kDa, and it is also able to convert *D*-dopachrome

to 5, 6-dihydroxyindole^{126,128}. D-dopachrome and p-hydroxyphenylpyruvate serve as substrates for the tautomerase. However, the murine MIF-2 and murine MIF have just a 28 % identity and 45 % homology when protein sequences are compared. However critical residues for the tautomerase activity are conserved in MIF and in MIF-2¹²⁹. In addition, the three-dimensional show that MIF-2 a significant homology with MIF. Not just the overall folding, also the subunit topology is almost identical when compared with human MIF¹²⁶. This positively charged property is also present in MIF-2 by the N-terminal proline¹³⁰, located at the bottom of a positively, in which the conformations of Lys32 and Ser63 are highly conserved. It is assumed that these characteristics related to the physiological role and tautomerase activity of MIF and D-dopachrome tautomerase. MIF-2 has been reported in different cellular locations, such as cytoplasmic membranous and nuclear as well. Besides, it is put in context to be associated with cancer, especially if high MIF levels are reported in Liver and prostate cancer, this is mostly attributed to the interaction with the CD74 receptor¹³¹. All in all, MIF-2 has been indicated for sharing with MIF, among others, an exacerbating role in endotoxic shock and in renal tumorigenesis. Besides it is mimicking the cardioprotective effect of MIF in a mouse model of ischemia/reperfusion injury of the heart^{125,127}.

However, state of the art research on the influence of MIF on cell survival and apoptosis is still controversial and complex. The receptor and molecular mechanism behind it are still unclear. All in all the biological function of MIF-2 has still barely been studied⁷⁶.

1.13. MIF: a crucial regulator of inflammation

Nowadays, inflammatory processes are described as “the impact on living tissue after injuries”^{132,133}. Macrophage migration inhibitory factor (MIF) is reported as a proinflammatory cytokine, which plays an important role of the inflammatory cascade. While studying the importance of MIF in the context of obesity IR, glucose intolerance and atherosclerosis, MIF deficient mice show significantly reduced inflammation in the liver. This is expressed by the lower fibrinogen levels at baseline under inflammatory conditions⁷⁹. These highlight the crucial role of chronic inflammation in the development of inflammatory response and atherosclerosis. This follows that one can deduce MIF as a potential therapeutic target, in order to decrease inflammatory responses within metabolic and cardiovascular disorders^{134,135}. MIF is known as a pleiotropic cytokine, which regulates the expression of several inflammatory molecules, such as TNF- α , nitric oxide and cyclooxygenase 2 (COX-2). Secretion of MIF secretion is regulated by immune stimuli, which in turn leads to pro inflammatory pathways^{136,137}. One should not forget

that MIF paralogue MIF-2 signals through the receptor CD74 and, therefore, should also not be disregarded in the context of inflammatory diseases. When focus is placed on CD74⁺ T cells, a distinct but synergistic role in CIA pathogenesis^{138,139} is observed. Chemokines can also be post-translationally modified by, among other things, nitration/nitrosylation. The modification can change chemokine activity¹⁴⁰.

1.14. MIF and its involvement in neurodegenerative disorders

Neurodegenerative diseases or ischemia is immune activation in the central nervous system (CNS). Not all immune responses in the CNS are harmful. They can also activate cascades of repairs and regeneration mechanisms. However, cell type-specific cascades can also be influenced, including the activation of microglia, which play an important role in controlling inflammatory processes^{80,141,142}. It can lead to a chronic activation of innate immune responses which are mediated by resident CNS macrophages. This in turn can activate neurotoxic pathways which further promote degeneration. Another key factor in neurodegenerative diseases is the adaptive immune response, which causes tissue damage, but also the resolution of inflammation as well as neuronal repair or protective mechanisms. It is becoming more and more clear that the immune system and the mediation of repair mechanism or damage within neurodegenerative diseases are inseparable. It is precisely for this reason that the modulation of the immune system has moved more and more into the focus of scientific work, but whether these approaches can be used in humans is still a matter of dispute. Today's research sees great potential for therapeutic approaches in MIF family member research. Therefore, it is essential to consider the topological function of MIF, as it plays an important role in future potential therapeutic approaches.

1.15. The multiple functions of MIF as a moonlighting protein

Considering the complexity of higher organisms, it turns out that mechanisms conserve the diversity among others, such as alternative splicing or post-translational modifications (PTMs) on the proteome level^{143,144}. Therefore, the proteome is assumed to be larger by a factor of >50-fold. Besides, the gene products are even more diverse in humans due to alternative promoter sites and transcript splicing. In addition, many non-coding RNAs (e.g, microRNAs) or small interfering RNAs (siRNAs) and long non-coding RNAs (lncRNAs) control the protein translation and mRNA stability.

As discussed with the focus on cytokine and chemokines, it is well known that due to PTMs, the enzyme function or even the interaction profile of a protein can change. Unexpected additional activities have even been discovered for cytokine such as MIF-2. The recent studies hold that several biomolecules show unexpected function, influenced by their different- locations, due to specific substrates or even various binding partners, such as AIF. Overall, the research shows more evidence of a “molecular multitasking” concept than the “one molecule, one function” paradigm. This concept of “multitasking moonlight proteins” was first described by Kapurniotu et al, 2019¹⁴⁵. New functionalities have also been discovered for the MIF family in recent years, including the MIF chaperone-like activity and the nuclease activity. However, it is still being discussed today whether the latter function takes place within the framework of repair mechanisms or during the PARP1 activated apoptosis or whether it performs its role in the trade depending on the location, the environment, and the given dysfunction. Intracellular proteins can have homeostatic and extracellular functions while promoting inflammation, among other functions. In this study, the remarkable multitasking potential of MIF and its family member MIF-2 will be described and examined. These molecules are called alarmins, released by dysfunctional or damaged cells, and can thus induce inflammatory reactions. The scientists have identified alarmins and DAMPs, terms for a class of molecules¹⁴⁶. In the event of cell stress or damage to the tissue, alarmins are passively released after cell death. On the one hand, a release can signal “danger” to the host and thus cause a local inflammatory reaction. These, in turn, contribute to the physiological healing of tissue. If these mechanisms are dysfunctional, however, pathological inflammation can occur. On the other hand, however, alarm release can be controlled to communicate early, sublethal cell stress. However, the focus of the MIF family is on the “multitasking” concept. For example, the principle of “multitasking” will be characterized with the help of the HMGB1. The HMGB1 is found in the cells as a transcriptional cofactor that can bind to the DNA^{145,147}. It can however also be secreted into the extracellular environment after cell damage. It can also be released into the extracellular milieu in a regulated manner via the autophagolysosomal pathway. Extracellular HMGB1 fulfills the task of intercellular cytokine and inflammation mediator. HMGB1 thus has two different functions, both of which are independent and topologically regulated. HMGB1 can act as a co-chemokine together with the CXCL12 (CXC chemokine). On the one hand, the HMGB1 / CXCL12 complex can bind with the CXCR4 receptor to stimulate the chemotactic cell migration of, among other things, macrophages. Alternatively, it binds to the receptor of advanced glycation endproducts (RAGE) to indicate autophagy. The later part of this work will make it clear that the MIF and its paralogue MIF-2 have similar function. MIF was first identified as a cytokine in 1966 and was newly declared as a

pleiotropic chemokine-like inflammatory cytokine. Furthermore, dysfunction of MIF promotes atherogenesis, cardiovascular diseases, and tumor development. Furthermore, the role of inflammatory cytokines of MIF and its homolog MIF-2 was described in the context of diseases. The molecular structure of MIF is unique and, in addition to cytokine classes, can also be assigned to a class of bacterial tautomerase with a sequence homology of only 20-30%. MIF shows a conserved catalytic tautomerase activity. MIF, as well as MIF-2, is expressed in many cell types. An upregulation of MIF in inflammation can be regulated by the release. MIF can be found in the cytosol after translation. MIF secretion occurs via the ABCA1 transporter, p115, and JAB1 / CSN5¹³⁰. Inflammation and immune stimulation control the non-canonical, regulated MIF secretion into the extracellular space. The circulating MIF can bind with receptors on myeloid cells. The CD74 plays an important role as a cytokine receptor for MIF and MIF-2, expressed by class II negative cells. This signaling activates the proliferative responses. Furthermore, in myocardial ischemia, the AMP kinase-mediated cardioprotective effects of MIF and MIF-2 are mediated by the CD74 receptor¹⁴⁸. In addition to neutrophils, CXCR2 is also expressed by macrophages and is upregulated under inflammatory stimulation. In addition to the extracellular functions, intracellular activities are also observed. These take place in both the cytosolic and the nuclear compartments. In the cytosol, MIF interacts with CSN5-JAB1, thereby regulating the COP9 signalosomes¹⁴⁹. In general, the cytosolic functions of MIFs are referred to as "cell-protecting", "homeostasis-promoting". These include the chaperone activity of MIF described in 2015. As already mentioned previously, MIF binds with the mutated superoxide dismutase (SOD1G93), it inhibits the accumulation of misfolded mutated SOD1 with the help of its chaperone activity. In doing so, it inhibits motor neuron damage²⁰. However, further questions are unclear in this regard and therefore the following studies are pending: chaperone activity in the cytoplasm in non-neuronal cells and a promotion of the breakdown of the misfolded protein through further enzymatic activity. One can be found in the cell nucleus. And another was observed in the nucleus, the nuclease activity. DNA damage promoted by ischemic or excitotoxic stress leads to an accumulation of cytosolic poly-ADP-ribose (PAR) trees. The PAR trees promote the release of AIF from the mitochondrion. In a complex tied to MIF. With AIF, MIF can also be escorted into the cell nucleus and develop its nuclease function there. This signal path leads to the promotion of cell death in Parthanatos^{150,151}. This study, which AIF and ischemic stress directly influenced, has been partially reproduced by an independent laboratory and repeatedly by the scientist who discovered the nuclease activity.

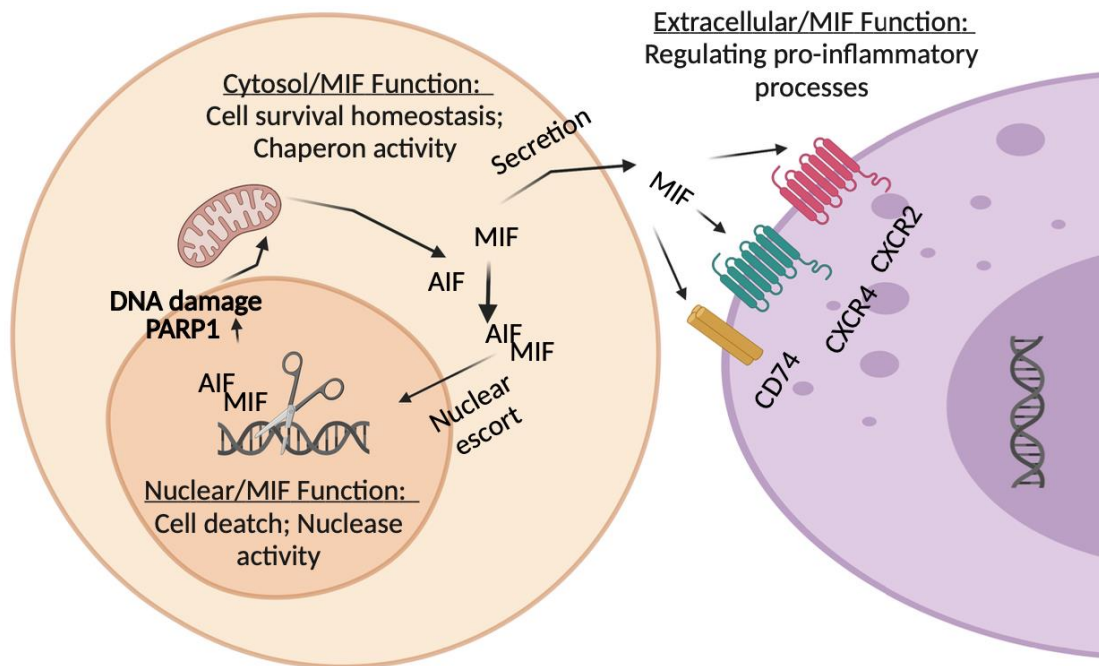


Figure 1-3: Schematic representation of summarized multitasking/moonlighting functions of MIF family member proteins.

This figure provides an overview of the multitasking/moonlighting functions of MIF family member proteins. Key abbreviations used in the figure include MIF (macrophage migration-inhibitory factor), AIF (apoptosis-inducing factor), PARP1 (Poly [ADP-ribose]-Polymerase 1), CD74 (MHC class II-associated invariant chain), CXCR-4 (C-X-C chemokine receptor type 4), and CXCR2 (C-X-C chemokine receptor 2).

In the schematic representation, the orange cell symbolizes MIF's nuclear function as a nuclease, indicating its involvement in nuclear processes. The extracellular interaction between the orange and violet cells represents the proinflammatory function of MIF, highlighting its role in mediating inflammatory responses. Please note that the depiction in this figure is a simplified representation aimed at summarizing the multifaceted functions of MIF family member proteins and their interactions.

This schematic representation provides an overview of the multitasking/moonlighting functions of MIF family member proteins, emphasizing their diverse roles in both intracellular and extracellular processes.

In summary, MIF has various functions in three independent compartments. The first, (i) in the extracellular space as cytokines, the second (ii) in the cytosol as a chaperone-like molecule, and the third (iii) in the cell nucleus as an AIF-dependent nuclear-translocated nuclease. All of these make the MIF family an incredible example of "topological multitasking". By and large, rough tasks in the various cell compartments are observed. However, the interaction of the MIF and its interactions with the individual areas of responsibility have not been clarified in detail. So important regulatory mechanisms are still unclear. It shows that MIF, as well as MIF-2, is a multitasking protein, which has functional versatility over three different topologies with several binding proteins.

1.15.1. The nuclease function of MIF

The family of nucleases is, among other things, structure, function and topology overarching. In summary, it can be said that nucleases can cleave phosphodiester bonds (between sugars and the DNA phosphate units) of nucleic acids. These include endo / exo, DNA / RNase, topoisomerases, recombinases, ribozymes and many others. This study deals with the nuclease of MIF and the potential nuclease function of MIF-2, but it is essential to understand mechanisms, structures and the metal ion dependency of the nuclease family. The control of the integrity and stability of genetic material is an important survival mode in living organisms. Environmental pollution is one of the greatest risk factors for DNA integrity. These can be caused by UV light, modification of the DNA by carcinogens, or ROS enrichment by by-products of the metabolism. However, the intrinsic errors during replication or recombination must not be ignored. These must be corrected by various repair protein mechanisms. However, it should be noted that a change in the base sequence could lead to serious neurodegenerative diseases. Since the molecules involved often work in a complex, each subunit is a limited factor. In these cases, nucleases play an important role in dissolving damage or activating the elimination of a cell. One of these important complexes in the repair mechanism, or rather in the replication apparatus, is DNA polymerase and its exonuclease. While the DNA polymerase contributes to the replication of the template DNA, the exonuclease degrades faulty DNA strands in the 3' to 5' direction. The deletion of this exonuclease, which contributes to proofreading, leads to increased cancer in mice¹⁵². In addition, another factor in DNA integrity is the removal of Okazaki fragments during replication. In addition to RNaseH, FEN1 endonucleases are involved in the elimination of the Okazaki fragments in eukaryotes and archaea^{75,153–156}. The flap endonuclease (FEN1) removes RNA and DNA 5' lobes. Members of this superfamily include XPG for nucleotide excision repair and EXO1 for mismatch repair. Studies however have also shown that FEN1 is assisted by human DNA2 protein in ATPase-dependent removing of long flaps in DNA replication¹⁵⁴. We know too those other nucleases take over important areas within various repair mechanisms. Base excision repair, through apurinic / apyrimidinic (AP) endonuclease, endonuclease IV (endoIV) and exonuclease III (exoIII) in *E. coli* cells also takes place. In this context, it is interesting to note that these two enzymes show no sequence similarities, but the AP endonuclease activities are conserved and are very similar. Within the mismatch repair mechanism, a complex of different proteins called the MutSLH (proteins) is the main actor¹⁵⁷. Nucleotide excision repair (NER) processes DNA after UV radiation, for example, unrepaired damage through base excision repair. Another DNA damage caused by

ionizing radiation and strand cut chemicals is double strand breaks. This is however not generated in meiosis and V (D) J recombination. In this context, Mre11 is shown as a multifunctional nuclease. Nucleases can also be classified according to the motifs in their primary sequences. The preservation of the motifs within the primary structure is however not always decisive, the 3D structure is another factor that must be taken into consideration. Functional preservation can be guaranteed by folding. These are shown above all in relation to the nucleases involved in DNA repair^{158,159}. It is assumed that the 3D structures diverge much less or have a greater correlation with the functions compared to the primary sequences. In fact, using the example of restriction endonucleases of type II, despite their primary sequence diversity, the common core motif leads to the formation of the active pocket site, based on their folding family. One of these classifications is the RNaseH-like fold (five-stranded β -sheet flanked by several α -helices), to which RNaseH or proofreading exonucleases belong. Parts of the active center are formed by the DDE motif, which is located on one side of the sheet. Three to four acidic radicals coordinate the metals that are essential for the catalytic reaction. Resolvase-like folds are also classified, for which FEN1 is also listed. Within the restriction endonuclease-like fold, the catalytic domains show a common fold architecture, which is a five-stranded β -sheet flanked by several α -helices. The strand order is 12345, with strand 2 and in some cases strand 5 being antiparallel to the others. The conserved PDXn (D / E) XK sequence can be found on one side of the β sheet. The folding of the Vsr endonuclease resembles this structure, with the (D / E) XK sequence being replaced by FXH. Furthermore, DNaseI, ExoIII and Ape1 (3F) belong to the class of the DNaseI-like fold. What they have in common is a four-layer structure that contains an α / β sandwich. The active site is on one side of the β sheet. The recognition of the DNA are roughly divided into two categories, DNA recognition by DNA repair nuclease, and the unspecific and specific associations^{160,161}. With the help of unspecific DNA binding, enzymes can quickly search for target sequences or damage by diffusion processes along the DNA. After that, specific interactions are performed to bind with the chemical groups within the DNA. Using the example of EcoRV or BamHI, it is shown that unspecific binding is a weak association, but in the specific complex DNA is bound sequence-specifically in the associated column of the protein. After the deformation of the DNA duplex, the cleavage is carried out¹⁶². As already mentioned, nucleases cleave phosphodiester bonds. There are two modes for this nucleophilic substitution: associative and dissociative. Many nucleases use metal cofactors for the hydrolytic reaction. For catalysis, some nucleases require magnesium cations, or other metals with positive charges.

1.15.2. Nucleases: key players in cell death processes

Most neurodegenerative diseases have one thing in common, the death of cells, which leads to an irreversible loss of function of organs. Sequentially, the primary goal for therapeutic studies of most diseases, is the prevention of cell death. Cell death is divided into different categories, but the first is divided into different clusters. Necrosis results from cell death, after an acute metabolic disorder (arterial circulatory disorder) such as ischemia or after severe toxic tissue damage^{163–165}. Affected cells are destroyed; this allows molecules to get into the extracellular space and activate the inflammatory response in the surrounding tissue. Of course, this reaction can also be triggered by mechanisms other than ischemia, such as mechanical injuries, burns, or frostbite. In addition to necrosis, another supergroup to be mentioned is, the apoptosis mechanisms. Whereas necrosis is a pathological process, i.e., which is triggered by damaging influences on the cell; apoptosis is a physiological and controlled mechanism for cell death. Programmed cell death, (called apoptosis), comes from the ancient Greek word for falling away. Apoptosis is also described as a "suicide program" by cells^{164,166–168}. Mechanisms are activated by stimuli, which in turn initiate programmed cell death. Necrosis can be abrupt, whereas apoptosis can last for hours. While cell death may be intricately divided into these two distinct categories, it's important not to prematurely conclude that these phenomena are entirely separate and independent. After necrotic cell death, there is cell lysis which activates inflammation. Furthermore, induced signal cascades cause neutrophils and monocytes to be recruited to the dead tissue, breaking down necrotic debris. Depending on the type of tissue or organ, healing can leave scars or, if possible, the necrosis areas are replaced by healthy tissue through cell proliferation. Dysfunction of these functions can lead to cirrhosis^{169–171}. The role of apoptosis can be pathological but also important for development; for example, apoptosis forms tissues and organs with the help of programmed gaps in the buds of the limbs so that fingers or toes can form apoptotic signals that activate caspases. In addition, caspase 3/7 contributes to the breakdown of the core lamina and cytokeratin, resulting in chromatin condensation and cell rounding.

Endonucleases contribute to DNA fragmentation. These can be detected using the comet assay (single-cell gel electrophoresis). In addition, when caspase is activated, cells shrink, which makes the translocation detection with the help of life imaging in MIF transfected cells culture difficult. Since cell shrinkage also makes it challenging to locate the cell compartments. However, not all apoptotic mechanisms are dependent on caspase 3/7 activation. An independent mechanism is an apoptosis-inducing factor (AIF) from the mitochondria. The translocation of AIF promotes DNA breakdown in the cell nucleus. In 2016 MIF was discovered as the most effective interaction partner of AIF and

thus also the searched associated nuclease^{19,116}. The missing partner of AIF was discovered, and a new enzymatic activity of the moonlight protein MIF. As mentioned at the beginning, the conjoint pathways of necrosis and apoptosis are also being discovered in new studies, and thus, new forms of programmed necrosis are being discovered. These include ferroptosis, pyroptosis, necroptosis, autophagic cell death, and PARP-dependent cell death¹⁷². These have the commonality that they regulate cell death independently of the caspase.

Ferroptosis is characterized as an iron-dependent process initiated by oxidative stress and subsequent lipid peroxidation. Various factors, including mitochondrial hyperpolarization and the generation of reactive oxygen species, can induce mitochondrial dysfunctions that ultimately lead to cell death. Consequently, ferroptosis predominantly occurs following events such as oxidative stress, ischemia-reperfusion, and drug-induced hepatotoxicity, activating a necrotic cell death pathway. Pyroptosis is induced by the formation of inflammasomes after an intracellular pathogen^{168,173,174}. Cell death promoted by pyroptosis removes pathogens and thus microbial killing by secondary phagocytes^{60,175,176}.

2. Aim of this study

In 2016, MIF's nuclease activity was discovered, which represented a significant breakthrough, despite the fact that previous research had detected MIF within the nucleus. The focus of this thesis was to study the nuclease activity of MIF, with a particular emphasis on identifying its critical amino acid and zinc finger domains. To ensure a complete understanding of MIF's nuclear activity, it was crucial to eliminate the possibility of contamination by other bacterial nucleases during purification or experimental environmental factors. By identifying these critical domains and conducting targeted mutation experiments and structural analyses. Furthermore, the objective was to determine if the identified domains could be inhibited without affecting the overall folding of the protein. This was crucial in confirming the specificity of MIF's nuclease activity and ruling out any potential contaminants from purification processes.

Therefore, to disrupt the active site of nuclear activity, it was crucial to use known MIF inhibitors or chelate it specifically in the reactant solution by binding it with an antibody, which was also a significant goal of the study. Furthermore, the study aimed to expand the scope by examining the nuclease activity of MIF-2. By comparing its structural attributes to MIF, the study sought to identify whether MIF-2 also exhibited nuclease activity. Crystallography and targeted mutation experiments were used to ascertain the presence of nuclease domains within MIF-2 and to determine its potential functional consequences. In addition, the study aimed to investigate whether MIF-2 was increasingly observed in the nucleus following a toxic insult with NMDA or MNNG and the potential collocation of MIF-2 with AIF. One another key target of my PhD thesis was to address whether there was an impact on DNA damage in MIF and MIF-2 deficient cells compared to WT cells. To investigate this, methods such as the comet assay and DSB marker analysis were employed. However, it was crucial to note that DSB markers may also increase during repair mechanisms. To overcome this limitation, live imaging was utilized to determine the number of intact cells within the culture before and after toxic insult. Another significant aspect of this research was to establish new research models for advancing scientific understanding in the field of MIF research.

3. Material

3.1. Chemicals and reagents

<u>Chemicals and Reagents</u>	<u>Manufacturer</u>
30 % Acrylamid-Lösung	BioRad, Munich
Albumin Fraktion V (BSA)	Carl Roth, Karlsruhe
Bacto-Agar	AppliChem, Darmstadt
Dimethylsulfoxid (DMSO)	Sigma, Munich
DNA-Ladder, 100 bp	Invitrogen, Gönningen, Netherlands
DNA-Ladder, 1kb	Invitrogen, Gönningen, Netherlands
Dynabeads® Protein G	Thermofisher Scientific
EDTA	AppliChem, Darmstadt
Ethanol	Carl Roth, Karlsruhe
FCS	Gibco, Eggenstein
Glycin	Fluka Chemie AG, Switzerland
Hoechst	Thermofisher Scientifi
Hydrochloric acid (HCl)	Fluka Chemie AG, Switzerland
Isopropanol	KMF, Lohmar
Magnesiumchlorid (MgCl ₂)	Sigma Aldrich
Matrigel	Collaborative Biomedical Products
MultiMark® Multi-Colored Protein Standard	Invitrogen, Karlsruhe
Penicillin/Streptomycin-Solution	Gibco, Eggenstein
Poly-L-Lysine	Sigma Aldrich
Protein Assay (Bradford-Reagenz)	BioRad, Munich
Sodium dodecyl sulfate Lauryl Sulfate (SDS)	Sigma Aldrich
Sodium hydroxide solution	Fluka Chemie AG, Switzerland
Saccharose	Sigma Aldrich
TEMED	BioRad, Munich
Tris	Carl Roth, Karlsruhe
Triton X-100	Fluka Chemie AG, Switzerland
Trypan Blue solution	Invitrogen, Karlsruhe
Trypsin/EDTA	Invitrogen, Karlsruhe
Tween 20	Fluka Chemie AG, Switzerland

3.2. MIF family protein samples

MIF	Manufacturer
Human MIF (MonoQ,C8/nativ)	Bernhagen lab, LMU, Munich
Mouse MIF (MonoQ,C8/nativ)	Bernhagen lab, LMU, Munich
Human MIF-2 (MonoQ,C8/nativ)	Bernhagen lab, LMU, Munich
Mouse MIF-2 (MonoQ,C8/nativ)	Bernhagen lab, LMU, Munich
Human MIF E22Q Nuclease Dead Mutant	Gokce lab, LMU, Munich / Bernhagen lab, LMU, Munich
Human MIF C81S Mutant	Bernhagen lab, LMU, Munich
Human MIF-2 E88Q Nuclease Dead Mutant	Gokce lab, LMU, Munich / Bernhagen lab, LMU, Munich

3.3. Buffer and solution

Buffer	Composition
PBS (pH 7.2)	137 mM NaCl, 2.7 mM KCl 1.5 mM KH_2PO_4 8.1 mM Na_2HPO_4 in ddH ₂ O
PBS-T	0.05 % (w/v) Tween 20 in PBS
TBS (pH 7.3)	20mM Tris-HCL 150mM NaCl in ddH ₂ O
TBS-T	1. Tween 20 in TBS

3.4. Buffer and solution (SDS-PAGE, western blot immunodetection)

Buffer	Composition
10 % Resolving gel	10 % (w/v) acrylamide/Bis solution 375 mM Tris-HCl, pH 8.8 0.1 % (w/v) SDS 0.1 % (w/v) APS 0.1 % (v/v) TEMED
4 % Stacking gel	4% (w/v) acrylamide/Bis solution 125 mM Tris-HCl, pH 6.8 0.1 % (w/v) SDS 0.1 % (w/v) APS 0.1 % (v/v) TEMED
5 x SDS running buffer	25 mM Tris-HCl 192 mM Glycine 1 % (w/v) SDS in ddH ₂ O
Transfer buffer	5 % (v/v) NuPage-transfer buffer (20x) 10 % (v/v) Methanol in ddH ₂ O
1 % Blocking solution	3 % (w/v) BSA in TBS-T
Immunoblot washing buffer (TBS-T)	0,1 % (w/v) Tween 20 in TBS

3.5. Media and solutions for culture of primary mouse neurons

Media and solutions	Composition
Hank's Balanced Salt Solution (HBS)	500mL Hanks without calcium or magnesium (Sigma H2387) 2.1875 ml of sterile Sodium bicarbonate solution 8% (w/v) NaHCO ₃ (350mg per L) 0.5ml sterile 1 mM HEPES pH 7.3
Common Medium: MEM	500 ml of MEM 12.5 ml of 20% glucose

	1.25 ml of 8% (w/v) NaHCO ₃ 50 mg Transferrin (thermo 11107-018, MW 77,000)
Plating Medium	88.3ml Common Medium 500ul of 100x antibiotics pen/strep (0.5X final) 10 ml FBS (or the one tested in house) (10% final) 1 ml 0.2M L-glutamine solution 200 µl Insuline solution
Growth Medium (0 Ara-C)	per 92.75 ml of Common Medium 5ml FBS(Heat inactivated at 57 °C for 30 min) 0.25 ml 0.2 M L-glutamine solution (GIBCO 12403) 2 ml B-27 supplement (Gibco 17504
Growth Medium (4µM Ara-C)	In 50ml Growth Medium 4 µM final concentration of Cytosine β-D- arabinofuranoside
Papain and 100X activator	Papain (0.25 mg/mL; Sigma-Aldrich; P3375) activated by L-cystein (1.25 mg/mL; Sigma-Aldrich; C7352) 0.5mM EDTA

3.6. Solutions for Coomassie brilliant blue staining

Buffer	Composition
Coomassie staining solution	0.25 % Coomassie Brilliant Blue R- 250 40 % methanol 10 % glacial acidic acid
Coomassie destaining solution	40 % methanol 1. glacial acidic acid

3.7. Bacteria and plasmids

Bacteria/ Plasmid	Description
E.coli	Gökce lab.
pET-22b/hMIF	Bernhagen lab;
Rosetta™(DE3) Competent Cells	Bernhagen lab;

3.8. Buffers and solutions for protein expression and purification

Buffer	Compositions
LB-media	1 % (w/v) NaCl 1 % (w/v) Bacto-Trypton 2 % (v/w) yeast extract.
LB-agar	LB-media + 1,5 % (w/v) Bacto-agar
Low salt buffer, pH 7.4	50 mM Tris-HCL, pH 7.4 50 mM NaCl
High salt buffer, pH 7.4	50 mM Tris-HCL, pH 7.4 1000 mM NaCl
Dialysis buffer 1	20 mM NaH ₂ PO ₄ 5 mM DTT
Dialysis buffer 2	20 M NaH ₂ PO ₄

3.9. Primary antibodies

Donkey anti-rabbit IRDye 800CW	Immunoblotting
Donkey anti-mouse IRDye 800CW	Immunoblotting
Donkey anti-mouse IRDye 680CW	Immunoblotting
Donkey anti-rabbit IRDye 800CW	Immunoblotting
Donkey anti-rabbit IRDye 680CW	Immunoblotting
Alexa Fluor 594, Donkey anti-goat IgG	IHC, ICC
Alexa Fluor 647, Donkey anti-mouse IgG	IHC, ICC
Alexa Fluor 647 Goat anti-rabbit IgG	IHC, ICC
Alexa Fluor 647 Goat anti-mouse IgG	IHC, ICC
Alexa Fluor 647 Goat anti-rat IgG	IHC, ICC

Alexa Fluor 555Goat anti-mouse IgG	IHC, ICC
Alexa Fluor 555 Goat anti-rabbit IgG	IHC, ICC
Alexa Fluor 488 Goat anti-mouse IgG	IHC, ICC
Alexa Fluor 488 Goat anti-rabbit IgG	IHC, ICC

3.10. Cell lines and primary cultures

Cell line	Use
HEK293	Preliminary experiments
Primary neuronal mix culture	Determinantal experiments
Primary astrocyte culture	Determinantal experiments

3.11. Mouse lines

Name	Background/Number
wildtype	C57BL/6j
MIF -/-	186
MIF-2 -/-	1313
MIF-2 -/-	1314

3.12. Consumables

Consumables	Manufacturer
Cell strainer 40 µm Nylon	BD, Heidelberg
Centrifuge tubes (15 ml, 50 ml)	Falcon, Heidelberg
Microtube	Eppendorf, Hamburg
NuPage combs	Invitrogen, Karlsruhe
NuPage cassettes	Invitrogen, Karlsruhe
Parafilm „M— Laboratory Film	American National Can, USA
Pipette tips 1000 µl	Brand, Wertheim
Pipette tips 200 µl	Brand, Wertheim
Pipette tips 10 µl	Sarstedt, Nürnbergrecht
Plastic vials	Sarstedt, Nürnbergrecht

PVDF (polyvinylidene difluoride) transfer membrane (0.2 µm)	Carl Roth, Karlsruhe
Reaction tube 1.5 ml	Sarstedt, Nürnberg
Reaction tube 2 ml	Carl Roth, Karlsruhe
Syringes (2 ml, 50 ml)	Dispomed, Gelnhausen
Whatman filter paper	Greiner Labortechnik, Frickenhausen

3.13. Kits

Kit	Manufacturer
Gibson Assembly® Master Mix	New Englan BioLabs
Mini and maxi preparation	QIAGEN

3.14. Devices

Devices	Manufacturer
-20 °C Freezer Premium	Liebherr, Ochsenhausen
-80 °C Freezer Ultra Low	Sanyo Electric Biomedical Co., Japan
4 °C Fridge Premium frost-free	Liebherr, Ochsenhausen
Centrifuge 5417R	Eppendorf, Wessling-Berzdorf
CO ₂ -Auto-Zero-Incubator	Heraeus, Hanau
Ice machine AF 100	Scotsman, Italien
Electrophoresis Power Supply 2909.1	Carl Roth, Karlsruhe
Hypoxic workstation INVIVO2 400	Ruskin, UK
LAS-3000 Image Reader	Fujifilm, Düsseldorf
Magnet stirrer MSH basic yellowline	IKA, Staufen
Neubauer counting chamber	Paul Marienfeld, Lauda-Königshofen
PHM82 Standard pH-Meter	Radiometer, Denmark
Pipettes	Gilson, USA
Pipettor Pipetboy	IBS integra biosciences, Fernwald
Rocking shaker Rocky	Fröbel Labortechnik, Lindau
Rocking Shaker PMR-30	Grant Instruments, Cambridge
Schott flasks	Schott, Mainz
SDS-PAGE NuPage	Invitrogen, Karlsruhe

Vortex MS2 Minishaker	IKA Works, Wilmington
Water bath type 1004	GFL, Burgwedel

3.15. Software

Software	Manufacturer
openComet Software	
ImageJ	ImagJ 1.51n
Graph Pad PRISM	8.2.1

4. Method

4.1. Cell culture

In order to ensure sterile conditions for working in cell culture, all experiments including cell lines or primary cultures were carried out in a laminar flow hood, approved for this purpose. The conditions under which cell lines and primary cell cultures grow can vary, but what they all have in common is a suitable container with a medium containing essential nutrients (amino acids, carbohydrates, vitamins, minerals). Growth factors are required for adequate maintenance, including hormones, the gas composition of the environment (O₂, CO₂) and above all, a regulated physical and chemical environment that includes the pH, temperature, and osmotic pressure. In addition to cell lines floating freely in the culture medium (suspension culture), there are also firmly bound lines (adherent or monolayer culture) that play an essential role in this work. These, in turn, require an additional layer of certain subsoil to attach.

4.1.1. Human embryonic kidney (HEK)

In this thesis, HEK293T cell lines were used for preliminary experiments to study the interaction of MIF and MIF-2 with AIF. The cell line was also used to establish life imaging and toxicity tests. The HEK cell line was kept in a DMEM culture medium supplemented with 10 % heat-inactivated fetal calf serum (FCS) and 1 % penicillin/streptomycin for both experiments. Cells were incubated in a humidified incubator (5 % CO₂) at 37 °C.

4.1.2. Neuronal culture isolation

In this study, mixed neuronal cultures were used for western blots, Immunocytochemistry staining (ICC), and live imaging purposes. For further microscopic analysis, a 24 well plate had to be prepared with round 12 mm cover slips (Hecht Assistent® /REF 41001112). Other culture plate formats (6 or 96 healthy plates) were first covered with Matrigel and placed in the incubator (5 % CO₂, 37 °C) for at least 1 hour. For neuronal cell isolation, the brain of P0-1-day old mouse pups were used. The cortex and hippocampus were removed and washed several times in a petri dish with a dissociation medium (4 °C) during preparation. All processes were performed on ice. The euthanized

pups were sacrificed by cutting off the animals' heads (with one single cut). For the following steps, blunt tweezers were used to fix the head through the eye sockets on the Petri dish's base. Then micro scissors were used to cut gently along the midline, starting at the cerebellum and going around the eye sockets. The skull was carefully opened. Now that the brain has been exposed, it was first transferred to a new petri dish with an ice-cold dissociation medium (enough to cover the brain completely). First the meninges (especially around the hippocampus), then the hippocampus and the cortex were removed, the animals' brains were individually dissected, and after each animal, all dissection tools were cleaned. For further dissociation steps, an activated papain solution was used. The papain solution (0.25 mg/mL) was diluted in a dissociation medium, the hippocampus and cortex were transferred into the enzyme-containing solution and incubated for 20 minutes at 37 °C. After the incubation, the papain solution was removed and covered with 3-5 ml preheated plating medium. The hippocampus and cortex's single cells were mechanically isolated in the plating medium using Transfer pipettes. By using a 40 µm filter incomplete dissociated tissue was removed. It is crucial to moisturize the filter beforehand to prevent unnecessary tissue destruction leading to DNA leakage, which creates an unwanted sticky cell solution. After the number of cells was determined (1.000.000 cells / mL) by TC20™ Automated Cell Counter, the cell suspension was seeded in a 24 well plate (~ 500.000 cells / well). After the cells had settled, the plating medium was removed and replaced with ARAC (50 %). The settling can take up to 60 hours.

4.1.3. Astrocyte culture isolation

To investigate the function of MIF-2, we established an astrocyte culture in which MIF-2 is present at high expression levels. The main differences between primary mixed neuronal culture and primary astrocyte culture start after cultivation in flasks. The dissociation of the brain and the plating and maintenance solution is the same (see section 3.1.2).

However, the dissected brain was transferred directly into flasks. This is followed by another step in which the cultures are split into the final plates (6-, 12-, 24-, or 96-well plates). Therefore, the astrocyte cultures were incubated in the same way as the mixed neuronal cultures until DIV 5-7. After reaching approximately 70 % confluence, the flask medium was changed from the usual maintenance media to Hibernate™ A medium containing 0.5 mM Glutamax™. After gentle shaking at

4°C, the remaining astrocytes were trypsinized, centrifuged, and resuspended in the freshly prepared AstroMACS medium. After checking the density and viability of the remaining cells, they were split into the designated plates. Cells were treated, fixed, or imaged between DIV 13-20.

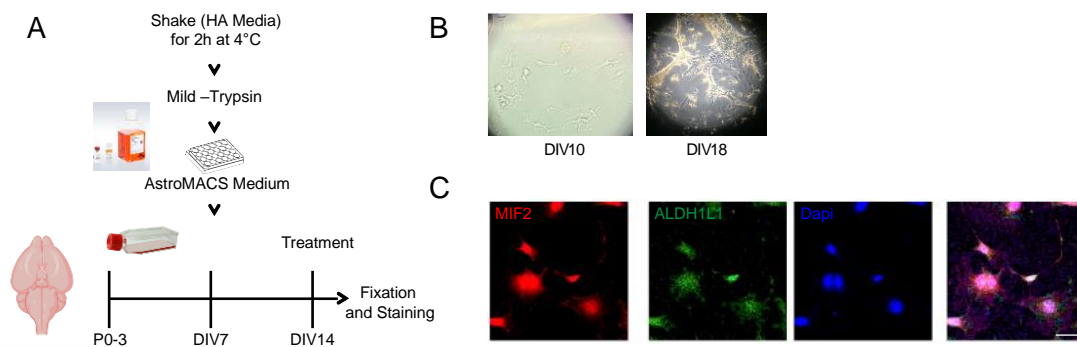


Figure 4-1: Schematic representation of primary astrocyte culture

(A) Schematic representation of the primary astrocyte culture protocol for mouse brain using AstroMACS medium. The timeline between dissociation and the experiment is depicted, illustrating the key steps involved in the culture process. (B) Representative images of primary astrocyte cultures at two time points: DIV10 (days in vitro 10) and DIV18 (days in vitro 18). The images were acquired using light microscopy, showcasing the morphological changes and growth of astrocytes over time. (C) Representative images of primary astrocyte culture demonstrate the colocalization of MIF-2 (red), the astrocyte marker ALDH1L1 (green), and the nucleus (DAPI/blue). The overlay of MIF-2 and the astrocyte marker is displayed in purple, while the colocalization of MIF-2, the astrocyte marker, and the nucleus is shown in white. These images provide visual evidence of successful primary astrocyte culture establishment and the specific localization of MIF-2 within astrocytes, as indicated by its colocalization with the astrocyte marker ALDH1L1 and the nucleus (The scale bar is 10 μ m).

4.2. Toxic treatments

Toxins have been used to study nuclear translocation and percentage cell death. The toxins N-methyl-N'-nitro-N-nitrosoguanidine (MNNG), N-methyl-D-aspartic (NMDA), etoposide, and 3-nitropropionic acid (3-NP) have been used to study nuclear translocation and cell death. To study the toxic effect, neuronal mixed cultures were introduced to toxicity, and cells were incubated (5% CO₂, 37 °C) for various time lengths. After this, the cells could be further processed in the described staining procedures. The cell culture plates were washed with PBS (MgCl₂ (0.9 mM) and CaCl₂ (0.5 mM)) and

fixed with 4% PFA / 4% sucrose in PBS (without $MgCl_2$ and $CaCl_2$) for 15 min at 4 °C. With a light microscope (Leica DMI8), the cells were live imaged during toxic introduction.

4.3. Digestion of DNA by restriction endonucleases

Restriction enzymes were used to monitor the cloning success. Besides, a control group for the MIF family's nuclease function was included using restriction enzymes, especially for the PD- (D / E) XK superfamily. Restriction enzymes (1U-1.5U) were used under ideal conditions for the analysis of the plasmids. The total volume of the reaction was filled up with DNase and RNase-free H₂O. The reaction mix was incubated at 37 °C for varying lengths of time (4-8 hours). After that, the reaction mixture was separated by agarose gel electrophoresis (0,7-1%). Digested plasmid DNA was visualized with SYBR® Safe (1:10000).

4.4. Nuclease agarose assay

Nuclease assays of pcDNA (200 ng/reaction) were carried out with human MIF / MIF-2, mouse MIF / MIF-2, or their recombinant mutants (hMIFC61S; hMIFE22Q; MIF-2E86Q). The nuclease assay has been performed with variable final concentrations of 0.2-8 μ M of MIF protein, in 10 mM Tris- HCl buffer (pH 7.0) and 10 mM $MgCl_2$ (pH 7.0) for 10-48 hours, incubated at 37 °C. When 50 mM EDTA was added to the reaction mixture, Mg^{2+} ions critical for the nuclease reaction were removed (chelated) from the reaction solution. 1x loading dye was added to the sample for a final concentration of 30-100 ng pcDNA the sample was loaded onto the agarose gel (0.7-1% agarose) supplemented with SYBR® Safe (1:10000). The agarose gel was embedded in 0.5 x TBE buffer and run for 45 minutes at 120 Volts in the electrophoresis chamber.

4.5. Real-time nuclease assay

The used nucleases were RNase-Free DNase I (Thermo Fisher Scientific), AGEI (New England Biolabs), ECORI (New England Biolabs), FEN1 (New England Biolabs), ECORV (New England Biolabs) and in-lab purified MIF and MIF-2. The individual restriction reaction mixture contained either a commercial reaction Buffer or the nuclease buffer containing Mg²⁺ (10mM). In addition, it has fluorescein-labeled oligonucleotide probes (0-20 μ M) as a substrate. DNase/RNase-Free ultra-pure Distilled Water (Invitrogen) was added until total reaction volume was reached. Samples were tested in a 384 multiplate (Roche Diagnostics). The plate was read in the Roche LightCycler 480 II – BIOTECON and analyzed by the corresponding software.

4.6. Agarose gel electrophoresis and DNA detection

To show the plasmid formation state or the degree of digestion, the samples containing DNA molecules were separated according to their molecular weight at 4 °C using a 0.7-1% agarose gel. In order to produce agarose, the algae genera *Gelidium* and *Gracilaria* were used. These consist of repeated agarose (L- and D-galactose) subunits. The agarose polymers do not form any covalent bonds when they polymerize. This creates networks of ribbons with a specific pore size which determines the molecular sieve properties of a gel. The DNA was loaded into the prepared wells (pockets) in the gel, and a current is applied. The DNA in the sample has a negative charge through the phosphate backbone of the DNA molecule. This causes the DNA to flow in an electrical field in the direction of the positively charged anode. The ratio of the mass of the DNA and its charge are in constant ratio. Therefore, the DNA molecules are separated according to their size and pattern; the distance covered is inversely proportional to their molecular weight.

With the help of "biased reptation," the DNA moves forward in the gel. The speed and rate of distance covered in a particular time are determined, but as already mentioned, the DNA molecule size is also determined by agarose concentration, applied voltage, electrophoresis buffer, and DNA conformation. An intact, co-pact DNA molecule (supercoiled) flows faster than an intact open circle DNA molecule or a DNA molecule with a linear conformation. Since the agarose gel in this study is supplemented with

SYBR® Safe, the DNA molecules were visualized using the Li-Cor Odyssey® Fc Imaging System at 600 nm channel.

4.7. Comet assay (single-cell gel electrophoresis)

The Trevigen (Gaithersburg, MD) protocol was used to aid comet testing and modified for this study. When studying the nuclease reaction, it is essential to determine the degree of DNA degradation. It is an established method of measuring the cellular percentage of DNA damage. Not only physiological DNA damage can be examined, but genotoxic effects can also be assessed. In general, the intact DNA ratio to its small DNA fragments that migrate towards the anode is measured. SybrGold staining enables a fluorometric recording of the degree of DNA damage.

In this study, neural mixed cultures or astrocyte cultures with or without treatment of toxins (MNNG) were washed 6 hours after treatment with ice-cold PBS (Mg²⁺ + and Ca²⁺) covered with 0.5 % trypsin (for 10 minutes at 37 °C). After harvesting the cells and centrifuging them at 700x g for 10 minutes at 4 °C, the cells were resuspended with ice-cold PBS (Ca²⁺ / Mg²⁺ free) (1 × 10⁵ cells / ml). The cell suspension (50 µL) was embedded in preheated (37 °C) 1% low melting point agarose in PBS (500 µL). The cell agarose mixture (70 µL) was pipetted onto the comet chip, which was pre-chilled / pre-cooled at 4 °C. The 20-well comet slide was placed in the dark at 4 °C for 30 minutes. After the cell, agarose mixtures have been attached to the chip; the comet slide was then immersed in the pre-cooled lysis solution and left overnight at 4 °C. An overnight incubation increases the sensitivity of DNA damage (double-strand breaks). Since the neutral comet assay was used in this study, the remaining lysis buffer was removed in the next step, and Neutral Electrophoresis Buffer was added and incubated for 30 minutes at 4 °C. Neutral Buffer houses Tris Base (mol. Wt. = 121.14) Sodium Acetate (mol. Wt. = 136.08) at a pH = 9.0. The same Neutral Electrophoresis Buffer had been added (~ 850 mL) in the electrophoresis chamber. The comet slides were placed in the electrophoresis slide tray before covering them with the slide tray overlay. The electrophoresis was run with a voltage of 21 V for 45 min at 4 °C. Neutral Electrophoresis Buffer was removed, and slides were immersed in DNA Precipitation Solution for 30 minutes at room temperature. In this step, the salt neutralizes the charge on the nucleic acid backbone. As a result, the DNA becomes less hydrophilic and precipitates out of solution. In order to wash away residual salt from the DNA, slides were immersed in 70% ethanol for 30 minutes at room temperature. The chips were dried at 4 °C for 2 h-10 h.

This ensures that the cells are in a single plane to facilitate observation. Samples can be stored at 4 °C or room temperature at this stage. To visualize the DNA, 100 µL of 0.3 X SYBR® Gold (in 10 mM Tris-HCl pH 7.5 and 1 mM EDTA) was added to every circle of dried agarose for 30 minutes at room temperature, in the dark. Excess SYBR® Gold was gently removed, and the samples were rinsed briefly in DNase and RNase free water. The slides were dried completely at 4 °C and were imaged with Leica DMI8 light microscope. The maximum excitation/emission of SYBR® Gold is 496 nm / 522 nm. The cells were analyzed individually with the supplied comet analysis software (Catalog # 4260-000-CS).

The undamaged DNA is supercoiled, or open circle (relaxed). For this reason, it migrates more slowly under the influence of an electric current compared to smaller fragments and therefore does not move further out of the nucleoid. However, in the cells with DNA damage, DNA fragments move out of the nucleoid (comet head) and form the comet tail. As with traditional gel electrophoresis, the DNA molecules migrate towards the anode. The DNA damage is described with the help of the percentage of DNA in the tail.

4.8. Cloning

In this study, human MIF E22Q, human MIF C61S, and MIF-2 E86Q were cloned to reduce or inhibit the nuclease activity. This means that bacterial contamination can be excluded during the purification steps. Therefore, the nuclease critical regions for MIF, E22, and C61 were mutated; for MIF-2, the region E86. The glutamic acid (E) was mutated to a glutamine (Q); the cysteine (C) to serine (S). To be more precise, the glutamic acid, which has electrically charged side chains, has been replaced by an amino acid with a polar uncharged side chain.

For this purpose, the nucleotide sequence of the nuclease activity of the hMIF was mutated. Therefore, the new insert with the mutant sequence was designed first. The guanine was replaced by the cytosine (5380). The Gibson assay has been used for MIF and MIF-2 nuclease dead cloning; for the insert, overlapping ends were designed according to the vector and ordered from IDT (<https://eu.idtdna.com>). The plasmid common in the laboratory for the wild type of MIF expression was used as a vector (pet11humanMIF). The same plasmid was also used for further MIF mutant production.

For this, however, the cysteine at point 61 was replaced with a serine molecule, which, like glutamine, is part of the amino acids with polar uncharged side chains.

In addition, a nuclease mutant of MIF-2 was cloned. The glutamic acid, with an electrically charged side class, was replaced by a glutamine (Q) with polar uncharged side chains. However, the vector had to be prepared with inserts. So, the backbone must first be cut at the place of the insert. The interfaces of Xba1 and BamH1 were used here to limit the insert placement (see restriction digestion). After digesting the plasmid with the restriction enzymes, 10 µl of 2X Gibson Assembly Master Mix solution was incubated in a final volume of 20 µl with 6 fragments (IDT). Since bacteria will only grow with an intact plasmid on the antibiotic added LB agar plate, the newly cloned plasmids were transformed into E. Coli 5 alpha bacteria (see transformation) and plated out. The colony was selected within 24 hours. These colonies were incubated with 5 ml of LB medium with the associated antibiotic. The following is the mini-preparation (mini-prep) for plasmid isolation (see plasmid isolation). The isolated plasmids were again examined for the correct size using restriction enzymes and contained the required insert (see restriction digestion). For enabling the expression of proteins, the plasmids were transformed into the bacteria BL21/DE3 to carry out protein overexpression with subsequent purification.

4.9. Trizol RNA isolation (brain tissue)

Per 50 - 100 mg of tissue, 1 ml of Trizol reagent was used and homogenized. After the additional sonicating step, the samples were incubated for 5 minutes at room temperature. After adding 200 µl of chloroform per 1ml of Trizol reagent, samples were shaken vigorously for 15 seconds and incubated at room temperature for 2 - 3 min. After the Centrifugation step (15 min at 12.000 x g at 4°C), the mixture separates into three parts, a lower red phenol-chloroform phase, interphase, and a colorless upper aqueous phase. The upper aqueous phase contains RNA. The aqueous phase is isolated, and 500 ul of isopropanol per 1ml of Trizol are added at room temperature (DNA or protein are able to find in the interphase and organic phase). After vortexing briefly, incubating for 10 minutes at RT and centrifuging for 10-30 min at 12.000 x g at 4°C, the supernatant

was discarded, and just the white gel-like pellet with DNA RNA was left. The pellet was resuspended in 1ml of cold 75% ethanol per 1ml of Trizol reagent used for lysis.

Afterward, the samples were next vortexed and centrifuged for 5 min at 7500 x g at 4°C. The supernatant was removed entirely, air-dried, and the RNA pellet was resuspended in RNase-free water. In order to dissolve the RNA, the samples were incubated in a heat block at 55-60°C for 15minutes.

4.10. Transgenic mice

As a key research tool, genetically modified mice models have played an important role in biomedical research in the last decades. One of the main reasons is that the mouse genome can be modified with very high precision. One of the diseases examined with different mouse models is Alzheimer's disease (AD), which leads to memory transmission through memory loss and corruption of personality. The neuropathology of AD is counteracted by the neuronal or synaptic loss as well as extracellular plaques formed from amyloid β (Ab) peptide and the intraneuronal neurofibrillary tangle (NFT), which is formed from microtubule-associated protein tau (MAPT). The genes encoding amyloid β precursor protein (APP) and presenilin 1 (PSEN1), presenilin 2 (PSEN2) are particularly associated with Alzheimer's disease.

The protein (APP) is formed by the enzymes β - and γ -secretase. During subsequent aggregation to form oligomers, fibrils and extracellular plaques develop. Various isoforms have been observed, which can be between 38 and 43 long. The main identified form is A β 40. However, A β 42 is more affine to aggregation. Hence, it is an important factor in AD pathology. Point mutations in the APP, presenilin 1 (PSEN1) or presenilin 2 (PSEN2) gene, promote an accumulation of the A β peptides. Dysfunction of the relationship between the control mechanisms A β clearance and the accumulation of A β production leads to tau hyperphosphorylation. Further formation of intracellular fibrils can lead to synaptic and neuronal losses and thus also to inflammatory reactions. Several animal models were created to analyze AD pathology. The mouse model 5xFAD is one of them. Mice of the 5xFAD model developed parenchymal plaque load at only two months of age. Furthermore, high APP expression identifications were identified in the mice; these are indicators of increasing stress and thus also an accumulation of amino acid types of A β . In addition, mice of the 5xFAD model show a hippocampus-dependent memory impairment and plaque pathology. At the age of 6 months, behavioral deficits in fear conditioning appear. The Alzheimer's disease mouse model, 5xFAD, was developed to overexpress the APP. The APP carries the Swedish (K670N, M671L), Florida (I716V),

and London mutations (V717I) as well as the human PS1 with the M146L and L286V mutations¹⁷⁷⁻¹⁷⁹. So as to characterize the transgenic 5xFAD mice, both transgenic and non-transgenic littermates were examined and compared. Examinations of the brain regions showed, an increased development of plaque load, as well as in the prefrontal cortex, cortex layer 5, and amygdala at the age of 2-3 months. From about the 4th month onwards, plaque loading can also be observed in the hippocampus and after about 8 months in the striatum. In addition, movement problems are observed at the age of 8-9 months. The elevated plus maze is an indicator of anxiety. Healthy wild-type mice tend to avoid open arms because they seek protection. In transgenic 5xFAD mice spend more time in open arms. The animal models known and developed today do not display a perfect representative of the human organism. However, they help to reflect aspects of the pathological pathology and thus allow us to generate a better understanding. The 5xFAD mouse model is also a great source for research for immunohistochemical and molecular studies.

4.10.1. Transgenic rat

In the last few decades, transgenic animals have been an important research tool. Transgenic rats represent an important resource for gaining new knowledge on gene functions in a wide variety of disease models. The production of transgenic mice is now widespread. As a result, the rodent is a good study model for human diseases. Research has now counted more than 250 strains of rats. Including those with targeted mutations so that researchers can study the various degrees of function loss. In addition to the extensive data available on the rat model, the practical size and the similarity of the animal's physiology to that of humans make it a good choice. The rat has also been used as a research animal in the field of strokes for decades. Its Genome Database (<http://rgd.mcw.edu/>) houses a lot of information for comparing genomics. Transgenic rats and mice have similar production methods: microinjecting DNA; isolating eggs; and identifying pregnancy. The methods might be similar but there is a significant difference in the actual production. These are in the process of superovulation and culture. The transformation rates in rats are approximately 0.2% and 3.5% of the injected eggs. With the help of hormone treatments, donor animals are brought to superovulate. The reason for this is to increase the rate of eggs available for manipulation. Serum gonadotropin (PMSG) from pregnant mares and human chorionic gonadotropin (HCG) are consumed during superovulation. Furthermore, follicle-stimulating hormone (FSH) can also be used for superovulation. In the next step, is to match females with fertile males.

The CRISPR / Cas9 method also revolutionized the production of transgenic rats because the CRISPR / Cas9 technology allows site-specific single-copy transgene integration. Specific chromosome breaks are induced using the Cas9 protein. These, in turn, stimulate the cellular DNA repair machinery in rat zygotes. Transgenes are inserted at specific locations, through a homology-directed repair mechanism. In addition to pronuclear microinjection, electroporation is also used for the administration of CRISPR / Cas9 reagents. Under controlled and optimal conditions, rat production can offer a success rate comparable to that of transgenic mouse production.

4.11. CRISPR/Cas

One of the breakthroughs in genome editing was establishing a simple method for inactivating, exchanging, or completely deleting genes. But at the same time, with an accuracy that enables researchers to switch off specific genes or insert new sections into these gaps simultaneously. As a result, it opens a quick method for genetic modification and an exact one at the same time. This method is applicable to humans, as organisms with nucleated cells. The main findings in this new method are the CRISPR (Clustered Regularly Interspaced Short Palindromic Repeats), repetitive DNA sections can be found commonly in bacteria and archaea genomes. The enzyme Cas9 is made up of two subunits; the RNA is embedded between the α -helix and the endonuclease domain. The HNH nuclease member domain, and the Cas9 enzymes, bind and cut the DNA strand attached to the crRNA while the opposite strand of RuvC is cut. The principle of the so-called genetics is described as simple and precise. To do this, however, various factors must be precisely coordinated. Since the first discoveries in 1987¹⁸⁰, this has still not fully explained how CRISPR / Cas9 works. Japan-based researchers made an unexpected discovery, a repeating region in the genome of bacteria. Although the meaning of this finding was unclear for many years, it became relevant very quickly by the year 2000 at the latest¹⁸¹. The so-called members of these Short Regularly Spaced Repeats (SRSRs) are first listed with their sequences. Two years later, the term CRISPR and the associated enzymes were discovered¹⁸². In phage infection, the acquisition machinery (Cas1, Cas2, and Csn2) builds a spacer into the CRISPR array. This consists of the invasive genetic code. The newly installed spacer is then co-transcribed with the remaining spacers to form the incomplete CRISPR RNA (pre-crRNA). The tracrRNA is transcribed separately; the crRNA is attached to the pre-crRNA repeats with the help of RNase III cleavage, among other things. Finally, the guide sequence is trimmed to 20nt at its 5' ends of the crRNA. Subsequently, the mature crRNA-tracrRNA structure binds

to the Cas9 endonuclease and recruits it to cut the foreign DNA, which contains a 20 nt long crRNA-complementary sequence in front of the protospacer adjacent motif (PAM) sequence¹⁸³.

Directs and activates the Cas 9 endonuclease during the interference of the crRNA-tracrRNA structure to cleave unknown DNA¹⁸⁴. The Cas9 enzyme is a 1368 amino acid long enzyme (158,441 Da) with a multifunctional DNA endonuclease domain. It has two different nuclease domains, one HNH-like and one RuvC-like nuclease domain, the first cleaves the DNA strand, which is complementary to the target RNA sequence, the second cleaves the non-target strand. Together they cut dsDNA 3 bp upstream of the PAM. It should also be said that there are more than 40 different Cas protein families, which are divided into three types, Type I-III, they bind and cut double-stranded DNA¹⁸⁵¹⁸⁶. Type IIIb, however, is single-stranded RNA. They have in common that the spacers in bacteria are formed by cas 1 and cas 2. Due to the structural relationship, one assumes a common origin of types I and III¹⁸⁷⁻¹⁸⁹. Nucleases play an essential role in the MIF and MIF-2 characterization and within the CRISPR/Cas machinery. The Cas9 nuclease domains reveal that the Cas9-RuvC domain shows similarities with the retroviral integrase superfamily. The distinctive feature is the RNase-H folding. Another nuclease domain is assigned to the family of the HNH nucleases, which show characteristic $\beta\beta\alpha$ metal folding. The RuvC is known for its double metal ion catalyst mechanism, used for the cleavage of the non-target DNA strand, a single metal ion mechanism is used for the DNA cleavage of the target strand by the HNH nuclease the end. For MIF as well as for MIF-2, the mutation of the conserved glutamic amino acid leads to a reduction or inhibition of the nuclease activity. For the Cas9 enzyme, the conserved base histidine or the aspartate is critical for the nuclease activity. If one of these regions is mutated, the endonuclease activity is inhibited, but binding to DNA is not impaired¹⁹⁰. After the separation of the DNA strand has ended, the cell's repair system is activated. This can be a non-homologous end joining (NHEJ) or homology-directed repair (HDR). During an NHEJ, end products with mutations arise, which is intended to silence a gene permanently. Since the cell can randomly incorporate nucleotides between the DNA break or deletions lead to gene disruption. From a therapeutic point of view, the NHEJ plays an important role in monogenic diseases, as a dominant-negative mutation can lead to a gene knockout. At the same time, this method can be used to switch off a particular gene in certain organisms. However, the repair can also be carried out homologous (HDR). The advantage here is that a selected gene section can be inserted within the breaking point.

4.12. Confocal microscopy analysis

The Leica DMI8 fluorescence wide-field microscope, confocal microscopy (ZEISS LSM 800) was also used here. This use of confocal microscopy is critical for all analyses in which protein intensities are inherent in the nucleus. This is because the necessary control is only given by using the pinhole in confocal microscopy to show the core surface's inner core layers. This made it possible to analyze the protein intensities with the ImageJ image analysis method's help by generating threshold values in the cell nuclei (Dapi). In addition to the pinhole function, other methods of confocal microscopy are essential. The light points captured by a photomultiplier tube through a pinhole are integrated into an image. For this purpose, pixel information is combined. The software displays this information. For an exact position within the cell, the aperture was set below 100 (89), while the total relative protein intensity could be measured by opening the aperture above 100 (300). With the help of GaAsP (Galliumarsenidphosphid) detection and the Airyscan method, further possibilities for qualitative image generation are possible. This leads to a higher quality of the images with confocal microscopy compared to DMI8 fluorescence wide-field microscopy. Besides, the Z-stack function was used not only to generate images but also to enable three-dimensional analysis. The target proteins can be localized and compared in different layers.

4.13. Statistics

To quantitatively analyze the results, GraphPad PRISM has been used. Differences between groups were determined either by one-way ANOVA, unpaired Student's t-test, or, if different, marked in the legend. A p-value < 0.05 was considered significant.

To quantitatively analyze the results, GraphPad PRISM has been used.

5. Results

5.1. Initial results

In 2016, MIF was identified as a member of the PD-D/E(x)K nuclease family, which includes restriction enzymes such as EcoRI, EcoRV, ExoIII, and PvuII4. ¹¹⁶. The critical residue for nuclease activity was discovered in previous studies as the glutamic acid at position 22. Our study has confirmed this. The glutamic acid at this point is largely preserved in other organisms. This residue was replaced by a glutamine (Q) in this study. This has an uncharged side chain, whereas the glutamic acid is negatively charged. In this study, the inhibition of the MIF nuclease activity has been validated by cloning the E22Q region in human MIF. This served to validate the study results from 2016. This also enabled the purity of the in-house purified MIF and MIF-2 proteins to be verified. It was given as a control for the nuclease reactions that chelate the Mg²⁺ ions, but contamination of DNase can also be inhibited since DNases are also Mg²⁺ and Ca²⁺ dependent. Therefore, a mutation of the critical core regions is mandatory to confirm the purity of MIF and MIF-2 recombinant house-purified proteins. C8 / nativ or C18 / nativ purifications grade was used for all nuclease experiments. Coomassie stainings also attest to the purity of the C8 / nativ and C18 / nativ proteins (Figure 5-1 A, E).

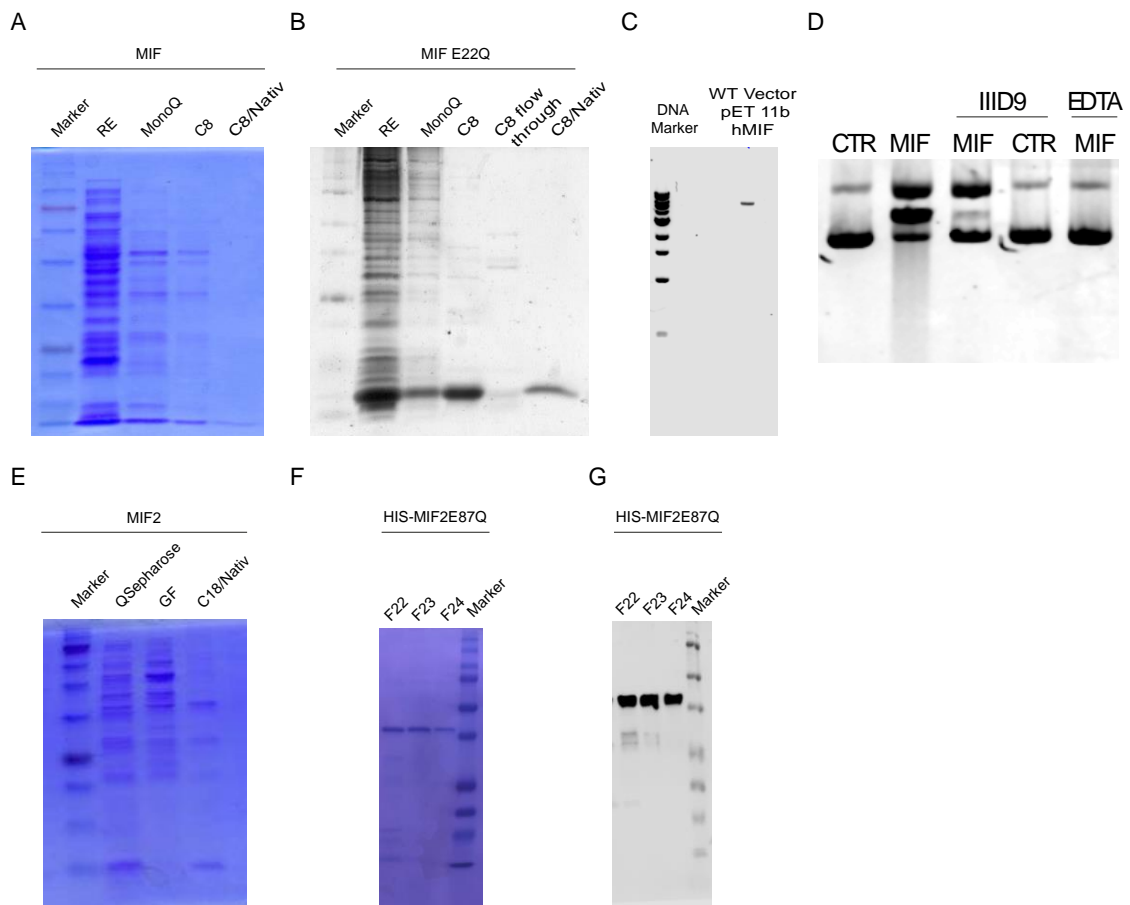


Figure 5-1: Presentation of the purity of the in-house produced recombinant MIF, MIF-2, and their mutants. (A) Coomassie staining of human MIF: raw extract (RE), MonoQ fraction, C8 column fraction, and nativ state of the C8 fraction. The samples and staining were prepared by Simona Gerra. (B) Coomassie staining of human MIF E22Q mutant: raw extract (RE), MonoQ fraction, C8 column fraction, C8 flow-through, and nativ state of the C8 fraction. (C) Agarose gel showing the cloning of the MIF mutant using the vector pET 11b. (D) *In vitro* agarose gel electrophoresis of human MIF (2 μ M) in a nuclease assay with plasmid DNA as the substrate. The assay was performed in a buffer containing Mg²⁺ (10 mM) with or without EDTA (50 mM) and with and without 400 nM (55 μ g/mL) IIIID9. (E) Coomassie staining of human MIF-2: QSepharose fraction, gel filtration fraction (GF), and nativ state of the C8 fraction. (F) Coomassie staining of human MIF-2 E88Q mutant: QSepharose fraction 22-24. (G) Western blot analysis of MIF-2 E88Q mutant in QSepharose fraction 22-24. The presented images and assays demonstrate the purity of the in-house produced recombinant MIF, MIF-2, and their respective mutants. Coomassie staining provides visual evidence of the protein fractions obtained through various purification steps. Agarose gel electrophoresis reveals the successful cloning of the MIF mutant, and the nuclease assay indicates the enzymatic activity of human MIF. Additionally, Western blot analysis confirms the presence of the MIF-2 E88Q mutant in the respective QSepharose fraction. Experiment shown in A has been performed by Simona Gerra.

At the outset of this study, we chose to use in-house purified MIF-2 as a control group. While the recombinant MIF-2 proteins undergo the same purification steps as human and mouse MIF, there are minor differences in their linear primary amino acid sequences, which focus on the nuclease domains postulated by Wang et al. in 2016.

This led us to initially hypothesize that MIF-2 may not share nuclease activity with its paralog MIF. However, our experimental results rejected this hypothesis. The agarose nuclease assay and the real-time nuclease assay both demonstrated nuclease activity for MIF-2, digesting plasmid DNA and probes that form hairpins. The differences between the amino acid sequences of MIF and MIF-2, particularly in the PD-D/E(x)K nuclease domains, will be explained below. However, it is important to note that the critical glutamic acid at position 22, which was first highlighted by the Dawson Lab, is conserved in a wide range of organisms (Figure 5-2). Although some domains are only partially conserved in the zebrafish and gorilla, the glutamic acid at position 22 is conserved in all organisms listed (Figure 5-2).

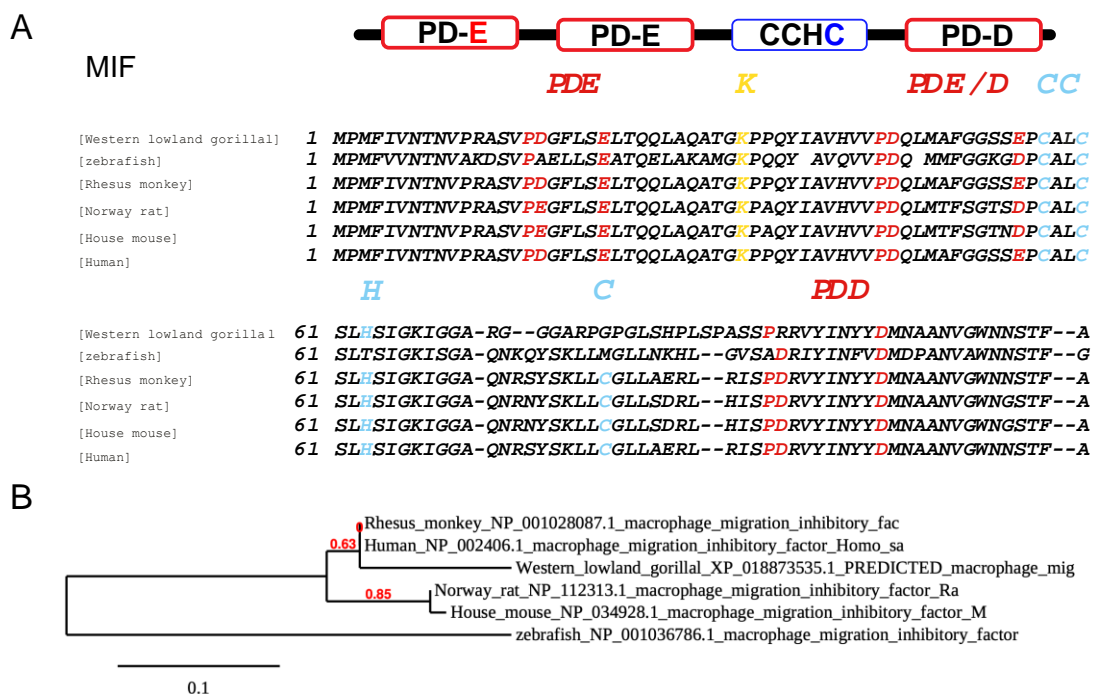


Figure 5-2: Representation of the sequence analysis of a variety of animals as well as human MIF and their schematic phylogenetic tree with the focus of the nuclease domains.

(A) Sequence alignment of MIF amino acid sequences from different animals and humans, emphasizing the conserved nuclease domains. The PD-D/E(x)K nuclease domains, characterized by the presence of glutamic acid at position 22, are highlighted. The PDE and PDD domains are marked in red, while the zinc finger domain is marked in blue.

(B) Phylogenetic tree generated using the amino acid sequences of MIF from the organisms depicted in panel A, with a specific focus on the nuclease domains. The tree was constructed using the Phylogeny.fr tool (<http://www.phylogeny.fr>).

The sequence alignment provides an overview of the similarities in the nuclease domains of MIF across various animal species and humans. The conserved PD-D/E(x)K motifs, along with other relevant domains,

are highlighted. The phylogenetic tree presents the evolutionary relationships between these organisms based on the sequence similarity of their MIF proteins, with a particular emphasis on the nuclease domains. The analysis was performed using the Phylogeny.fr tool, aiding in the visualization of the evolutionary conservation of MIF and its nuclease functionality among different species.

Before delving into the details of the MIF-2 nuclease domains and the related phylogenetic tree, we will briefly highlight the differences in expression levels between MIF and other nucleases or actors in context. MIF is expressed in the regions mentioned in Figure 5-3 of the brain, but to a slightly varying extent. When compared with other nucleases such as DNA2 or flap nuclease (FEN1) and their receptors, MIF shows a higher expression level. Important questions related to the expression level include differences in expression within organs, cell types, and gender, as well as whether the expression levels of the individual components listed change between the adult and fetal stages, or between diseases in general or neurodegenerative diseases. It would also be interesting to analyze whether MIF or MIF-2 knockout differs in single-cell RNAseq expression levels from other proteins that are normally expressed under healthy and diseased conditions. Additionally, it would be of interest to examine the expression levels in the event of a knockout of both genes, MIF and MIF-2^{195,196}.

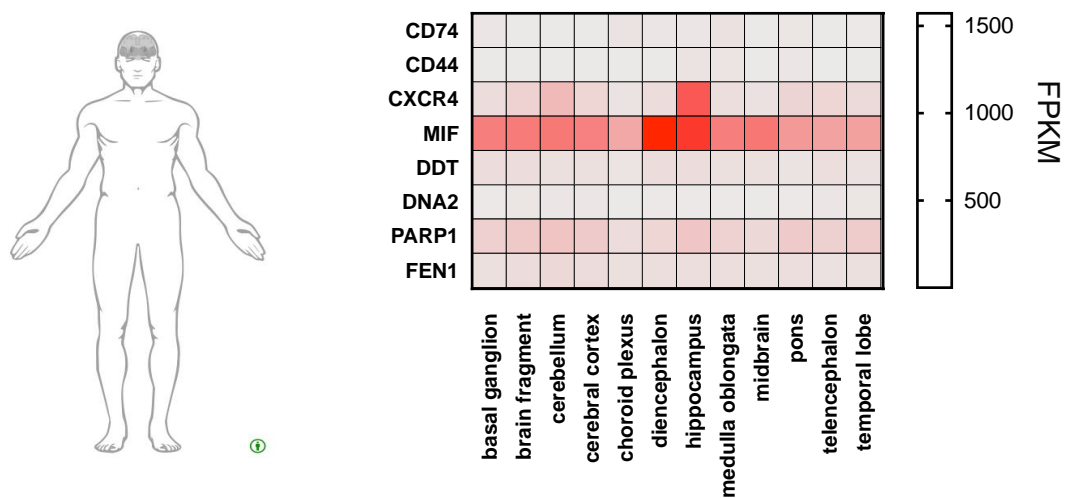


Figure 5-3: Heatmap of MIF family proteins and their receptors, nucleases DNA2 and FEN1 as well as PARP1 in human tissues.

This heatmap represents the reanalysis of RNA-seq data obtained from 53 human tissue samples from the Genotype-Tissue Expression (GTEx) Project dataset. The focus of this reanalysis was on the expression patterns of MIF family proteins, their corresponding receptors, nucleases DNA2 and FEN1, as well as PARP1. The analysis was performed using RNA-seq data of coding RNA in Human Developmental Biology Resource (HDBR), specifically investigating prenatal human brain development. The heatmap visually

illustrates the expression levels of these genes across multiple tissue types, highlighting potential patterns and differences in their expression profiles¹⁹⁷.

5.2. Nuclease properties of MIF and MIF-2

This study highlights that MIF-2 as MIF paralogues share the newly discovered enzyme functions as a nuclease. However, it is not seen as a backup protein. Therefore, it is pending that a deficiency of one of the MIF-like proteins can partially compensate for the phenotype. Highlighting human fetal development in the weeks after conception and in the Carnegie phase, MIF shows higher expression levels than MIF-2. In addition, CXCR4 has a higher expression level among the known receptors, which were provided in the bulk RNAseq study (Figure 5-4). The well-known MIF receptor, CXCR4, is being investigated in various autoimmune diseases, including rheumatoid arthritis and autoimmune diseases of the central nervous system such as multiple sclerosis. In addition, it is assumed that leukocyte chemotaxis plays an important role in certain inflammatory disorders. The CXCL12 / CXCR4 axis is of great importance in homing stem and progenitor cells in the bone marrow^{198,199}. It is also assumed that the CXCR4 signaling pathway plays an important role in the clustering activity of neurons in vitro as well as for dorsal root ganglia (DRG) accumulation²⁰⁰.

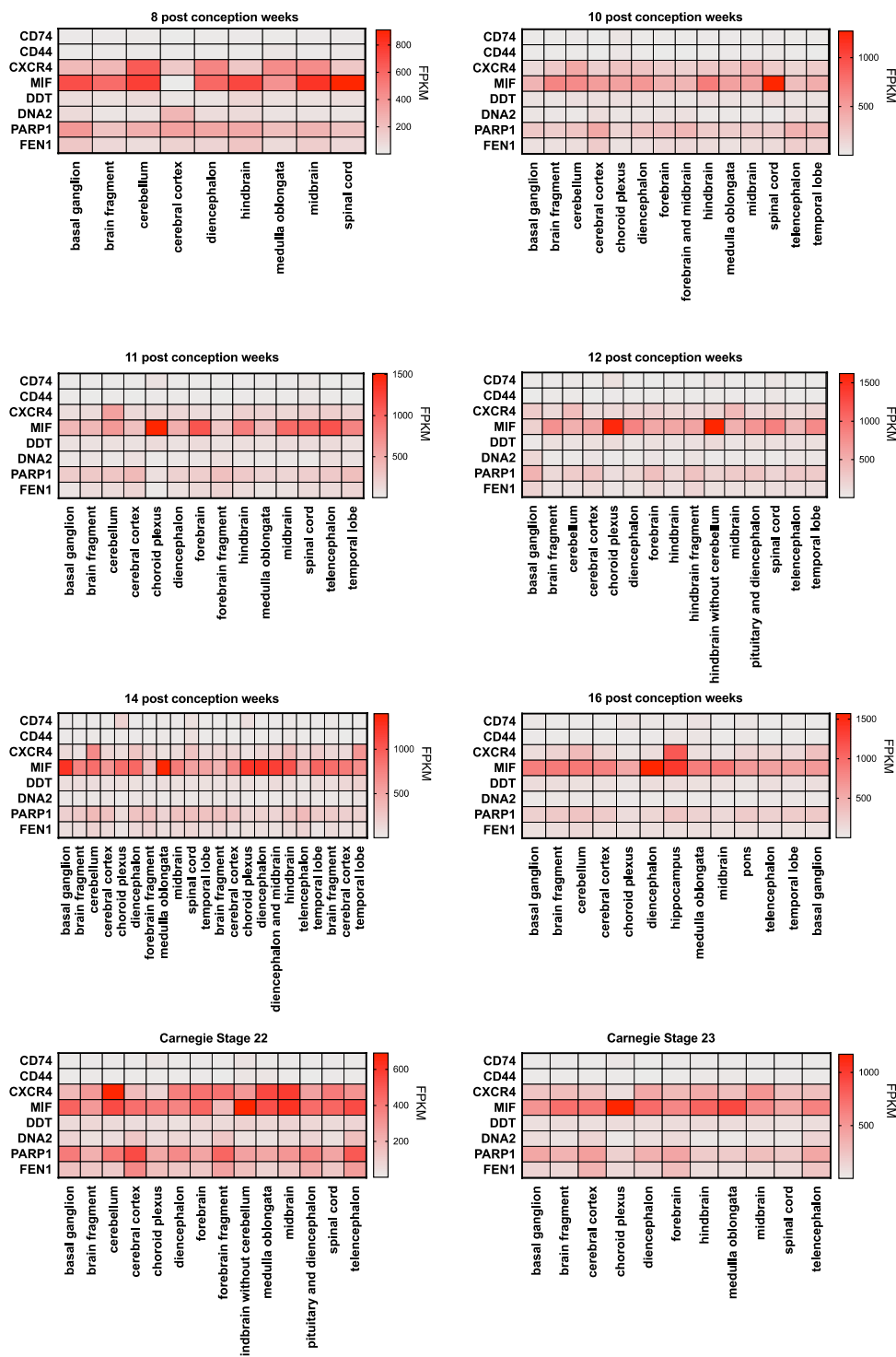


Figure 5-4 : Heatmap of MIF family proteins and their receptors, nucleases DNA2 and FEN1as well as PARP1 during prenatal human brain development.

This heatmap presents the reanalysis of RNA-seq data obtained from 53 human tissue samples sourced from the Genotype-Tissue Expression (GTEx) project dataset. The focus of this reanalysis was to investigate the expression patterns of MIF family proteins, their associated receptors, nucleases DNA2 and FEN1, as

well as PARP1 during prenatal human brain development. The analysis utilized RNA-seq data derived from coding RNA in the Human Developmental Biology Resource (HDBR), specifically focusing on prenatal human brain development. The heatmap visualizes the expression levels of these genes across different stages of prenatal brain development, providing valuable insights into their temporal expression patterns and potential regulatory dynamics. The reanalysis of the GTEx project dataset, combined with the Human Developmental Biology Resource (HDBR) expression data, enhances our understanding of the intricate roles played by MIF family proteins, their receptors, nucleases DNA2 and FEN1, and PARP1 in the developmental processes of the human brain. The Expression Atlas (www.ebi.ac.uk)¹⁹⁷. served as the data source for the prenatal human brain development expression resource, contributing to the comprehensive analysis of these genes during crucial stages of brain development.

The distribution of MIF, MIF-2 and the proteins in the various cell types was examined. Whereas FEN1 is mostly less expressed than MIF, there is an exception in the erythroblasts. Here is a significant increase in FEN1 expression in the study of the BLUEPRINT epigenome project^{201,202}. The tasks that FEN1 is assigned to, are linked to the body's DNA replication and repair. FEN1 is a Mg²⁺-dependent nuclease with 5'-flap endonuclease and 5'-3'exonuclease activities. The DNA polymerase cleaves the 5'overhanging valve structure that meets the 5' end of a downstream Okazaki fragment. It is also related to mitochondrial DNA repair. However, the data also shows a higher expression of PARP1, MIF, and partly of MIF-2 with other nucleases, which are also associated with the caspase-independent apoptosis pathway. A correlation between MIF, MIF-2 expression level, and that of PARP1 cannot be verified based on the study results. Furthermore, no statement can be made as to whether there is a connection between EndoG and MIF expression levels. It would be interesting here, to find out whether the MIF-2 expression levels change with MIF low expression levels in human or *Mif KO* in animal models and whether it has an effect on other proteins such as PARP1²⁰³. If one compares the receptors, the expression levels of CXCR4 stand out and do so again while comparing different cell types and that of CD74. So when we compare proteins such as PARP1, DNA2, and mTOR, with each other and with other proteins, the expression levels stand out^{204,205}. Whether MIF and MIF-2 levels are compared in the various age- stages of embryonal development or between the cell types, the function of the multipotent proteins cannot be directly concluded. Naturally, an increase in the associated receptors and their downstream pathways indicate their possible role. However, the topology of MIF and MIF-2 within the cell is decisive for their function. Various locations within the cell were observed before the nuclease function for MIF was not even recorded yet²⁰³. In summary, this study showed that the multipotent proteins MIF and MIF-2 can perform different tasks. They are also described as moon-like enzymes because their activity adapts to the function of the areas and circumstances

surrounding the cells. Above all, the topological localization within the cell plays a significant role in the activity of MIF and MIF-2. For this reason, it would be interesting in future studies to distinguish between organs or cell types and between individual cell segments, especially with a view to neurodegenerative diseases.

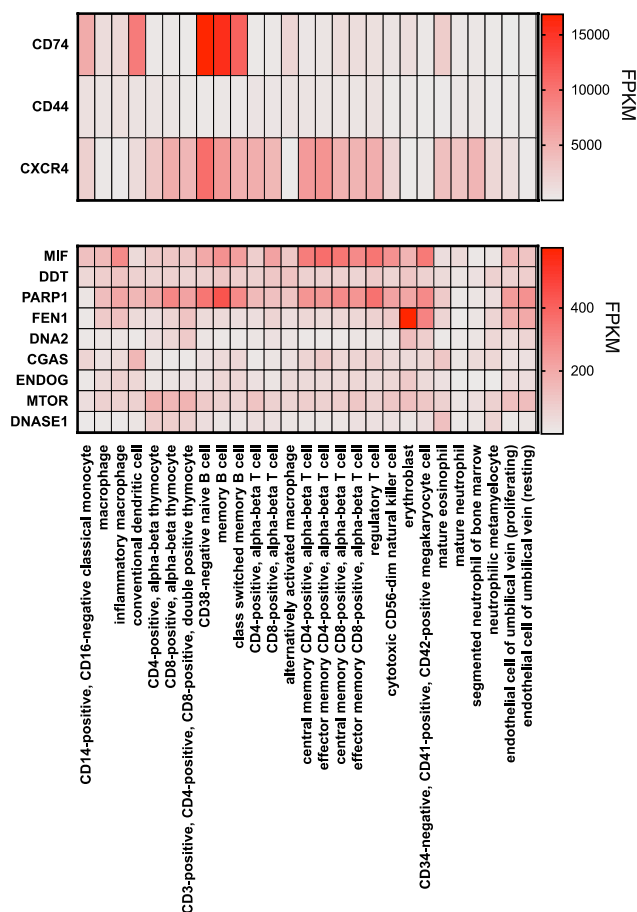


Figure 5-5: Heatmap of MIF-receptor family proteins, nucleases (*DNA2*, *Dnase1* and *FEN1*), proteins involved in DNA sensing process (Cyclic GMP-AMP synthase (*CGas*)) and mechanistic Target of Rapamycin (*MTOR*).

This heatmap represents a comprehensive reanalysis of strand-specific RNA-Seq data derived from rRNA-depleted total RNA obtained from common types of cultured or uncultured primary cells belonging to various hematopoietic lineages. The data was collected from healthy individuals as part of the BLUEPRINT epigenome project. The focus of this analysis was to investigate the expression levels and patterns of MIF-receptor family proteins, nucleases including *DNA2*, *Dnase1*, and *FEN1*, proteins involved in the DNA sensing process such as *CGas*, and the mechanistic Target of Rapamycin (*MTOR*) across different haematopoietic lineages²⁰¹.

To assess high expression levels of MIF-associated proteins in adult humans, we can analyze their distribution in the lungs and spleen and compare it to other tissues. CXCR4

receptor expression is notably high in the blood and spleen, whereas MIF-2 shows higher expression levels in the liver^{197,206}.

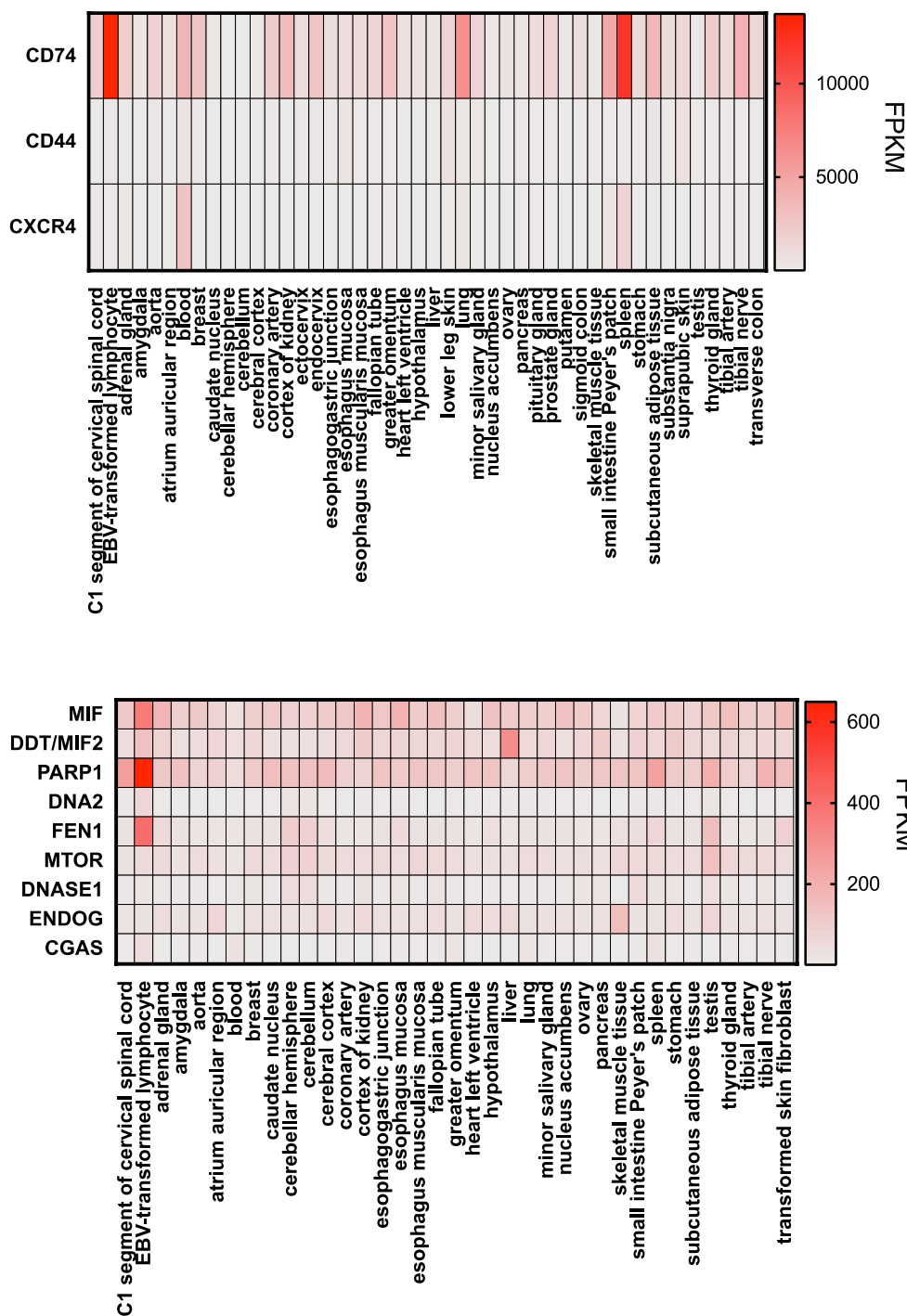


Figure 5-6 : Heatmap of MIF family proteins and their receptors, nucleases (DNA2, Dnase1 and FEN1), DNA sensing process proteins (Cyclic GMP-AMP synthase (CGas)) and mechanistic Target of Rapamycin (MTOR).

This heatmap represents a comprehensive reanalysis of RNA-seq data obtained from the Genotype-Tissue Expression (GTEx) Project dataset¹⁹⁷. The analysis focused on examining the expression levels and patterns of MIF family proteins, their receptors, nucleases (DNA2, Dnase1, and FEN1), DNA sensing

process proteins (CGas), and the mechanistic Target of Rapamycin (MTOR) across a variety of tissues. The heatmap provides a visual representation of the expression levels of these genes in different tissues, allowing for a comparative analysis of their expression patterns. By examining the relative expression levels across tissues, this analysis offers insights into the tissue-specific expression profiles of MIF family proteins, their receptors, nucleases, DNA sensing process proteins, and MTOR.

Neurodegenerative disease, is a term, used to refer to a number of diseases of the human brain that all have neuronal cell loss in common. These can be roughly divided into three different classes. Firstly, based on their clinical characteristics (e.g., dementia, Parkinson's or motor neuron diseases). Secondly, based on their anatomical distribution of neurodegeneration (e.g., frontotemporal degenerations, extrapyramidal disorders, or spinocerebellar degenerations) and thirdly, through their main molecular anomalies, these are commonly amyloidosis.

Differences in MIF-associated proteins have been observed in glioma and glioblastoma multiforme tissues when compared to healthy brain tissue. Specifically, the upregulation of MIF-2 becomes apparent in disease-associated tissue. One such protein, S100A9, belongs to the S100 protein family and contains two EF-hand calcium-binding motifs. Like MIF, S100A9 is localized in the cytoplasm and cell nucleus of many cells, and it is involved in cellular processes such as cell cycle progression and differentiation. S100A9 is also a calcium and zinc-binding protein. S100A9 is a calcium and zinc-binding protein that plays a key role in inflammatory process regulations. This makes it very interesting in the context of MIF family members. It is also known for its apoptosis-inducing activities or for promoting cytokine and chemokine production^{207,208}. In addition, it belongs to the class of alarmin or a danger-associated molecular pattern (DAMP)²⁰⁹. The protein S100A9 is often mentioned in studies together with MIF-2. In addition, MIF is associated with the protein BAZ1A (Bromodomain Adjacent To Zinc Finger Domain 1A) in the context of the pathway of liver fibrosis²¹¹ (Figure 5-7).

In summary, the expressions of the degrees of the listed comparative proteins between that of the regular and daily stages cannot give any direct information about the function of MIF and MIF-2. Each can provide information on the possible interaction partners that have not yet been discovered.

Within this study, a translocation or an enrichment of MIF and MIF-2 in the nucleus could be shown. At the same time, the enrichment of AIFs was also observed. However, no direct evidence of interaction could be provided. For this reason, it would be an exciting challenge to identify a possible third party involved and prove it with various methods.

The translocation results of this study will be discussed in more detail in the following section.

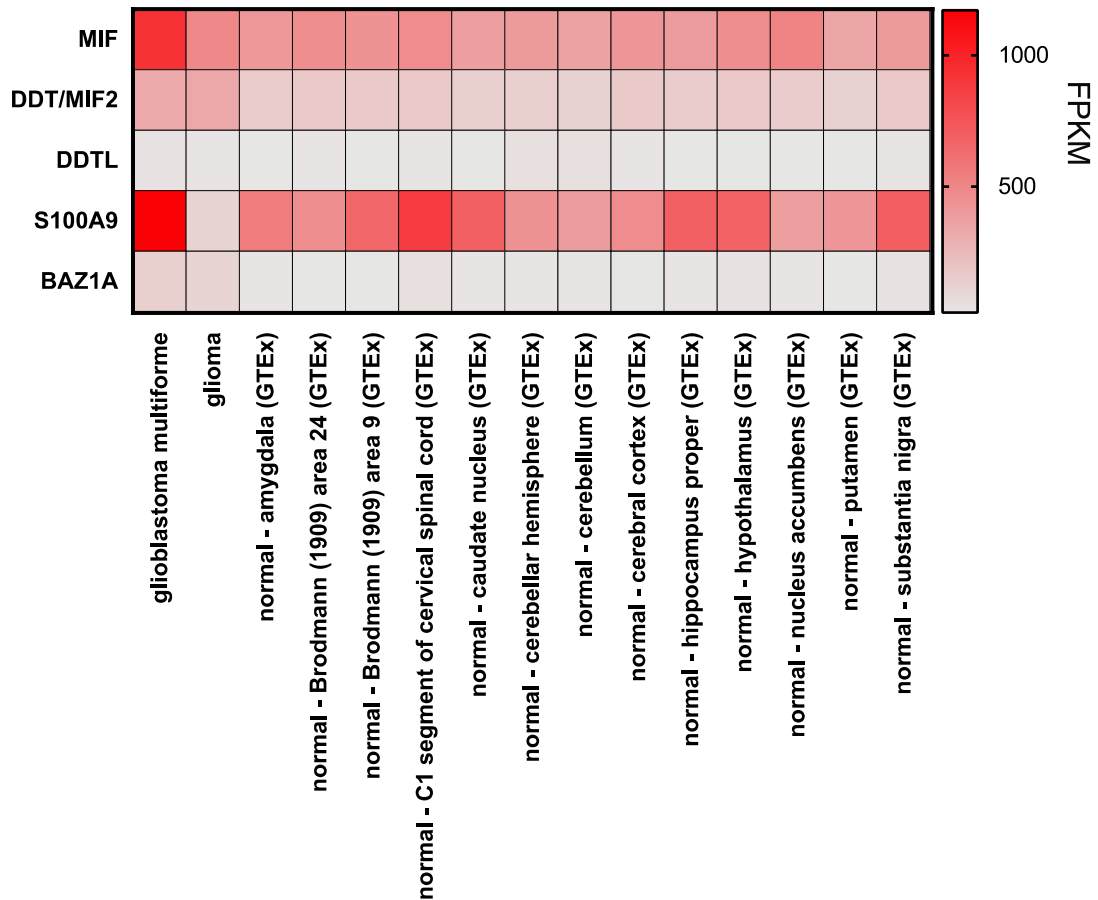


Figure 5-7: Heatmap of MIF family proteins and their receptors, S100A9 also known as migration inhibitory factor-related protein 14 (MRP14), and Bromodomain Adjacent to Zinc Finger Domain 1A, including (BAZ1A).

This heatmap represents a reanalysis of RNA-Seq mRNA baseline data obtained from the International Cancer Genome project, specifically the Pan-Cancer Analysis of Whole Genomes (PCAWG) dataset. The analysis focused on examining the expression levels and patterns of MIF family proteins, their receptors, S100A9, and BAZ1A in *Homo sapiens*²¹².

The PCAWG dataset is a comprehensive resource for studying the genomic and transcriptomic alterations in various areas. This reanalysis contributes to our understanding of the transcriptional landscape and potential implications of MIF family proteins, their receptors, S100A9, and BAZ1A.

After a nuclease activity for MIF-2 was observed in this study, important aspects, such as possible contamination by bacterial nuclease, were excluded. The question arises as to which regions in the MIF-2 sequence are decisive for their nuclease activity. In addition, whether MIF-2 will be added to the well-known PD-D / E (x) K family or should be sorted into a different class of nucleases. When the crystal structures of human MIF and mouse MIF are superimposed, it turns out that the glutamic acid at position 88 for MIF-2 folds to the same position where the glutamic acid is at position 22 of MIF. So the

protein structure is conserved, whereas the amino acid sequence is only partially conserved or even differently at point 22 of MIF.

PD-D / E (x) K domains for MIF and MIF-2 are:

Human MIF (P16D17E22K33) (P44D45E55K67) (P92D93E81K)

Human MIF-2 (P16E20E88) (P44D7E55) (P102E104D94).

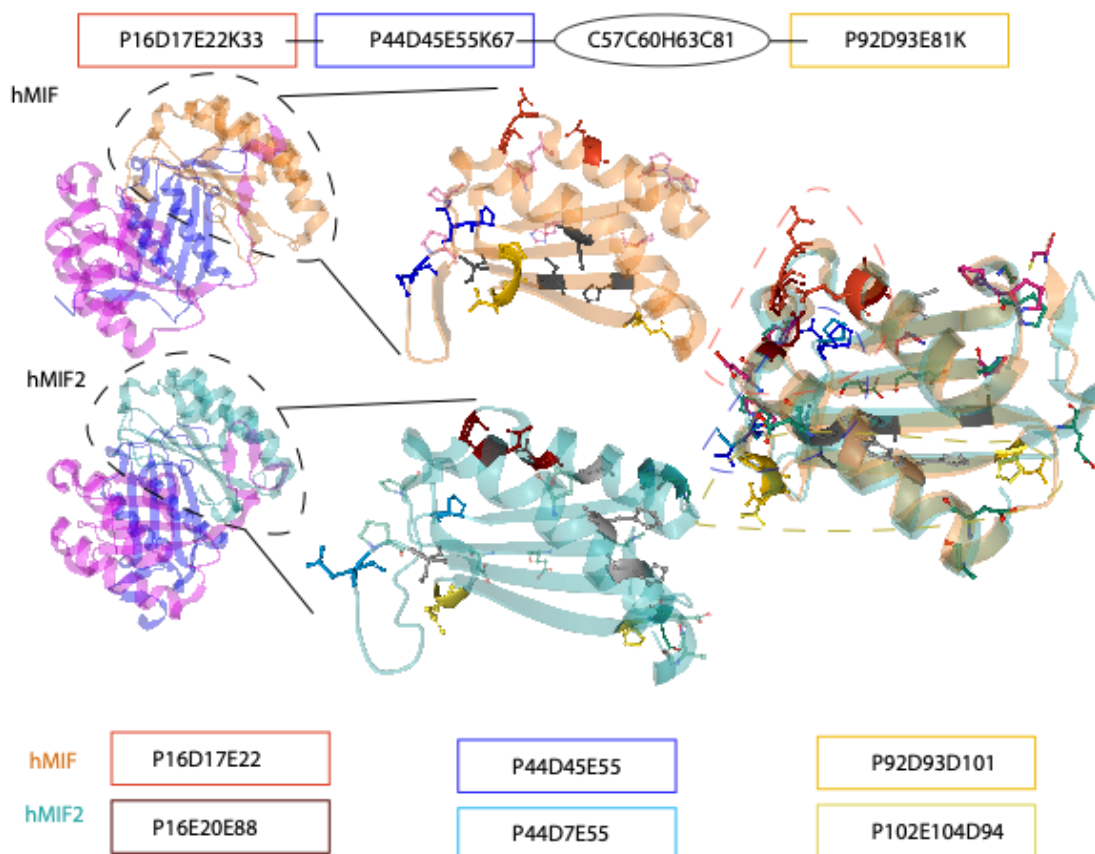


Figure 5-8: Identifying the possible Nuclease domains by the crystal structure of human MIF and MIF-2. The crystal structure was generated using PDP protein data bank tools (<https://www.rcsb.org>). human MIF and human MIF-2 nuclease domains are highlighted. Different red colors are representing first PDE or PEE domain, blue colors representing the second PDE domain and yellow colors are representing the third inspected PDE or PDD domain. In grey zinc finger domains are visualized.

Since similar PD-D / E (x) K domains can also be identified for MIF-2, we assume that MIF-2 can also be counted to the same group of nucleases. However, the assignment of the zinc finger domain cannot be done simply. Two different structures for MIF and MIF-2 were observed here.

The zinc finger domain of MIF-2 may bear little resemblance to the class of zinc fingers to which MIF (CCHC superfamily) also belongs²¹³. While in hMIF the zinc domain consists of (C57C60H63C81), in MIF-2 a possible zinc finger domain is C24C57H77H80

(Figure 5-8). From what we know, it is assumed that the MIF-2 zinc finger motif can be classified among those of the C2H2 zinc fingers^{214,215}. Zinc finger (Znf) domains, have in their structure, handles that resemble fingers. These can bind zinc and most other metals, such as iron, but they don't bind to all metals. The binding properties depend, on the amino acid sequence of the zinc finger domain; the structures between the fingers and the properties of the higher structural order, and the number of zinc finger domains. The tasks of zinc finger domains can range from DNA recognition to transcriptional activation or regulation of apoptosis and protein folding^{216,217,218}. Transposable elements occupy significant roles in genome evolution, both in bacteria and eukaryotes^{219–221}. The class of transposases can generally be divided into two groups, forming covalent intermediates with the DNA, including serine or rolling circles, also called Y2 transposases. The second group consists of those collected that do not develop covalent intermediates with the DNA²²². Within the group that does not have a covalent bond with the DNA, the best-known transposases have conserved the DDE motif in their amino acid sequence. They coordinate metal ions, which are required for DNA cleavage²²³. In comparison to MIF-2, two motifs can be compared with the transposases: the DDE motif and the C2H2 zinc finger motif. Similar positions of the two H atoms can be seen in the crystal structure for MIF-2, ISHp608 transposase, and ZBED1.

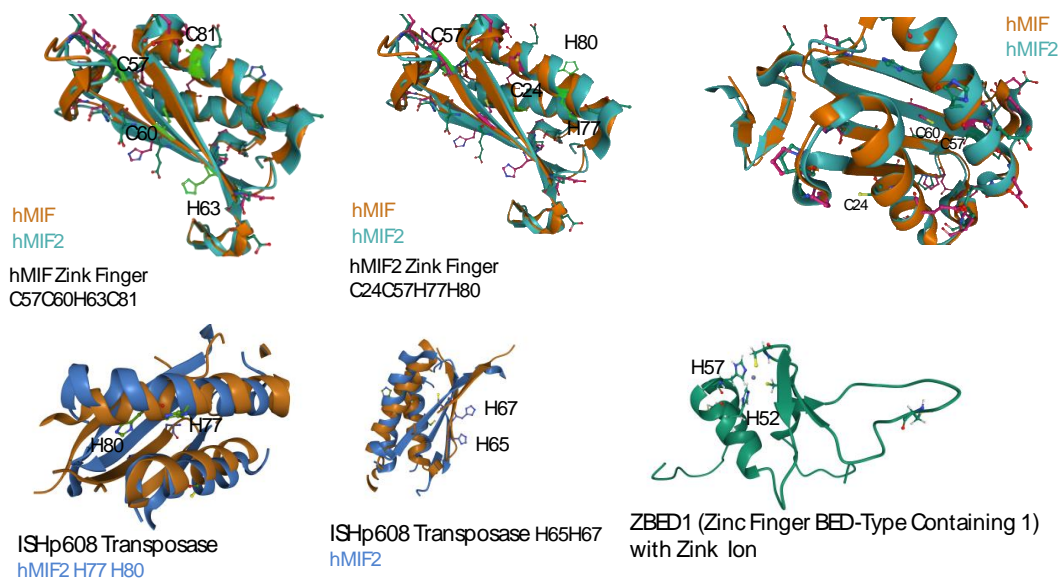


Figure 5-9: Identifying the possible Zinc finger domains.

Human MIF and MIF-2 have been overlaid by using PDP protein data bank tools (<https://www.rcsb.org>). Zinc finger domains were highlighted for human MIF (C57C60H63C81) and for human MIF-2 (C24C57H77H80). ISHp608 transposase was overlaid with human MIF-2, focusing on the zinc finger domain. ZBED1 crystal structure represents a similar zinc finger family as seen for MIF-2 (C2H2- zinc finger motif)

Comparing the zinc finger domain and the nuclease domain, the zinc finger domain C2H2 is only partially conserved within the organisms. Still, the critical region of glutamic acid at site 88 is always conserved (Figure 5-9).

Summarizing the observations of this study and those made in advance regarding MIF and MIF-2 as a nuclease, we arrive at the following findings. We assume that MIF and MIF-2 possess nuclease properties that can be assigned to one or more domains of the PD-D / E(x) K nucleases. The zinc finger domains, however, are different for MIF and MIF-2. Whereas MIF belongs to the CCHC superfamily, we assume that MIF-2 could be assigned to the C2H2 zinc finger family. The critical regions for the nuclease function are possibly E22 for MIF and E88 for MIF-2 since this region shows high evolutionary conservation.

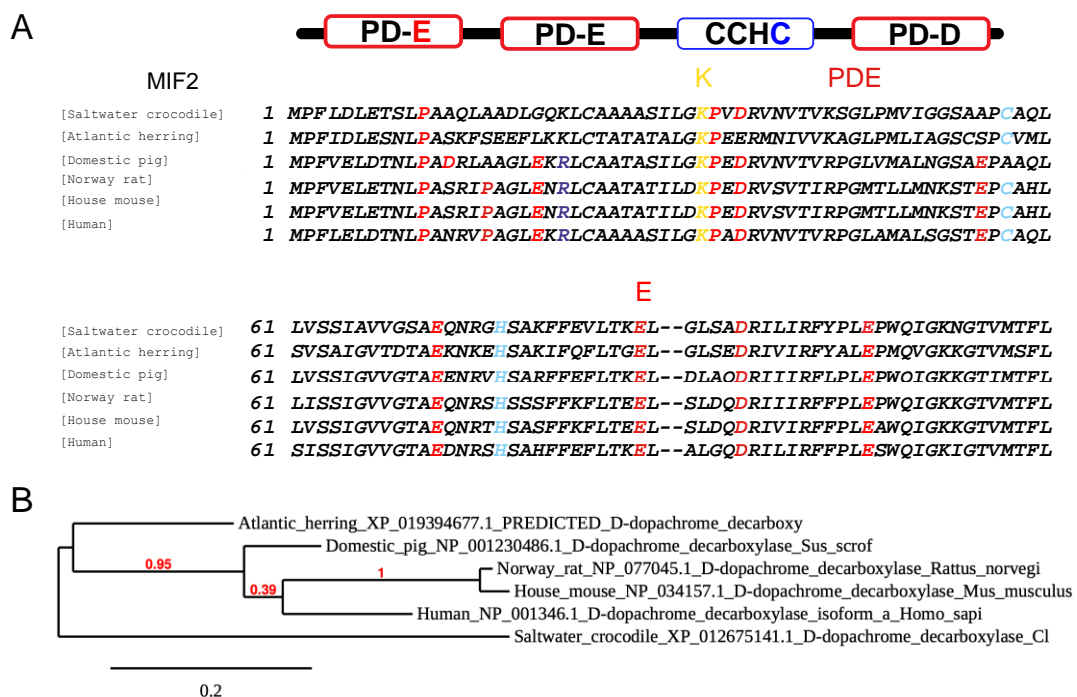


Figure 5-10: Sequence analysis of a variety of animals as well as human MIF-2 and their schematic phylogenetic tree.

(A) Highlighting PD-D/E(x)K nuclease domains with glutamic acid at place 88, which is conserved through the different kingdoms. The PDE and PDD domains are highlighted in red, while the zinc finger is highlighted in blue. (B) Visualization of the variety of organisms used in A with a focus of MIF-2 by generating their Phylogenetic tree (<http://www.phylogeny.fr>).

5.3. MIF-2 is a novel nuclease

In the face of increasing life expectancies and improved health in age, we are facing new medical and scientific challenges. One of these, is the process of apoptosis, in which the critical mechanisms involved are quite complex. Those physiological apoptosis mechanisms are especially relevant, as various factors such as the embryonic development or aging affect the cell and induce an activation of nucleases²⁶⁶. Cell death resulting in DNA degradation also acts as a defense mechanism in immune reactions and also after cell damage by injuries. The focus of this study is on MIF-2 also called D-dopachrome tautomerase (D-DT), which is the paralogue of macrophage migration inhibitory factor (MIF). MIF's active center for tautomerase activity is located at the interface between pairs of subunits (lined with amino acid residues 1, 33-34 and 64-66)^{113,227}. This substrate binding site is highly conserved among the MIF homologues. A new role was only recently discovered for MIF, in addition to the already characterized ones. MIF was found to be the previously unknown nuclease of the AIF dependent apoptosis pathways when screening for AIF interacting proteins. MIF has been classified as a member of the PD-D/E(x)K restriction enzyme family similar to EcoRI, EcoRV, ExoIII and PvuII^{116,117}. However, the state-of-the-art influence of MIF on cell survival and apoptosis is still controversial and not completely understood^{30,116,228-230}. To determine the similarity of the critical nuclease structures, MIF sequence homologues were compared: mouse and human MIF contain PD-D/E(X)K superfamily motifs and the first domain has been identified as the critical domain for MIF nuclease activity. MIF also shares this nuclease motive with other nucleases, such as APEI or the staphylococcal nuclease^{119,160,231}.

5.3.1. MIF-2 exhibits nuclease activity similar to MIF

In this study, we questioned the nuclease function of MIF-2 as a homologue of MIF to further comprehend the physiological role of the MIF family and its potential effects on cell death. Therefore, we first aligned MIF and MIF-2 protein structures. The primary structure of MIF-2 shows only partial conservation of the nuclease critical amino acids. The glutamic acid at site 22 differs in human and mouse MIF-2; as it is replaced by an arginine (Figure 5-11:A). However, the nuclease domains are partially conserved, but rather the zinc finger domain of MIF (CxxCxxHx(n)C) is different in the primary structure compared to MIF-2 (C2H2). The zinc finger is found mainly as a critical factor in DNA-damage-response proteins^{232,233}. To determine whether MIF-2 shares nuclease activity with MIF we incubated plasmid DNA (200ng) with an in-lab purified mouse and human recombinant MIF (2 μ M); MIF-2 (2 μ M); as well as the nuclease deficient mutants human MIF E22Q (2 μ M) and human MIF-2 E88Q (2 μ M); in which glutamic (E) acid is replaced by glutamine (Q). Human and mouse MIF or MIF-2 cleaved plasmid DNA (Figure 5-11: D) in a concentration, and buffer dependent manner (Figure 5-13 A-F). To determine Mg²⁺ dependence, we added EDTA, which inactivates the nuclease activity, by chelating the divalent cation from the buffer (Figure 5-11:D). Next to EDTA, MIF nuclease activity could be decreased by adding IIID9, a known neutralizing anti-MIF monoclonal antibody (clone IIID9, IgG1 isotype)^{234,235} (Figure 5-11:F). These primary sequence analyses indicated partially conserved PD-D/E(X)K nuclease domains. However, three-dimensional (3D) modeling results showed that human MIF-2 (PDB: 6C5F) missing glutamic acid at position 22, is functionally replaced by its glutamic acid at 88 (Figure 5-11:B). This is also observed for mouse MIF-2 (PDB: 3KER) in comparison to human MIF (PDB: 1GDO) (Figure 5-11:C), and when comparing mouse MIF 3D structure (PDB: 2GDG) with mouse MIF-2 (PDB: 3KER) (Figure 5-11:F).

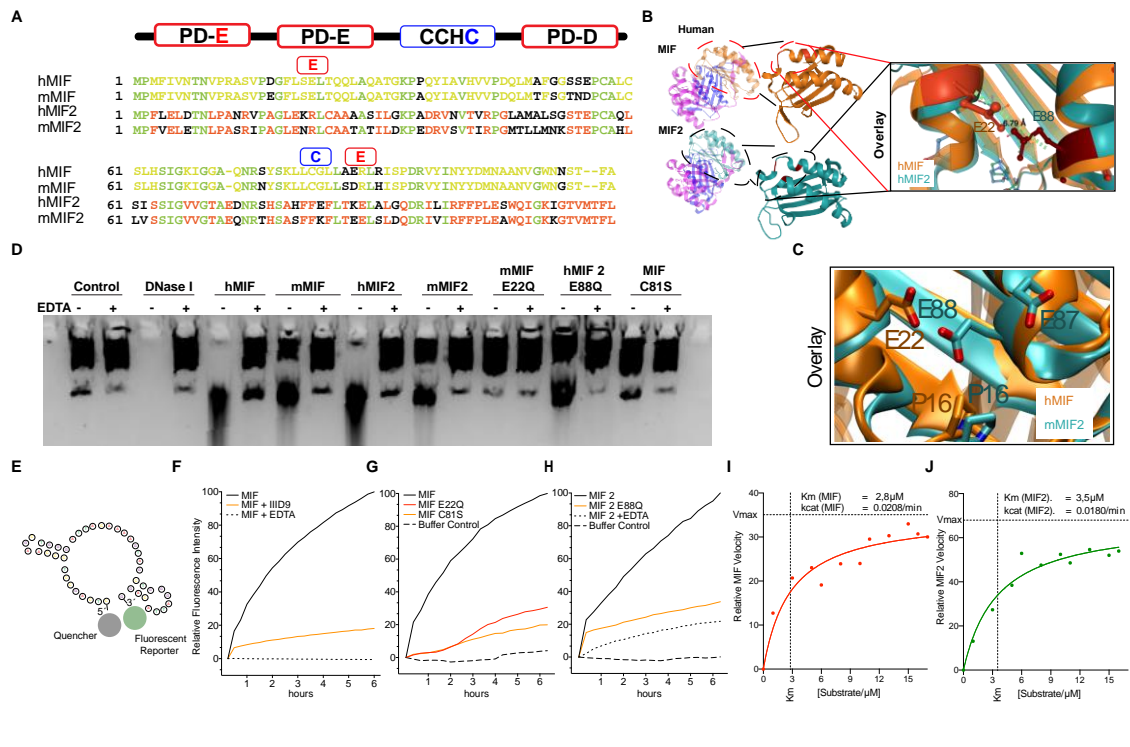


Figure 5-11: MIF-2 nuclease function is conserved within the crystal structure.

MIF and MIF-2 show nuclease function. The critical glutamic acid for the nuclease domains of MIF-2 has been identified at place 88. Real time nuclease assay identifies K_m values of $2.8 \mu M$ for MIF (SEM = 1.483) and $3.5 \mu M$ for MIF-2 (SEM = 1.059). MIF nuclease inhibition shown by MIF E22Q and MIF C81S mutant. IIID9 inhibition of MIF nuclease activity. MIF-2 nuclease inhibition is shown for the MIF-2 E88Q mutant.

(A) Schematic representation of nuclease superfamily PD-D/E(X)K domains and DNA binding zinc finger domains CxxCxxHx(n); A, Ala; C, Cys; D, Asp; E, Glu; F, Phe; G, Gly; H, His; I, Ile; K, Lys; L, Leu; M, Met; N, Asn; P, Pro; Q, Gln; R, Arg; S, Ser; T, Thr; V, Val; W, Trp; Y, Tyr; and X, any amino acid. The color coding of the sequence alignments is according to the conservation, trough MIF and trough species (dark green); trough mouse and human MIF (light green), mouse and human MIF-2 (red); no conservation trough MIF and MIF-2 species (black); (B) Highlighting human MIF and human MIF-2 structural differences, first PDE Domain region and glutamate of human MIF (PDB: 4GUM) position 22 and human MIF-2 (PDB: 6C5F) position 88. (C) Overlay of human hMIF (PDB: 1GDO) and mouse mMIF-2 (PDB: 3KER) Crystal structure, highlighting E, glutamate of MIF position 22 and MIF-2 position 88. (D) In vitro agarose gel electrophoresis of human MIF ($2 \mu M$), mouse MIF, human MIF-2, mouse MIF-2 and mutants ($2 \mu M$) nuclease assay with plasmid DNA as a substrate in buffer containing Mg^{2+} with or without EDTA. (E) Schematic representation of Real time nuclease Probe sequence: CCAAGCTGGGATTACAAAAGTAGCTGGGATTACAGG. (F) Quantification of real time nuclease assay of MIF, $n = 6$ replicates of 3 independent experiments; with and without ($55 \mu g/mL$) IIID9 (IgG), or with and without EDTA, by measuring the relative fluorescence rate. (G) Relative fluorescence rate quantification of real time nuclease assay of MIF, $n = 6$ replicates of 3 biologically independent experiments; MIFE22Q, $n = 4$ replicates of 2 independent experiments; MIFC81S $n = 4$ replicates of 2 independent experiments; buffer control containing Mg^{2+} . (H) Relative fluorescence rate quantification of real time nuclease assay of MIF-2, $n = 6$ replicates of 3 independent experiments; MIF-2E88Q, $n = 4$ replicates of 2 independent experiments; with and without EDTA and buffer control containing

Mg^{2+} . (I) Quantification of Michaelis-Menten constant (K_m) ($2.8\mu M$) and turnover number k_{cat} ($0.0208/min$) for human MIF $n=4$ replicates of 4 independent experiments by real time nuclease assay. (J) Quantification of Michaelis-Menten constant (K_m) ($3.5\mu M$) and turnover number k_{cat} ($0.0180/min$) for human MIF-2, $n=7$ replicates of 4 independent experiments by using the real time nuclease assay.

We monitored the increase of cleaved probe fluorescence signal intensity of MIF, MIF-2 and their nuclease deficient mutant (Figure 5-11.G-H). In the presence of MIF, and MIF-2, fluorescein amidites (FAM) labeled probes with non-identical sequences show a nonlinear regression of the fluorescence signal increase (Figure 5-11 A, C). However, they reach different relative fluorescent intensities. In addition, we compared MIF and MIF-2 with different restriction enzymes (AGEI, EcoRV and EcoRI) as a control since their sequence-specific palindromes cannot be found in our fluorescein-labeled oligonucleotide probes (P6) (Figure 5-12 B, D).

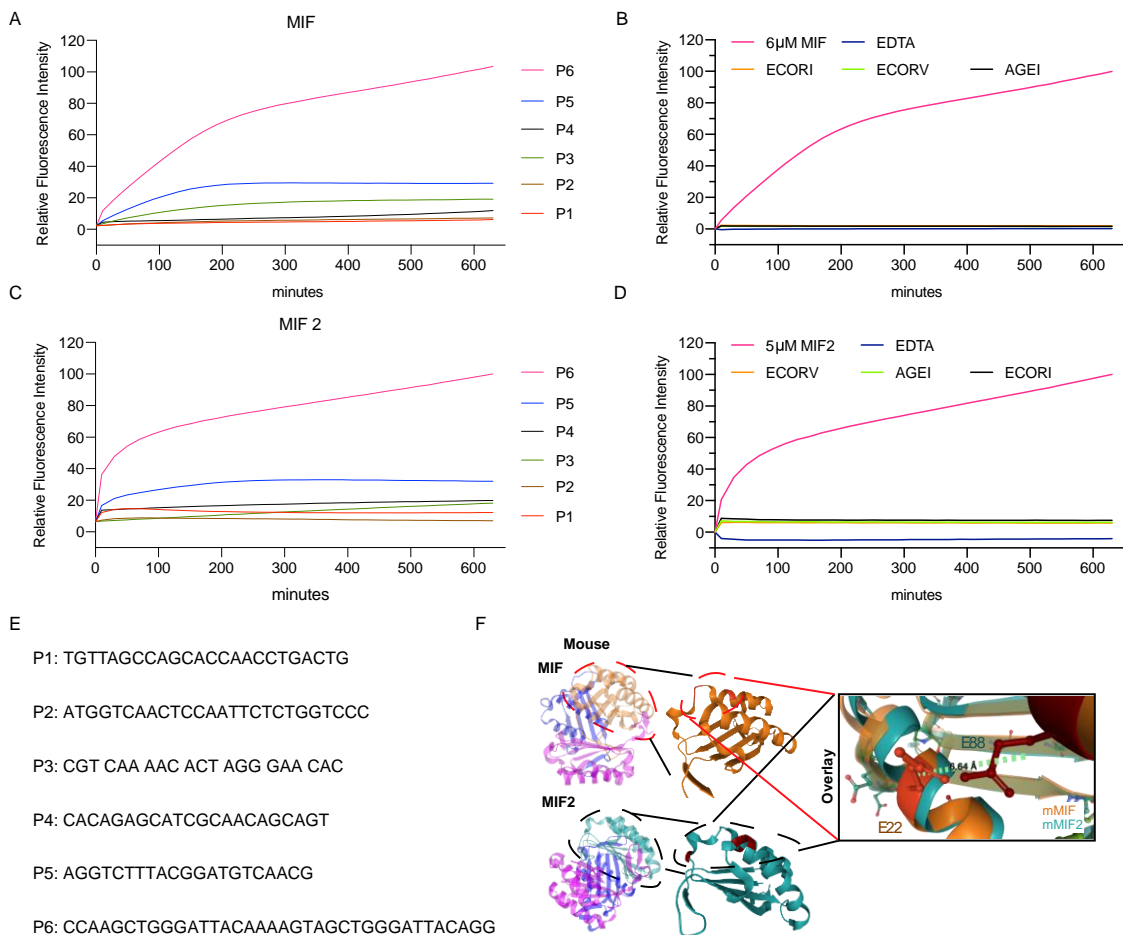


Figure 5-12: Quantification of the relative fluorescence intensity indicates different sequence affinities of MIF and MIF-2 by using the real time nuclease assay.

Results: MIF-2 is a nuclease

Restriction enzymes show no nuclease function for linear substrate without cutting motive, as a negative control. (A) Quantification of the relative fluorescence Intensity by using the real time nuclease assay of human MIF (6 μ M), with different probe sequences P1-P6 (n= 3 replicates). (B) Quantification of the relative fluorescence Intensity of human MIF (6 μ M) with and without EDTA, and ECORI (0.5U), ECORV (0.5U), AGEI (0.5U), P6: CCAAGCTGGGATTACAAAAGTAGCTGGGATTACAGG as substrate (n= 3 replicates of 3 independent experiments); (C) Relative fluorescence rate quantification of real time nuclease assay of human MIF-2 (5 μ M), with different probe sequences P1-P6 (n= 3 replicates) (D) Relative fluorescence Intensity quantification of real time nuclease assay of human MIF-2 (5 μ M) with and without EDTA, and ECORI (0.5 U), ECORV (0.5 U), AGEI (0.5 U), with Substrate P6: CCAAGCTGGGATTACAAAAGTAGCTGGGATTACAGG (n= 3 replicates of 3 independent experiments);. (E) Representative of P1-P6 Sequence code. (F) Highlighting mouse MIF (PDB: 2GDG) and mouse MIF-2 (PDB: 3KER), first PDE Domain region and glutamate of mouse MIF position 22 and mouse MIF-2 position 88.

We further investigated the Michaelis-Menten constant K_m and turnover number k_{cat} and received a K_m value of 2.8 μ M and a k_{cat} of 0.0208/min for human MIF. For human MIF-2 a K_m of 3.5 μ M, and a k_{cat} of 0.0180/min was measured (Figure 5-11:I-J). In addition, with the real-time nuclease method we repeatedly observed a lower cleaved probe fluorescence signal intensity for MIF E22Q nuclease dead mutant and MIF C81S zinc finger mutant, compared to the recombinant MIF fluorescence intensity (Figure 5-11: I). The results seen in Figure 5-11: J also indicate higher cleaved probe fluorescence signal intensity compared to MIF-2 E88Q nuclease deficient mutant. Further, we investigated MIF by incubating it with the MIFIID9 antibody which is also known to inhibit MIF. We found a decreased cleaved probe signal, compared to MIF alone (Figure 5-11).

Results: MIF-2 is a nuclease

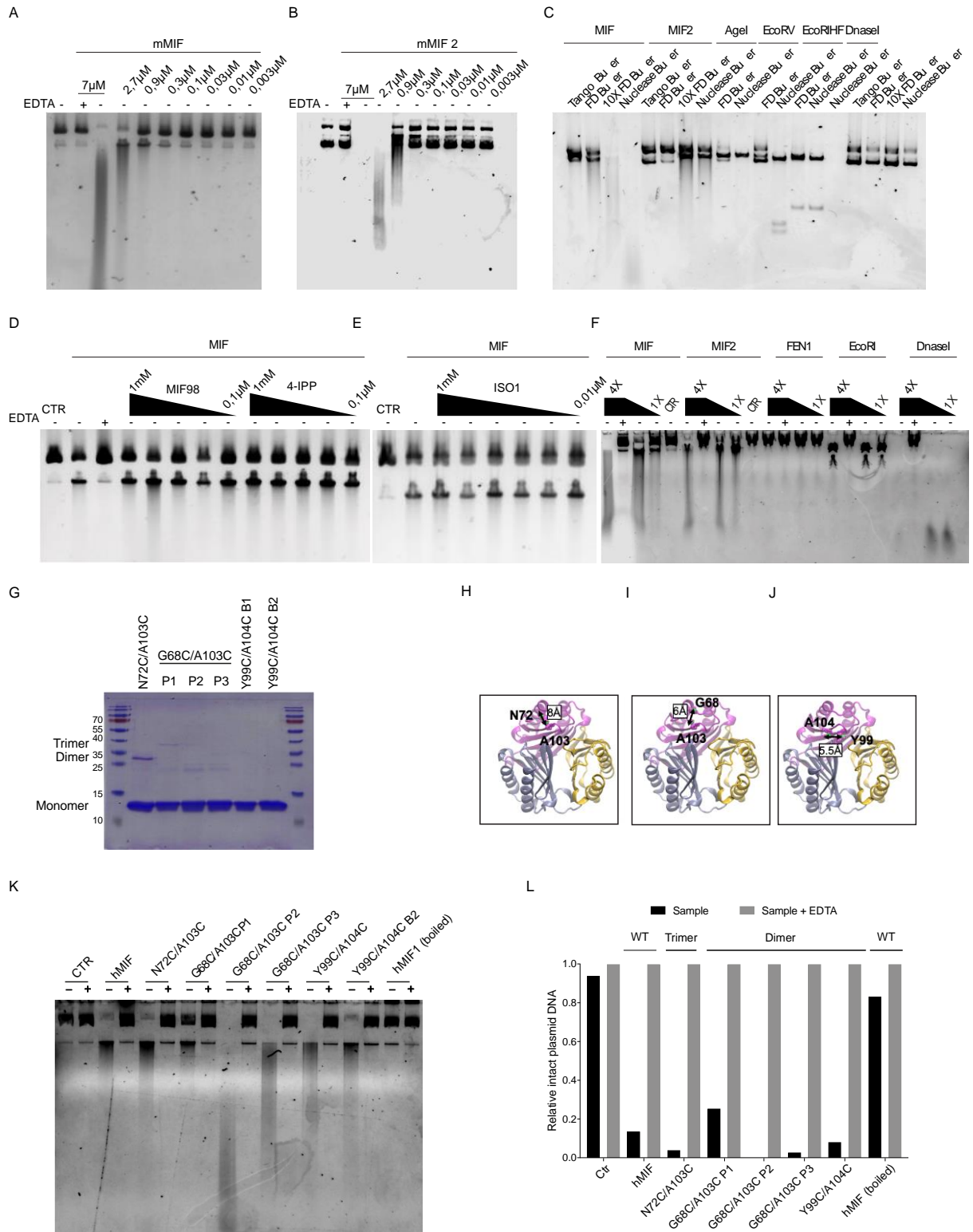


Figure 5-13: In vitro agarose gel electrophoresis nuclease assay of MIF and MIF-2 with various concentrations, and buffer conditions, with known inhibitors as well as with different MIF mutants.

(A) In vitro agarose gel electrophoresis of mouse MIF with different concentration, with and without EDTA (n= 3 independent experiments). (B) In vitro agarose gel electrophoresis of mouse MIF-2 with different concentrations, with and without EDTA (n= 3 independent experiments). (C) In vitro agarose gel electrophoresis of mouse MIF (2 μ M) with Fast Digest (FD) buffer or 10X FD buffer or nuclease buffer

containing Mg^{2+} , mouse MIF-2, with FD Buffer or 10X FD Buffer or nuclease buffer containing Mg^{2+} (10mM), AGEI (0.5 U), ECORV (0.5 U) with FD buffer or nuclease buffer containing Mg^{2+} (10mM), DNaseI (0.5 U) with nuclease buffer containing Mg^{2+} (10mM) (n= 2 replicates). (D) In vitro agarose gel electrophoresis of mouse MIF (2 μ M) with and without EDTA, or with Inhibitor MIF98, 4-IPP (n=1). (E) In vitro agarose gel electrophoresis of mouse MIF with and without ISO1 (1mM-0.01 μ M) (n=1 independent experiment). (F) In vitro agarose gel electrophoresis of human MIF with and without EDTA (50mM), human MIF-2 with and without EDTA, FEN1, EcoRI (1-0.25U), DnaseI(1-0.25U) (n=4 independent experiments). (G) SDS-PAGE: MIF mutants' purity and concentration; provided by Najat Haj Yahya and the Dal Peraro lab. (H-J) Highlighting N72C/A103C, G68C/A103C and Y99C/A104C mutants' Crystal structure; provided by Najat Haj Yahya and the Dal Peraro lab. (K) In vitro agarose gel electrophoresis of human MIF, N72C/A103C, G68C/A103C and Y99C/A104C mutants with or without EDTA or boiled) (n=1 independent experiment). (L) Quantification of Relative intact plasmid DNA) (n=1 independent experiment).

However, the MIF tautomerase inhibitor ISO-1, had no effect on the nuclease activity (Figure 5-13). Similar results were observed after incubating MIF with MIF receptor antagonist, MIF98, or 4-IPP, which are known to block the MIF/CD74 internalization (Figure 5-13 D).

5.3.2. MIF and MIF-2 nuclear enrichment after excitotoxicity

It is known that MIF translocates to the nucleus by interacting with AIF. Mitochondrial AIF is released due to PARP1 activation by, among other factors, excitotoxicity and oxidative stress^{116,117,236}. Wild type primary neuronal culture was treated with 500 μ M NMDA, 500 μ M 3-NP, and 500 μ M MNNG. MIF enriched in the nucleus after 6 hours of incubation with toxic insult in WT primary mixed neuronal culture, as compared to the control (Figure 5-14 A-F).

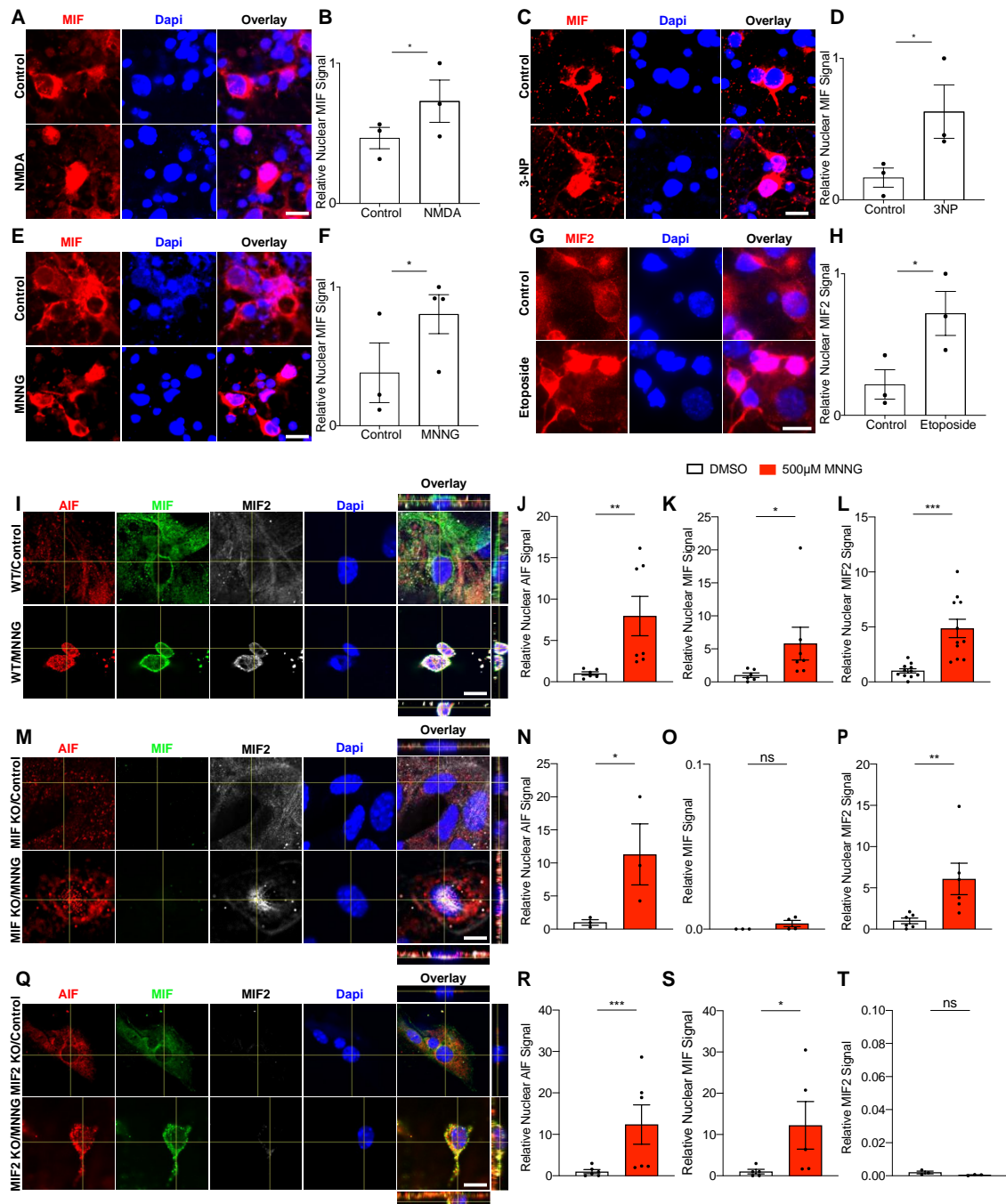


Figure 5-14: MIF and MIF-2 enrichment in the nucleus in excitotoxicity in astrocyte culture and neuronal primary culture. AIF translocation is not affected by MIF or MIF-2 deficiency.

(A) Images of nuclear enrichment of MIF after NMDA treatment in WT primary mixed culture. The purple color indicates the overlay of MIF and 4',6'-diamidino-2-phenylindole (DAPI), showing the nuclear enrichment (The scale bar is 10 µm). (B) Quantification of the relative nuclear MIF levels after 500µM NMDA treatment in WT (* $p < 0.0378$ one-way ANOVA, corrected with Bonferroni); the relative total MIF levels after NMDA treatment in WT (ns $p < 0.880$ one-way ANOVA, corrected with Bonferroni). Experiment was replicated in 3 independent cultures/animals for each group ($n = 3$). (C) Images of nuclear enrichment of MIF after 3-NP treatment in WT primary mixed culture (The scale bar is 10 µm). (D) Quantification of the relative nuclear MIF levels after 3-NP in WT (* $p < 0.0146$ one-way ANOVA, corrected with Bonferroni); and the relative total

MIF levels after 3-NP treatment in WT ($ns\ p>0.6798$ one-way ANOVA, corrected with Bonferroni). Experiment was replicated in 3 independent cultures/animals for each group ($n=3$). (E) Images of nuclear enrichment of MIF after MNNG treatment in WT primary mixed culture (The scale bar is $15\ \mu m$). (F) Quantification of the relative nuclear MIF levels after MNNG in WT ($*p<0.0358$ one-way ANOVA, corrected with Holm-Sidak); the relative total MIF levels after MNNG treatment in WT ($ns\ p<0.4953$ one-way ANOVA, corrected with Holm-Sidak). Experiment was replicated in 3 independent cultures/animals for each group ($n=3$). (G) Images of nuclear enrichment of MIF-2 after Etoposide treatment in WT primary mixed culture (The scale bar is $12\ \mu m$). (H) Quantification of the relative nuclear MIF-2 levels after etoposide treatment in WT ($*p<0.0216$ one-way ANOVA, corrected with Holm-Sidak); the relative total MIF-2 levels after $500\ \mu M$ Etoposide treatment in WT primary mixed cultures ($ns\ p<0.1332$ one-way ANOVA, corrected with Holm-Sidak) in 3 independent cultures/animals for each group ($n=3$). (I) Representative of nuclear enrichment of AIF, MIF, and MIF-2 after MNNG treatment in WT, primary astrocyte culture (The scale bar is $10\ \mu m$). (J) Quantification of the relative nuclear AIF levels after MNNG treatment in WT ($*p<0.0123$ one-way ANOVA. Experiment was replicated in the control ($n=6$) and treatment ($n=7$) group with independent cultures of 3 individual animals ($n=3$). (K) Quantification of the relative nuclear MIF levels after MNNG treatment in WT ($*p<0.0300$ one-way ANOVA). Experiment was replicated in the control ($n=6$) and treatment ($n=7$) group with independent cultures of 3 individual animals ($n=3$). (L) Quantification of the relative nuclear MIF-2 levels after MNNG treatment in WT ($***p<0.0002$ one-way ANOVA). Experiment was replicated in the control ($n=11$) and treatment ($n=11$) group with independent cultures of 6 individual animals ($n=6$). (M) Representative of nuclear enrichment of AIF, MIF and MIF-2 after MNNG treatment in Mif KO, primary astrocyte cultures (The scale bar is $8\ \mu m$). (N) Quantification of the relative nuclear AIF levels after $500\ \mu M$ MNNG treatment in Mif KO ($*p<0.0248$ one-way ANOVA) of 3 individual animals for each group ($n=3$). (O) Quantification of the relative nuclear MIF level with and without MNNG treatment in Mif KO, primary astrocyte culture ($ns\ p=0.1878$ t-test unpaired) of 3 individual animals for the control group ($n=3$) and 4 individual animals for the $500\ \mu M$ MNNG treated group ($n=4$). (P) Quantification of the relative nuclear MIF-2 levels after MNNG treatment in Mif KO ($**p<0.0103$ one-way ANOVA) of 6 individual animals for each group ($n=6$). (Q) Representative of nuclear enrichment of AIF, MIF and MIF-2 after MNNG treatment in Mif-2 KO, primary astrocyte culture (The scale bar is $10\ \mu m$). (R) Quantification of the relative nuclear AIF levels after MNNG treatment in Mif-2 KO ($**p<0.0047$ one-way ANOVA) of 6 individual animals for each group ($n=6$). (S) Quantification of the relative nuclear MIF level after MNNG treatment in Mif-2 KO, primary astrocyte culture ($*p=0.0103$ one-way ANOVA) of 5 individual animals for each group ($n=5$). (T) Quantification of the relative nuclear MIF-2 levels with and without MNNG treatment in Mif-2 KO primary astrocyte culture ($ns\ p=0.1251$ one-way ANOVA) of 3 individual animals for each group ($n=3$).

In addition, MIF-2 enriched in the nucleus compared to the control after a 6-hour treatment with $500\ \mu M$ etoposide, which is an inhibitor of topoisomerase II, in WT primary mixed neuronal culture (Figure 5-14 G-H). Due to the topoisomerase II inhibition, etoposide induces DNA damage and therefore promotes cell death^{39,237–239}. Besides primary neuronal cultures, primary astrocyte cultures have been established with the focus of observing AIF, MIF, and MIF-2 nuclear enrichment after toxic insult with $500\ \mu M$ MNNG. WT, Mif KO, and Mif-2 KO primary astrocyte cultures were treated with $500\ \mu M$ MNNG. Endogenous MIF, MIF-2 and AIF were subsequently enriched in the nucleus (Figure 5-14 I-T). Neither the depletion of MIF nor MIF-2 influenced AIF translocation,

(Figure 5-14 N, and R). In addition, we could not detect any effect of MIF nuclear enrichment after toxic insult in *Mif-2* KO or MIF-2 nuclear enrichment after toxic insult. Furthermore, we show AIF, MIF, and MIF-2 enrichment after 6 hours of 250 μ M MNNG and 750 μ M MNNG toxic insult in a HEK-293 cell line (Figure 5-15 A-F).

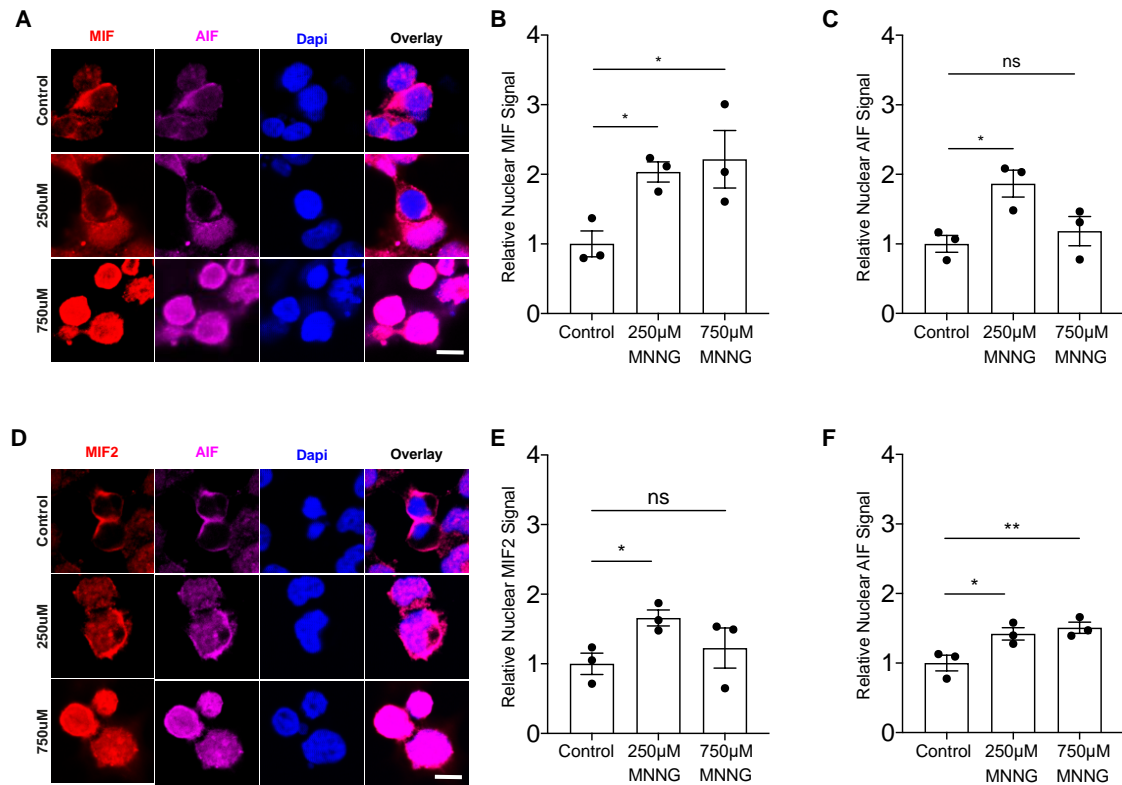


Figure 5-15: AIF, MIF and MIF-2 enrichment in the nucleus after MNNG excitotoxicity in HEK-cells.

(A) Representative of nuclear enrichment of MIF and AIF after MNNG treatment in HEK cell cultures. Overlay of AIF, MIF and MIF-2 with 4',6'-diamidino-2-phenylindole (Dapi), showing the nuclear enrichment (The scale bar is 10 μ m). (B) Quantification of the relative nuclear MIF levels after MNNG treatment in HEK cell cultures (control/250 μ M * $p=0.0378$ one-way ANOVA, Control/750 μ M * $p=0.0205$ one-way ANOVA) of 3 individual cultures for each group ($n=3$). (C) Quantification of the relative nuclear AIF levels after MNNG treatment in HEK cell culture (control/250 μ M * $p=0.0139$ one-way ANOVA, Control/750 μ M ns $p=0.4930$ one-way ANOVA) of 3 individual cultures for each group ($n=3$). (D) Representative of nuclear enrichment of MIF-2 and AIF after 500 μ M MNNG treatment in HEK cell culture (The scale bar is 10 μ m). Overlay of AIF, MIF and MIF-2 with 4',6'-diamidino-2-phenylindole (Dapi), showing the nuclear enrichment. (E) Quantification of the relative nuclear MIF-2 levels after MNNG treatment in HEK cell culture (Control/250 μ M * $p=0.0290$ one-way ANOVA, control/750 μ M ns $p=0.5380$ one-way ANOVA) of 3 individual cultures for each group ($n=3$). (F) Quantification of the relative nuclear AIF levels after MNNG treatment in HEK cell culture (control/250 μ M * $p=0.0201$ one-way ANOVA, Control/750 μ M ** $p=0.0089$ one-way ANOVA) of 3 individual cultures for each group ($n=3$).

5.4. Indication of DSB and cell survival change in *Mif* KO and *Mif-2* KO

We also found that *Mif* KO as well as *Mif-2* KO in primary astrocyte cultures had decreased levels of tail moment indicated in the neutral comet assay (Figure 5-16 A, B). In addition, we also observed substantial numbers of γ H2AX foci per cell in wildtype primary astrocyte cultures, whereas the number of γ H2AX foci per cell was reduced in *Mif-2* KO astrocyte cultures (Figure 5-16 D). Similar results are observed for DNA damage marker 53BP1. We found that Mif-2 KO decreased the fluorescence intensity of 53BP1 (Figure 5-16 E).

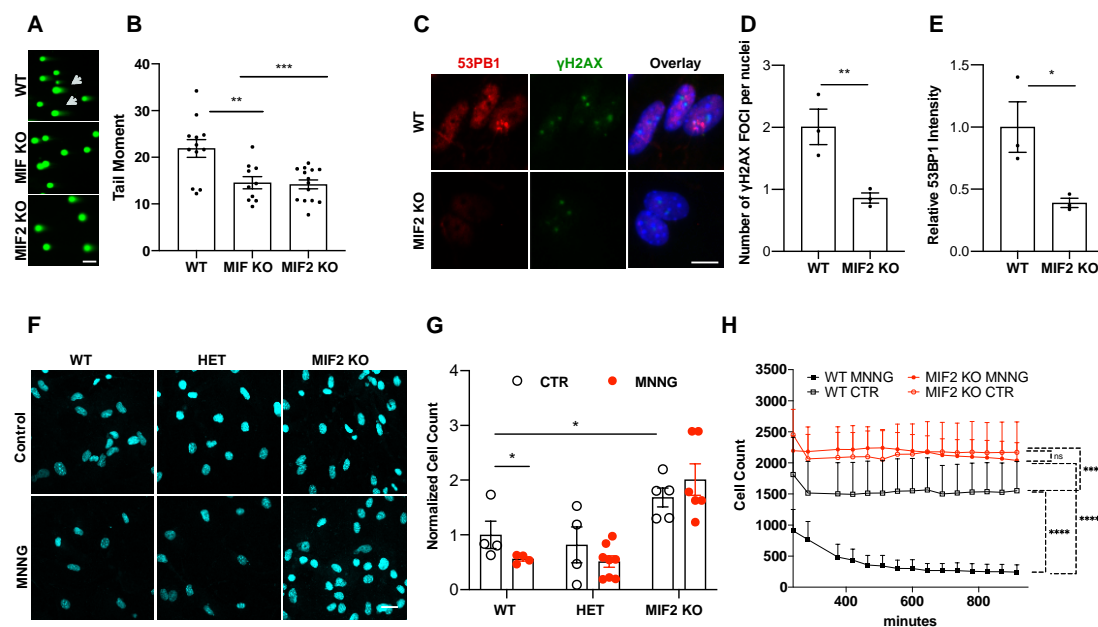


Figure 5-16: Decrease of DSB in *Mif* KO and *Mif-2* KO indicated by the neutral comet assay analysis of the tail moment, and by DSB marker γ H2AX, 53BP1, as well as increase of cell survival after MNNG excitotoxicity.

(A) Tail Moment content was quantified with Trevigen Comet Analysis Software. Primary astrocyte cultured cells from WT, *Mif* KO and *Mif-2* KO animals were assessed for DSB levels by the comet assay at neutral pH (The scale bar is 40 μ m). (B) Quantification of the percentage of the tail moment, determined by the comet assay in WT, *Mif* KO and *Mif-2* KO (*Mif* KO ** p <0.0014 one-way ANOVA) and (*Mif-2* KO *** p <0.0004 one-way ANOVA). Experiment was performed for WT n =12; *Mif* KO n =10 *Mif-2* KO n =14 individual cultures (C) Representative γ H2AX-positive foci (green) and 53BP1 intensity (red) in immunostained primary neuronal culture from WT and *Mif-2* KO of primary astrocyte cultures. Cultures were visualized by confocal microscopy (The scale bar is 10 μ m). (D) Quantification of γ H2A.X-positive foci (green) per nuclei in WT and *Mif-2* KO astrocyte cultures (n =3) (** p =0.0091 one-tailed t -test). (E) Quantification of 53BP1 intensity (red) in WT and *Mif-2* KO astrocyte cultures (n =3) (* p =0.0209 one-tailed t -test). (F) Representative of primary astrocyte culture from WT, *Mif-2* Het and *Mif-2* KO animals (The scale bar is 15 μ m). (G) Quantification of

Results: MIF-2 is a nuclease

*relative cell count after 500 μ M MNNG treatment for 6 hours; (WT CTR/WT MNNG * $p=0.0286$ one-tailed t -test; WT CTR/Mif-2 KO CTR * $p=0.0317$ one-tailed t -test) and (Het CTR/ Het MNNG ns $p=0.3414$ one-tailed t -test). (H) Live Imaging quantification of Cell count after 500 μ M MNNG treatment; (WT CTR/Mif-2 KO CTR *** $p < 0.0001$ ordinary one-way ANOVA; WT CTR/WT MNNG *** $p < 0.0001$ ordinary one-way ANOVA; Mif-2 KO CTR/Mif-2 KO MNNG ns $p=0.7930$ ordinary one-way ANOVA; WT MNNG /Mif-2 KO MNNG *** $p < 0.0001$ ordinary one-way ANOVA); Experiment was performed for WT/ CTR $n=6$; WT/MNNG $n=9$; Mif-2 KO/CTR $n=5$; MIF-2 MNNG $n=9$ individual WT astrocyte culture independent cultures/animals for each group.*

Next to DNA damage levels, we also observed an increase in cell number after excitotoxicity of 500 μ M MNNG in MIF-2 knockout primary astrocyte culture compared to the cell count in wild type and heterozygous cultures (Figure 5-16F, G). In addition, we found that MIF-2 control and MNNG treated cultures show less cell loss compared to wild type controls as well as MNNG treated primary astrocyte cultures (Figure 5-16 H).

5.5. MIF related to DNA damage

Neuronal damage is often incurable and leads to life-limiting diseases, such as Alzheimer's, Parkinson's, or Huntington's disease. These cause a slowly progressive loss of neurons in the

Central nervous system, which in turn, leads to a deterioration in certain brain functions and the memory or movement controlled by the affected CNS region. This loss of neurons in the central nervous system (CNS)¹⁴¹ is also the main cause of cognitive and motor dysfunction in neurodegenerative diseases. Other factors such as aging and exposure to environmental factors such as systemic infections are also present in humans. For this reason, this thesis aims to understand better how immune responses are involved in the damage and regeneration of neurons and astrocytes. This is intended to provide assistance for effective therapies that can improve the quality of life or at least dampen the personal, social effects of these diseases. The economic effect must also not be ignored.

5.5.1. MIF's topological driven function

Proteins are macromolecules that have various enzymatic activities and functions. However, some have a single role that they fulfill, but before cytokines, a phenomenon of the multifunctional protein also called moonlighting, is discovered. This particular class of multifunctional proteins has several autonomous and dissimilar functions and enzymatic activities. The enzymatic activities are detected in various domains of the protein. However, not only the domains can define the process, also the topological position in the cell as well. This phenomenon of moonlighting proteins was first described in 1980 by Piatigorsky and Wistow. In 2019, the Kapurniotu, Gokce, and Bernhagen lab put MIF in the focus of the moonlighting proteins and their function in their topological location in the cell. With the help of the Imaris software and the primary neuronal culture, it was shown that MIF was found both outside the Dapi-labeled nucleus (magenta) and inside colocalized with Dapi MIF (green) (Figure 5-17)

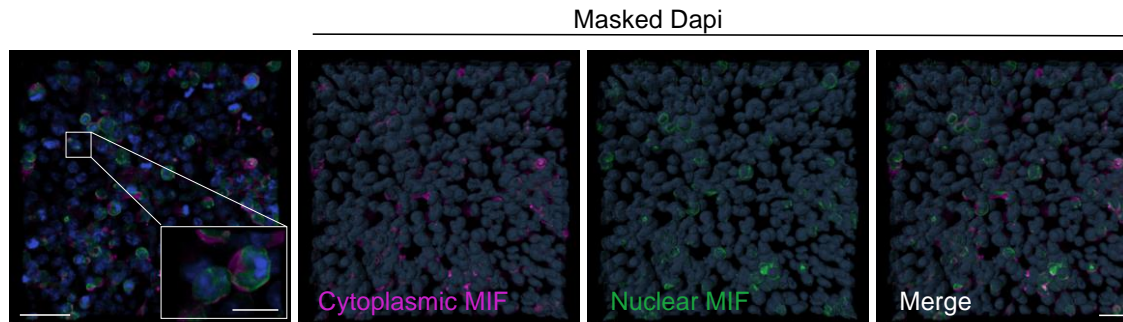


Figure 5-17: Imapris representative of cellular MIF topology in primary neuronal mixed culture.

Imaris Image of WT Primary neuronal mixed culture, magenta is indicating cytoplasmic MIF, in green nuclear MIF is represented. To gain insights into the subcellular location of MIF, 3D renderings of confocal data were generated using Imapris. Confocal images were acquired from multiple cellular layers. Subsequently, Imapris applied DAPI thresholding to differentiate the constituents within the nucleus and the extranuclear space ($n=3$ individual cultures), scale bar: 70 μm ; 20 μm (insets).

Single cell gel electrophoresis, also known as the comet assay, is a technique used to quantify DNA damage. When examining the embedded cells of the WT and *Mif* KO culture or the agarose-embedded brain tissue that was lysed under neutral conditions, the various head and DNA-tail ratios were measured. In the neutral PH, the cells were lysed, and DNA denatured so that the DNA can escape and, depending on its size, can also flow differently during electrophoresis. The intact DNA collects in the comet's head and the DSBs in the tail (Figure 5 18 A). In this study, the comet assay was carried out under neutral conditions to recognize DSBs. In the neutral comet assay, DNA was found in the tail for WT and MIF knocked out mice. However, they differ in the amount of DNA in the tail compared to the DNA in the head. In addition to the comet assay, co-labeling of MIF and DSB markers was also detected. The antibody γ -H2AX (Foci) detects the phosphorylated form of the histone protein H2AX, thereby representing the formation of DNA double-strand breaks. DNA damage can be triggered by endogenous mechanisms or by exogenous factors. The creation and accumulation of DSBs are a threat to cell health. In addition to γ -H2AX (Foci), the p53-binding protein (53BP1) is another well-known DNA damage reaction marker, and accordingly, also a way of quantifying DSBs. 53BP1 is recruited on the DNA damage side. We also observed co-staining of MIF with the DSB marker of γ -H2AX and 53BP1 in the nucleus indicated by the cyan staining. (Figure 5 18 B). In addition to the findings obtained from primary neuronal cultures, we established primary astrocyte culture for our study. In these astrocyte cultures, we also detected the DSBs with the help of the marker γ -H2AX (green) as well as MIF-2 (red). Overlapping fluorescence signals from both markers were detected, indicating their co-localization within the nuclei structure (blue). These co-localizations were carefully

examined within the nuclear structures. The results showed that, similar to primary neuronal cultures, staining with MIF-2 and the DSB marker γ -H2AX occurred within the nuclei structure in primary astrocyte cultures as well (Figure 5 18 C).

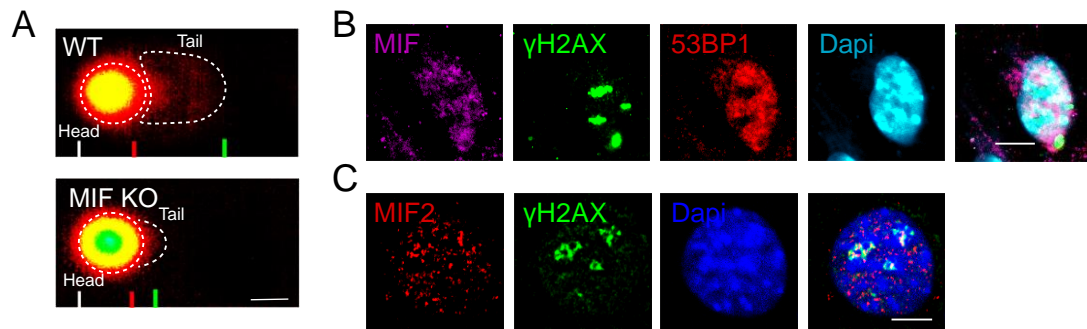


Figure 5-18: Representative of DNA damage related with MIF and MIF deficient cells by the neutral comet assay as well as the Co-staining of MIF , MIF-2 with DSB-marker γ H2AX and 53BP1.

(A) Representative of the Comet assay (neutral) Tail DNA content Cells from WT and Mif KO animals. were isolated from hippocampus and cortex; homogenates were assessed for DSB levels by the comet assay at neutral pH. Green to yellow color represents higher intact DNA density. Red color represents less DNA density and outside of the comet core, the DSB tail accumulation (scale bar: 10 μ m). (B) Co-staining of DSB-marker γ H2AX (green) and 53BP1 (red) with MIF (MIF-n20/violet), (n= 3 WT animals) Scale bar: 5 μ m. Representative of DNA damage related with MIF-2 in astrocyte culture with DSB marker γ H2AX. (C) Representative of DNA damage related with MIF-2 in astrocyte culture with DSB marker γ H2AX. Co-staining of DSB-marker γ H2AX (green) and MIF-2 (red), within the nuclei (blue/Dapi). MIF-2 (red) also spotted outside of the nuclei (n=3 individual cultures), scale bar: 5 μ m.

In WT primary neuronal mixed cultures, we observed the topological distribution of MIF in various cellular compartments, including the nucleus, cytoplasm, and extracellular space (Figure 5 19 A). Similarly, we investigated the cellular localization of MIF-2 in astrocyte cultures (Figure 5 19 B).

The results revealed that both MIF and MIF-2 exhibited colocalization with extracellular DAPI staining besides their nuclear and cytoplasmic presence. This extracellular Dapi staining may be due to DNA damage (Figure 5 19).

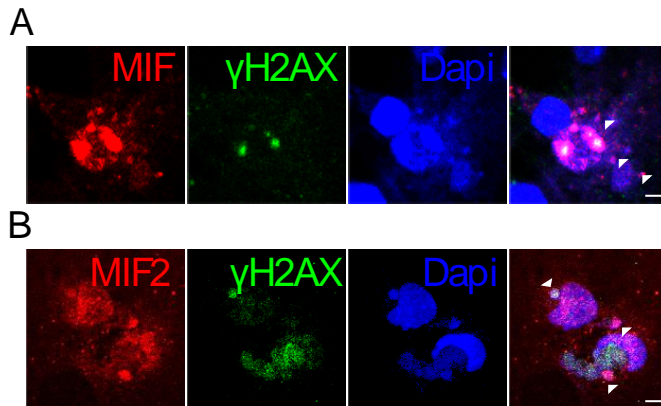


Figure 5-19: Representative of DNA (Dapi) and (extracellular) DNA damage, colocalized MIF and MIF-2. Upper panel MIF (red) colocalized within the nuclei (dapi/blue) and with the extracellular DNA (dapi/blue). DNA damage indicated by DSB marker γ H2AX (green) ($n=1$), scale bar: 5 μ m. Lower panel MIF-2 (red) colocalized within the nuclei (blue/dapi) and with the extracellular DNA (dapi/blue). DNA damage indicated by DSB marker γ H2AX (green). Colocalization with MIF-2 and γ H2AX (green) within the nuclei structure (dapi/blue) and extracellular (blue/dapi) ($n=1$), scale bar: 5 μ m.

To summarize, in some cells, that show extracellular Dapi stainings, an overlap of the DSB marker with Dapi, MIF, and MIF-2 was observed. However, further analysis could not be performed in this regard. Therefore, in the next course of this work, the DNA damage levels in brain tissue of WT and transgenic mice will be investigated in more detail using the Comet assay (Figure 5-20)

To show whether MIF deficient brain tissue shows differences in DNA damage loading, brain tissue was dissected from WT and *Mif* KO mice. The hippocampus and cortex regions of both genotypes were examined. When measuring with the help of the neutral comet assay, a method for measuring DSBs, *Mif* KO tissue compared with WT tissue showed a reduction in the % DNA in the tail. However, this difference is significantly more pronounced in the cortex (Figure 5-20). In addition to the DNA damage detected by the comet assay, we also performed immunocytochemistry (ICC) by using 53BP1 DSB marker to show the difference between WT and *Mif* KO of primary neuronal culture. The transgenic primary neuronal *Mif* KO mixed culture shows a lower 53BP1 staining intensity than the primary neuronal WT mixed culture.

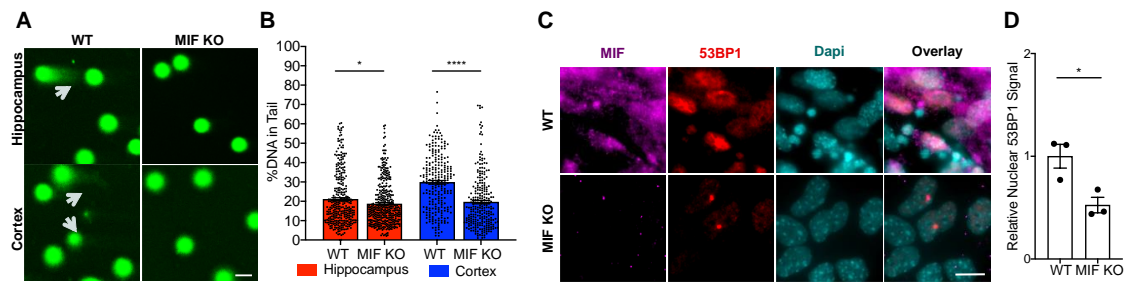


Figure 5-20: Decrease of DSB in *Mif* KO indicated by the neutral comet assay from brain tissue and immunocytochemistry primary neuronal culture.

(A) Tail DNA content was quantified with Trevigen Comet Analysis Software. Cells from WT and *Mif* KO animals were isolated from hippocampus and cortex; homogenates were assessed for DSB levels by the comet assay at neutral pH, scale bar: 15 μ m. (B) Quantification of the percentage of DNA in the tail, determined by the comet assay in WT ($n=3$ animals), or *Mif* KO cells isolated from the Hippocampus ($n=3$ animals) ($*p<0.015$ one-way ANOVA, corrected with Holm-Sidak) and Cortex ($****p<0.0001$ one-way ANOVA, corrected with Holm-Sidak). (C) Representative MIF (magenta) and 53BP1 intensity (red) in immunostained primary neuronal culture from WT and *Mif* KO of primary neuronal mixed culture. Cultures were visualized by confocal microscopy, scale bar: 15 μ m. (D) Quantification of 53BP1 intensity (red) in WT and *Mif* KO neuronal mixed Culture ($n=3$ animals) ($*p=0.0131$ one-tailed t -test).

As in the previous DNA damage analyses using neutral comet assay, brain tissues from WT, *Mif* KO, 5XFAD, and 5XFAD/*Mif* KO animals were removed and dissected.

Using the neutral comet assay, a significant reduction of the percentage of DNA in the tail, which indicates the level of DNA damage, was observed in MIF deficient transgenic mice. This means that compared to the WT, *Mif* KO mice showed lower DNA damage, whereas 5XFAD/*Mif* KO mice also showed lower amounts of DNA damage than the 5XFAD control. When comparing WT mice, a significant increase in DSB was shown in 5XFAD mice. However, no significant result was obtained when comparing *Mif* KO and 5XFAD/*MIF*KO transgenic animals (Figure 5-21).

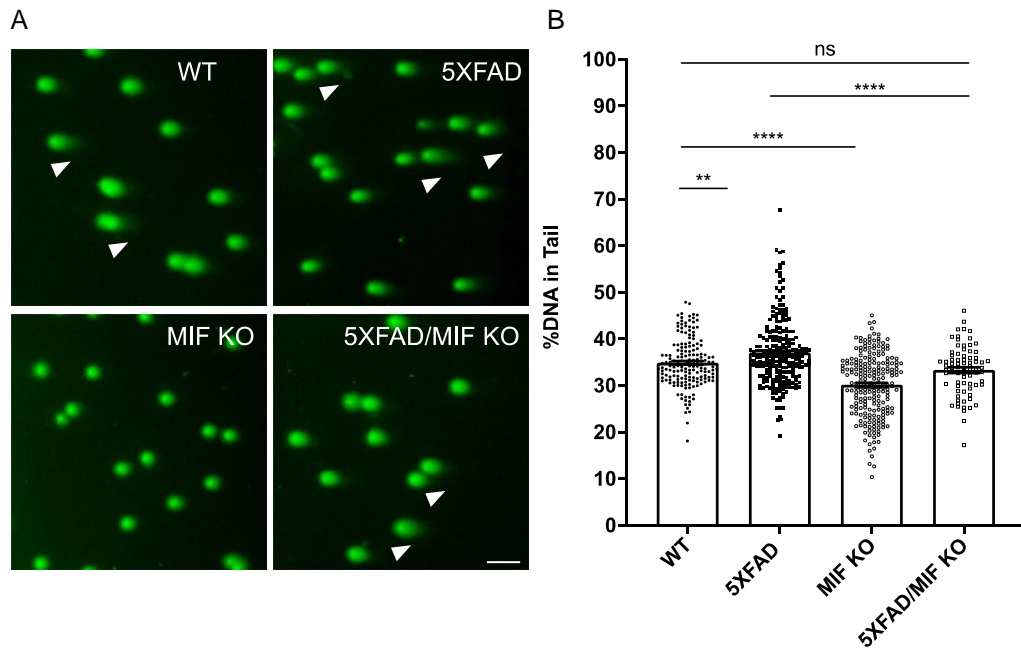


Figure 5-21: Decrease of DSB in *Mif* KO transgenic mice indicated by the neutral comet assay of brain tissue from WT, *Mif* KO, transgenic 5XFAD and 5XFAD/*Mif* ko mice.

(A) Cells isolated from mouse brain were assessed for DSB levels by the comet assay at neutral pH. DNA of the agarose-embedded nuclei was stained with SYBR-gold after separation of DNA fragments by electrophoresis. Images were captured by fluorescence microscopy (DMI 8), scale bar: 70 μ m. (B) Quantification of the percentage of DNA in comet tails for each nucleus indicative of DSBs. Percentage of DNA in the Tail indicating the extent of DNA fragmentation, was measured for each cell. Ordinary one way ANOVA Test Bars represent means \pm SEM.) Quantification of the percentage of DNA in the tail, determined by the comet assay in WT(n=7), *Mif* KO (n=4), 5XFAD (n=8) and 5xRAD/*Mif* KO (n=6) animals(WT vs. *Mif* KO **** $p < 0.0001$ one-way ANOVA; WT vs. 5XFAD $p = 0.0032$ one-way ANOVA; WT vs. 5XFAD/MIFKO $p = ns$ one-way ANOVA and 5XFAD vs. 5XFAD/MIFKO $p = KO$ **** $p < 0.0001$ one-way ANOVA).

5.6. *Mif KO* rat

Decades of research resulted in many translational approaches successfully screening for MIF inhibitors and anti-MIF / anti-CD74 antibodies in phase I / II clinical studies (e.g., <https://www.clinicaltrials.gov/ct2/show/NCT01845740>). However, future studies should also focus on intracellular functions such as nuclease activity. Because these also represent critical therapeutic approaches that should not remain unexplored. Suppose one considers that MIF and MIF-2 play an important role in neurobiology, cardiology, and immunology. In that case, it is essential to expand the translational potential and research other MIF models other than the mouse. Therefore, the rat as a model, is the focus of research. As mentioned initially, a rat is not just a larger mouse; accordingly, a MIF knockout rat model (*Mif KO* rat) is a new research model that enables new research approaches. The advantage of a rat model, besides many other requirements, is that the model system is in many ways closer to human physiology²⁴⁰. This opens practical benefits for research into behavioral analysis that are already known and new, simpler operations, as well as serial blood withdrawals. In addition, the new research opportunities provided by the *Mif-KO* rat model can clear up the contradicting results. Many studies have been carried out on mouse models in the area of ischemic stroke models. However, partly contradicting results were received so that no precise results could be assigned to the role of MIF, even less for MIF-2^{116,241}. With the help of the established stroke models, combined with *Mif KO* rats, it would be possible to obtain a better one to clear up the contradicting facts. This could make MIF the focus of a therapeutic approach, namely stroke research. The main focus of the research is to characterize the role of MIF on microglia or astrocytes using the in-house scRNAseq pipeline. Because there are only minor studies of transgenic rats within the MIF family, cell-specific questions cannot be limited to the microglia or astrocytes. Still, they could also investigate the maturation of rat B cells. In addition, the new research opportunities provided by the *Mif KO* rat model can clear up the contradicting results. Many studies have been carried out on mouse models in ischemic stroke models. The scRNA sequence could characterize *Mif KO* in rats, which is a partial contradiction. In addition, the role of MIF in the maturation of B-cell in mice could be repeated and used for the rat animal model. This would give a closer insight into possible treatment methods for atherosclerosis. Overall, the *Mif KO* rat model offers excellent potential for research and the establishment of a broader biomedical research community, particularly in the cardiovascular field.

The current work focuses on the nuclease activity of MIF. In this regard, it must also be mentioned in this section, that the protein sequence of the rat for MIF, the critical residues, shows that these would be the glutamic acid at position 22 and the cysteines at position 81. Both regions are also conserved in the rat (Figure 5-22). In addition, MIF was also observed in the cytosol and the nucleus of the rat cells²⁴².

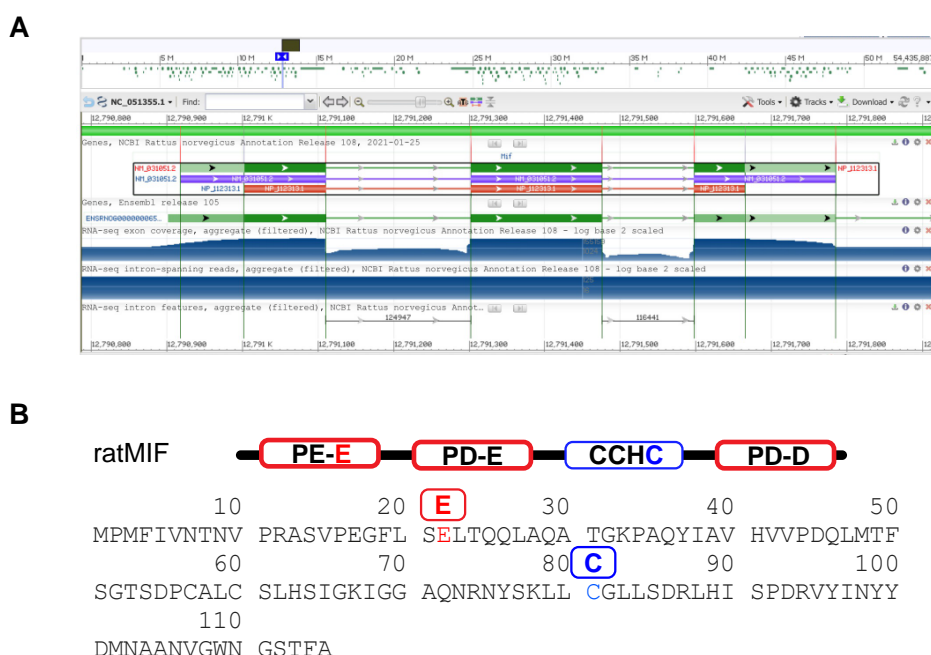


Figure 5-22: Targeted MIF gene in rat genome with the help of uniprot tools (<https://www.uniprot.org>).

(A) Illustration of MIF graphic: [A0A0F7RQL3 P30904](#). (B) Protein Sequence of rat MIF, highlighting critical glutamic acid at the place 22 for the nuclease activity and critical domain at the place 81 for the zinc finger.

The CRISPR / Cas system was initially described in this paper, revolutionizing the scientific world. With the help of this new method, ticked genetic sections could be cut, modified, or desired genomes could be inserted. For the transgenic rat project, the innovative system of CRISPR / Cas was used to remove the MIF gene from the net with genetic scissors^{243–245}.

CRISPR was initially found as a specific piece of DNA in a bacteria's genome. The reason for this being that the CRISPR with the enzyme Cas9 forms part of the bacterial immune system, which helps the bacteria to defend themselves against viruses. The CRISPR / Cas system protects bacteria from viruses or bacteriophage infections. In bacteria, the mechanism is divided into three phases. The first phase is an acquisition,

in which the bacteria build parts of the virus DNA as spacers in their genome. This sequence serves as a "memory" for the bacterium. In the second phase, the Cas protein's expression is assembled with the RNA. Finally, the RNA serves the Cas protein as a template for the correct sequences to detect sections. The third phase that occurs is the interference; in this case, if the same Virus is attached again, the foreign DNA is recognized, docked, and cut. In this way, the injected virus DNA is rendered harmless. The targeted degradation of the foreign DNA sequences takes place. The CRISPR array is read, resulting in a precursor RNA, which can also be referred to as pre-crRNA. These palindromic repeats form hairpin loops. The short crRNAs are bundled with a spacer each. These are combined with a Cas9 enzyme, a tracrRNA (trans-encoded crRNA). With the help of the PAM sequence, it is ensured that a similar sequence of one's organism is not accidentally cut^{184,246–249}. The RNA molecules point the Cas9 enzyme to the correct DNA sequence. So that the enzyme can recognize and cut the DNA strand, it must first be wound up so that the recognition sequence is exposed. This makes it possible for the RNA molecules to attach themselves to the complementary piece of DNA. the strand is then cut enzymatically so that a double-strand break occurs. This study used this method to perform a direct change in the DNA. Two researchers were recognized for discovering the CRISPR / Cas system in 2020. However, these systems and their basic structures were developed and discovered years ago and have already been investigated by the Zhang Lab^{250–252}. Looking at the transgene model with a *Mif* KO, we see that an integrated "guide RNA" was designed for the Cas9 enzyme, recognizing the target DNA interface. The endonuclease Cas9 can subsequently cut the recognized double strands. As mentioned before, DSB arises normally under natural conditions through oxidative stress or other mechanisms of aging. To reduce DNA damage, organisms have built-in repair mechanisms. The intentionally dispatched DSB can be repaired by a random (non-homologous) or targeted (homologous)^{73,253,254}. The repair itself leads to its inactivation, when the DSB ends are joined directly together so that the cut-out section is missing, or when new random base pairs are inserted. However, the breaks could also be repaired by an additionally inserted homologous sequence. At this point, a new or modified form of a gene (mutation) can be inserted²⁵³. In addition to the production of genetic modification, this information must also be developed in an organism, and the organism must be bred. Another achievement in genetic engineering has made it possible to create transgenic rats, known as in vitro fertilization (IVF)^{255,256}. With the help of in vitro fertilization, fundamental physiological, morphological, and molecular processes in gametes can be examined. In addition, the reproduction of animals can be ensured.

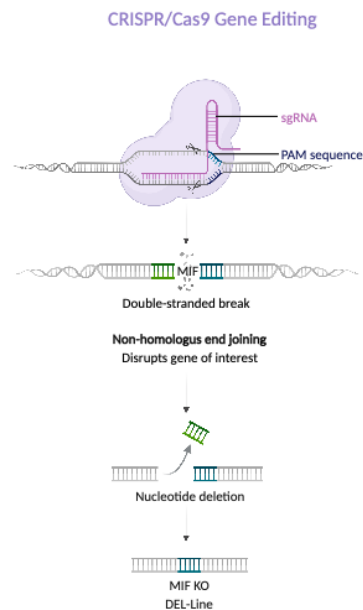


Figure 5-23: Schematic representation of MIF gene Editing by CRISPR/Cas9 method, modified by using Biorender.

Schematic presentation of the CRISPR/Cas9 process of gene editing. In purple, the complex of Single Guide RNA (sgRNA) and protospacer adjacent motif (PAM) sequence is represented. Double strand break and non-homologous end joining is targeted in the MIF encoding gene sequence. Further nucleotide deletion leads to MIF gene deletion of the genome.

5.6.1. Designing CRISPR/Cas9 guide RNA

With the help of the CRISPR / Cas method, the editing process could be carried out much more efficiently. Furthermore, embryonic and spermatogonial stem cells can be injected into adult animals to breed transgenic offspring directly²⁵⁷. As already mentioned, the CRISPR-Cas system consists of two main components, a guide RNA (gRNA) and a CRISPR-associated (Cas) nuclease (Cas9). With the help of the guide RNA, the Cas nuclease recognizes the target DNA region, which is why it consists of a specific RNA sequence, individual to the research interest. The gRNA itself is also made up of two parts ; on the one hand, the CRISPR-RNA (crRNA), which is approx. 17-20 nucleotide sequence long and naturally complementary to the target DNA, and on the other hand, a tracr-RNA, which acts as a binding structure for the Cas nuclease, is used. The CRISPR-associated protein, usually the Cas9 nuclease from *Streptococcus*

pyogenes, is a non-specific endonuclease, but with the help of the gRNA, it is transferred to the specific DNA locus. At the desired point, the nuclease generates a double-strand break. The crRNA is integrated into the gRNA. Therefore, it is the component that has to be adapted to the research aim so that the specificity of the Cas9 nuclease is guaranteed (*Figure 5-23 A*). There is a single RNA molecule in the single guide RNA (sgRNA) in which the crRNA sequence and the tracrRNA sequence are fused. This sgRNA can be produced synthetically. In nature, crRNAs and tracrRNAs occur as two separate RNA molecules. In contrast, sgRNAs are popular in research, and the terms sgRNAs and gRNA often have the same meaning in the CRISPR community. Correct design of the CRISPR Guide RNA sequence is critical as it affects the efficiency of DNA cleavage at the target site. Therefore it is essential to consider all important parameters. A Protospacer Neighbor Motif (PAM) was therefore designed. The PAM sequence identifies the locations where the nuclease divides 3-4 nucleotides upstream of the PAM sequence. For an efficient generation of transgenic rats with a Mif KO, various PAM ounces were identified. These are marked in green and yellow. However the yellow mark indicates a less efficient PAM sequence compared to the green label (*Figure 5-24 B*). Next to the PAM sequence, the Primer sequences were also indicated (*Figure 5-24 C*). The primer sequences are designed with the aim to delete the whole MIF gene (*Figure 5-24 D*). The PAM sequence "NGG" can be added to the oligo but is not mandatory during the design of the target spacer. However, it is important that the NGG PAM sequence immediately follows the target on the genome but not on the oligo. Therefore, the PAM sequence and its location are marked purple, the designed oligos in the desired gene region are marked yellow. The actual oligos correspond to the following motif :

5'-CACCGN ... N-3 '
 3'-CN ... NCAAA-5 '.



Figure 5-24: Design of Targeted gene side, with the help of the PAM sequence and sgRNA. (A) Illustration of Cas 9 enzyme with sgRNA and tracrRNA. (B) Sequence and PAM region detection. (C) Analyzing of sgRNA cutting site (<http://crispor.tefor.net/crispor.py?batchId=fsuAE7PvZzA0GS95RJCu>). (D) Representing cutting side; sgRNA side in yellow and PAM sequence in blue; summary of the primer, sequence and the amplification product. Sequence analysis by courtesy of Marie-Christine Birling (Phenomin), generated as part of the Infrafrontier project of Profs. Gokce and Bernhagen.

With the help of a KIT, the CRISPR / Cas9 genomic editing method was carried out. The Agilent SureGuide gRNA Synthesis Kit (P / N 5190-7719) is recommended for synthesizing your gRNAs. In *Figure 5-25* analyses of Control Cas9 digestion are shown. The Cas9 protein is a protein that ensures that the target region is cut out. This cuts the PCR product, including the area of interest. A guide is validated when it cuts the target PCR fragment. However, the amount of cut DNA fragments is not a further indicator and does not guarantee the in vivo efficiency of the guides. The bands are indicating the PCR bands of the different guide RNAs.

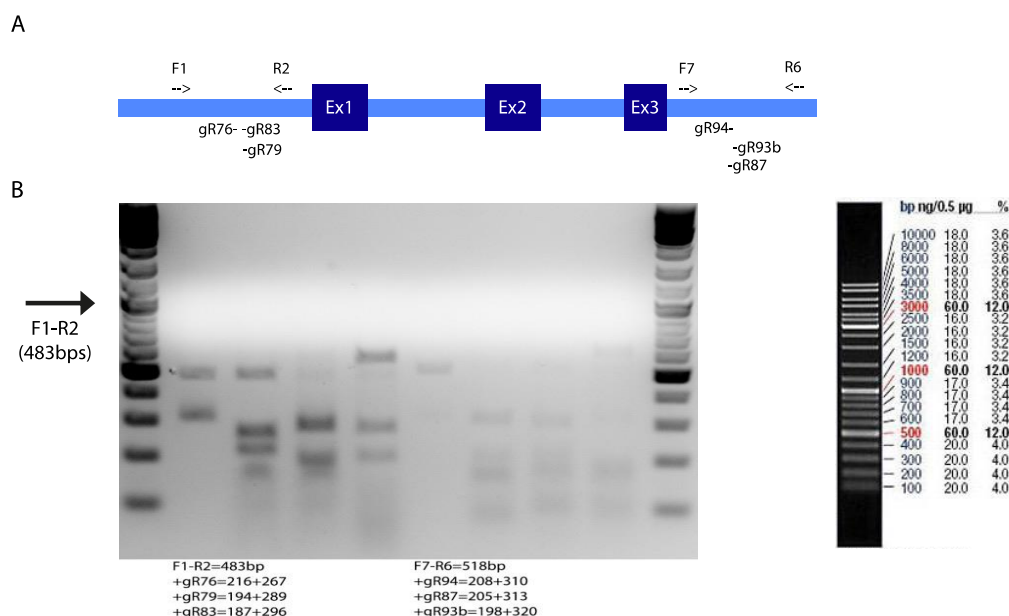


Figure 5-25: Representation of CRISPR guide efficiency (Agilent Technologies 5190-7716).

(A) Representative of MIF gene environment (B) CRISPR guide efficiency in vitro test by using Sureguide kit (Agilent Technologies 5190-7716). The gel image is by courtesy of Marie-Christine Birling

After the primers F2 and R7 were used, the F0 generation was characterized for the pup screening. In addition, the F1 was genotyped. A visible band identifies the deletion at 540bp and 531bp. The aim is to delete the whole MIF gene (~1kb). The visible del allele fragment is identified through the black band in the agarose gel (*Figure 5-25*). With the help of the CRISPR / Cas9 method and the rat research model, a new research species was created to investigate the effects of MIF. Therefore, the most critical trademarks were to synthesize guide RNAs in vitro and validate them. Then, the validated sgRNAs

were selected for microinjection. Sprague Dawley (rat) eggs were fertilized by microinjection in this study.

The F0 generation was characterized and genotyped. The F0 founders of interest were bred to obtain germline transmission. F1 animals were validated by genotyping to collect the F1 and F2 animals for organ removal.

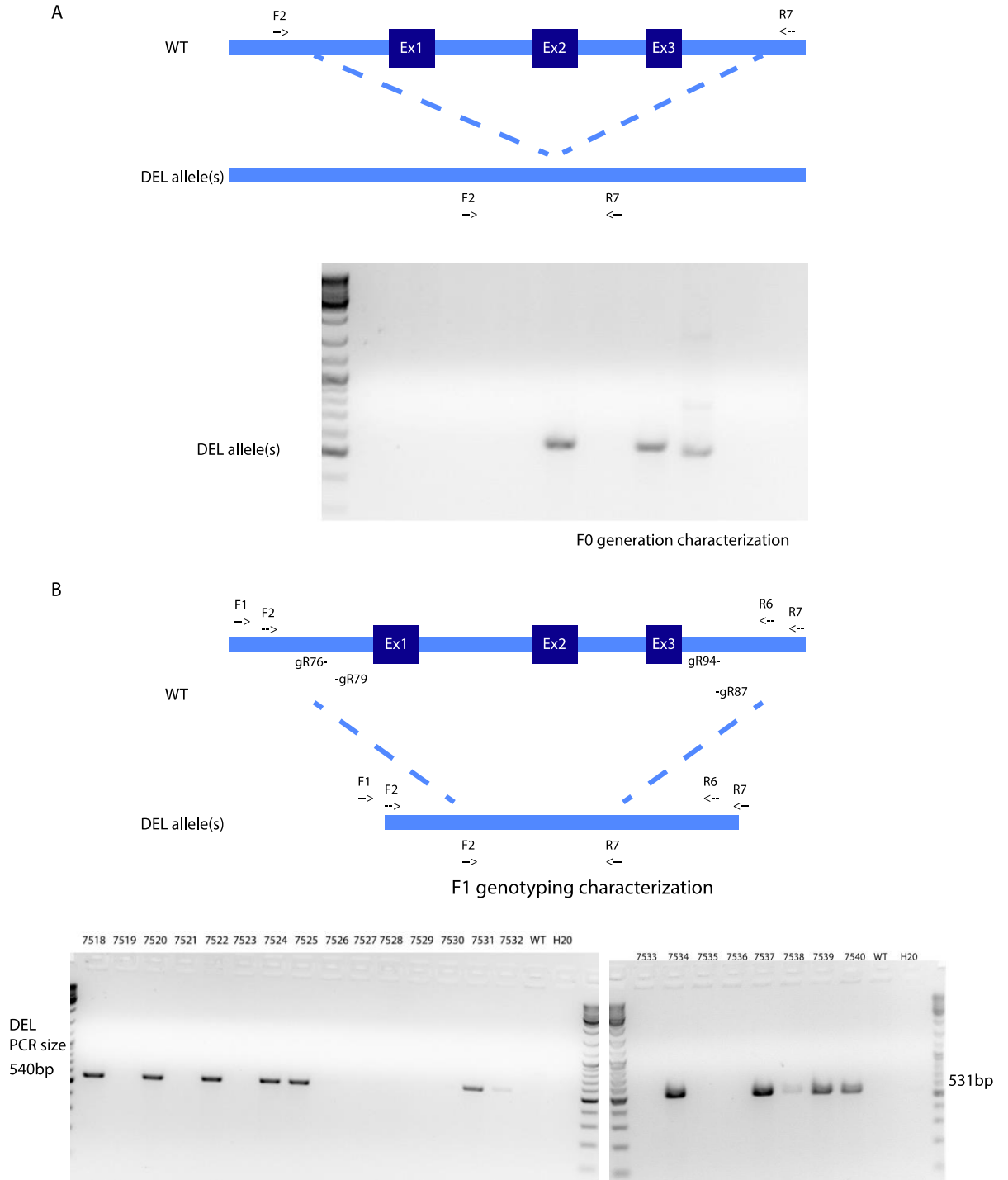


Figure 5-26: Selection of targeted gene side (PCR F2-R7) of F0 and F1 genotyping results.

(A) F0 genotyping results using PCR F2 and F7 for pups screening (B) F1 genotyping results using PCR F2 and F7; fKur7103-6979-DEL left gel and Kur7103-6981-DEL line right gel. Gel images are by courtesy of Marie-Christine Birling

Three founders have been identified and have been validated by Sanger sequencing (F0-6979, F0-6981, and F0-6982). They were bred with wild-type animals after eight weeks (Figure 5-27).

The Sprague Dawley (SD) rats with a Mif gene knockout (*Mif*-KO) were generated using the CRISPR/Cas9 nuclease system.

Oligo F2 (Forward) Oligo R7 (Reverse) Insertion

Kur7103-6979-DEL line

```

ttcgtctaaagtcctgcatctaccactggcaggagagataaggccaacctaccggtccatcaatggcctaagttcctctacttggtaca
aatctctcagacctgaactgtctcctaataacggttaactgtacagcatctacttgcaatgtctcgacgaacctaatacgtagagtaag
cctcactacctagcttattaatagggcatcctcgtttc-----JUNCTION DEL-----
cgtgctgagtggtgatggcagactgaaattggcagttggtggtttacatagctttgctgggctttctctaaactgtgctgacctac
gtccaaaagaagccgacttagtaaaactggtcagagtgatcagaactcccgggcagttgtgcatcctgagctaggttctccgctggg
cggaatcctgaattgtgccctcctacctctgtggcaaatggaaggggagttgagtgggcaaaagtatagggataaataatagtgagg
cagctggcctgtatctttcagccccattt

```

Kur7103-6981-DEL line

```

ttcgtctaaagtcctgcatctaccactggcaggagagataaggccaacctaccggtccatcaatggcctaagttcctctacttggtaca
aatctctcagacctgaactgtctcctaataacggttaactgtacagcatctacttgcaatgtctcgacgaacctaatacgtagagtaag
cctcactacctagcttatta-----JUNCTION DEL-----
cgTCCATGCACGTAACGatggggcgtgatggcagactgaaattggcagttggtggtttacatagctttgctgggctttctctaa
actgtgctgacctacgtccaaaagaagccgacttagtaaaactggtcagagttgatcagaactcccgggcagttgtgcatcctgagctag
ggttctccgctggggggaatcctgaattgtgccctcctacctctgtggcaaatggaaggggagttgagtgggcaaaagtatagggatt
aaataatagtgccgagctggcctgtatctttcagccccattt

```

Kur7103-6982

```

ttcgtctaaagtcctgcatctaccactggcaggagagataaggccaacctaccggtccatcaatggcctaagttcctctacttggtaca
tacttggtacaaatctcagacctgaactgtctcctaataacggttaactgtacagcatctacttgcaatgtctcgacg
aacctaatacgtagagtaagctcactacctagct---JUNCTION DEL---
ggggcgtgatggcagactgaaattggcagttggtggtttacatagctttgctgggctttctctaaactgtgctgacct
acgtccaaaagaagccgacttagtaaaactggtcagagttgatcagaactcccgggcagttgtgcatcctgagctagg
ttctccgctggggggaatcctgaattgtgccctcctacctctgtggcaaatggaaggggagttgagtgggcaaaagt
atagggataaataatagtgccgagctggcctgtatctttcagccccattt

```

Kur7103-7131

```

ttcgtctaaagtcctgcatctaccactggcaggagagataaggccaacctaccggtccatcaatggcctaagttcctctacttg
gtacaaatctcagacctgaactgtctcctaataacggttaactgtacagcatctacttgcaatgtctcgacgaacctaatacgt
agagtcaagtcctcactaccta---JUNCTION DEL---
atggggcgtgatggcagactgaaattggcagttggtggtttacatagctttgctgggctttctctaaactgtgctgacctacgt
ccaaaagaagccgacttagtaaaactggtcagagttgatcagaactcccgggcagttgtgcatcctgagctaggttctccgct
gggcgggaatcctgaattgtgccctcctacctctgtggcaaatggaaggggagttgagtgggcaaaagtatagggataaataa
tagtgccgagctggcctgtatctttcagccccattt

```

Figure 5-27: Sanger Sequencing results of the founder animals for the transgenic *Mif* KO rat.

(A) F0 sequences; red color indicates forward oligo F2; green color indicates reverse oligo R7; cyan indicates insertions.

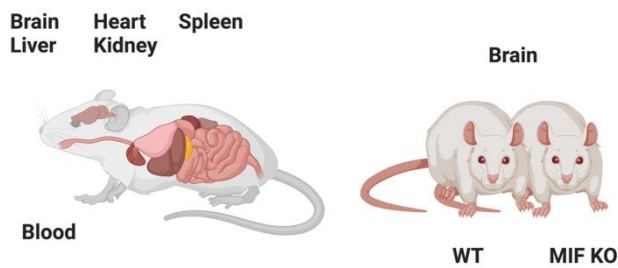


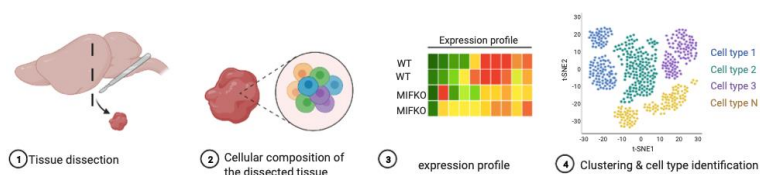
Figure 5-28: Illustration of experimental design for rat tissue collection.

Different Tissue samples were collected (brain, heart, kidney spleen and liver) for western blot, tissue staining and RNAseq (bulk) as well as serum of WT and *Mif* KO rats.

Various organs were removed from WT and *Mif* KO rats and collected for subsequent staining, Western blots, and RNAseq analyses (Figure 5-28). The brain, heart, spleen, kidney, liver, and blood were collected as freshly frozen tissue. For further RNA seq analyses, different areas of the brain were brought together, the prefrontal cortex, hippocampus, cerebellum, and corpus callosum. In order to investigate the biological role of Migration Inhibitory Factor (MIF), a pleiotropic cytokine, mouse strains without MIF were generated in embryonic stem cells by gene targeting in earlier research projects. However, no ratlines are known with a MIF deletion.

A wide variety of results were achieved in mouse trunks with MIF deficits. In the lethal effect of high-dose bacterial lipopolysaccharide (LPS) or *Staphylococcus aureus* enterotoxin B (SEB) with D-galactosamine, *Mif* KO mice showed resistance compared to wild-type mice. However, one of the most interesting observations was made a decade ago when MIF-deficient mice showed longer lifespans. Compared to control mice, *Mif* KO mice are significantly extending lifespan in response to calorie restriction (CR)²⁵⁸.

Rnaseq tissue collection



Serum Collection



Figure 5-29: Illustration of experimental design for WT and *Mif* KO rat tissue collection.

Different Tissue samples for western blot, tissue staining and Rnaseq (bulk) as well as serum collected of brain, heart, kidney spleen and liver.

Various methods can validate genes, and multiple techniques can confirm a gene deletion in addition to the examination of transgenic standard PCR with subsequent agarose gel electrophoresis or real-time PCR for genotyping.

The subsequent analysis uses the western blot technique, in which β -actin is used as a housekeeping gene. The description of housekeeping genes is used for genes that are not subject to any regulation in the cell's transcription process. Housekeeping genes can be used as a control, or the target proteins can be normalized to the housekeeping protein concentration. The western blot results were normalized for each animal with respect to its β -actin band intensity. Monomeric AIF shows a band at the height of about 67Kd, MIF about 12.5kD, and β -actin at around 42Kd. On the PVDF membrane, all wild-type (Animal ID: 9041, 8908, 9366 and 9052) and heterozygous (Animal ID: 9046, 9049, 9912 and 9050) rat samples showed a band for β -actin, AIF, and MIF. Only for the *Mif* KO (Animal ID: 9365, 9051, 8907 and 9053) animals were no band for MIF detected (Figure 5-30). There are no significant differences based on the MIF concentration of wild-type and heterozygous rat samples. However, *Mif*-KO rats show a significant MIF protein deficiency.

The mean values of the AIF protein level show slight differences. Still, the results are similarly slightly spread for all genotypes so that no difference in the AIF expression can be determined based on the genotypes.

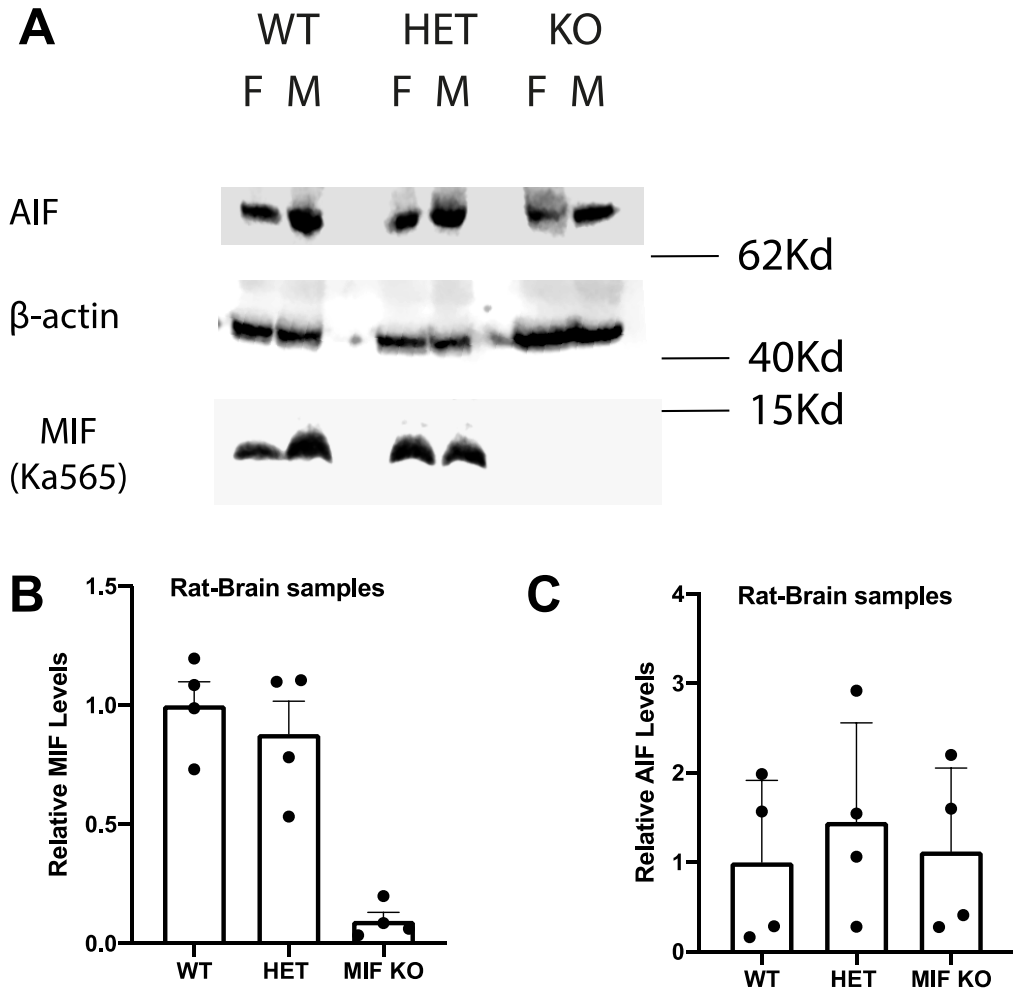


Figure 5-30: Western Blot Validation of the CRISPR/Cas9 transgenic WT and Mif KO rat, by AIF and MIF detection, by using brain tissue.

Analysis of MIF and AIF detection in WT, het and Mif KO rat brain tissue. Dissected and collected under the guidance of Prof. Dr. Özgün Gökçe. (A) Western Blot of AIF; β -actin und MIF (B) MIF expression quantification normalized to β -actin (n=4). (C) AIF expression quantification normalized to β -actin (n=4); quantification by LI-COR Software for Proteomics Imaging and Analysis.

6. Discussion

6.1. Aging associated neurodegenerative diseases

The past few decades have seen significant advancements in the fields of science and medicine. As a result, there has been a notable improvement in life expectancy and overall health at an advanced age. However, these advancements have presented new challenges to society, particularly in dealing with conditions that are commonly associated with old age. One such class of age-related diseases is neurodegenerative diseases, which include well-known conditions such as Alzheimer's disease, frontotemporal dementia (FTD), Parkinson's disease (PD), and motor neuron diseases like amyotrophic lateral sclerosis (ALS)²⁵⁹. These diseases are characterized by diverse pathophysiological processes that can affect different bodily functions. For instance, some of these disorders can lead to speech, movement, or breathing difficulties, while others primarily cause memory and cognitive impairments^{260,261}. To gain a better understanding of neurodegenerative disorders and develop effective treatments, it is crucial to decipher their causes and the molecular mechanisms that govern them. One key mechanism that affects every cellular life cycle is apoptosis, which plays a critical role in cell physiology. Each individual mechanism involved in apoptosis is complex. Apoptosis is particularly relevant when the cell is affected by factors such as caspases, B-cell lymphoma 2 (Bcl2), tumor necrosis factor- α (TNF- α), or reactive oxygen species (ROS). The disruption of regular cellular processes, such as apoptosis, due to aging or harmful environmental influences, can lead to detrimental neurodegenerative disorders^{262,263}. Neurodegenerative diseases are often characterized independently, but there is frequently an overlap between Alzheimer's disease and Lewy body pathologies. Biomarkers are crucial in diagnosing neurodegenerative diseases and tracking their progression in clinical trials. Aging leads to many changes in the organism, including the gradual decline of various tissues and organs. Neurodegenerative diseases are particularly associated with aging and are characterized by cognitive and motor impairments. With life expectancy increasing, there has been a rise in neurodegenerative diseases. The accumulation of cellular stresses, such as oxidative stress and DNA damage, contributes to the aging process and can exacerbate neurodegenerative diseases. PARP1 is a protein that is linked to aging and neurodegenerative diseases and is also involved in cell death mechanisms in neurons, called parthanatos. In addition, PARP1 suppresses autophagy but also plays a role in DNA repair and neuroinflammation. PARP1 inhibitors have been the focus of drug research for the

treatment of breast cancer, pancreatic cancer, and other diseases, but drug discovery is still in its early stages for central nervous system disorders. Therefore, it is essential to conduct comprehensive studies on PARP1 and its downstream mechanisms. However, the nature of the BBB and the structural changes following post-translational modifications make it challenging to control PARP1 with an inhibitor drug and establish effective medication for central nervous system diseases.

PARP1 activation can lead to DNA degradation by nucleases and activation of pro-inflammatory gene transcription. Interestingly, inhibition of PARP1 leads to the accumulation of cytosolic self-DNA, which activates the cGAS-STING signaling pathway. These findings suggest that PARP1 activity is diverse and that various factors interact, which ultimately determines the activity of specific pathways^{264–266}.

However, it represents an important research area for future in-depth studies of PARP1 as it is still a critical avenue to solve these problems^{265,267}. This study, aims to focus on the activation of apoptosis, also known as parthanatos, by PARP1-induced DNA degradation by MIF as a nuclease.

The activation of the poly-ADP-ribose polymerase 1 (PARP1) and, thus, the parthanatos signaling pathways is additionally increased by the strongly oxidative environment after a stroke. Another study showed that resveratrol preconditioning (RPC) induced ischemic tolerance by inhibiting PARP1 overexpression and, thus, parthanatos²⁶⁸.

6.2. MIF-2 is a potential nuclease

The family of nucleases is structure, function, and topology overarching. In general nucleases can cleave phosphodiester bonds (between sugars and the DNA phosphate units) of nucleic acids. These include endo- / exonucleases, DNases / RNases, topoisomerases, recombinases, ribozymes and many others^{74,269}. The families of nucleases, such as the members of the PD-(D/E) XK nuclease, are not only diverse, but can often also show low sequence similarities. The main features of this family are the similar core folds and the critical residues in the active sites. For this very reason, it was not only a challenge to establish MIF as a new member, but also, in the case of this study, MIF-2 because the standard sequence analysis needs to be revised to obtain evidence²⁷⁰. MIF was recognized as a new member of the (D/E) XK nucleases in 2016. the similarity to the restriction endonuclease was demonstrated by comparing the critical motifs within the sequence that represents the active site for nucleic acid cleavage. However, our investigations have shown that the evolutionary conservation of the active center was only preserved with the help of the crystal structure, which was not immediately recognizable from the amino acid sequence. The experiments of this study

aimed to investigate the predicted active sites of nuclease activity, DNA cleavage sites, as well as the potential biological role of this newly discovered nuclease function of MIF, but also of MIF-2. MIF has been identified as endonuclease as well as an exonuclease based on the MIF trimer^{19,116,271}.

While the DNA polymerase contributes to the replication of the template DNA, the exonuclease degrades faulty DNA strands in the 3' to 5' direction. The deletion of this exonuclease, which contributes to proofreading, leads to increased cancer in mice¹⁵². Another factor in DNA integrity is the removal of Okazaki fragments during replication. RNaseH, FEN1 endonucleases are also involved in the elimination of the Okazaki fragments in eukaryotes and archaea^{75,153–155}. The flap endonuclease (FEN1) removes RNA and DNA 5'flaps^{75,154}. In this study we tested FEN1 next to MIF and MIF-2 as negative controls. The nuclease assay, visualized by the agarose gel showed no degradation of the plasmid DNA by FEN1, whereas MIF and MIF-2 show a clear DNA cleavage. However, no observation of FEN1 nuclease activity was not unexpected in this experimental design since 5'flaps were not present in the used plasmid DNA as substrate. However, it also shows no risk of contamination from the excipients used in the reaction design. Although, this approach cannot disprove whether the in-house purified proteins MIF and MIF-2 carry contamination by bacterial nucleases. Next to FEN1 also restriction enzymes such as AGEI, EcoRV, EcoRI and DNase1 have been used as a positive control for plasmid DNA cleavage (nuclease agarose gel assay). Similar to previous studies, the nuclease assay works, and the established restriction enzymes, likewise nuclease associated with the PD-(D/E) XK family show nuclease activity and cut the plasmid DNA. We were able to show how similar previous studies were that the assay itself works and the established restriction enzymes, which are also associated with the PDX nucleases, show nuclease activity, and cut the plasmid DNA. However, to determine the K_d of MIF and MIF-2, besides if both show an affinity for specific sequences or binding sites, the real-time nuclease assay was established for this purpose. Simultaneously it was not expected that the restriction enzymes show nuclease activity in this assay. Due to the missing specific cutting site, AGEI, EcoRI and EcoRV have been used as a negative control site in the probe based real-time nuclease assay. Nucleases can be classified according to their motifs in their primary sequences, however functional properties can be conserved in 3D crystal structure sequences in comparisons with other known nucleases. In 2016 MIF was identified as a Mg²⁺-dependent nuclease showing 3' exonuclease and endonuclease activities¹¹⁶. Specifically, the goal of this study is to minimize the possibility of artifact. Therefore, various positive and negative controls were used to exclude the observation of nuclease activity due to a manufacturing or testing procedure. In this study, the 3D crystal structure

was also observed of human MIF with human MIF-2, mouse MIF with mouse MIF-2, human MIF and mouse MIF-2, and mouse MIF-2 with staphylococcal nuclease. We focused on either the glutamic acid at the region 22 for mouse and human MIF, or the glutamic acid at the region 88 for mouse and human MIF-2, as functional moiety necessary for the respective nuclease function. We observed that in all cases the glutamic acid (E88) for human and mouse MIF-2 is in proximity to the critical glutamic region E22 for mouse MIF and MIF-2 and next to the glutamic acid E44 for the staphylococcal nuclease. In addition, nuclease deficient mutants showed no (MIFE22Q) to little nuclease activity (MIFC81S; MIF-288Q) detected by agarose gel nuclease assay as well as real-time nuclease assay. Using the MIFE22Q mutant, the results of Wang et al. 2016, have been reproduced. In which the mutation specifically affects the function of the active site. Now, enzymes of the PD-(D/E) XK nuclease family are endowed with multiple active sites. Therefore, inhibition of nuclease activity by mutation of MIFE22Q may disrupt the one critical active site, but it is likely that a misfolding resulted from the mutation, leading to a significant reduction in nuclease activity. The PD-(D/E)XK motifs could only be partially found in the sequence compared to MIF. However, our study showed that the fold conserves the critical active site where the E88 of MIF-2 is missing, resulting in glutamic acid at position 22 being replaced. A nuclease activity for MIF-2 could also be measured after the mutation. Again, it is believed that this is not the only domain that plays an important role in the nuclease function. In addition, the folding of the protein is not disturbed by this weakening so that the other nuclease domains, which are responsible for the function, are preserved. The S-nitrosylation site of MIF, Cys81, has been an area of research for years. The focus is on the decreasing MIF activity. Among other things, MIF can stimulate the transcription of BDNF, while SNO-modified MIF shows less effect. In addition, S-nitrosylation of MIF is believed to cause a conformational change. Which in turn impairs trimer formation. It is still unclear whether nuclease activity is affected by homotrimer formation by MIF. However, our studies do not show a clear effect of trimer and dimer on nuclease activity²⁷². In this study, it was observed that the MIFC81S mutant, which mimics the SNO-modified MIF, as well as the MIF zinc finger mutant, which is the DNA-binding site. In addition, reduced nuclease activity was noted in this study. Using the MIF and MIF-2 mutants in this study, it was shown that the assay works and carries no risk of artifacts due to contamination from nucleases in the environment. However, a conformational change and the possible bacterial nuclease contamination during the purification of the MIF was not completely ruled out. Therefore, it was necessary to establish the nuclease assay directly affecting MIF. Our validation approach led us to add a MIF-neutralizing antibody to the nuclease assay. In the presence of a neutralizing anti-MIF monoclonal antibody (clone IID9, IgG1

isotype) we also showed a decrease of plasmid DNA degradation and probe cleavage. Overall, we were able to determine the critical nuclease residues and independence from the MIF and MIF-2 nuclease activity, in addition we can rule out bacterial nuclease contamination. Through the antibody neutralization of MIF, a successful reduction of the inflammatory symptoms could be shown in studies^{273,274}. However, there is a consensus that understanding the molecular structures and their dynamics responsible for the functional properties can help influence the disease state. This is because, by conformational change or inhibition, targeting the active sites accountable for nuclease function can lead to inhibition of DNA degradation and, thus, cell death via the PARP1-activating AIF-dependent apoptosis pathway. However, MIF and MIF-2 are topologically controlled, meaning that, among others, unwanted symptoms could be promoted by also modifying extracellular MIF or MIF-2^{19,275}. It is known that MIF and MIF-2 have overlapping functions, including transcriptional activation of pro-inflammatory factors, which is promoted, for example, by binding to the CD74 receptor^{276,277}. Further controls were conducted using the in vitro agarose nuclease assay and real-time nuclease assay. The inhibitory effect of MIF in connection with diseases has been proven in many studies. Therefore, many known MIF inhibitors were tested with the agarose-nuclease assay. However, nothing was able to inhibit or stop the nuclease activity except for the antibody IIID9, which is used in many studies as a neutralizer anti-MIF monoclonal Ab (clone IIID9, IgG1 isotype)^{65,234,278}. ISO-1, known as MIF antagonist, a cell-permeable inhibitor of MIF tautomerase (IC₅₀ = 7 μM for D-dopachrome tautomerase), could not inhibit the nuclease activity. The MIF antagonist MIF98 was also unable to show any inhibition of nuclease activity^{279,280}. We obtained similar results after a 4-IPP addition to the nuclease reaction mix²⁸¹. In summary, we assume that the nuclease activity has been verified in our laboratory, and the possible contamination by bacterial nuclease could be decidedly refuted with the help of the purification of a nuclease-deficient mutant (MIFE22Q). In addition, this result was supported by the inhibition of the nuclease activity by the neutralizer anti-MIF monoclonal Ab (IIID9). However, it is assumed that the MIF antibody IIID chelates out the MIF molecules in the reaction mix). There is no evidence that the antibody binds directly to the nuclease active pocket of the MIF proteins. At the same time, it would be very exciting to investigate this in the future by means of a crystallization analysis.

In general, can be confirmed that the nuclease activity could be verified for human and mouse MIF using all control resources available. However, the question of folding correctness after cloning processes remains unanswered, which could be explored in future studies. A malfunction caused by the mutation could also influence the nuclease activity, but this does not affect the question of the general nuclease activity. The reason

is that the contamination-free purification is still proven by inhibiting nuclease activity due to sequences/conformation changes. We could visualize a nuclear accumulation of MIF as well as MIF-2 upon excitotoxicity in primary mixed neuronal culture after treatment with NMDA, MNNG and etoposide. In primary astrocyte culture we showed similar AIF, MIF and MIF-2 nuclear increases after toxic insult with MNNG. We could not detect any effect of MIF nuclear increase in *Mif-2 KO* cultures or MIF-2 nuclear increases in *Mif KO* culture. In addition, neither *Mif KO* nor *Mif-2 KO* cultures influenced AIF translocation into the nucleus. Whether a MIF deficiency leads to a decrease in apoptotic cells or a decrease in repair processes in damaged cells is still unclear, as is the exact mechanism behind it. Since MIF was referred to as an AIF-dependent nuclease in initial studies, its deficiency decreased apoptotic cells. However, recent studies discovered MIF as a 3' flap nuclease critical for DNA replication. In this study, which at first glance seems contradictory, it must not be forgotten that MIF and MIF-2 are complex proteins with different enzymatic abilities and functions. However, this makes their study all the more difficult since the experimental environment appears to be crucial for the functional unfolding of MIF and MIF-2.

In 2016, Wang et al. reported reduced levels of DNA damage in *Mif KO* and MIF nuclease deficient cultures. To confirm this finding, we conducted experiments using the neutral comet assay to assess DNA damage in primary astrocyte cells from *Mif KO* transgenic mice. Our results showed a significant decrease in double-strand breaks (tail moment) in these cells, as well as in *Mif-2 KO* primary astrocytes. The comet assay is a microscopic method that allows for visualization of DNA breaks or damage. The shape of the comet tail can provide insight into the amount or length of DNA breaks, and therefore the extent of damage. However, it should be noted that DNA breaks can also occur as part of a repair mechanism, indicating an intact or increasing repair process. In our study, we propose that MNNG-stimulated apoptosis activates the MIF or MIF-2 nuclease function, leading to comet assay tail formation as a result of DNA damage. With the help of two independent DSB markers (γ H2AX and 53BP1), we showed a DNA damage decrease in *Mif-2 KO* primary astrocyte culture. However, it was still unclear if the decrease of DSB in *Mif KO* and *Mif-2 KO* cells is due to the missing nuclease activity in the AIF dependent apoptosis pathway, during the repair mechanism, or a decrease in the proliferation rate. It is known that MIF has regulatory properties that can, among other things, stimulate the growth of cell lines, for example, endothelial cells²⁸². Therefore, this proliferation-promoting function of MIF should also be a fact that makes the study of cell loss due to AIF-dependent apoptosis even more complex.

To clarify some of these questions, we plated the same number of primary astrocyte cells, treated with MNNG, and counted them after the incubation time. We observed a

decrease of the cell count in WT control compared to MNNG treated primary astrocyte cells. We saw a significant effect of MNNG in WT, while in our heterozygote WT/*Mif-2* KO cultures the toxic insult was not significant. Same was observed for *Mif-2* KO samples compared to the MNNG treated and the control group. These results indicate a decreased risk for apoptosis upon MIF or MIF-2 deletion. However, WT control samples compared with *Mif* KO significantly increased in cell numbers. To explore this finding more in detail, the cell number in culture during a longer period of time was monitored. We established the live imaging, during toxic insult and counted the cells every ~30 minutes. After initially incubating the cells with Hoechst and treating them with MNNG we readily detected less cells in WT MNNG samples. Cell numbers were gradually decreasing within 13 hours. Compared to WT MNNG samples we also detected a decrease in cell count in the WT control group. These decreases were, however, not at the same level as for the MNNG groups. Therefore, the difference between WT control and MNNG groups was still significant. A significant decrease was not given between *Mif-2* KO control and *Mif-2* KO MNNG groups. If we compare WT control groups with the *Mif-2* KO control and if we also compare the WT MNNG group with the *Mif-2* KO MNNG samples, we see significant increases of cell numbers for *Mif-2* KO, regardless of the control or MNNG group. Therefore, we assume a protective effect of MIF-2 deficiency upon toxic insult.

Studies have shown that treatment with MNNG activates Neuro2a cell death in vitro. However, cultures deficient in MIF show a reduction in cell loss. Previous research has also demonstrated a protective effect of modified MIF, such as through acetylation²⁸³. It remains unclear whether this modification prevents binding to AIF or whether conformational changes lead to a reduction in the promotion of apoptosis by MIF. Nevertheless, these findings do not contradict previous studies that have identified MIF as essential for the DNA repair mechanism.

In this study, we were able to replicate the toxic effect of MNNG on astrocyte cultures. Similar protective observations were made in MIF and MIF-2 deficient cultures, leading us to hypothesize that MIF-2 also plays a critical role during apoptosis. However, it remains to be confirmed whether this pathway is also AIF-dependent. Additionally, MIF-2-deficient cultures were observed to have higher cell counts despite MNNG treatment. This observation suggests that cells with MIF-2-deficiency may be protected during experimental handling. Therefore, in vitro MIF deficiency appears to promote cell survival. In conclusion, it was found that (1) MIF-2 is a novel nuclease and can digest plasmid DNA and fluorescein-labeled oligonucleotide probes. Although it is the paralogue of MIF, the critical nuclease sequence is partially conserved. However, these were restored within the crystal structure, and thus the active center for the nuclease

function could be preserved. (2) MIF-2 critical nuclease domain is identified as E88. With the help of the simulation of the critical structures, the most important domains for MIF and MIF-2 could be superimposed. Note that the glutamic acid of MIF-2 at position 88 overlaps with the glutamic acid at position 22. In addition, our investigations were able to show a decrease of the nuclease reaction for the mutant MIF-2 E88Q. (3) MIFE22Q show loss of nuclease activity, MIFC81S as well as for MIF-2 E88Q have reduced nuclease activity. Therefore, previous studies with the MIFE22Q mutant could be reproduced. In addition, the MIFC81S mutant was discovered, which also resulted in a loss of MIF nuclease function. (4) Neither MIF nor MIF-2 deficiency influences AIF nuclear translocation. We could detect nuclear AIF in WT, MIF or MIF-2 deficient cells. (5) MIF deficiency does not alter MIF-2 nuclear enrichment upon toxic insult as well as MIF-2 deficiency is not altering MIF nuclear increase after MNNG treatment in astrocyte culture. (6) MIF and MIF-2 deficiency show less DNA damage levels in primary astrocyte cultures. However, it is unclear whether decreased DSB markers in MIF and MIF-2 deficient cells are due to apoptotic protection or a reduction in cell repair mechanisms. (7) In *Mif-2* KO primary astrocyte culture, we detect higher cell numbers than WT astrocyte culture, regardless of a toxic insult.

6.3. MIF is related to DNA damage

Cell death is a crucial mechanism that helps to maintain tissue and regulate organ size and function. However, it plays an even more critical role in neuronal cells. This is because postmitotic neurons, after the development phase, need to maintain circuits, and therefore, the longevity of these cells is of utmost importance. Cell death can occur during both the development phase and in postmitotic neurons that have already formed a differentiated neuronal population. During the development phase, cell death helps to regulate optimal target innervation by eliminating a specific number of neurons that migrate into ectopic positions or innervate incorrect targets. The overall balance of programmed cell death is an important factor in acute and chronic neurodegenerative diseases. While targeted cell death can contribute to the formation of functional circuits, aberrant cell death mechanisms are one of the main causes of neurodegenerative diseases. Although neuronal cell death shares similarities with other cell types, there are also significant differences. Due to the neuronal excitability, a high turnover of ATP¹⁶⁸ is converted, so neurons can be tapped against ischemia-induced death. In addition, the voltage-controlled sodium channels are an area of attack for sodium overload and,

consequential swelling. However, precisely this feature is used in this study to induce neuronal cell death *in vitro*.

However, in addition to neurons in the brain, one must not lose sight of other important cell types such as glial cells. They themselves have important roles, as do astrocytes which support neurons metabolically. In addition, they modulate synaptic activity. This however concludes that an impairment of the astrocyte functions has a major influence on neuronal survival²⁸⁴.

Today, astrocytes are increasingly in the focus of many acute and chronic neurodegenerative diseases. Within neurodegenerative diseases such as cerebral ischemia or Alzheimer's disease, apoptotic astrocytes are increasingly the focus of studies. Astrocytes are also an important factor in fighting off antioxidants^{8,285,286}. Oxidative stress is known to be implicated in neurodegenerative diseases. Although the cerebrum measures only a small body mass (2%) compared to the total body weight, it still uses around 20% of the oxygen required by the body. If at the same time one considers that ROS are continuously generated as a by-product during oxidative metabolism, everything involved in these cascades plays a key role in neurodegenerative diseases. If, contrary to the antioxidative capacity, there is an imbalance in the direction of the reactive oxygen species (ROS), one speaks of oxidative stress. This inequality can be fueled by numerous factors such as amyloid P peptides, inflammatory cytokines or decouples of mitochondrial electron transport, to name a few. The formation of oxygen species (ROS) can be prevented with the help of antioxidants such as ascorbic acid or antioxidant enzymes such as glutathione peroxidase. Astrocytes contain many of these antioxidants. Above all, glutathione metabolism of astrocytes, via extracellular forerunner, plays an important role in the disposal of exogenous peroxides, thereby protecting astrocytes in coculture neurons from the toxicity of ROS²⁸⁷. More recent findings however, provide additional evidence (*in vivo*) for the glutamate-glutamine cycle in the brain between neurons and astrocytes^{288,289}. In addition early studies suggest MIF as member of the theta-class glutathione S-transferase²⁹⁰. However this assumption has been questioned by later investigation²⁹¹. This study not only emphasizes the importance of the networking of neurons and astrocytes, but also the role of the MIF family (MIF and MIF-2) as a key function within the programmed cell death mechanism. In the context of stroke, the involvement of the macrophage migration inhibition factor (MIF) in cell death was examined in detail, even if some studies present controversial results²²⁹. The importance of the MIF family in this context is not overshadowed. In connection with the neurological deficits after an experimental stroke, it was shown that a disruption of the MIF gene in mice resulted in lower infarct volumes^{116,229}. In addition, after a temporary occlusion of the middle cerebral

artery (tMCAo) in MIF-KO mice, less damage to the sensory-motor function was measured^{229,292}. Furthermore, the finding confirms that neurons in the peri-infarct region show an enrichment of the MIF expression. This is particularly the case with interneurons of the cortical area. To emulate this, in-vitro studies have also shown that cultured cortical neurons in neuronal mixed culture increase the MIF level during oxygen and glucose deprivation. It is assumed that the molecular composition within the cells and as a result, also the macrophage and microglial reactions are influenced. This has a major influence on the neurological deficits after a stroke. Without neglecting the role of the MIF family within different cell mechanisms, this study aims to highlight the nuclease function of the MIF family and the resulting key role in the pathogenesis of neural injury caused by stroke or other neurodegenerative diseases^{44,116,236}. The importance of this aspect in this study is supported by the assumption that Parthanatos belongs to regulated cell death (RCD). This in turn stands in the context of DNA damage, which is triggered for various reasons. The mechanism of regulated cell death, which is influenced by the apoptosis-inducing factor (AIF), sheds further light on the effects of the MIF family within neurodegenerative diseases with the discovery of MIF as the missing nuclease. Signal transduction pathways, mechanisms and functions of MIF are still better characterized than those of MIF-2. MIF-2 shows 34% homology with MIF, and both can be seen as a homotrimer structure. Earlier studies are known in which the role of MIF-2 in cancer is characterized. When MIF and MIF-2 are inhibited in the pancreatic cell line PANC-1, this results in a reduced activation of ERK1 / 2 and AKT. In addition, the p53 expression levels were increased, and in this context the tumor growth was inhibited in vitro and in vivo at the same time^{293,294}. In addition, post-translational modifications are present in MIF, and they are also observed in MIF-2. Both share the removal of the N-terminal methionine and the resulting exposure of a proline residue. This is believed to be necessary for enzymatic activity. Interestingly, the same post-translational modification and the exposed proline residue can bind isothiocyanate. This leads to the loss of tautomerase activity¹⁹⁶.

MIF, a cytokine family member, is a true mediator of inflammation and innate immunity. After stimulation by microbial products and proinflammatory cytokines, it can be released quickly and, in turn, stimulates the production of proinflammatory mediators by immune cells. Accordingly, the extracellular MIF is characterized by its function as a cytokine and atypical chemokine. In previous studies MIF has been observed in the cytoplasm and nucleus^{19,116,295}. MIF was stained in a primary mixed neural culture in this study, and a confocal microscopy Z-stack image was generated. This enabled the MIF localization to be determined. In addition, MIF was calculated and visualized inside and outside the Dapi marker. In this study, all three topological localizations within the cell could be

shown in MIF and MIF-2. Within the Cell, MIF can be colocalized with other proteins. In this thesis, we observed that known DSB markers such as γ H2AX and 53BP1 are colocalized with MIF and MIF-2 in the cell nucleus. DNA damage is one of the reasons for this instability and thus for neurodegenerative diseases. DNA strand breaks can occur as single-strand breaks, and the others as double-strand breaks (DSB). The DNA double-strand break (DSB) is a type of DNA damage that can have severe consequences in cells, particularly if it is left unrepaired. This damage can result in programmed cell death (apoptosis) or mutations in genes that lead to cancer. Additionally, the missing nuclease in AIF-induced apoptosis was identified as MIF, and since then, nuclear MIF has been closely associated with apoptosis mechanisms. In published research, the histone variant H2AX and its phosphorylation on Ser 139 (γ H2AX) have been recognized as a marker of DSBs. However, it is not limited to DNA damage detection but also plays an important role in various tasks, such as DNA repair⁵⁵. The 53BP1 (p53 binding protein 1) was used as an enhancer for the transcription of p53. With the help of the 53BP1, late DNA damage reactions (DDR) can be detected. In addition, as a DSB marker, DNA damage marker Comet Assay (single-cell gel electrophoresis) can also be used. With the help of this technique, DSB can be recognized under neutral conditions and SSBs under alkalic conditions. Cells are embedded in agarose, lysed, and exposed to an electric field. Depending on how severe the DNA damage is, comet-like stripes appear behind the cell body. The more DNA that accumulates in the tail, and the longer it is, the more advanced the DNA damage has become²⁹⁶. This study found that depletion of MIF or MIF-2 resulted in reduced DNA damage, as indicated by a decrease in 53BP1 intensity and γ H2AX foci. These findings were validated using the Comet assay, which showed less DNA damage in MIF and MIF-2. The results were obtained from primary mixed neuronal cultures, as well as hippocampus and cortex tissue from both MIF knockout and wild-type animals. However, it should be noted that cellular stress occurs within the cell cultures, and the cells are also tested for the Comet assay during dissociation. In summary, *Mif* KO cell cultures and tissues appear to be less susceptible to DSB breaks in stressful situations. However, further investigation is required to determine whether *Mif*-KO animals exhibit minor DNA damage under physiological or tumor-related conditions, as this is inconsistent with the research.

6.4. Validation of MIF/MIF-2 enzymatic activity

A specific family of proteins has evolved as a key regulator in the pathway of neurodegenerative diseases over the last few years^{116,297,298}. This is the MIF protein family, which consists of the macrophage migration inhibitory factor (MIF)^{116,299} and its paralogue MIF-2, also known as D-dopachrome tautomerase (D-DT)^{121,126,127}. As already mentioned, the common neurodegenerative diseases, such as AD, FTD and ALS are incurable conditions nor can the disease progression be suppressed^{179,261,300}. These diseases are related with an accumulation of abnormal or misfolded proteins, for example amyloid in the context of AD. An accumulation of improperly folded or aggregated protein leads consecutively to a cellular response of inflammation and to an impairment of normal microglia activity in the brain. This is where the role of the MIF family fits in, since the MIF proteins are known mediators of inflammation and participate in immune responses (in the periphery). Recent studies have identified MIF as a key mediator in the brain. It has been found that these group of proteins are important in microglial activity, inflammation, as well as blood brain barrier function. A key finding is that in addition to its inflammatory role nuclear MIF is a PD-(D/E)XK nuclease that is calcium and magnesium dependent. Since the decomposition of DNA is a step in the apoptosis cascade, it is vital to investigate the role of MIF as a nuclease, as this could provide a clearer insight into the molecular mechanisms that govern neuronal death in neurodegenerative diseases^{205,231,301,302}.

In summary, this work highlights the multipotent function of MIF. Furthermore, where it is shown that MIF and its family members, such as MIF-2 and their receptors, play a central role in the regulation of innate and adaptive immunity, it is also studied widely as one of the most important factors involved in various pathologies, such as autoimmune and neurodegenerative diseases. This study validated nuclease activity for MIF and observed by chance the nuclease function of MIF-2. Important achievements were the finding of similar nuclease domains in the crystal structure of MIF and MIF-2 and the experimental exclusion of a possible artifact of nuclease activity through contamination of the experimental set-up by bacterial nucleases during protein purification. While nuclease activity was discovered early in the work, validation and potential functionality pose the greater challenge. There are several methods to validate enzymatic purity. This can be evaluated using inhibitor-based, substrate-based, or comparative studies. Studies based on inhibitors to validate enzymatic purity are the most common. For these

reasons, some of the known MIF and MIF-2 inhibitors and antibodies were tested. Unfortunately, none of the known MIF, MIF-2, or specific for their receptors could reduce, let alone wholly inhibit, the nuclease activity detected in this study by the agarose nuclease assay. However, a reduction in the nuclease activity of MIF was detected after the addition of the known MIF antibody IIID9 using the real-time nuclease assay. In addition, the nuclease activity could be stopped by adding the chelator EDTA, which removes the positively charged ions from the nuclease buffer. However, the purity of the MIF nuclease activity is not adequately demonstrated only with the addition of EDTA since possible contamination of bacterial nucleases may also be ion dependent. So enzymatic purity is only possible with the addition of inhibitors specific for MIF and MIF-2, or the catalytic pocket responsible for the enzyme reaction is altered by a mutation such that the protein activity is inhibited. In this study, the critical regions for the nuclease activity were mutated to show another possibility for detecting the purity of the enzyme activity. However, the purity of the proteins produced in the house should not be doubted. It should be emphasized that, unless otherwise stated, all experiments were performed with recombinant proteins that were not only purified by HPLC but also by a complex purification process of C18 or C8 columns to remove contaminations.

6.5. MIF and MIF-2 are key players in various diseases

MIF and MIF-2 belong to the protein family of chemotactic cytokines, which regulate the innate immune system. Macrophage Migration Inhibitory Factor (MIF) is an evolutionarily conserved protein, which is also known, for its pro-inflammatory mechanisms. In addition, MIF and its paralogue MIF-2 play an important role in regulating many processes in biology and pathophysiology. MIF belongs to the family of chemokine-like functions, which share the classic chemokine receptor-mediated chemotaxis and cell recruitment activities. Still, MIF does not have the canonical N-terminal cysteine residues nor the chemokine fold^{103,147}. Human MIF (hMIF) is 114 amino acids long, similar in length to its paralogue human MIF (hMIF-2), which measures 118 amino acids. Since MIF was discovered in 1966, it has been commonly used, and so the interacting receptors discovered. The MIF and also MIF-2 family include the type II receptor proteins CD74 and also CXCR2 and CXCR4 receptors^{91,94,95,125,276,303}. The interactions between MIF and MIF-2 and their receptors have been partially researched, but the mechanisms for structure-activity properties or the topologically regulated functions have not yet been fully researched. In addition, over-expressions of MIF and MIF-2 have been shown in the context of diseases^{304,305}. During apoptosis, the nucleases take over the task of destroying the cell nucleus. This is an important step in the so-called PARP1 activated

parthanatos, a particular form of apoptosis. Given that MIF has been recognized as the sought-after nuclear in the AIF-dependent apoptosis pathway, it plays a vital role in destroying the nucleus. Accordingly, its translocation to the nucleus plays a critical role in the degradation of DNA degradation and the gain of apoptosis.

For this reason, next to the direct observation of an enzymatic reaction, research into the role and chain of effects represents a major challenge. It is known that the MIF family consists of unique proteins. However, this is what makes it exciting to recognize the mode of action in the biological context because MIF and MIF-2 act as cytokines, chemokines like protein, but it is also known to have tautomerase and the nuclease activity. The latter is examined in more detail in this work. However, the biological relevance of tautomerase and nuclease function has only been researched to a limited extent, whereas this enzymatic activity offers a high therapeutic potential. The functioning and mode of action of MIF and MIF-2 depend on the cell context and the state of induction. This is because MIF and MIF-2 can lead to different downstream activation and signaling pathways. However, this aspect has not been investigated in depth. A basic summary of what is known so far will be explained in the next section. A proliferative effect is observed in connection with the ERK1/2 pathway, and growth inhibition related to MIF with JAB1/CSN5 could be shown. When observing MIF in the context of angiogenesis, its associated receptor CD74 plays an essential role in cell proliferation and cell differentiation processes. MIF and MIF-2 are promising therapeutic approaches but are therefore also out of the question. If you summarize the literature, it often seems misleading to be contradictory. Especially concerning the ischemic core area after stroke, studies appear where an MIF deficit reduces the damaged region, but studies also appear in which the damage size has been promoted. How exactly different modes of action can be explained depends, as already mentioned, on the cellular context but also on the physiological conditions through unknown pathways. However, the known and possible unknown interaction partners of MIF and MIF-2 also play a major role. It is explained using the example of MIF; it is known to act as a pro-inflammatory cytokine. At the same time, known since 2016, it induces cell death through its nuclease activity, promoted by a pre-switched PARP1 activity.

MIF interacts with both JAB1 and CD74. When JAB1 and MIF interact, cell cycle arrest is promoted, but the CD74 receptor, in turn, promotes the proliferation of tissue precursor cells. Furthermore, it promotes proliferation by inhibiting HTAR1/p53. In this work, we were also able to show nuclease activity for MIF-2. Accordingly, we also postulate that MIF-2 has a multipotent ability, which is regulated by cell topology, timing, and physiological state. Therefore, with new approaches to the modulation of diseases, a deep understanding of MIF and MIF-2 and their interaction partners is essential.

Furthermore, because the opposite functionalities can also cause undesirable side effects, the function, position in the cell, and their possible interaction partners must be defined concerning MIF and MIF-2 depending on the disease. One takes a closer look at the location of MIF and MIF-2 within the cell. Thus, MIF/MIF-2 is found to be extracellular, cytosolic, and nuclear. The position in the nucleus has only been investigated since 2016, with the focus on the nuclease activity of MF. At the same time, MIF had been sighted in the nucleus decades earlier. Accordingly, it is undisputed that MIF/MIF-2 resides at different top pole locations in the cell. However, a more difficult question that is important to answer is how exactly it crosses the different compartments and what factors initiate these factors. It is important to research how exactly individual MIF functions are controlled because these can provide information on a disease state of the pathology. Since this study focuses primarily on the translocation from the cytosol into the nucleus and the associated nuclease reaction, the results of the nuclear translocation by interaction with mitochondrial AIF, will be described in more detail in the next section. Apoptosis-inducing factor (AIF) is a protein observed in normal cells, exclusively in the mitochondria. AIF increase is observed in the nucleus, during PARP1 activity, apoptosis induction by staurosporine, c-Myc, or etoposide. Studies suggest that Bcl-2 protein also influences or prevents AIF translocation into the nucleus from the mitochondrion^{306–308}. Due to DNA damage, the Activation of PARP1 leads to a release of mitochondrial AIF molecules in the cytoplasm, where it binds to MIF proteins and forms a complex. MIF can be transported to the nucleus within this complex, where it can eventually act as a nuclease^{116,151}. Within this study, an increase in nuclear AIF upon toxic treatment could be shown. This could be shown in vitro for HEK cells as well as for WT, Mif KO, and Mif-2 KO astrocytes. In addition, this study showed that MIF intensity in the nucleus, upon toxic insult, increased in WT and *Mif-2 KO* astrocytes. Similar results were observed for MIF-2 in WT and MFI KO primary astrocyte culture. Simultaneously, AIF intensity also increases in the nuclease. However, no clear correlation could be observed between AIF and MIF or MIF-2. It would be interesting to observe the enrichment of MIF and MIF-2 in AIF KO astrocyte culture in future studies. As well as a dual genetic deficit of AIF/MIF double KO, or AIF/MIF-2 double KO. This could allow validating if MIF translocates only in complex with AIF into the nucleus and if its paralog MIF-2 forms a similar complex with AIF to be escorted into the nucleus. The observations collected so far also explain the reduction of DNA damage detected by the comet assay and the known DSB marker, in vitro or in vivo. The detailed description will now be explained. The apoptosis in which PARP1 activation promotes AIF-dependent cell death is classified as parthanatos, which is a form of regulated cell death (RCD). This in turn is associated with DNA damage. Since In 2016 ,when MIF was described as nuclear for

the first time, in apoptosis-inducing factor (AIF)-dependent cell death, the changes in DNA damage related to MIF deficiencies are being studied¹¹⁶. However, controversial results have generally been obtained in the relationship between MIF and the mediated DNA strand breaks. Compared with the WT group, some studies show a reduction in DNA strand breaks in MIF-deficient cells, especially with H₂O₂ expansion. Some studies contradict this. They are related to repair mechanisms and cancer cells with high replication stress. In this study from 2021, one was described as a 3' flap nuclease. Besides, MIF was observed translocating to the nucleus in the S phase. In addition, PAPR1 at the DNA replication fork was colocalized with MIF. The deficiency of MIF reportedly promotes mutation frequency and promotes cell cycle delay. In the context of stroke, mice were subjected to a 45-minute transient middle cerebral artery occlusion (MCAO). The observation showed a similar intensity of ischemic insult but differences in infarct volume. In MIF knockout mice, lower infarct volumes were measured compared with the wild-type group. Whether this result is due to nuclear activity and thus death induced by the AIF is explained by the fact that the wild-type observations were restored by expression of wild-type MIF but not with the nuclear dead MIF mutants such as MIF E22Q¹¹⁶.

Stroke is one of the leading causes of death worldwide. However, strokes are categorized into different groups, with ischemia and hemorrhagic strokes. The obstructed cerebral arteries, thrombus formation, emboli, or atherosclerosis underlie ischemic stroke. Hemorrhagic strokes are caused by intracerebral hemorrhage³⁰⁹. Neuronal apoptosis after stroke is considered the leading cause of neurological deficits. In this context, MIF has been studied in different directions. However, it should not be forgotten that MIF belongs to the multipotent, atypical chemokines, which are also referred to as "multitaskers." Inflammation in the acute phase of stroke leads to a nuclear shift of NFκB in affected cells in the infarct area. In addition, MIF is also known to induce NF-κB activity. Independent of NF-κB, MIF, and MIF-2 play essential roles in inflammation, cell stress, and cell death. Moreover, poststroke events cause inflammation or cell death, among other effects^{310,311}. Neurons and glial cells, such as astrocytes, dysfunctional Ca²⁺ extruders, Excitotoxicity, or Cytoskeletal degradation, lead to Apoptosis or necrosis³¹². This study treated primary neuronal mixed culture with NMDA and primary astrocyte culture with MNNG. The aim was to demonstrate the effect of Mif KO and Mif-2 KO on DNA damage and survival, respectively.

In studies with H₂O₂ or other toxins significantly inducing cell death, a reduction in cell death was observed in MIF knockdown cells (adenovirus, MIF-shRNA), even in those showing translocation of AIF to the nucleus^{116,310}. In addition, the effects of MIF on DNA integration were observed using the Comet assay. It was found that Mif KO cells showed

less DNA strand breaks compared to the wild type. Whether the MIF deficit protects the cells from parthanatos under physiological conditions or during induced stress such as dissection/cell preparation, is unclear.

Here we investigate, using primary mixed neuronal culture and primary astrocyte culture, the behavior of MIF and MIF-2 deficit on cell survival after a toxic insult or in general, compared to the wildtype. Some studies suggest that knocking down MIF may be a promising therapy for rescuing neurons. However, in other studies, MIF or MIF-2 is described as a survival-promoting factor, primarily through its interaction with the CD74 receptor^{30,127,203,230}. But then, the studies differ in organ, cell, and/or age of interest. We observed less DSB in MIF- and MIF-2-deficient cultures in this study. In addition, we observed a higher cell number for *Mif-2 KO* primary astrocyte culture regardless of whether it was toxic insult or not. We observed less DSB in MIF- and MIF-2-deficient cultures too. In addition, we observed a higher cell number for *Mif-2 KO* primary astrocyte culture regardless of toxic insult or not. The individual functions and main interaction partners are known. However, critical control partners that trigger the function and mode of MIF and MIF-2 may still be missing. It is possible that there is a coupled response loop. Another protein is involved in the activation of apoptosis by the AIF pathway.

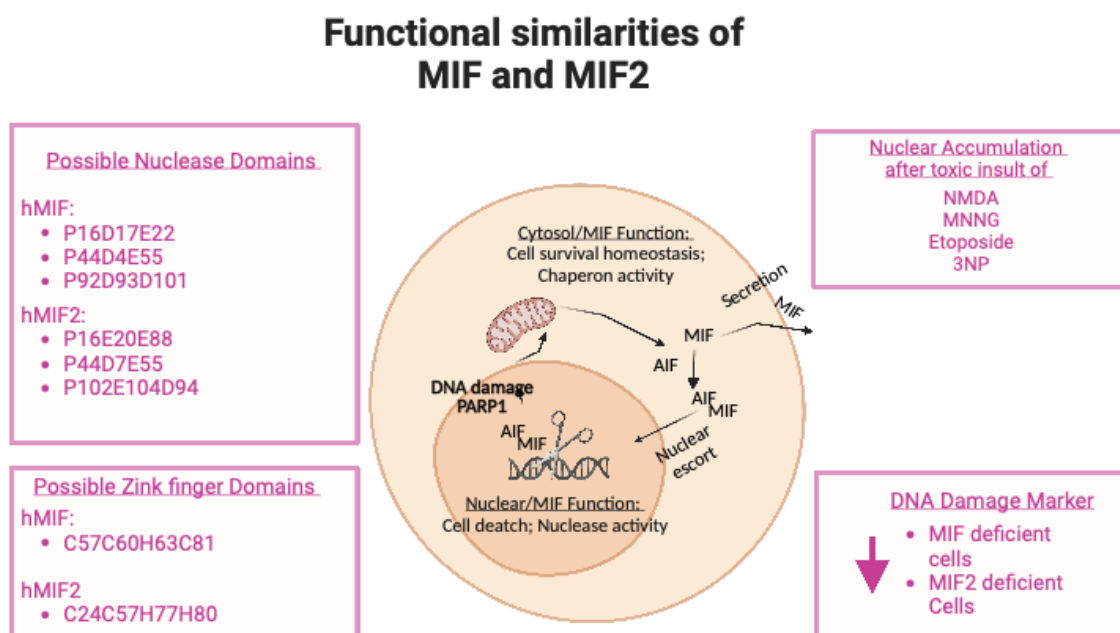


Figure 6-1: Schematic representation of summarized MIF and MIF function.

MIF, macrophage migration-inhibitory factor; AIF, apoptosis-inducing factor; PARP1, Poly (ADP-ribose)-Polymerase 1; orange cell represents schematic MIF's nuclear function as a nuclease. Indicating possible nuclease and zinc finger domains of human MIF and MIF-2. C, Cys; D, Asp; E, Glu; G, Gly; H, His; P, Pro; any amino acid. Nuclear Accumulation of MIF and MIF-2 after excitotoxicity with the help of NMDA, MNNG, Etoposide and 3NP. Decrease of DNA damage, indicated by DSB marker γ H2AX and 53BP1.

Considering the functions of MIF and MIF-2 together, both essential proteins can be ascribed to disease-promoting and inhibitory effects. However, these vary depending on the disease process, cell type, interacting proteins, and typological location of MIF and MIF-2.

6.6. Validation of *Mif*-deficient rat

The CRISPR / Cas9 system is still considered a new process that is characterized above all by its simplicity and yet precision. It is a “gene scissors” method from bacteria, but after optimization, it works in almost all living cells and organisms. It is being used to research AIDS, cancer, and several hereditary diseases as well as in the culturing of plants and breeding of animals. For this reason, this study also used the safe and fast genome editing method called CRISPR / Cas9. The procedure is based on three steps; The desired location in the target organism's genome, which consists of billions of base pairs (DNA building blocks), must first be recognized, and identified so that the Cas9 protein can target the aim area. For this reason, a suitable “probe” was constructed, which is called guide RNA. Since the target region of the MIF gene is in the rat genome for this study, a suitable DNA sequence was designed to match the respective target sequence. Here, the guide RNA is coupled with the Cas9 protein to find the right position and, as a nuclease, creates a DSB at the desired location. The MIF gene was recognized in the rat genome, and the regions around the gene segment were marked. With the help of primers and small PAM sequences, which are only a few nucleotides long, the guide RNA could be synthesized. Then, using a KIT, the CRISPR guide efficiency was identified from the various gRNAs. The goal of this study was to cut out the entire MIF gene (~ 1kb)^{313–315}. In retrospect, this method is the most efficient and the safest way of getting an overall impression of the impact of MIF on rat physiology. However, if subsequent observations, changes should be assigned to a specific MIF or MIF-2 gene function. So it is possible not to remove the whole genome but relatively certain smaller regions, or it is possible to incorporate a defective gene in the target region. In addition to *Mif* KO rat, MIF nuclease deficient rat could also be designed in the future so that the transgenic phenotype has a specific function of the multipotent MIF and MIF-2^{116,158,316}. The F0 (generation), F1, and F2 generations were gene typed to check the possible deletion and plan the matings. However, the founder lines had to be sequenced. This is because even with a CRISPR / Cas9 method, the cell's repair systems can influence the results. The repair systems are responsible for mending the severed DNA strand back together. So that individual DNA building blocks or short sequences can be reintegrated into the DNA strand. Only the Kur7103-6981 DEL line showed a minor sequence insertion in this study. Overall, the WT genotype four, heterozygous four, and *Mif* KO four animals were bred. There are however only two females and two males per genotype. So it is therefore difficult to analyze a gender-specific phenotype^{317–320}. The earlier microarrays were replaced by RNA-Seq analysis (bulk and single-cell) with a breakthrough in the latter part of the year 2000. This method is employed to assess the

mean expression level of each gene within a substantial population of input cells. In this way, transcriptomes can be compared, and disease studies can be carried out. The bulk RNA Seq can be used to gain insight into the gene expression of an entire sample. However, if a differentiation between cell types is needed. In that case, this will have to be sorted in a cell-type-specific manner before, by fluorescence-activated cell sorting (FACS) and then sorted in small population groups of around 50 cells. For these studies, different regions were removed from the rat's brain (prefrontal cortex, hippocampus, cerebellum, and corpus callosum). In addition to the RNA-seq samples, the brain and other essential organs were also collected. This is intended to investigate the results of the bulk sequencing so that the desired regions can be verified with staining or western blots. In the case of RNA-seq, however, it should be noted that compared to DNA, which represents a stable structure, RNA is very sensitive, particularly to oxidation and hydrolytic cleavage of its phosphodiester bonds by RNases. For this reason, the samples for these bulk RNA Seq studies were placed on ice and immediately chilled to -80. This prevents the breakdown of the RNA and thus prevents distortion of the RNA-Seq. This research is based on the differences in RNAseq results from wild-type and MIF-KO rats. However, this is the first known study on transgenic rats with MIF deficiency in general. Studies with scRNA-seq show that high and low MIF cells have been identified. However, there is no general characterization of the MIF-KO effect on the organism. Therefore, this study is essential to establish the rat as a scientific model for the MIF family and characterize the differences in expression of MIF-KO organisms compared to the wild type^{321,322}.

Western blotting is mainly used to detect MIF proteins to verify the generated transgenic rats with the CRISPR / Cas9 method in our area of work. Among other things, a piece of the brain was removed from each rat. These were used for verification. Each rat sample showed a band at the level of monomeric AIF and β -actin. However, only wild-type and heterozygous samples showed a band at 12.5 kD for MIF (MIF Ka565). A significant difference was observed in comparing *Mif*-KO samples and those of the wild type and heterozygous. However, no significant differences or trends were found between the wild type and the heterozygous samples. This may be because the western blot method is not sensitive enough, or the intact gene segment compensates for MIF expression. The AIF values do not differ significantly among all three genotypes, but individual animals show slightly different expression levels when looking at the results. However, this broader distribution is observed for all three genotypes.

6.7. Mif-deficient rat as a novel research model

The extraordinary impact that laboratory mice and rats have on biomedical research is undisputed in the research community. In the next section, however, the merits of the rat model in general and especially for the MIF family research will be discussed in more detail.

Rats and mice belong to the largest order within the class of mammals, the order of Rodentia. The derived strains of *Mus musculus* and *Rattus norvegicus* are most often used in the current research. One of the most critical differences between rats and mice is size and weight. Namely, rats are several times larger and heavier. This, in turn, provides advantages in surgical procedures. In addition, in spinal cord injury studies, rats are of great translational value³²³. For studies within the research of MIF family members, the rat research model offers a new, largely unexplored platform that could be the focus of stroke³²⁴ or Alzheimer's disease studies³²⁵. For this reason, a MIF-deficient rat model was created using the CRISPR Cas9-Das method for the upcoming studies. Therefore, this project aims to produce a genetically modified rat model using the CRISPR Cas9 method and investigate the possible physiological differences of a MIF-deficient rat model. In addition, it is helpful for the upcoming research to focus on programmed cell death to alter AIF expression or unintentionally affect MIF-2 by MIF genetic deletion. In this study, we demonstrated that deletion of MIF by the CRISPR Cas9 method was successful. By using Western blot, deletion of MIF was shown in rat *Mif KO* animals, whereas in WT and Het animals, MIF is expressed. In summary, we succeeded in creating a MIF-deficient rat model. In this model, AIF expression does not change.

A singular focus on MIF KO within this model may not yield the desired insights into MIF's function. However, the establishment of the MIF KO rat model remains critical, providing an opportunity to replicate and validate essential findings from mouse models.

The studies from 2010 suggest a correlation between the absence of MIF in mice and an extended lifespan²⁵⁸. However, the certainty of this assertion is moderated by potential genetic disparities between the MIF-KO mice and the control mice utilized in prior studies. Therefore, to validate the previously reported increase in lifespan attributed to MIF deficiency, our newly established rat model provides an avenue for such validation.

Furthermore, within the context of atherosclerosis, the validation of outcomes could be pursued. Given the three-decade exploration of MIF's role in inflammatory modulation, the initial findings highlighting MIF's activation from central and peripheral sources in response to inflammatory stimuli emphasize its pivotal role in systemic tissue invasion response. Subsequent studies indicate that MIF deficiency is linked to reduced

inflammation within atherosclerotic lesions. Given MIF's pro-inflammatory nature, its absence may contribute to diminished inflammatory processes³²⁶. Additionally, MIF deficiency has been associated with alterations in plaque composition, potentially enhancing plaque stability. Plaques lacking MIF may exhibit fewer macrophages and inflammatory cells, suggesting a role in plaque stability³²⁷.

However, it also presents an opportunity to investigate and validate various neurological processes. For instance, utilizing the new rat model in the study of MIF deficiency could allow for the examination of whether altered expression of genes related to neuronal survival and synaptic plasticity is indeed associated with MIF deficiency, thereby suggesting a potential role for MIF in preserving neural homeostasis³²⁸.

In addition to these research focuses, the investigation of mechanisms in which MIF plays an essential role has been directed towards emerging apoptosis following stroke, as well as the potential activity of MIF as a chaperone in relation to ALS conditions. Functioning as a chaperone, MIF aids in the proper folding of other proteins, thereby ensuring their structural integrity and functional activity. MIF's interactions with proteins, including enzymes and signaling molecules, have been demonstrated, facilitating their attainment of accurate three-dimensional configurations.²⁰

Furthermore, the Macrophage Migration Inhibitory Factor (MIF) has been implicated in the context of stroke, contributing to the comprehension of intricate mechanisms underpinning this cerebrovascular event. In stroke, MIF's engagement surpasses its conventional functions, impacting diverse processes like oxidative stress, neuroinflammation, and neuronal apoptosis¹¹⁶. The distinct roles of MIF introduce an additional layer of complexity to understanding its biological functions. It underscores MIF's adaptability as a molecule that not only engages in immune responses but also exerts influence over broader cellular dynamics. Exploring MIF's distinct roles within the established rat model could yield valuable insights into its participation in both health and disease. It is noted that our ability to conduct these experiments was hindered by the constraints imposed by the Corona restrictions, which prevented the breeding of a rat line.

For decades, inspiring research has been done in the MIF family field. However, it is becoming increasingly clear that the multipotent MIF and its paralog MIF-2 have other unexplored functions and play an essential but complex role in many cascades. For this reason, MIF and MIF-2 research will play an important role in drug discovery in areas ranging from stroke research, Alzheimer's disease, ALS to other inflammatory diseases.

References

1. Morimoto, K. & Nakajima, K. Role of the Immune System in the Development of the Central Nervous System. *Frontiers in Neuroscience* (2019) doi:10.3389/fnins.2019.00916.
2. Gokce, O. *et al.* Cellular Taxonomy of the Mouse Striatum as Revealed by Single-Cell RNA-Seq. Gokce, O. *et al.* Cellular Taxonomy of the Mouse Striatum as Revealed by Single-Cell RNA-Seq. *Cell Rep.* 16, (2016). *Cell Reports* (2016) doi:10.1016/j.celrep.2016.06.059.
3. Skaper, S. D., Facci, L., Zusso, M. & Giusti, P. An inflammation-centric view of neurological disease: Beyond the neuron. *Frontiers in Cellular Neuroscience* (2018) doi:10.3389/fncel.2018.00072.
4. Keren-Shaul H, Spinrad A, Weiner A, Matcovitch-Natan O, Dvir-Szternfeld R, Ulland TK, David E, Baruch K, Lara-Astaiso D, Toth B, Itzkovitz S, Colonna M, Schwartz M, Amit I. A Unique Microglia Type Associated with Restricting Development of Alzheimer's Disease. *Cell.* 2017 Jun 15;169(7):1276-1290.e17. doi: 10.1016/j.cell.2017.05.018. Epub 2017 Jun 8. PMID: 28602351.
5. Linnerbauer M, Wheeler MA, Quintana FJ. Astrocyte Crosstalk in CNS Inflammation. *Neuron.* 2020 Nov 25;108(4):608-622. doi: 10.1016/j.neuron.2020.08.012. Epub 2020 Sep 7. PMID: 32898475; PMCID: PMC7704785.
6. Gleichman, A. J. & Carmichael, S. T. Glia in neurodegeneration: Drivers of disease or along for the ride? *Neurobiology of Disease* (2020) doi:10.1016/j.nbd.2020.104957.
7. Sharif Y, Jumah F, Coplan L, Krosser A, Sharif K, Tubbs RS. Blood brain barrier: A review of its anatomy and physiology in health and disease. *Clin Anat.* 2018 Sep;31(6):812-823. doi: 10.1002/ca.23083. Epub 2018 Oct 18. PMID: 29637627.
8. Huang SF, Othman A, Koshkin A, Fischer S, Fischer D, Zamboni N, Ono K, Sawa T, Ogunshola OO. Astrocyte glutathione maintains endothelial barrier stability. *Redox Biol.* 2020 Jul;34:101576. doi: 10.1016/j.redox.2020.101576. Epub 2020 May 19. PMID: 32502899; PMCID: PMC7267730.
9. Qiu, C., Kivipelto, M. & Von Strauss, E. Epidemiology of Alzheimer's disease: Occurrence, determinants, and strategies toward intervention. *Dialogues in Clinical Neuroscience* (2009) doi:10.31887/dcns.2009.11.2/cqiu.
10. Rocca WA, Petersen RC, Knopman DS, Hebert LE, Evans DA, Hall KS, Gao S, Unverzagt FW, Langa KM, Larson EB, White LR. Trends in the incidence and prevalence of Alzheimer's disease, dementia, and cognitive impairment in the

- United States. *Alzheimers Dement.* 2011 Jan;7(1):80-93. doi: 10.1016/j.jalz.2010.11.002. PMID: 21255746; PMCID: PMC3026476.
11. McDaniel, M. A. & Einstein, G. O. The neuropsychology of prospective memory in normal aging: A componential approach. *Neuropsychologia* (2011) doi:10.1016/j.neuropsychologia.2010.12.029.
 12. Lashuel HA, Aljabari B, Sigurdsson EM, Metz CN, Leng L, Callaway DJ, Bucala R. Amyloid fibril formation by macrophage migration inhibitory factor. *Biochem Biophys Res Commun.* 2005 Dec 16;338(2):973-80. doi: 10.1016/j.bbrc.2005.10.040.
 13. Sorrentino, Z. A., Giasson, B. I. & Chakrabarty, P. α -Synuclein and astrocytes: tracing the pathways from homeostasis to neurodegeneration in Lewy body disease. *Acta Neuropathologica* (2019) doi:10.1007/s00401-019-01977-2.
 14. Lau A, So RWL, Lau HHC, Sang JC, Ruiz-Riquelme A, Fleck SC, Stuart E, Menon S, Visanji NP, Meisl G, Faidi R, Marano MM, Schmitt-Ulms C, Wang Z, Fraser PE, Tandon A, Hyman BT, Wille H, Ingelsson M, Klenerman D, Watts JC. α -Synuclein strains target distinct brain regions and cell types. *Nat Neurosci.* 2020 Jan;23(1):21-31. doi: 10.1038/s41593-019-0541-x.
 15. El Haj M, Antoine P, Amouyel P, Lambert JC, Pasquier F, Kapogiannis D. Apolipoprotein E (APOE) ϵ 4 and episodic memory decline in Alzheimer's disease: A review. *Ageing Res Rev.* 2016 May;27:15-22. doi: 10.1016/j.arr.2016.02.002.
 16. Moore, A. M. *et al.* APOE ϵ 4-specific associations of VEGF gene family expression with cognitive aging and Alzheimer's disease. *Neurobiology of Aging* (2020) doi:10.1016/j.neurobiolaging.2019.10.021.
 17. Jackson J, Jambrina E, Li J, Marston H, Menzies F, Phillips K, Gilmour G. Targeting the Synapse in Alzheimer's Disease. *Front Neurosci.* 2019 Jul 23;13:735. doi: 10.3389/fnins.2019.00735.
 18. Koller, E. J. & Chakrabarty, P. Tau-Mediated Dysregulation of Neuroplasticity and Glial Plasticity. *Frontiers in Molecular Neuroscience* (2020) doi:10.3389/fnmol.2020.00151.
 19. Wang Y, Chen Y, Wang C, Yang M, Wang Y, Bao L, Wang JE, Kim B, Chan KY, Xu W, Capota E, Ortega J, Nijhawan D, Li GM, Luo W, Wang Y. MIF is a 3' flap nuclease that facilitates DNA replication and promotes tumor growth. *Nat Commun.* 2021 May 19;12(1):2954. doi: 10.1038/s41467-021-23264-z.
 20. sraelson A, Ditsworth D, Sun S, Song S, Liang J, Hruska-Plochan M, McAlonis-Downes M, Abu-Hamad S, Zoltsman G, Shani T, Maldonado M, Bui A, Navarro M, Zhou H, Marsala M, Kaspar BK, Da Cruz S, Cleveland DW. Macrophage migration inhibitory factor as a chaperone inhibiting accumulation of misfolded

- SOD1. *Neuron*. 2015 Apr 8;86(1):218-32. doi: 10.1016/j.neuron.2015.02.034.
21. Leyton-Jaimes, M. F., Kahn, J. & Israelson, A. AAV2/9-mediated overexpression of MIF inhibits SOD1 misfolding, delays disease onset, and extends survival in mouse models of ALS. *Proceedings of the National Academy of Sciences of the United States of America* (2019) doi:10.1073/pnas.1904665116.
 22. Bueno M, Papazoglou A, Valenzi E, Rojas M, Lafyatis R, Mora AL. Mitochondria, Aging, and Cellular Senescence: Implications for Scleroderma. *Curr Rheumatol Rep*. 2020 Jun 19;22(8):37. doi: 10.1007/s11926-020-00920-9.
 23. Calcinotto A, Kohli J, Zagato E, Pellegrini L, Demaria M, Alimonti A. Cellular Senescence: Aging, Cancer, and Injury. *Physiol Rev*. 2019 Apr 1;99(2):1047-1078. doi: 10.1152/physrev.00020.2018.
 24. Ng, Y. Y. *et al*. T Cells Expressing NKG2D CAR with a DAP12 Signaling Domain Stimulate Lower Cytokine Production While Effective in Tumor Eradication. *Molecular Therapy* (2021) doi:10.1016/j.ymthe.2020.08.016.
 25. von Herrmann, K. M. *et al*. NLRP3 expression in mesencephalic neurons and characterization of a rare NLRP3 polymorphism associated with decreased risk of Parkinson's disease. *npj Parkinson's Disease* (2018) doi:10.1038/s41531-018-0061-5.
 26. Yan, S. *et al*. Pharmacological Inhibition of HDAC6 Attenuates NLRP3 Inflammatory Response and Protects Dopaminergic Neurons in Experimental Models of Parkinson's Disease. *Frontiers in Aging Neuroscience* (2020) doi:10.3389/fnagi.2020.00078.
 27. Kelley, N., Jeltema, D., Duan, Y. & He, Y. The NLRP3 inflammasome: An overview of mechanisms of activation and regulation. *International Journal of Molecular Sciences* (2019) doi:10.3390/ijms20133328.
 28. Schulz, R. *et al*. Inhibiting the HSP90 chaperone destabilizes macrophage migration inhibitory factor and thereby inhibits breast tumor progression. *Journal of Experimental Medicine* (2012) doi:10.1084/jem.20111117.
 29. Rossaert, E. & Van Den Bosch, L. HDAC6 inhibitors: Translating genetic and molecular insights into a therapy for axonal CMT. *Brain Research* (2020) doi:10.1016/j.brainres.2020.146692.
 30. Chatterjee, M. *et al*. Macrophage migration inhibitory factor limits activation-induced apoptosis of platelets via CXCR7-dependent Akt signaling. *Circulation Research* (2014) doi:10.1161/CIRCRESAHA.115.305171.
 31. Kunkel TA, Erie DA. Eukaryotic Mismatch Repair in Relation to DNA Replication. *Annu Rev Genet*. 2015;49:291-313. doi: 10.1146/annurev-genet-112414-054722.
 32. Satoh MS, Lindahl T. Role of poly(ADP-ribose) formation in DNA repair. *Nature*.

- 1992 Mar 26;356(6367):356-8. doi: 10.1038/356356a0.
33. Zhang, Z. yong *et al.* Activation of mGluR5 Attenuates Microglial Activation and Neuronal Apoptosis in Early Brain Injury After Experimental Subarachnoid Hemorrhage in Rats. *Neurochemical Research* (2015) doi:10.1007/s11064-015-1572-7.
 34. Kim, B. W., Jeong, Y. E., Wong, M. & Martin, L. J. DNA damage accumulates and responses are engaged in human ALS brain and spinal motor neurons and DNA repair is activatable in iPSC-derived motor neurons with SOD1 mutations. *Acta Neuropathologica Communications* (2020) doi:10.1186/s40478-019-0874-4.
 35. Butterfield, D. A. & Halliwell, B. Oxidative stress, dysfunctional glucose metabolism and Alzheimer disease. *Nature Reviews Neuroscience* (2019) doi:10.1038/s41583-019-0132-6.
 36. Akbar, M., Shabbir, A., Rehman, K., Akash, M. S. H. & Shah, M. A. Neuroprotective potential of berberine in modulating Alzheimer's disease via multiple signaling pathways. *Journal of Food Biochemistry* (2021) doi:10.1111/jfbc.13936.
 37. Liu, J. Y. *et al.* Cells exhibiting strong p16 INK4a promoter activation in vivo display features of senescence. *Proceedings of the National Academy of Sciences of the United States of America* (2019) doi:10.1073/pnas.1818313116.
 38. Hernandez, B. Y. *et al.* Human papillomavirus DNA detection, p16 INK4a , and oral cavity cancer in a U.S. population. *Oral Oncology* (2019) doi:10.1016/j.oraloncology.2019.03.001.
 39. Hsieh, M. H. *et al.* Topoisomerase II inhibition suppresses the proliferation of telomerase-negative cancers. *Cellular and Molecular Life Sciences* (2015) doi:10.1007/s00018-014-1783-0.
 40. Jebaraj, B. M. C. & Stilgenbauer, S. Telomere Dysfunction in Chronic Lymphocytic Leukemia. *Frontiers in Oncology* (2021) doi:10.3389/fonc.2020.612665.
 41. Zhang, P. *et al.* Senolytic therapy alleviates A β -associated oligodendrocyte progenitor cell senescence and cognitive deficits in an Alzheimer's disease model. *Nature Neuroscience* (2019) doi:10.1038/s41593-019-0372-9.
 42. Kumari, S., Kumar, P., Kumar, M., Singh, S. & Narayan, G. Expression of p27 and p16 and their clinical significance in gastric cancer. *Clinical and Translational Oncology* (2021) doi:10.1007/s12094-020-02479-4.
 43. Chen, S. *et al.* TREM2 activation attenuates neuroinflammation and neuronal apoptosis via PI3K/Akt pathway after intracerebral hemorrhage in mice. *Journal of Neuroinflammation* (2020) doi:10.1186/s12974-020-01853-x.
 44. Baeza Garcia, A. *et al.* Neutralization of the Plasmodium-encoded MIF ortholog

- confers protective immunity against malaria infection. *Nature Communications* (2018) doi:10.1038/s41467-018-05041-7.
45. Rossi D, Brambilla L, Valori CF, Roncoroni C, Crugnola A, Yokota T, Bredesen DE, Volterra A. Focal degeneration of astrocytes in amyotrophic lateral sclerosis. *Cell Death Differ.* 2008 Nov;15(11):1691-700. doi: 10.1038/cdd.2008.99.
 46. Rai, A. *et al.* CDK5-induced p-PPAR γ (Ser 112) downregulates GFAP via PPREs in developing rat brain: Effect of metal mixture and troglitazone in astrocytes. *Cell Death and Disease* (2014) doi:10.1038/cddis.2013.514.
 47. Karmon, O. & Ben Aroya, S. Spatial Organization of Proteasome Aggregates in the Regulation of Proteasome Homeostasis. *Frontiers in Molecular Biosciences* (2020) doi:10.3389/fmolb.2019.00150.
 48. Cristofani, R. *et al.* A Crucial Role for the Protein Quality Control System in Motor Neuron Diseases. *Frontiers in Aging Neuroscience* (2020) doi:10.3389/fnagi.2020.00191.
 49. Mandrioli, J., Mediani, L., Alberti, S. & Carra, S. ALS and FTD: Where RNA metabolism meets protein quality control. *Seminars in Cell and Developmental Biology* (2020) doi:10.1016/j.semcdb.2019.06.003.
 50. Tubbs A, Nussenzweig A. Endogenous DNA Damage as a Source of Genomic Instability in Cancer. *Cell.* 2017 Feb 9;168(4):644-656. doi: 10.1016/j.cell.2017.01.002.
 51. Keefe DL. Telomeres and genomic instability during early development. *Eur J Med Genet.* 2020 Feb;63(2):103638. doi: 10.1016/j.ejmg.2019.03.002.
 52. Ernst, A. *et al.* Telomere dysfunction and chromothripsis. *International Journal of Cancer* (2016) doi:10.1002/ijc.30033.
 53. Srinivas, U. S., Tan, B. W. Q., Vellayappan, B. A. & Jeyasekharan, A. D. ROS and the DNA damage response in cancer. *Redox Biology* (2019) doi:10.1016/j.redox.2018.101084.
 54. Li, F. *et al.* The histone mark H3K36me3 regulates human DNA mismatch repair through its interaction with MutS α . *Cell* (2013) doi:10.1016/j.cell.2013.03.025.
 55. Turinetto, V. & Giachino, C. Survey and summary multiple facets of histone variant H2AX: A DNA double-strand-break marker with several biological functions. *Nucleic Acids Research* (2015) doi:10.1093/nar/gkv061.
 56. Hall, B. M. *et al.* Aging of mice is associated with p16(Ink4a)- and β -galactosidase-positive macrophage accumulation that can be induced in young mice by senescent cells. *Aging* (2016) doi:10.18632/aging.100991.
 57. Azam, S., Haque, M. E., Balakrishnan, R., Kim, I. S. & Choi, D. K. The Ageing Brain: Molecular and Cellular Basis of Neurodegeneration. *Frontiers in Cell and*

- Developmental Biology* (2021) doi:10.3389/fcell.2021.683459.
58. Hou Y, Dan X, Babbar M, Wei Y, Hasselbalch SG, Croteau DL, Bohr VA. Ageing as a risk factor for neurodegenerative disease. *Nat Rev Neurol*. 2019 Oct;15(10):565-581. doi: 10.1038/s41582-019-0244-7.
 59. Liu, Y. *et al.* MIF inhibitor ISO-1 alleviates severe acute pancreatitis-associated acute kidney injury by suppressing the NLRP3 inflammasome signaling pathway. *International Immunopharmacology* (2021) doi:10.1016/j.intimp.2021.107555.
 60. Kasper, L. *et al.* The fungal peptide toxin Candidalysin activates the NLRP3 inflammasome and causes cytolysis in mononuclear phagocytes. *Nature Communications* (2018) doi:10.1038/s41467-018-06607-1.
 61. Song, K. *et al.* Oxidative Stress-Mediated Blood-Brain Barrier (BBB) Disruption in Neurological Diseases. *Oxidative Medicine and Cellular Longevity* (2020) doi:10.1155/2020/4356386.
 62. Sardana, R. & Emr, S. D. Membrane Protein Quality Control Mechanisms in the Endo-Lysosome System. *Trends in Cell Biology* (2021) doi:10.1016/j.tcb.2020.11.011.
 63. Oyama, R., Yamamoto, H. & Titani, K. Glutamine synthetase, hemoglobin α -chain, and macrophage migration inhibitory factor binding to amyloid β -protein: Their identification in rat brain by a novel affinity chromatography and in Alzheimer's disease brain by immunoprecipitation. *Biochimica et Biophysica Acta - Protein Structure and Molecular Enzymology* **1479**, 91–102 (2000). doi: 10.1016/s0167-4838(00)00057-1. PMID: 11004532.
 64. Volpe, E., Sambucci, M., Battistini, L. & Borsellino, G. Fas-fas ligand: Checkpoint of t cell functions in multiple sclerosis. *Frontiers in Immunology* (2016) doi:10.3389/fimmu.2016.00382.
 65. Abe, R., Peng, T., Sailors, J., Bucala, R. & Metz, C. N. Regulation of the CTL Response by Macrophage Migration Inhibitory Factor. *The Journal of Immunology* (2001) doi:10.4049/jimmunol.166.2.747.
 66. Galatro, T. F. *et al.* Transcriptomic analysis of purified human cortical microglia reveals age-associated changes. *Nature Neuroscience* (2017) doi:10.1038/nn.4597.
 67. Shahidehpour, R. K. *et al.* Dystrophic microglia are associated with neurodegenerative disease and not healthy aging in the human brain. *Neurobiology of aging* (2021) doi:10.1016/j.neurobiolaging.2020.12.003.
 68. Satrom, K. M. *et al.* Neonatal hyperglycemia induces CXCL10/CXCR3 signaling and microglial activation and impairs long-term synaptogenesis in the hippocampus and alters behavior in rats. *Journal of Neuroinflammation* (2018)

- doi:10.1186/s12974-018-1121-9.
69. Shanbhag, N. M. *et al.* Early neuronal accumulation of DNA double strand breaks in Alzheimer's disease. *Acta Neuropathologica Communications* (2019) doi:10.1186/s40478-019-0723-5.
70. Zhang, F. & Gong, Z. Regulation of DNA double-strand break repair pathway choice: a new focus on 53BP1. *Journal of Zhejiang University: Science B* (2021) doi:10.1631/jzus.B2000306.
71. Kumari, R. & Jat, P. Mechanisms of Cellular Senescence: Cell Cycle Arrest and Senescence Associated Secretory Phenotype. *Frontiers in Cell and Developmental Biology* (2021) doi:10.3389/fcell.2021.645593.
72. Löbrich, M. *et al.* γ H2AX foci analysis for monitoring DNA double-strand break repair: Strengths, limitations and optimization. *Cell Cycle* (2010) doi:10.4161/cc.9.4.10764.
73. Román-Rodríguez, F. J. *et al.* NHEJ-Mediated Repair of CRISPR-Cas9-Induced DNA Breaks Efficiently Corrects Mutations in HSPCs from Patients with Fanconi Anemia. *Cell Stem Cell* (2019) doi:10.1016/j.stem.2019.08.016.
74. Lee, K. I. *et al.* Etoposide induces pancreatic β -cells cytotoxicity via the JNK/ERK/GSK-3 signaling-mediated mitochondria-dependent apoptosis pathway. *Toxicology in Vitro* (2016) doi:10.1016/j.tiv.2016.07.018.
75. Henneke, G., Koundrioukoff, S. & Hübscher, U. Phosphorylation of human Fen1 by cyclin-dependent kinase modulates its role in replication fork regulation. *Oncogene* (2003) doi:10.1038/sj.onc.1206606.
76. Kobold, S. *et al.* The macrophage migration inhibitory factor (MIF)-homologue D-dopachrome tautomerase is a therapeutic target in a murine melanoma model. *Oncotarget* (2014) doi:10.18632/oncotarget.1560.
77. Popp, J. *et al.* Macrophage migration inhibitory factor in mild cognitive impairment and Alzheimer's disease. *Journal of Psychiatric Research* **43**, 749–753 (2009) doi: 10.1016/j.jpsychires.2008.10.006.
78. Djudjaj S, Martin IV, Buhl EM, Nothofer NJ, Leng L, Piecychna M, Floege J, Bernhagen J, Bucala R, Boor P. Macrophage Migration Inhibitory Factor Limits Renal Inflammation and Fibrosis by Counteracting Tubular Cell Cycle Arrest. *J Am Soc Nephrol.* 2017 Dec;28(12):3590-3604. doi: 10.1681/ASN.2017020190. Epub 2017 Aug 11. PMID: 28801314; PMCID: PMC5698074.
79. Verschuren, L. *et al.* MIF deficiency reduces chronic inflammation in white adipose tissue and impairs the development of insulin resistance, glucose intolerance, and associated atherosclerotic disease. *Circulation Research* (2009) doi:10.1161/CIRCRESAHA.109.199166.

80. Cunningham, C. *et al.* Systemic Inflammation Induces Acute Behavioral and Cognitive Changes and Accelerates Neurodegenerative Disease. *Biological Psychiatry* (2009) doi:10.1016/j.biopsych.2008.07.024.
81. Bucala, R. Neuroimmunomodulation by macrophage migration inhibitory factor (MIF). in *Annals of the New York Academy of Sciences* (1998). doi:10.1111/j.1749-6632.1998.tb09551.x.
82. Stojanovic, I., Saksida, T. & Stosic-Grujicic, S. Beta cell function: The role of macrophage migration inhibitory factor. *Immunologic Research* (2012) doi:10.1007/s12026-012-8281-y.
83. Bloom, B. R. & Bennett, B. Mechanism of a reaction in vitro associated with delayed-type hypersensitivity. *Science* (1966) doi:10.1126/science.153.3731.80.
84. David, J. R. Delayed hypersensitivity in vitro: its mediation by cell-free substances formed by lymphoid cell-antigen interaction. *Proceedings of the National Academy of Sciences of the United States of America* (1966) doi:10.1073/pnas.56.1.72.
85. Nathan, C. F., Remold, H. G. & David, J. R. Characterization of a lymphocyte factor which alters macrophage functions. *Journal of Experimental Medicine* (1973) doi:10.1084/jem.137.2.275.
86. Hallowell Churchill, W., Piessens, W. F., Sulis, C. A. & David, J. R. Macrophages activated as suspension cultures with lymphocyte mediators devoid of antigen become cytotoxic for tumor cells. *Journal of Immunology* (1975).
87. Tau, G. Z., Cowan, S. N., Weisburg, J., Braunstein, N. S. & Rothman, P. B. Regulation of IFN- γ Signaling Is Essential for the Cytotoxic Activity of CD8 + T Cells . *The Journal of Immunology* (2001) doi:10.4049/jimmunol.167.10.5574.
88. Stubblefield Park, S. R., Widness, M., Levine, A. D. & Patterson, C. E. T Cell-, Interleukin-12-, and Gamma Interferon-Driven Viral Clearance in Measles Virus-Infected Brain Tissue. *Journal of Virology* (2011) doi:10.1128/jvi.01496-10.
89. Weiser, W. Y. *et al.* Molecular cloning of a cDNA encoding a human macrophage migration inhibitory factor. *Proceedings of the National Academy of Sciences of the United States of America* (1989) doi:10.1073/pnas.86.19.7522.
90. Bernhagen, J. *et al.* Purification, Bioactivity, and Secondary Structure Analysis of Mouse and Human Macrophage Migration Inhibitory Factor (MIF). *Biochemistry* (1994) doi:10.1021/bi00251a025.
91. Bernhagen, J. *et al.* MIF is a pituitary-derived cytokine that potentiates lethal endotoxaemia. *Nature* (1993) doi:10.1038/365756a0.
92. Bozza, M. *et al.* Targeted disruption of migration inhibitory factor gene reveals its critical role in sepsis. *Journal of Experimental Medicine* (1999) doi:10.1084/jem.189.2.341.

93. Ghoochani, A. *et al.* MIF-CD74 signaling impedes microglial M1 polarization and facilitates brain tumorigenesis. *Oncogene* (2016) doi:10.1038/onc.2016.160.
94. Leng, L. *et al.* MIF signal transduction initiated by binding to CD74. *Journal of Experimental Medicine* (2003) doi:10.1084/jem.20030286.
95. Bernhagen, J. *et al.* MIF is a noncognate ligand of CXC chemokine receptors in inflammatory and atherogenic cell recruitment. *Nature Medicine* (2007) doi:10.1038/nm1567.
96. Renner, P., Roger, T. & Calandra, T. Macrophage migration inhibitory factor: Gene polymorphisms and susceptibility to inflammatory diseases. in *Clinical Infectious Diseases* (2005). doi:10.1086/432009.
97. Ito, K., Yoshiura, Y., Ootake, M. & Nakanishi, T. Macrophage migration inhibitory factor (MIF) is essential for development of zebrafish, *Danio rerio*. *Developmental and Comparative Immunology* (2008) doi:10.1016/j.dci.2007.10.007.
98. Faria, M. R. *et al.* Spatiotemporal patterns of macrophage migration inhibitory factor (Mif) expression in the mouse placenta. *Reproductive Biology and Endocrinology* (2010) doi:10.1186/1477-7827-8-95.
99. Chai, X. *et al.* Profile of MIF in Developing Hippocampus: Association With Cell Proliferation and Neurite Outgrowth. *Frontiers in Molecular Neuroscience* (2020) doi:10.3389/fnmol.2020.00147.
100. Roger, T. *et al.* High expression levels of macrophage migration inhibitory factor sustain the innate immune responses of neonates. *Proceedings of the National Academy of Sciences of the United States of America* (2016) doi:10.1073/pnas.1514018113.
101. Roger, T. *et al.* Plasma levels of macrophage migration inhibitory factor and d-dopachrome tautomerase show a highly specific profile in early life. *Frontiers in Immunology* (2017) doi:10.3389/fimmu.2017.00026.
102. Kobayashi, S. *et al.* Expression pattern of macrophage migration inhibitory factor during embryogenesis. *Mechanisms of Development* (1999) doi:10.1016/S0925-4773(99)00057-X.
103. Schober, A., Bernhagen, J. & Weber, C. Chemokine-like functions of MIF in atherosclerosis. *Journal of Molecular Medicine* (2008) doi:10.1007/s00109-008-0334-2.
104. Schmitz, C. *et al.* Mif-deficiency favors an atheroprotective autoantibody phenotype in atherosclerosis. *FASEB Journal* (2018) doi:10.1096/fj.201800058R.
105. Presti, M. *et al.* Overexpression of macrophage migration inhibitory factor and functionally-related genes, D-DT, CD74, CD44, CXCR2 and CXCR4, in glioblastoma. *Oncology Letters* (2018) doi:10.3892/ol.2018.8990.

106. Shimizu, T. Role of macrophage migration inhibitory factor (MIF) in the skin. *Journal of Dermatological Science* (2005) doi:10.1016/j.jdermsci.2004.08.007.
107. Guda, M. R. *et al.* Pleiotropic role of macrophage migration inhibitory factor in cancer. *American journal of cancer research* (2019).
108. Zhang, S. *et al.* Upregulation of MIF as a defense mechanism and a biomarker of Alzheimer's disease. *Alzheimer's Research and Therapy* (2019) doi:10.1186/s13195-019-0508-x.
109. Bacher, M. *et al.* The role of macrophage migration inhibitory factor in alzheimer's disease. *Molecular Medicine* (2010) doi:10.2119/molmed.2009.00123.
110. Oikonomidi, A. *et al.* Macrophage migration inhibitory factor is associated with biomarkers of Alzheimer's disease pathology and predicts cognitive decline in mild cognitive impairment and mild dementia. *Journal of Alzheimer's Disease* (2017) doi:10.3233/JAD-170335.
111. Sun, H. W., Bernhagen, J., Bucala, R. & Lolis, E. Crystal structure at 2.6-Å resolution of human macrophage migration inhibitory factor. *Proceedings of the National Academy of Sciences of the United States of America* (1996) doi:10.1073/pnas.93.11.5191.
112. Jaworski, D. C., Jasinskas, A., Metz, C. N., Bucala, R. & Barbour, A. G. Identification and characterization of a homologue of the pro-inflammatory cytokine Macrophage Migration Inhibitory Factor in the tick, *Amblyomma americanum*. *Insect Molecular Biology* (2001) doi:10.1046/j.0962-1075.2001.00271.x.
113. Sparkes, A. *et al.* The non-mammalian MIF superfamily. *Immunobiology* (2017) doi:10.1016/j.imbio.2016.10.006.
114. Prudovsky, I. *et al.* The non-classical export routes: FGF1 and IL-1 α point the way. *Journal of Cell Science* (2003) doi:10.1242/jcs.00872.
115. Lodish H, Berk A, Zipursky SL, E. A. Overview of the Secretory Pathway. *Molecular Cell Biology*. (2000).
116. Wang Y, An R, Umanah GK, Park H, Nambiar K, Eacker SM, Kim B, Bao L, Harraz MM, Chang C, Chen R, Wang JE, Kam TI, Jeong JS, Xie Z, Neifert S, Qian J, Andrabi SA, Blackshaw S, Zhu H, Song H, Ming GL, Dawson VL, Dawson TM. A nuclease that mediates cell death induced by DNA damage and poly(ADP-ribose) polymerase-1. *Science*. 2016 Oct 7;354(6308):aad6872. doi: 10.1126/science.aad6872. PMID: 27846469; PMCID: PMC5134926.
117. Park, H., Kam, T. I., Dawson, T. M. & Dawson, V. L. Poly (ADP-ribose) (PAR)-dependent cell death in neurodegenerative diseases. in *International Review of Cell and Molecular Biology* (2020). doi:10.1016/bs.ircmb.2019.12.009.

118. Zhao, G., Zhao, B., Tong, Z., Mu, R. & Guan, Y. Effects of 2'-O-Methyl Nucleotide Substitution on EcoRI Endonuclease Cleavage Activities. *PLoS ONE* (2013) doi:10.1371/journal.pone.0077111.
119. Loenen, W. A. M., Dryden, D. T. F., Raleigh, E. A., Wilson, G. G. & Murray, N. E. Highlights of the DNA cutters: A short history of the restriction enzymes. *Nucleic Acids Research* (2014) doi:10.1093/nar/gkt990.
120. Odh, G., Hindemith, A., Rosengren, A. M., Rosengren, E. & Rorsman, H. Isolation of a new tautomerase monitored by the conversion of D-dopachrome to 5,6-dihydroxyindole. *Biochemical and Biophysical Research Communications* (1993) doi:10.1006/bbrc.1993.2524.
121. Sugimoto, H. *et al.* Crystal structure of human D-Dopachrome tautomerase, a homologue of macrophage migration inhibitory factor, at 1.54 Å resolution. *Biochemistry* (1999) doi:10.1021/bi982184o.
122. Sonesson, B., Rosengren, E., Hansson, A. S. & Hansson, C. UVB-induced inflammation gives increased D-dopachrome tautomerase activity in blister fluid which correlates with macrophage migration inhibitory factor. *Experimental Dermatology* (2003) doi:10.1034/j.1600-0625.2003.120307.x.
123. Valiño-Rivas, L. *et al.* CD74 in kidney disease. *Frontiers in Immunology* (2015) doi:10.3389/fimmu.2015.00483.
124. Kim, B. S. *et al.* The clinical significance of the MIF homolog D-dopachrome tautomerase (MIF-2) and its circulating receptor (sCD74) in burn. *Burns* (2016) doi:10.1016/j.burns.2016.02.005.
125. Qi, D. *et al.* The vestigial enzyme D-dopachrome tautomerase protects the heart against ischemic injury. *Journal of Clinical Investigation* (2014) doi:10.1172/JCI73061.
126. Merk, M. *et al.* The D-dopachrome tautomerase (DDT) gene product is a cytokine and functional homolog of macrophage migration inhibitory factor (MIF). *Proceedings of the National Academy of Sciences of the United States of America* (2011) doi:10.1073/pnas.1102941108.
127. Merk, M., Mitchell, R. A., Endres, S. & Bucala, R. D-dopachrome tautomerase (DDT or MIF-2): Doubling the MIF cytokine family. *Cytokine* (2012) doi:10.1016/j.cyto.2012.03.014.
128. Coggan, M., Whitbread, L., Whittington, A. & Board, P. Structure and organization of the human theta-class glutathione S-transferase and D-dopachrome tautomerase gene complex. *Biochemical Journal* (1998) doi:10.1042/bj3340617.
129. Rosengren, E. *et al.* The macrophage migration inhibitory factor MIF is a phenylpyruvate tautomerase. *FEBS Letters* (1997) doi:10.1016/S0014-

- 5793(97)01261-1.
130. Fingerle-Rowson, G. *et al.* A Tautomerase-Null Macrophage Migration-Inhibitory Factor (MIF) Gene Knock-In Mouse Model Reveals That Protein Interactions and Not Enzymatic Activity Mediate MIF-Dependent Growth Regulation. *Molecular and Cellular Biology* (2009) doi:10.1128/mcb.01907-08.
 131. Gai, J. W. *et al.* Expression of CD74 in bladder cancer and its suppression in association with cancer proliferation, invasion and angiogenesis in HT-1376 cells. *Oncology Letters* (2018) doi:10.3892/ol.2018.8309.
 132. Alksne, J. F. THE PASSAGE OF COLLOIDAL PARTICLES ACROSS THE DERMAL CAPILLARY WALL UNDER THE INFLUENCE OF HISTAMINE. *Quarterly Journal of Experimental Physiology and Cognate Medical Sciences* (1959) doi:10.1113/expphysiol.1959.sp001376.
 133. Fleming, J. C., Norenberg, M. D., Ramsay, D. A., Dekaban, G. A., Marcillo, A. E., Saenz, A. D., ... & Weaver, L. C. (2006). The cellular inflammatory response in human spinal cords after injury. *Brain*, 129(12), 3249-3269.
 134. Zerneck, A., Bernhagen, J. & Weber, C. Macrophage migration inhibitory factor in cardiovascular disease. *Circulation* (2008) doi:10.1161/CIRCULATIONAHA.107.729125.
 135. Cui, J. *et al.* Macrophage migration inhibitory factor promotes cardiac stem cell proliferation and endothelial differentiation through the activation of the PI3K/Akt/mTOR and AMPK pathways. *International Journal of Molecular Medicine* (2016) doi:10.3892/ijmm.2016.2542.
 136. *MIF Family Cytokines in Innate Immunity and Homeostasis. MIF Family Cytokines in Innate Immunity and Homeostasis* (2017). doi:10.1007/978-3-319-52354-5.
 137. Calandra T, Roger T. Macrophage migration inhibitory factor: a regulator of innate immunity. *Nat Rev Immunol.* 2003 Oct;3(10):791-800. doi: 10.1038/nri1200. PMID: 14502271; PMCID: PMC7097468.
 138. Gu, R. *et al.* Macrophage migration inhibitory factor is essential for osteoclastogenic mechanisms in vitro and in vivo mouse model of arthritis. *Cytokine* (2015) doi:10.1016/j.cyto.2014.11.015.
 139. Tilstam, P. V. *et al.* A selective small-molecule inhibitor of macrophage migration inhibitory factor-2 (MIF-2), a MIF cytokine superfamily member, inhibits MIF-2 biological activity. *Journal of Biological Chemistry* (2019) doi:10.1074/jbc.RA119.009860.
 140. Luedike, P. *et al.* Cardioprotection through S-nitros(yl)ation of macrophage migration inhibitory factor. *Circulation* (2012) doi:10.1161/CIRCULATIONAHA.111.069104.

141. Amor, S., Peferoen, L. A., Vogel, D. Y., Breur, M., van der Valk, P., Baker, D., & van Noort, J. M. (2014). Inflammation in neurodegenerative diseases—an update. *Immunology*, 142(2), 151-166 doi:10.1111/imm.12233.
142. Stephenson, J., Nutma, E., van der Valk, P. & Amor, S. Inflammation in CNS neurodegenerative diseases. *Immunology* (2018) doi:10.1111/imm.12922.
143. Ouertatani-Sakouhi, H. *et al.* Identification and characterization of novel classes of macrophage migration inhibitory factor (MIF) inhibitors with distinct mechanisms of action. *Journal of Biological Chemistry* (2010) doi:10.1074/jbc.M110.113951.
144. Molina-Sánchez, P., Chèvre, R., Rius, C., Fuster, J. J. & Andrés, V. Loss of p27 phosphorylation at Ser10 accelerates early atherogenesis by promoting leukocyte recruitment via RhoA/ROCK. *Journal of Molecular and Cellular Cardiology* (2015) doi:10.1016/j.yjmcc.2015.04.013.
145. Kapurniotu, A., Gokce, O. & Bernhagen, J. The multitasking potential of alarmins and atypical chemokines. *Frontiers in Medicine* (2019) doi:10.3389/fmed.2019.00003.
146. Murao, A., Aziz, M., Wang, H., Brenner, M. & Wang, P. Release mechanisms of major DAMPs. *Apoptosis* (2021) doi:10.1007/s10495-021-01663-3.
147. Degryse, B. & De Virgilio, M. The nuclear protein HMGB1, a new kind of chemokine? *FEBS Letters* (2003) doi:10.1016/S0014-5793(03)01027-5.
148. Miller, E. J. *et al.* Macrophage migration inhibitory factor stimulates AMP-activated protein kinase in the ischaemic heart. *Nature* (2008) doi:10.1038/nature06504.
149. Qin, N., Xu, D., Li, J. & Deng, X. W. COP9 signalosome: Discovery, conservation, activity, and function. *Journal of Integrative Plant Biology* (2020) doi:10.1111/jipb.12903.
150. Fatokun, A. A., Dawson, V. L. & Dawson, T. M. Parthanatos: Mitochondrial-linked mechanisms and therapeutic opportunities. *British Journal of Pharmacology* (2014) doi:10.1111/bph.12416.
151. Wang, Y., Dawson, V. L. & Dawson, T. M. Poly(ADP-ribose) signals to mitochondrial AIF: A key event in parthanatos. *Experimental Neurology* (2009) doi:10.1016/j.expneurol.2009.03.020.
152. Goldsby, R. E. *et al.* Defective DNA polymerase- δ proofreading causes cancer susceptibility in mice [1]. *Nature Medicine* (2001) doi:10.1038/88963.
153. Guo, E. *et al.* FEN1 endonuclease as a therapeutic target for human cancers with defects in homologous recombination. *Proceedings of the National Academy of Sciences of the United States of America* (2020) doi:10.1073/pnas.2009237117.
154. Pawłowska, E., Szczepanska, J. & Blasiak, J. DNA2—An important player in DNA

- damage response or just another DNA maintenance protein? *International Journal of Molecular Sciences* (2017) doi:10.3390/ijms18071562.
155. Tsutakawa, S. E. *et al.* Human flap endonuclease structures, DNA double-base flipping, and a unified understanding of the FEN1 superfamily. *Cell* (2011) doi:10.1016/j.cell.2011.03.004.
 156. Hanzlikova, H. *et al.* The Importance of Poly(ADP-Ribose) Polymerase as a Sensor of Unligated Okazaki Fragments during DNA Replication. *Molecular Cell* (2018) doi:10.1016/j.molcel.2018.06.004.
 157. Fukui, K., Kosaka, H., Kuramitsu, S. & Masui, R. Nuclease activity of the MutS homologue MutS2 from *Thermus thermophilus* is confined to the Smr domain. *Nucleic Acids Research* (2007) doi:10.1093/nar/gkl735.
 158. Kim, H., Kim J.S. A guide to genome engineering with programmable nucleases. *Nat Rev Genet.* 2014 May;15(5):321-34. doi: 10.1038/nrg3686.
 159. Mimitou, E. P. & Symington, L. S. Nucleases and helicases take center stage in homologous recombination. *Trends in Biochemical Sciences* (2009) doi:10.1016/j.tibs.2009.01.010.
 160. Yang W. Nucleases: diversity of structure, function and mechanism. *Q Rev Biophys.* 2011 Feb;44(1):1-93. doi: 10.1017/S0033583510000181.
 161. Lehman, I. R. DNA ligase: Structure, mechanism, and function. *Science* (1974) doi:10.1126/science.186.4166.790.
 162. Carroll D. Genome engineering with zinc-finger nucleases. *Genetics.* 2011 Aug;188(4):773-82. doi: 10.1534/genetics.111.131433.
 163. Liu Z. G., Jiao D. Necroptosis, tumor necrosis and tumorigenesis. *Cell Stress.* 2019 Dec 19;4(1):1-8. doi: 10.15698/cst2020.01.208.
 164. D'Arcy, M. S. Cell death: a review of the major forms of apoptosis, necrosis and autophagy. *Cell Biology International* (2019) doi:10.1002/cbin.11137.
 165. Del Re, D. P., Amgalan, D., Linkermann, A., Liu, Q. & Kitsis, R. N. Fundamental mechanisms of regulated cell death and implications for heart disease. *Physiological Reviews* (2019) doi:10.1152/physrev.00022.2018.
 166. Adams, J. M. & Cory, S. The Bcl-2 protein family: Arbiters of cell survival. *Science* (1998) doi:10.1126/science.281.5381.1322.
 167. Cavallucci, V. & D'Amelio, M. Matter of Life and Death: the Pharmacological Approaches Targeting Apoptosis in Brain Diseases. *Current Pharmaceutical Design* (2011) doi:10.2174/138161211795049705.
 168. Fricker, M., Tolkovsky, A. M., Borutaite, V., Coleman, M. & Brown, G. C. Neuronal cell death. *Physiological Reviews* (2018) doi:10.1152/physrev.00011.2017.
 169. Li, J., Qin, C., Lai, D., Hu, Y. & Wang, L. Safety and effectiveness of inguinal

- hernia repair in patients with liver cirrhosis: a retrospective study and literature review. *Hernia* (2020) doi:10.1007/s10029-019-02087-4.
170. Bernsmeier, C., van der Merwe, S. & Périanian, A. Innate immune cells in cirrhosis. *Journal of Hepatology* (2020) doi:10.1016/j.jhep.2020.03.027.
171. Jover, R. *et al.* Brain edema and inflammatory activation in bile duct ligated rats with diet-induced hyperammonemia: A model of hepatic encephalopathy in cirrhosis. *Hepatology* (2006) doi:10.1002/hep.21180.
172. Andrabi, S. A. *et al.* Iduna protects the brain from glutamate excitotoxicity and stroke by interfering with poly(ADP-ribose) polymer-induced cell death. *Nature Medicine* (2011) doi:10.1038/nm.2387.
173. Fang, Y. *et al.* Pyroptosis: A new frontier in cancer. *Biomedicine and Pharmacotherapy* (2020) doi:10.1016/j.biopha.2019.109595.
174. Zheng, Z. & Li, G. Mechanisms and therapeutic regulation of pyroptosis in inflammatory diseases and cancer. *International Journal of Molecular Sciences* (2020) doi:10.3390/ijms21041456.
175. Schiwon M, Weisheit C, Franken L, Gutweiler S, Dixit A, Meyer-Schwesinger C, Pohl JM, Maurice NJ, Thiebes S, Lorenz K, Quast T, Fuhrmann M, Baumgarten G, Lohse MJ, Opdenakker G, Bernhagen J, Bucala R, Panzer U, Kolanus W, Gröne HJ, Garbi N, Kastenmüller W, Knolle PA, Kurts C, Engel DR. Crosstalk between sentinel and helper macrophages permits neutrophil migration into infected uroepithelium. *Cell*. 2014 Jan 30;156(3):456-68. doi: 10.1016/j.cell.2014.01.006.
176. Di Liberto G, Pantelyushin S, Kreutzfeldt M, Page N, Musardo S, Coras R, Steinbach K, Vincenti I, Klimek B, Lingner T, Salinas G, Lin-Marq N, Staszewski O, Costa Jordão MJ, Wagner I, Egervari K, Mack M, Bellone C, Blümcke I, Prinz M, Pinschewer DD, Merkler D. Neurons under T Cell Attack Coordinate Phagocyte-Mediated Synaptic Stripping. *Cell*. 2018 Oct 4;175(2):458-471.e19. doi: 10.1016/j.cell.2018.07.049.
177. Gendron W. H., Fertan E, Pelletier S, Roddick KM, O'Leary TP, Anini Y, Brown RE. Age related weight loss in female 5xFAD mice from 3 to 12 months of age. *Behav Brain Res*. 2021 May 21;406:113214. doi: 10.1016/j.bbr.2021.113214.
178. Oakley H, Cole SL, Logan S, Maus E, Shao P, Craft J, Guillozet-Bongaarts A, Ohno M, Disterhoft J, Van Eldik L, Berry R, Vassar R. Intraneuronal beta-amyloid aggregates, neurodegeneration, and neuron loss in transgenic mice with five familial Alzheimer's disease mutations: potential factors in amyloid plaque formation. *J Neurosci*. 2006 Oct 4;26(40):10129-40. doi: 10.1523/JNEUROSCI.1202-06.2006.

179. Jawhar, S., Trawicka, A., Jenneckens, C., Bayer, T. A. & Wirths, O. Motor deficits, neuron loss, and reduced anxiety coinciding with axonal degeneration and intraneuronal A β aggregation in the 5XFAD mouse model of Alzheimer's disease. *Neurobiology of Aging* **33**, 196.e29-196.e40 (2012).
180. Ishino, Y., Shinagawa, H., Makino, K., Amemura, M. & Nakamura, A. Nucleotide sequence of the iap gene, responsible for alkaline phosphatase isoenzyme conversion in *Escherichia coli*, and identification of the gene product. *Journal of Bacteriology* (1987) doi:10.1128/jb.169.12.5429-5433.1987.
181. Mojica, F. J. M., Díez-Villaseñor, C., Soria, E. & Juez, G. Biological significance of a family of regularly spaced repeats in the genomes of Archaea, Bacteria and mitochondria. *Molecular Microbiology* (2000) doi:10.1046/j.1365-2958.2000.01838.x.
182. Jansen, R., Van Embden, J. D. A., Gaastra, W. & Schouls, L. M. Identification of genes that are associated with DNA repeats in prokaryotes. *Molecular Microbiology* (2002) doi:10.1046/j.1365-2958.2002.02839.x.
183. Anders, C., Bargsten, K. & Jinek, M. Structural Plasticity of PAM Recognition by Engineered Variants of the RNA-Guided Endonuclease Cas9. *Molecular Cell* (2016) doi:10.1016/j.molcel.2016.02.020.
184. Chen, H., Choi, J. & Bailey, S. Cut site selection by the two nuclease domains of the Cas9 RNA-guided endonuclease. *Journal of Biological Chemistry* (2014) doi:10.1074/jbc.M113.539726.
185. Haft, D. H., Selengut, J., Mongodin, E. F. & Nelson, K. E. A guild of forty-five CRISPR-associated (Cas) protein families and multiple CRISPR/Cas subtypes exist in prokaryotic genomes. *PLoS Computational Biology* (2005) doi:10.1371/journal.pcbi.0010060.eor.
186. Chylinski, K., Makarova, K. S., Charpentier, E. & Koonin, E. V. Classification and evolution of type II CRISPR-Cas systems. *Nucleic Acids Research* (2014) doi:10.1093/nar/gku241.
187. Van Der Oost, J., Westra, E. R., Jackson, R. N. & Wiedenheft, B. Unravelling the structural and mechanistic basis of CRISPR-Cas systems. *Nature Reviews Microbiology* (2014) doi:10.1038/nrmicro3279.
188. Taylor DW, Zhu Y, Staals RH, Kornfeld JE, Shinkai A, van der Oost J, Nogales E, Doudna JA. Structural biology. Structures of the CRISPR-Cmr complex reveal mode of RNA target positioning. *Science*. 2015 May 1;348(6234):581-5. doi: 10.1126/science.aaa4535.
189. Wiedenheft, B., Sternberg, S. H. & Doudna, J. A. RNA-guided genetic silencing systems in bacteria and archaea. *Nature* (2012) doi:10.1038/nature10886.

190. Brezgin, S., Kostyusheva, A., Kostyushev, D. & Chulanov, V. Dead cas systems: Types, principles, and applications. *International Journal of Molecular Sciences* (2019) doi:10.3390/ijms20236041.
191. Picelli, S. *et al.* Full-length RNA-seq from single cells using Smart-seq2. *Nature Protocols* (2014) doi:10.1038/nprot.2014.006.
192. Du, Y., Huang, Q., Arisdakessian, C. & Garmire, L. X. Evaluation of STAR and kallisto on single cell RNA-seq data alignment. *G3: Genes, Genomes, Genetics* (2020) doi:10.1534/g3.120.401160.
193. Love, M. I., Soneson, C. & Robinson, M. D. Importing transcript abundance datasets with tximport. *dim (txi. inf. rep \$ infReps \$ sample1)* (2017).
194. Varet, H., Brillet-Guéguen, L., Coppée, J. Y. & Dillies, M. A. SARTools: A DESeq2- and edgeR-based R pipeline for comprehensive differential analysis of RNA-Seq data. *PLoS ONE* (2016) doi:10.1371/journal.pone.0157022.
195. Florez-Sampedro, L. *et al.* Genetic regulation of gene expression of MIF family members in lung tissue. *Scientific Reports* (2020) doi:10.1038/s41598-020-74121-w.
196. Illescas, O., Pacheco-Fernández, T., Laclette, J. P., Rodriguez, T. & Rodriguez-Sosa, M. Immune modulation by the macrophage migration inhibitory factor (MIF) family: D-dopachrome tautomerase (DDT) is not (always) a backup system. *Cytokine* (2020) doi:10.1016/j.cyto.2020.155121.
197. Ardlie, K. G. *et al.* The Genotype-Tissue Expression (GTEx) pilot analysis: Multitissue gene regulation in humans. *Science* (2015) doi:10.1126/science.1262110.
198. Rajasekaran, D. *et al.* Macrophage migration inhibitory factor-CXCR4 receptor interactions: Evidence for partial allosteric agonism in comparison with CXCL12 chemokine. *Journal of Biological Chemistry* (2016) doi:10.1074/jbc.M116.717751.
199. Döring, Y., Pawig, L., Weber, C. & Noels, H. The CXCL12/CXCR4 chemokine ligand/receptor axis in cardiovascular disease. *Frontiers in Physiology* (2014) doi:10.3389/fphys.2014.00212.
200. Terheyden-Keighley, D., Zhang, X., Brand-Saberi, B. & Theiss, C. CXCR4/SDF1 signalling promotes sensory neuron clustering in vitro. *Biology Open* (2018) doi:10.1242/bio.035568.
201. Fernández, J. M. *et al.* The BLUEPRINT Data Analysis Portal. *Cell Systems* (2016) doi:10.1016/j.cels.2016.10.021.
202. Baião, A. M. T. *et al.* cDNA microarray analysis of cyclosporin A (CsA)-treated human peripheral blood mononuclear cells reveal modulation of genes associated with apoptosis, cell-cycle regulation and DNA repair. *Molecular and Cellular*

- Biochemistry* (2007) doi:10.1007/s11010-007-9505-7.
203. Verjans, E. *et al.* Dual role of macrophage migration inhibitory factor (MIF) in human breast cancer. *BMC Cancer* (2009) doi:10.1186/1471-2407-9-230.
204. Wang, J. *et al.* Feedback activation of STAT3 limits the response to PI3K/AKT/mTOR inhibitors in PTEN-deficient cancer cells. *Oncogenesis* (2021) doi:10.1038/s41389-020-00292-w.
205. Zheng, L., Meng, Y., Campbell, J. L. & Shen, B. Multiple roles of DNA2 nuclease/helicase in DNA metabolism, genome stability and human diseases. *Nucleic Acids Research* (2020) doi:10.1093/nar/gkz1101.
206. Aguet, F. *et al.* The GTEx Consortium atlas of genetic regulatory effects across human tissues. *Science* (2020) doi:10.1126/SCIENCE.AAZ1776.
207. Miyasaki, K. T. *et al.* In vitro Antimicrobial Activity of the Human Neutrophil Cytosolic S-100 Protein Complex, Calprotectin, Against *Capnocytophaga sputigena*. *Journal of Dental Research* (1993) doi:10.1177/00220345930720020801.
208. Li, C. *et al.* A novel p53 target gene, S100A9, induces p53-dependent cellular apoptosis and mediates the p53 apoptosis pathway. *Biochemical Journal* (2009) doi:10.1042/BJ20090465.
209. Björk, P. *et al.* Identification of human S100A9 as a novel target for treatment of autoimmune disease via binding to quinoline-3-carboxamides. *PLoS Biology* (2009) doi:10.1371/journal.pbio.1000097.
210. Kerkhoff, C., Klempt, M. & Sorg, C. Novel insights into structure and function of MRP8 (S100A8) and MRP14 (S100A9). *Biochimica et Biophysica Acta - Molecular Cell Research* (1998) doi:10.1016/S0167-4889(98)00144-X.
211. Liu, Z. *et al.* Integrative omics analysis identifies macrophage migration inhibitory factor signaling pathways underlying human hepatic fibrogenesis and fibrosis. *Journal of Bio-X Research* (2019) doi:10.1097/jbr.0000000000000026.
212. Pan-cancer analysis of whole genomes. *Nature*, 2020, 578. Jg., Nr. 7793, S. 82-93.
213. Kratz, K. *et al.* Deficiency of FANCD2-Associated Nuclease KIAA1018/FAN1 Sensitizes Cells to Interstrand Crosslinking Agents. *Cell* (2010) doi:10.1016/j.cell.2010.06.022.
214. Iuchi, S. Three classes of C2H2 zinc finger proteins. *Cellular and Molecular Life Sciences* (2001) doi:10.1007/PL00000885.
215. Fedotova, A. A., Bonchuk, A. N., Mogila, V. A. & Georgiev, P. G. C2H2 zinc finger proteins: The largest but poorly explored family of higher eukaryotic transcription factors. *Acta Naturae* (2017) doi:10.32607/20758251-2017-9-2-47-58.

216. Chang, G. T. G. *et al.* Characterization of a zinc-finger protein and its association with apoptosis in prostate cancer cells. *Journal of the National Cancer Institute* (2000) doi:10.1093/jnci/92.17.1414.
217. Brayer, K. J. & Segal, D. J. Keep your fingers off my DNA: Protein-protein interactions mediated by C2H2 zinc finger domains. *Cell Biochemistry and Biophysics* (2008) doi:10.1007/s12013-008-9008-5.
218. Laity, J. H., Lee, B. M. & Wright, P. E. Zinc finger proteins: New insights into structural and functional diversity. *Current Opinion in Structural Biology* (2001) doi:10.1016/S0959-440X(00)00167-6.
219. Chain, P. S. G. *et al.* Insights into the evolution of *Yersinia pestis* through whole-genome comparison with *Yersinia pseudotuberculosis*. *Proceedings of the National Academy of Sciences of the United States of America* (2004) doi:10.1073/pnas.0404012101.
220. Parkhill, J. *et al.* Comparative analysis of the genome sequences of *Bordetella pertussis*, *Bordetella parapertussis* and *Bordetella bronchiseptica*. *Nature Genetics* 2003 Sep;35(1):32-40. doi:10.1038/ng1227.
221. Waterston, R. H., Lander, E. S. & Sulston, J. E. On the sequencing of the human genome. *Proceedings of the National Academy of Sciences of the United States of America* (2002) doi:10.1073/pnas.042692499.
222. Derbyshire, K. M. & Grindley, N. D. F. DNA Transposons: Different Proteins and Mechanisms but Similar Rearrangements. in *The Bacterial Chromosome* (2014). doi:10.1128/9781555817640.ch26.
223. Nesmelova IV, Hackett PB. DDE transposases: Structural similarity and diversity. *Adv Drug Deliv Rev.* 2010 Sep 30;62(12):1187-95. doi: 10.1016/j.addr.2010.06.006.
224. Elmore S. Apoptosis: a review of programmed cell death. *Toxicol Pathol.* 2007 Jun;35(4):495-516. doi: 10.1080/01926230701320337.
225. Papaliagkas V, Anogianaki A, Anogianakis G, Ilonidis G. The proteins and the mechanisms of apoptosis: a mini-review of the fundamentals. *Hippokratia.* 2007 Jul;11(3):108-13.
226. Akematsu T, Endoh H. Role of apoptosis-inducing factor (AIF) in programmed nuclear death during conjugation in *Tetrahymena thermophila*. *BMC Cell Biol.* 2010 Feb 11;11:13. doi: 10.1186/1471-2121-11-13.
227. Ouertatani-Sakouhi, H. *et al.* Kinetic-based high-throughput screening assay to discover novel classes of macrophage migration inhibitory factor inhibitors. *Journal of Biomolecular Screening* (2010) doi:10.1177/1087057110363825.
228. Lue, H. *et al.* Macrophage migration inhibitory factor (MIF) promotes cell survival

- by activation of the Akt pathway and role for CSN5/JAB1 in the control of autocrine MIF activity. *Oncogene* (2007) doi:10.1038/sj.onc.1210318.
229. Inácio, A. R., Ruscher, K., Leng, L., Bucala, R. & Deierborg, T. Macrophage migration inhibitory factor promotes cell death and aggravates neurologic deficits after experimental stroke. *Journal of Cerebral Blood Flow and Metabolism* (2011) doi:10.1038/jcbfm.2010.194.
230. Soppert, J. *et al.* Soluble CD74 reroutes MIF/CXCR4/AKT-mediated survival of cardiac myofibroblasts to necroptosis. *Journal of the American Heart Association* (2018) doi:10.1161/JAHA.118.009384.
231. Steczkiewicz, K., Muszewska, A., Knizewski, L., Rychlewski, L. & Ginalski, K. SURVEY AND SUMMARY: Sequence, structure and functional diversity of PD-(D/E)XK phosphodiesterase superfamily. *Nucleic Acids Research* (2012) doi:10.1093/nar/gks382.
232. Gamsjaeger R, Liew CK, Loughlin FE, Crossley M, Mackay JP. Sticky fingers: zinc-fingers as protein-recognition motifs. *Trends Biochem Sci.* 2007 Feb;32(2):63-70. doi: 10.1016/j.tibs.2006.12.007.
233. Sulej, A. A., Tuszyńska, I., Skowronek, K. J., Nowotny, M. & Bujnicki, J. M. Sequence-specific cleavage of the RNA strand in DNA-RNA hybrids by the fusion of ribonuclease H with a zinc finger. *Nucleic Acids Research* (2012) doi:10.1093/nar/gks885.
234. Malu, D. T. *et al.* Macrophage Migration Inhibitory Factor: A Downregulator of Early T Cell-Dependent IFN- γ Responses in Plasmodium chabaudi adami (556 KA)-Infected Mice . *The Journal of Immunology* (2011) doi:10.4049/jimmunol.1003355.
235. Yang, N. *et al.* Reversal of established rat crescentic glomerulonephritis by blockade of macrophage migration inhibitory factor (MIF): Potential role of MIF in regulating glucocorticoid production. *Molecular Medicine* (1998) doi:10.1007/bf03401748.
236. Yang, D. *et al.* Knockdown of macrophage migration inhibitory factor (MIF), a novel target to protect neurons from parthanatos induced by simulated post-spinal cord injury oxidative stress. *Biochemical and Biophysical Research Communications* (2020) doi:10.1016/j.bbrc.2019.12.115.
237. Yeo, C. Q. X. *et al.* P53 Maintains Genomic Stability by Preventing Interference between Transcription and Replication. *Cell Reports* (2016) doi:10.1016/j.celrep.2016.03.011.
238. Loza-Mejía, M. A. *et al.* Synthesis, cytotoxic activity, DNA topoisomerase-II inhibition, molecular modeling and structure-activity relationship of 9-

- anilinothiazolo[5,4-b]quinoline derivatives. *Bioorganic and Medicinal Chemistry* (2009) doi:10.1016/j.bmc.2009.03.052.
239. Cattrini, C., Capaia, M., Boccardo, F. & Barboro, P. Etoposide and topoisomerase II inhibition for aggressive prostate cancer: Data from a translational study. *Cancer Treatment and Research Communications* (2020) doi:10.1016/j.ctarc.2020.100221.
240. Szpirer, C. Rat models of human diseases and related phenotypes: A systematic inventory of the causative genes. *Journal of Biomedical Science* (2020) doi:10.1186/s12929-020-00673-8.
241. Turtzo, L. C. *et al.* Deletion of macrophage migration inhibitory factor worsens stroke outcome in female mice. *Neurobiology of Disease* (2013) doi:10.1016/j.nbd.2013.01.016.
242. Garai J, Adlercreutz H. Estrogen-inducible uterine flavonoid binding sites: is it time to reconsider? *J Steroid Biochem Mol Biol.* 2004 Apr;88(4-5):377-81. doi: 10.1016/j.jsbmb.2004.01.001.
243. Jiang F, Doudna JA. CRISPR-Cas9 Structures and Mechanisms. *Annu Rev Biophys.* 2017 May 22;46:505-529. doi: 10.1146/annurev-biophys-062215-010822.
244. Bäck S, Necarsulmer J, Whitaker LR, Coke LM, Koivula P, Heathward EJ, Fortuno LV, Zhang Y, Yeh CG, Baldwin HA, Spencer MD, Mejias-Aponte CA, Pickel J, Hoffman AF, Spivak CE, Lupica CR, Underhill SM, Amara SG, Domanskyi A, Anttila JE, Airavaara M, Hope BT, Hamra FK, Richie CT, Harvey BK. Neuron-Specific Genome Modification in the Adult Rat Brain Using CRISPR-Cas9 Transgenic Rats. *Neuron.* 2019 Apr 3;102(1):105-119.e8. doi: 10.1016/j.neuron.2019.01.035.
245. Liu, J. *et al.* Construction and Characterization of CRISPR/Cas9 Knockout Rat Model of Carboxylesterase 2a Gene. *Molecular Pharmacology* (2021) doi:10.1124/molpharm.121.000357.
246. Zhang, Y. *et al.* Processing-Independent CRISPR RNAs Limit Natural Transformation in *Neisseria meningitidis*. *Molecular Cell* (2013) doi:10.1016/j.molcel.2013.05.001.
247. Bao, Z. *et al.* Homology-Integrated CRISPR-Cas (HI-CRISPR) System for One-Step Multigene Disruption in *Saccharomyces cerevisiae*. *ACS Synthetic Biology* (2015) doi:10.1021/sb500255k.
248. Karvelis, T., Gasiunas, G. & Siksnys, V. Methods for decoding Cas9 protospacer adjacent motif (PAM) sequences: A brief overview. *Methods* (2017) doi:10.1016/j.ymeth.2017.03.006.

249. Mekler, V., Kuznedelov, K. & Severinov, K. Quantification of the affinities of CRISPR–Cas9 nucleases for cognate protospacer adjacent motif (PAM) sequences. *Journal of Biological Chemistry* (2020) doi:10.1074/jbc.RA119.012239.
250. Zhang, F. *et al.* Efficient construction of sequence-specific TAL effectors for modulating mammalian transcription. *Nature Biotechnology* (2011) doi:10.1038/nbt.1775.
251. Sanjana NE, Cong L, Zhou Y, Cunniff MM, Feng G, Zhang F. A transcription activator-like effector toolbox for genome engineering. *Nat Protoc.* 2012 Jan 5;7(1):171-92. doi: 10.1038/nprot.2011.431.
252. Cong L, Ran FA, Cox D, Lin S, Barretto R, Habib N, Hsu PD, Wu X, Jiang W, Marraffini LA, Zhang F. Multiplex genome engineering using CRISPR/Cas systems. *Science.* 2013 Feb 15;339(6121):819-23. doi: 10.1126/science.1231143.
253. Liang, P. *et al.* CRISPR/Cas9-mediated gene editing in human tripronuclear zygotes. *Protein and Cell* (2015) doi:10.1007/s13238-015-0153-5.
254. Pickar-Oliver, A. & Gersbach, C. A. The next generation of CRISPR–Cas technologies and applications. *Nature Reviews Molecular Cell Biology* (2019) doi:10.1038/s41580-019-0131-5.
255. Capuzzi, E. *et al.* Is in vitro fertilization (IVF) associated with perinatal affective disorders? *Journal of Affective Disorders* (2020) doi:10.1016/j.jad.2020.08.006.
256. Honda A, Tachibana R, Hamada K, Morita K, Mizuno N, Morita K, Asano M. Efficient derivation of knock-out and knock-in rats using embryos obtained by in vitro fertilization. *Sci Rep.* 2019 Aug 9;9(1):11571. doi: 10.1038/s41598-019-47964-1.
257. Neff, E.P. CRISPR improves prospects for transgenic rats. *Lab Animal* 48, 167 (2019). <https://doi.org/10.1038/s41684-019-0316-8>
258. Harper, J. M., Wilkinson, J. E. & Miller, R. A. Macrophage migration inhibitory factor-knockout mice are long lived and respond to caloric restriction. *The FASEB Journal* (2010) doi:10.1096/fj.09-152223.
259. Ray Dorsey, E., George, B. P., Leff, B. & Willis, A. W. The coming crisis: Obtaining care for the growing burden of neurodegenerative conditions. *Neurology* (2013) doi:10.1212/WNL.0b013e318293e2ce.
260. Abeliovich, A. & Gitler, A. D. Defects in trafficking bridge Parkinson's disease pathology and genetics. *Nature* (2016) doi:10.1038/nature20414.
261. Holtzman, D. M., Morris, J. C. & Goate, A. M. Alzheimer's disease: The challenge of the second century. *Science Translational Medicine* (2011)

- doi:10.1126/scitranslmed.3002369.
262. Obulesu, M. & Lakshmi, M. J. Apoptosis in Alzheimer's Disease: An Understanding of the Physiology, Pathology and Therapeutic Avenues. *Neurochemical Research* (2014) doi:10.1007/s11064-014-1454-4.
 263. Petersen RC, Smith GE, Waring SC, Ivnik RJ, Kokmen E, Tangelos EG. Aging, memory, and mild cognitive impairment. *Int Psychogeriatr*. 1997;9 Suppl 1:65-9. doi: 10.1017/s1041610297004717.
 264. Zhong, J., Li, G., Xu, H., Wang, Y. & Shi, M. Baicalin ameliorates chronic mild stress-induced depression-like behaviors in mice and attenuates inflammatory cytokines and oxidative stress. *Brazilian Journal of Medical and Biological Research* (2019) doi:10.1590/1414-431x20198434.
 265. Mao K, Zhang G. The role of PARP1 in neurodegenerative diseases and aging. *FEBS J*. 2022 Apr;289(8):2013-2024. doi: 10.1111/febs.15716.
 266. Akbari M, Shanley DP, Bohr VA, Rasmussen LJ. Cytosolic Self-DNA-A Potential Source of Chronic Inflammation in Aging. *Cells*. 2021 Dec 15;10(12):3544. doi: 10.3390/cells10123544.
 267. Unnisa, A., Greig, N. H. & Kamal, M. A. Nanotechnology: A Promising Targeted Drug Delivery System for Brain Tumours and Alzheimer's Disease. *Current Medicinal Chemistry* (2022) doi:10.2174/0929867329666220328125206.
 268. Koronowski, K. B. *et al.* Resveratrol Preconditioning Induces a Novel Extended Window of Ischemic Tolerance in the Mouse Brain. *Stroke; a journal of cerebral circulation* (2015) doi:10.1161/STROKEAHA.115.009876.
 269. Montecucco A, Zanetta F, Biamonti G. Molecular mechanisms of etoposide. *EXCLI J*. 2015 Jan 19;14:95-108. doi: 10.17179/excli2015-561.
 270. Knizewski, L., Kinch, L. N., Grishin, N. V., Rychlewski, L. & Ginalski, K. Realm of PD-(D/E)XK nuclease superfamily revisited: Detection of novel families with modified transitive meta profile searches. *BMC Structural Biology* (2007) doi:10.1186/1472-6807-7-40.
 271. Philo, J. S., Yang, T. H. & LaBarre, M. Re-examining the oligomerization state of macrophage migration inhibitory factor (MIF) in solution. *Biophysical Chemistry* (2004) doi:10.1016/j.bpc.2003.10.010.
 272. Nakahara, K. *et al.* Attenuation of macrophage migration inhibitory factor-stimulated signaling via S-nitrosylation. *Biological and Pharmaceutical Bulletin* (2019) doi:10.1248/bpb.b19-00025.
 273. Rajasekaran D, Zierow S, Syed M, Bucala R, Bhandari V, Lolis EJ. Targeting distinct tautomerase sites of D-DT and MIF with a single molecule for inhibition of neutrophil lung recruitment. *FASEB J*. 2014 Nov;28(11):4961-71. doi:

- 10.1096/fj.14-256636.
274. Yaddanapudi K, Putty K, Rendon BE, Lamont GJ, Faughn JD, Satoskar A, Lasnik A, Eaton JW, Mitchell RA. Control of tumor-associated macrophage alternative activation by macrophage migration inhibitory factor. *J Immunol*. 2013 Mar 15;190(6):2984-93. doi: 10.4049/jimmunol.1201650.
275. Kleemann R, Hausser A, Geiger G, Mischke R, Burger-Kentischer A, Flieger O, Johannes FJ, Roger T, Calandra T, Kapurniotu A, Grell M, Finkelmeier D, Brunner H, Bernhagen J. Intracellular action of the cytokine MIF to modulate AP-1 activity and the cell cycle through Jab1. *Nature*. 2000 Nov 9;408(6809):211-6. doi: 10.1038/35041591.
276. Cavalli, E. *et al.* Upregulated expression of macrophage migration inhibitory factor, its analogue d-dopachrome tautomerase, and the cd44 receptor in peripheral cd4 t cells from clinically isolated syndrome patients with rapid conversion to clinical defined multiple sclerosis. *Medicina (Lithuania)* (2019) doi:10.3390/medicina55100667.
277. Bozza, M. T., Lintomen, L., Kitoko, J. Z., Paiva, C. N. & Olsen, P. C. The Role of MIF on Eosinophil Biology and Eosinophilic Inflammation. *Clinical Reviews in Allergy and Immunology* (2020) doi:10.1007/s12016-019-08726-z.
278. Burger-Kentischer, A. *et al.* Reduction of the aortic inflammatory response in spontaneous atherosclerosis by blockade of macrophage migration inhibitory factor (MIF). *Atherosclerosis* (2006) doi:10.1016/j.atherosclerosis.2005.03.028.
279. Huang, H. *et al.* The small molecule macrophage migration inhibitory factor antagonist MIF098, inhibits pulmonary hypertension associated with murine SLE. *International Immunopharmacology* (2019) doi:10.1016/j.intimp.2019.105874.
280. Ma, F. *et al.* Protease activated-receptor 4 activation as a model of persistent bladder pain: Essential role of macrophage migration inhibitory factor and high mobility group box 1. *International Journal of Urology* (2018) doi:10.1111/iju.13778.
281. Winner, M. *et al.* A novel, macrophage migration inhibitory factor suicide substrate inhibits motility and growth of lung cancer cells. *Cancer Research* (2008) doi:10.1158/0008-5472.CAN-07-6227.
282. Zhang, B. *et al.* Role of macrophage migration inhibitory factor in the proliferation of smooth muscle cell in pulmonary hypertension. *Mediators of Inflammation* (2012) doi:10.1155/2012/840737.
283. Hu, J.-X. *et al.* Macrophage migration inhibitory factor (MIF) acetylation protects neurons from ischemic injury. *Cell Death & Disease* **13**, 466 (2022).
284. Takuma, K., Baba, A. & Matsuda, T. Astrocyte apoptosis: Implications for

- neuroprotection. *Progress in Neurobiology* (2004) doi:10.1016/j.pneurobio.2004.02.001.
285. Barros, L. F. & Deitmer, J. W. Glucose and lactate supply to the synapse. *Brain Research Reviews* (2010) doi:10.1016/j.brainresrev.2009.10.002.
286. Dringen, R., Pfeiffer, B. & Hamprecht, B. Synthesis of the antioxidant glutathione in neurons: Supply by astrocytes of CysGly as precursor for neuronal glutathione. *Journal of Neuroscience* (1999) doi:10.1523/jneurosci.19-02-00562.1999.
287. Hertz L, Zielke HR. Astrocytic control of glutamatergic activity: astrocytes as stars of the show. *Trends Neurosci.* 2004 Dec;27(12):735-43. doi: 10.1016/j.tins.2004.10.008.
288. Lebon, V. *et al.* Astroglial contribution to brain energy metabolism in humans revealed by ¹³C nuclear magnetic resonance spectroscopy: Elucidation of the dominant pathway for neurotransmitter glutamate repletion and measurement of astrocytic oxidative metabolism. *Journal of Neuroscience* (2002) doi:10.1523/jneurosci.22-05-01523.2002.
289. Danbolt N. C. Glutamate uptake. *Prog Neurobiol.* 2001 Sep;65(1):1-105. doi: 10.1016/s0301-0082(00)00067-8.
290. Blocki, F. A., Ellis, L. B. M. & Wackett, L. P. MIF proteins are theta-class glutathione S-transferase homologs. *Protein Science* (1993) doi:10.1002/pro.5560021210.
291. Rossjohn, J., Board, P. G., Parker, M. W. & Wilce, M. C. J. A structurally derived consensus pattern for theta class glutathione transferases. *Protein Engineering* (1996) doi:10.1093/protein/9.4.327.
292. Zhou, J. *et al.* The prolyl 4-hydroxylase inhibitor GSK360A decreases post-stroke brain injury and sensory, motor, and cognitive behavioral deficits. *PLoS ONE* (2017) doi:10.1371/journal.pone.0184049.
293. Cavalli, E. *et al.* Emerging role of the macrophage migration inhibitory factor family of cytokines in neuroblastoma. Pathogenic effectors and novel therapeutic targets? *Molecules* (2020) doi:10.3390/molecules25051194.
294. Hudson, J. D. *et al.* A proinflammatory cytokine inhibits p53 tumor suppressor activity. *Journal of Experimental Medicine* (1999) doi:10.1084/jem.190.10.1375.
295. Yao, Y. *et al.* MIF Plays a Key Role in Regulating Tissue-Specific Chondro-Osteogenic Differentiation Fate of Human Cartilage Endplate Stem Cells under Hypoxia. *Stem Cell Reports* (2016) doi:10.1016/j.stemcr.2016.07.003.
296. Singh, N. P., McCoy, M. T., Tice, R. R. & Schneider, E. L. A simple technique for quantitation of low levels of DNA damage in individual cells. *Experimental Cell Research* (1988) doi:10.1016/0014-4827(88)90265-0.

297. Perry, V. H. The influence of systemic inflammation on inflammation in the brain: Implications for chronic neurodegenerative disease. *Brain, Behavior, and Immunity* (2004) doi:10.1016/j.bbi.2004.01.004.
298. Peferoen, L., Kipp, M., van der Valk, P., van Noort, J. M. & Amor, S. Oligodendrocyte-microglia cross-talk in the central nervous system. *Immunology* (2014) doi:10.1111/imm.12163.
299. Lolis E, Bucala R. Macrophage migration inhibitory factor. *Expert Opin Ther Targets*. 2003 Apr;7(2):153-64. doi: 10.1517/14728222.7.2.153.
300. Alzheimer's Disease International. World Alzheimer Report 2019: Attitudes to Dementia. *Alzheimer's Disease International: London* (2019).
301. Masuda-Sasa, T., Polaczek, P., Peng, X. P., Chen, L. & Campbell, J. L. Processing of G4 DNA by Dna2 helicase/nuclease and replication protein A (RPA) provides insights into the mechanism of Dna2/RPA substrate recognition. *Journal of Biological Chemistry* (2008) doi:10.1074/jbc.M802244200.
302. Kosinski, J., Feder, M. & Bujnicki, J. M. The PD-(D/E)XK superfamily revisited: Identification of new members among proteins involved in DNA metabolism and functional predictions for domains of (hitherto) unknown function. *BMC Bioinformatics* (2005) doi:10.1186/1471-2105-6-172.
303. Petralia, M. *et al.* Transcriptomic analysis reveals moderate modulation of macrophage migration inhibitory factor superfamily genes in alcohol use disorders. *Experimental and Therapeutic Medicine* (2020) doi:10.3892/etm.2020.8410.
304. Cavalli, E. *et al.* Overexpression of macrophage migration inhibitory factor and its homologue d-dopachrome tautomerase as negative prognostic factor in neuroblastoma. *Brain Sciences* (2019) doi:10.3390/brainsci9100284.
305. Caltabiano, R. *et al.* Macrophage Migration Inhibitory Factor (MIF) and Its Homologue d-Dopachrome Tautomerase (DDT) Inversely Correlate with Inflammation in Discoid Lupus Erythematosus. *Molecules (Basel, Switzerland)* (2021) doi:10.3390/molecules26010184.
306. Daugas E, Susin SA, Zamzami N, Ferri KF, Irinopoulou T, Larochette N, Prévost MC, Leber B, Andrews D, Penninger J, Kroemer G. Mitochondrio-nuclear translocation of AIF in apoptosis and necrosis. *FASEB J*. 2000 Apr;14(5):729-39. PMID: 10744629.
307. Yang, S., Huang, J., Liu, P., Li, J. & Zhao, S. Apoptosis-inducing factor (AIF) nuclear translocation mediated caspase-independent mechanism involves in X-ray-induced MCF-7 cell death. *International Journal of Radiation Biology* (2017) doi:10.1080/09553002.2016.1254833.

308. Xing, Y. *et al.* Pak5-mediated aif phosphorylation inhibits its nuclear translocation and promotes breast cancer tumorigenesis. *International Journal of Biological Sciences* (2021) doi:10.7150/ijbs.58102.
309. Feigin, V. L. *et al.* Global and regional burden of stroke during 1990-2010: Findings from the Global Burden of Disease Study 2010. *The Lancet* (2014) doi:10.1016/S0140-6736(13)61953-4.
310. Zhang S, Zis O, Ly PT, Wu Y, Zhang S, Zhang M, Cai F, Bucala R, Shyu WC, Song W. Down-regulation of MIF by NFκB under hypoxia accelerated neuronal loss during stroke. *FASEB J.* 2014 Oct;28(10):4394-407. doi: 10.1096/fj.14-253625.
311. Kim, M. J. *et al.* Macrophage migration inhibitory factor interacts with thioredoxin-interacting protein and induces NF-κB activity. *Cellular Signalling* (2017) doi:10.1016/j.cellsig.2017.03.007.
312. Sekerdag, E., Solaroglu, I. & Gursoy-Ozdemir, Y. Cell Death Mechanisms in Stroke and Novel Molecular and Cellular Treatment Options. *Current Neuropharmacology* (2018) doi:10.2174/1570159x16666180302115544.
313. Sakai, M., Nishihira, J., Hibiya, Y., Koyama, Y. & Nishi, S. Glutathione binding rat liver 13k protein is the homologue of the macrophage migration inhibitory factor. *Biochemistry and Molecular Biology International* (1994).
314. Blocki FA, Schlievert PM, Wackett LP. Rat liver protein linking chemical and immunological detoxification systems. *Nature.* 1992 Nov 19;360(6401):269-70. doi: 10.1038/360269a0.
315. Suzuki M, Sugimoto H, Nakagawa A, Tanaka I, Nishihira J, Sakai M. Crystal structure of the macrophage migration inhibitory factor from rat liver. *Nat Struct Biol.* 1996 Mar;3(3):259-66. doi: 10.1038/nsb0396-259.
316. Wang, H., Park, H., Liu, J. & Sternberg, P. W. An efficient genome editing strategy to generate putative null mutants in *Caenorhabditis elegans* using CRISPR/Cas9. *bioRxiv* (2018) doi:10.1101/391243.
317. Villa, A. *et al.* Sex-Specific Features of Microglia from Adult Mice. *Cell Reports* (2018) doi:10.1016/j.celrep.2018.05.048.
318. Geurs, T. L., Hill, E. B., Lippold, D. M. & French, A. R. Sex differences in murine susceptibility to systemic viral infections. *Journal of Autoimmunity* (2012) doi:10.1016/j.jaut.2011.12.003.
319. Howell, M. D. *et al.* TIA1 is a gender-specific disease modifier of a mild mouse model of spinal muscular atrophy. *Scientific Reports* (2017) doi:10.1038/s41598-017-07468-2.
320. Aloisi, A. M. *et al.* Gender-related effects of chronic non-malignant pain and opioid

- therapy on plasma levels of macrophage migration inhibitory factor (MIF). *Pain* (2005) doi:10.1016/j.pain.2005.02.019.
321. Xu, J. *et al.* Intratumor Heterogeneity of MIF Expression Correlates With Extramedullary Involvement of Multiple Myeloma. *Frontiers in Oncology* (2021) doi:10.3389/fonc.2021.694331.
322. Kuksin, M. *et al.* Applications of single-cell and bulk RNA sequencing in onco-immunology. *European Journal of Cancer* (2021) doi:10.1016/j.ejca.2021.03.005.
323. Kjell J, Olson L. Rat models of spinal cord injury: from pathology to potential therapies. *Dis Model Mech.* 2016 Oct 1;9(10):1125-1137. doi: 10.1242/dmm.025833. PMID: 27736748; PMCID: PMC5087825.
324. Popp, A., Jaenisch, N., Witte, O. W. & Frahm, C. Identification of ischemic regions in a rat model of stroke. *PLoS ONE* (2009) doi:10.1371/journal.pone.0004764.
325. Tsai Y, Lu B, Ljubimov AV, Girman S, Ross-Cisneros FN, Sadun AA, Svendsen CN, Cohen RM, Wang S. Ocular changes in TgF344-AD rat model of Alzheimer's disease. *Invest Ophthalmol Vis Sci.* 2014 Jan 29;55(1):523-34. doi: 10.1167/iovs.13-12888.
326. Calandra, T., Bernhagen, J., Mitchell, R. A. & Bucala, R. The macrophage is an important and previously unrecognized source of macrophage migration inhibitory factor. *Journal of Experimental Medicine* (1994) doi:10.1084/jem.179.6.1895.
327. Bäck M, Weber C, Lutgens E. Regulation of atherosclerotic plaque inflammation. *J Intern Med.* 2015 Nov;278(5):462-82. doi: 10.1111/joim.12367. PMID: 25823439.
328. Vratarić, M. *et al.* Fructose diet ameliorates effects of macrophage migration inhibitory factor deficiency on prefrontal cortex inflammation, neural plasticity, and behavior in male mice. *BioFactors* (2023) doi:10.1002/biof.1802.

Acknowledgement

During my Ph.D., I studied the role of MIF and its paralogue MIF-2 in cell death mechanisms of neurons and astrocytes. As a result, I contributed to the establishment of a new experimental animal model for the MIF family.

Therefore, in the first place, I would like to thank my doctoral advisor, Univ. Prof. Dr. Jürgen Bernhagen, for his support in MIF family research. Additionally, I extend my sincere thanks to my supervisor Prof. Dr. Özgün Gokce, for providing me with the invaluable opportunity to pursue and complete my Ph.D. Both have played pivotal roles, engaging in constructive discussions and offering continuous support, showcasing their expertise and interest in my research project.

I appreciate Prof. Dr. Özgün Gokce for his trust and support, which I consider instrumental for my future career trajectory, paving the way for me to evolve into a dedicated scientist. Finally, I want to thank Prof. Dr. med. Martin Dichgans for running the institute innovatively, progressively, and continuously focusing on research breakthroughs.

I would also like to thank all the laboratory staff at the AG Gokce and AG Bernhagen and all the employees at the ISD, especially the animal facility. Furthermore, special thanks go to Fumere Usifo, Simon Besson-Girard and Yijing Wang from the Gokce Lab, Markus Brandhofer, Simona Gerra, and Dr. Omar El Bounkari from the Bernhagen Lab, for ongoing scholarly discussions that have contributed significantly to the progress of my work.

For this study, it was essential to generate recombinant human and mouse MIF and MIF-2. Therefore, I would like to acknowledge Simona Gerra for her invaluable assistance in purifying and providing the wild-type proteins and the MIF-C81S mutant. Additionally, I would like to express gratitude to Markus Brandhofer for providing considerable help in purifying the MIF-2 E88Q mutant.

I would also like to thank my internal and external collaborators Prof. Dr. med Plesnila Nikolaus, and Josh Shrouder. It was fun to establish pericytes sorting of the ischemic cortex for Bulk RNA sequencing and Single Cell RNAseq.

I would also like to thank my external collaborators Marie-Christine Birling and all members of phenomin and the institute clinic de la souris. They contributed to establishing a novel animal model for MIF research in rats. I look forward to expanding our MIF research related to Alzheimer's disease, atherosclerosis, and related cardiovascular diseases.

Here, I would like to once again acknowledge the support of Yijing Wang for the collaboration and assistance in RNA extraction, as well as the sequencing analysis, together with Simon Besson Girard.

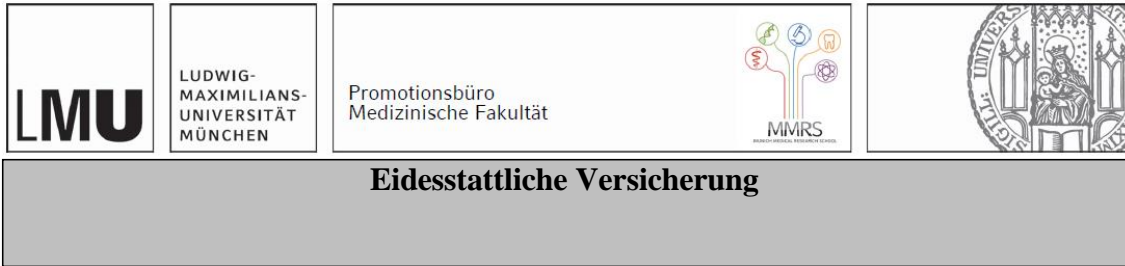
Last but not least, I would like to thank the strong women around me who constantly inspire me. Starting with my mother, mother-in-law, and Mrs. Bader (also for proofreading my thesis 😊). Thank you for believing in me the most when I least do it. Thank you for setting an example that women can “be” and “do” anything they desire. Next, I would like to thank Christine Krammer and Lisa Behrend (birth name: Schindler) for always having suggestions and advice for me, not just work-related but also in all private areas. I look forward to our future adventures together. I am so lucky to have you as my friends.

I would also like to thank the people who mean the most to me in life. Starting with my brother Kemal, and my parents. You have given me tireless support, motivation, and encouragement at all times. You were, are, and will always be "my Rock in the Waves."

Finally, special thanks go to my friend, partner in crime, and for almost 1.5 years now, my husband, Ibrahim. You are my Nastenka forever and ever. Of course, thank you for being so patient and caring, but I thank you forever indebted for letting me be who I wanted to be.

Ich liebe dich mein Balli Lokma!

Affidavit



Bulut-Impraim, Buket

Name, Vorname

Ich erkläre hiermit an Eides statt, dass ich die vorliegende Dissertation mit dem Titel:

Investigating the Nuclease Activity of MIF and MIF-2 and Their Effects on DNA Damage.

selbständig verfasst, mich außer der angegebenen keiner weiteren Hilfsmittel bedient und alle Erkenntnisse, die aus dem Schrifttum ganz oder annähernd übernommen sind, als solche kenntlich gemacht und nach ihrer Herkunft unter Bezeichnung der Fundstelle einzeln nachgewiesen habe.

Ich erkläre des Weiteren, dass die hier vorgelegte Dissertation nicht in gleicher oder in ähnlicher Form bei einer anderen Stelle zur Erlangung eines akademischen Grades eingereicht wurde.

Immenstadt im Allgäu, 07.07.2024
Ort, Datum

Buket Bulut Impraim
Unterschrift Doktorandin bzw. Doktorand

List of publications

Published paper:

Dissociation of microdissected mouse brain tissue for artifact free single-cell RNA sequencing

Liu L, Besson-Girard S, Ji H, Gehring K, Bulut B, Kaya T, Usifo F, Simons M, Gokce O. Dissociation of microdissected mouse brain tissue for artifact free single-cell RNA sequencing. STAR Protoc. 2021 Jun 10;2(2):100590. doi: 10.1016/j.xpro.2021.100590. PMID: 34159323; PMCID: PMC8196224.

High-Resolution RNA Sequencing from PFA-Fixed Microscopy Sections

Hao Ji, Simon Besson-Girard, Peter Androvic, Buket Bulut, Lu Liu, Yijing Wang & Ozgun Gokce; Methods in Molecular Biology, vol 2616; pp 205–212.

Submitted Papers:

Capillary pericytes promote no-reflow after experimental stroke in vivo.

Shrouder, Joshua; Filser, Severin; Varga, Daniel Peter; Besson-Girard, Simon; Mamrak, Uta; Bulut-Impraim, Buket; Seker, Fatma Burcu; Gesierich, Benno; Laredo, Fabio; Wehn, Antonia Clarissa; Khalin, Igor; Bayer, Patrick; Liesz, Arthur; Gokce, Ozgun; Plesnila, N. currently under review at Nature Communications

Manuscripts in preparation:

The Role of MIF and his paralogue MIF-2, after toxic insult in primary neuronal mixed and astrocyte cultures.

Buket Bulut¹, Simon Besson-Girard¹, Peter Androvic¹, Hao Ji¹, Lu Liu¹, Yijing Wang¹, Jürgen Bernhagen, Ozgun Gokce^{1,2};

MIF's multipotent role in Alzheimer's disease mouse model (5XFAD).

Lu Liu¹, Simon Besson-Girard¹, Buket Bulut¹, Peter Androvic¹, Hao Ji¹, Yijing Wang¹, Jürgen Bernhagen, Ozgun Gokce^{1,2};